Establishment of maize resistance to fungal diseases by host-induced gene silencing and site-directed mutagenesis

Von der Naturwissenschaftlichen Fakultät der
Gottfried Wilhelm Leibniz Universität Hannover

zur Erlangung des Grades
Doktor der Naturwissenschaften (Dr. rer. nat.)

genehmigte Dissertation
von
Krishna Mohan Pathi, M.Sc.

2021

Referent: Prof. Dr. Thomas Debener

Korreferent: Prof. Dr. Jens Boch

Tag der Promotion: 03.05.2021

Zusammenfassung

Schlagworte: *Genome Engineering*, Suszeptibilitätsfaktor, Pflanze-Pathogen-Interaktion, Gen-Knock-down, short interfering RNAs

Mais ist eine der am meisten angebauten Nutzpflanzen der Welt. Die als Anthraknose bezeichnete Krankheit kann für bis zu 80% der Verluste in der Maisproduktion verantwortlich sein. Diese Krankheit wird durch den hemibiotrophen Pilz *Colletotrichum graminicola* verursacht. Leider ist die Krankheit prinzipiell schwer zu bekämpfen, da entsprechende Wirtsresistenzmechanismen kaum bekannt sind. In der vorliegenden Studie wurde zum Schutz der Maispflanzen vor *C. graminicola*-Infektionen das biotechnologische Prinzip der Wirts-induzierten Gen-Repression (*host-induced gene silencing*, HIGS) angewendet. HIGS ist ein auf RNA-Interferenz (RNAi) basierender Prozess, bei dem *short interfering* RNAs (siRNAs) von den Pflanzen gebildet und vom Pilz aufgenommen werden, um einen Abbau Sequenz-entsprechender Transkripte im Pilz auszulösen. Mit Hilfe dieser Strategie wurden in der vorliegenden Studie die *C. graminicola* Gene *β-Tubulin 2* (*Tub2*) und *Succinatdehydrogenase 1* (*Sdh1*) adressiert, die für Fungizidziele kodieren. Zu diesem Zweck wurden RNAi-Vektoren unter Verwendung geeigneter Zielgenregionen entworfen. Transgene, RNAi-Konstrukte exprimierende Pflanzen wurden mit *C. graminicola* infiziert, wodurch in einigen Fällen eine quantitative Resistenz erzielt werden konnte.

Neben dem HIGS-Ansatz wurde eine weitere Strategie verfolgt, die darin bestand einen Suszeptibilitätsfaktor gegenüber *C. graminicola* mittels zielgerichteter Mutagenese auszuschalten. Dabei handelte es sich um das 9-LIPOXYGENASE *LOX3*-Gen aus Mais, das durch Expression RNA-geleiteter Cas9-Endonuclease gelungen ist in mehreren Pflanzen zu mutieren. Homozygote *lox3*-Mutanten wurden in *C. graminicola*-Infektionsassays getestet um den Effekt der Mutation zu testen. Die Quantifizierung von Pilzbiomasse ergab, dass die *lox3*-Mutanten im Vergleich zum nicht-mutierten Wildtyp signifikant weniger von *C. graminicola* besiedelt wurden.

Der Maisbeulenbrand, eine ebenfalls bedeutende Pilzkrankheit, wird durch das biotrophe Pathogen *Ustilago maydis* verursacht. Während des Infektionsverlaufes mit *U. maydis* erhobene Transkriptionssdaten zeigten (Doehlemann et al., 2008), dass in Abhängigkeit der Infektion mehrere Mitglieder der *LOX*-Genfamilie hochreguliert werden, von denen eines *LOX3* ist. Daher wurden die zur Verfügung stehenden *lox3* Mutanten ebenfalls bezüglich ihrer Reaktion auf die Infektion mit *U. maydis* überprüft. Die Quantifizierung der Krankheitssymptome ergab, dass die *lox3* Mutanten eine mäßige Resistenz gegen *U. maydis*-Infektionen aufwiesen. Darüber hinaus ergab die Quantifizierung der Biomasse von *U. maydis*, dass die *lox3* Mutanten im Vergleich zum Wildtyp in geringerem Maß vom Pilz besiedelt wurden. Zudem wurden Infektionstests anhand von unabhängig entstandenen *lox3* Mutanten durchgeführt, die durch Transposon-

Insertionsmutagenese erzeugt worden waren. Diese Linien zeigten ein ähnliches Resistenzverhalten wie die Cas9-induzierten Mutanten, wodurch konvegente Evidenz erzielt werden konnte. Aus der Literatur geht hervor, dass *U. maydis* die Akkumulation reaktiver Sauerstoffspezies (*reactive oxygen species*, ROS) unterdrückt, um seinen biotrophen Pathogenesemodus etablieren zu können. Der in dieser Arbeit durchgeführte ROS-Akkumulationstest zeigte, dass die *lox3*-Mutanten im Vergleich zum Wildtyp eine erhöhte ROS Akkumulation aufwiesen, was darauf hindeutet, dass die durch Pathogen-assozierte molekulare Strukturen (pathogen-associated molecular pattern, PAMP) ausgelöste Immunität der Mutanten zu einer Verringerung der Schwere der Pilzinfektion führte. Dies ist die erste Studie, die zeigt, dass *lox3* Mutanten eine moderate Resistenz gegen *U. maydis* aufweisen. Angesichts dieser Ergebnisse wird vermutet, dass *LOX3* auch ein Suszeptibilitätsfaktor für *U. maydis* ist.

Abstract

Keywords: genome engineering, susceptibility factor, plant-pathogen interaction, gene knock-down, short interfering RNAs

Maize is one of the most cultivated crops in the world. A disease called anthracnose accounts for up to 80% of the loss in maize production. It is caused by the hemibiotrophic fungus *Colletotrichum graminicola*. Unfortunately, the disease is notoriously difficult to combat, since host resistance mechanisms are hardly available. In the present investigation, the principle of host-induced gene silencing (HIGS) was employed to protect maize plants from *C. graminicola* infection. HIGS is an RNA-interefence (RNAi)-based process, wherein plant-produced short interfering RNAs (siRNA) are taken up by the fungus and trigger the silencing of cognate genes of the latter. In the present study, genes encoding fungicide targets were chosen as HIGS targets, namely *C. graminicola β-Tubulin 2* and *Succinate dehydrogenase 1*. RNAi vectors were designed using appropriate regions of these target genes. Transgenic plants expressing RNAi constructs were infected with *C. graminicola*, whereby the plants showed quantitative resistance.

In addition to the HIGS approach, a further strategy was pursued, which consisted in knocking out a susceptibility factor against *C. graminicola* by means of targeted mutagenesis. This factor was the 9-LIPOXYGENASE *LOX3* gene from maize, for which several mutated plants were generated by expression of RNA-directed Cas9 endonuclease. Homozygous *lox3* mutants were tested in *C. graminicola* infection assays to analyze the consequences of their mutations. Quantification of fungal biomass revealed that the *lox3* mutants were significantly less colonized by *C. graminicola* compared to the non-mutated wild-type.

Corn common smut, another important fungal disease, is caused by the biotrophic pathogen *Ustilago maydis*. Transcriptional data (Doehlemann et al., 2008) collected during the course of infection with *U. maydis* showed that, depending on the infection, several members of the *LOX* gene family are upregulated, one of which is *LOX3*. Therefore, the available *lox3* mutants were tested for their response to infection with *U. maydis*. The quantification of the disease symptoms showed that the *lox3* mutants showed a moderate resistance against *U. maydis* infections. Furthermore, the quantification of the biomass of *U. maydis* revealed that the *lox3* mutants were colonized by the fungus to a lesser extent compared to the wild-type. Furthermore, infection tests were performed using *lox3* mutants independently produced by transposon insertion mutagenesis. These lines showed a resistance behavior similar to that of Cas9-induced mutants, by which the anticipated role of *LOX3* for the interaction of maize and *U. maydis* was corroborated. From the literature it is known that *U. maydis* suppresses the accumulation of reactive oxygen species (ROS) to establish its biotrophic mode of pathogenesis. A ROS accumulation test revealed that *lox3* mutants feature increased ROS accumulation

compared to the wild-type, suggesting that the immunity of the mutants triggered by pathogen-associated molecular pattern (PAMP) led to a reduction in the severity of fungal infection. This is the first study showing that *lox3* mutants show moderate resistance to *U. maydis*. In view of these results, it is concluded that *LOX3* is a susceptibility factor for *U. maydis* as well.

Table of content

Abbreviations and Technical terms

% w/v	Percent by mass
% v/v	Percentage by volume
μ	Micro
A. thaliana	*Arabidopsis thaliana*
Z. mays	*Zea mays*
U. maydis	*Ustilago maydis*
C. graminicola	*Colletotrichum graminicola*
A. tumefaciens	*Agrobacterium tumefaciens*
bp	Base pair(s)
Cas9	CRISPR-associated protein
cDNA	complementary DNA
CRISPR	Clustered Regularly Interspaced Short Palindromic Repeats
DBD	DNA binding domain
ddH_2O	double distilled water
DMSO	Dimethylsulfoxid
DNA	Deoxyribonucleic acid
DSB	DNA double-strand break
E. coli	*Escherichia coli*
F_1, F_2	Filial generation 1, 2
FokI	Type II restriction enzyme from *Flavobacterium okeanokoites*
gfp; GFP	green fluorescent protein (Green Fluorescent Protein)
gRNA	*guide* RNA
h	hour
HDR	*Homolgy-Directed Repair*
LB, RB	Left and Right recognition sequence of the T-DNA
M	Molar
min	Minutes
mM	Millimolar
NHEJ	*Non-Homologous End-Joining*
NLS	*Nuclear Localization Signal*
nm	Nanometer
OD	optical density
PCR	*Polymerase Chain Reaction*
pDNA	Plasmid DNA
RGEN(s)	RNA-guided endonuclease(s)
RNA	Ribonucleic acid
rpm	rotation per minute
RT	Room temperature
RT-qPCR	Reverse transcriptase quantitative PCR
s	Seconds
S. pyogenes	*Streptococcus pyogenes*
T_0	Primarily transgenics
T_1	Transgenic filial generation 1
T_2	Transgenic filial generation 2
TALEN(s)	Transcription activator-like effector Nuclease(s)
T-DNA	Transfer DNA
WT	Wild-type

qPCR	quantitative PCR
ROS	Reactive Oxygen Species
SE	Standard error
HIGS	Host induced gene silencing
SIGS	Spraying induced gene silencing
deCAMV35s	Double enhanced cauliflower mosaic virus 35s promotor
Ubi-int	Intron of ubiquitin
Lox	lipoxygenases
PR proteins	Pathogenesis related proteins
OPR	12-oxo-phytodienoic Acid Reductase
P450	cytochrome P450
CC9	Corn Cystatin 9
PAL	Phenylalanine-ammonia-lyase
HYD	Hydrolase
AOS	Allene oxide synthase
GST	Glutathione S-transferase
ACX	acylcoenzyme A (CoA) oxidases
MPI	Maize protease inhibitor
PAM	Protospacer adjacent motif
hpt	hygromycin phosphotransferase
OsU3t	Rice U3 terminator
JA	Jasmonic acid
ET	Ethylene
SA	Salicylic acid
hpi	Hours post infection
dpi	Days post infection
PAMP	Pathogen associated molecular pattern
WGA	wheat germ agglutinin
PTI	PAMP triggered immunity
β	Beta
PRB	Plant reproductive biology
FRAC	Fungicide resistance action committee
TCA	Tricarboxylic acid
dpi	days post inoculation
Mlk	Mixed lineage kinases
CPR	constitutive expression of PR genes
Mla	Mildew resistance locus a

List of Figures and Tables

1. Introduction

1.1 Importance of maize

Maize (*Zea mays* L.) is one of the most valuable cereal crops in the world. It belongs to the Poaceae family and was domesticated about 10,000 years ago by indigenous people in southern Mexico (Benz, 2001). It is a fast-growing C4 annual plant. Maize grains are used for direct human consumption as they are rich sources of fiber, vitamins, minerals and anti-oxidants (Gwirtz and Garcia-Casal, 2014). It is also used as a primary nutrient source for animal feed. Many industries have been using maize as a raw material for the production of commercial products such as oil, syrup, alcohol, biofuel, biodegradable plastics and ethanol. Furthermore, maize is employed as a model organism to study various biological events such as paramutation, transposition, allelic diversity and heterosis (Kynast, 2012; Pathi et al., 2013; Pathi et al., 2020). Owing to its importance, the demand for maize production has dramatically increased at a global level over recent decades.

However, environmental factors, namely abiotic (i.e. drought, salinity, high and low temperatures, and nutrient deficiency) and biotic (pathogens) stresses pose severe threats to maize production, which can lead to substantial yield losses and diminished grain quality. This causes a significant impact on the economy and threatening the livelihood of millions of people. On a worldwide scale, annual losses of maize caused by pathogens account for approximately 75 million metric tons (http://faostat.fao.org). The most important and destructive diseases are stalk rots, leaf blights, seedling diseases as well as ear and kernel rots (Ali and Yan, 2012; Pechanova and Pechan, 2015). Anthracnose is a globally important fungal disease of maize (Boa, 2001; Balint-Kurti and Johal, 2009). In addition to this, smut fungi are distributed worldwide and are important pathogens of maize (Hoefnagels, 2005). The present thesis mainly focuses on the establishment of resistance to maize anthracnose and common smut diseases.

1.2 Anthracnose disease

Maize anthracnose is caused by the hemi-biotrophic fungal pathogen *Colletotrichum graminicola* (Wilson, 1914)*.* Hemi-biotrophs parasitize in living tissue for a while, which is followed by a necrotrophic phase. Besides maize, *C. graminicola* infects other economically important grain crops such as barley, wheat and sorghum. In addition to this, members of the genus *Colletotrichum* are infesting at least 42 plant genera of the Poaceae family (Crouch and Beirn, 2009). In addition, many economically important dicotyledonous plant species are affected by anthracnoses; e.g. tomato is infected by *C. coccodes*, Cucurbits by *C. lagenarium,* Bean by *C. lindemuthianum,* Onion by *C. circinans,* Cotton by *C. gossypii,* Pepper by *C. capsici,* Strawberry by *C. acutaum,* Mango by *C. gloeosporioides,* Papaya by *C. papaya,* Grape*s* by *C. godetiae* and Apple by *C. gleosporioides* (Jeger et al., 1992). In some cases, the yield reduction can be more than 40%, which mainly depends on the crop (Bergstrom and Nicholson, 1999;

Tsror et al., 1999). Anthracnose stalk rot reduces the yield, which can cost around 750 million dollars annually (Frey et al., 2011). Perkins and Hooker (1979) described the yield penalty in Illinois as being up to 17%. Yield Losses are predominantly due to the premature death of the plant before the grain is completely filled. However, some losses may also occur at harvest if the plants are lodged (Figure 1) (Robertson, 2013). This disease affects all parts of the maize plant, and notably, it can be found at any period during the growing season.

Figure 1: Maize field lodged with anthracnose disease (Picture credit to T. Jackson-Ziems, University of Nebraska)

1.2.1 Disease symptoms
The anthracnose disease is commonly associated with leaf blight (ALB), top die-back and stalk rot (ASR).

1.2.1.1 Anthracnose leaf blight
The leaf-blight phase is characterized by spindle- to oval-shaped necrotic areas which may appear to be water-soaked or chlorotic (Figure 2A). The lesions are often found first on the lower leaves and may progress to the upper leaves. Small, black, hair-like fungal structures known as setae often occur in necrotic tissue. The lesions are usually brown with yellow to reddish-brown edges. Heavily infected leaves lead to atrophy and die.

1.2.1.2 Top die-back

Top die-back is defined as the premature death of the cob, although the lower part of the plant remains green (Figure 2B). This symptom appears as early as 1 to 3 weeks after tasseling. Top die-back serves for stalk rot. As the stalk rotting phase progresses, the pitch and vascular system decay, which is reducing the shift of water to the upper leaves. Consequently, the upper leaves tend to dry out and die off.

1.2.1.3 Stalk rot

Stalk rot is observed as browning of the stalk with black and shiny lesions that usually start appearing in the lower part of the stalk (Figure 2C). The stalk rot phase begins soon after tasseling, yet it becomes noticeable only in the middle of the grain-filling period. As the fungus grows, these black lesions combine to form massive black spots or stripes that form on the lower internodes, or on the entire stalk. When the stalk is divided into two halves, a deterioration of the inner stalk is seen with dark discoloration at the nodes (Figure 2D).
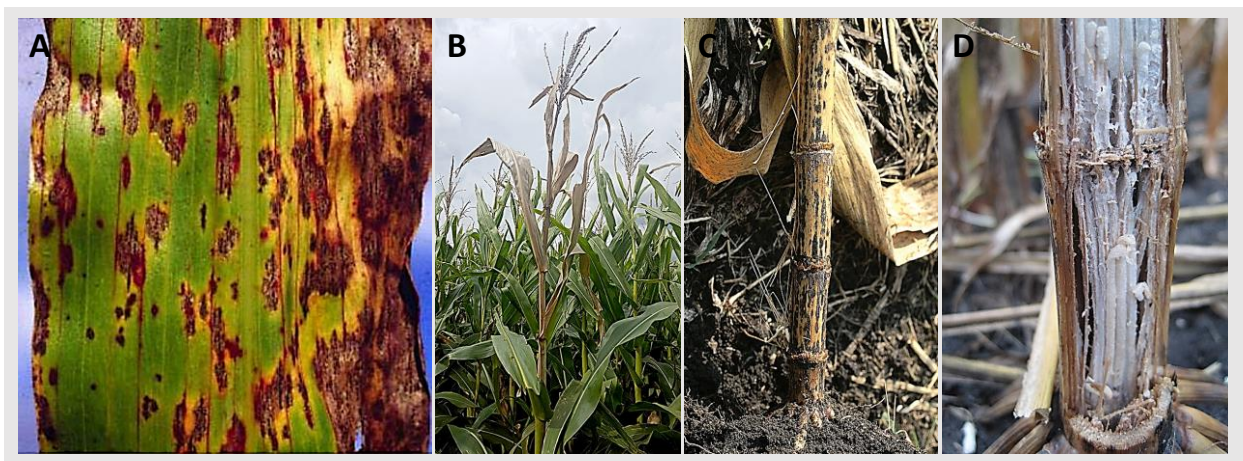
Figure 2: Anthracnose disease symptoms. (A) Leaf blight, (B) Top die-back, (C) Stalk rot, (D) Split stalk of stalk rot phase (top-die back and stalk rot phase picture credit to K. Broderick, the University of Nebraska, leaf blight picture credit to IITA)

1.2.2 Disease cycle

C. graminicola has adapted its lifestyle to live in maize-based agro-ecosystems. It is an aggressive pathogen which lives on maize plants and is a facultative saprophyte on residues of maize. The maize anthracnose life cycle (Figure 3) can be characterized into five temporal phases (Bergstrom and Nicholson, 1999). **Primary inoculum phase:** primary inoculum for leaf blight generally comes from the overwintered maize residues which remain on the surface of the soil. The primary infection of the seedling leaves is caused by spores that are produced in the acervuli. Spores spread from infested debris which is further spreading by splashing and blowing of raindrops. **Seedling blight phase:** During the seedling development stage, the symptoms

3

usually consist of oval-shaped lesions that often give rise to concentrically expanding zones. Plants in the seedling stage grow so quickly that when new leaves emerge from the whorl, they appear resistant and often do not show any disease. Leaf blight of young plants can even lead to seedling death. **Leaf blight phase:** The secondary inoculum for the further development of the disease comes from lesions on the lower leaves. Conidia are spread vertically in the canopy of the plants by splashing rain. Repeated cycles of production and spreading of the secondary inoculum occur during the complete development of the plant. Conidia serve as a secondary inoculum for leaf infections, but can also serve as an inoculum for stalk infections. **Systemic colonization/stalk rot phase:** The stalk rind epidermis appears to be infected in a similar way as the leaf epidermis. Hence, the stalk rind infection may be a prolongation of the leaf blight phase. Conidia formed on leaves may be washed behind the leaf sheath and initiate rind infection. Penetration of the pathogen into the stems of non-senescent plants often occurs through wounds that break through the rind. The most common wounds in maize are those caused by stalk-boring insects, especially by larvae of the European corn borer. *C. graminicola* is an aggressive vascular pathogen in the late vegetative phase, and in the early stages of plant reproductive development. It is a well-suited colonist of xylem, since it promptly uses sucrose as a carbon source and constitutively produces invertase. Small, oval conidia are formed in the xylem vessels. Under favourable conditions, this fungus begins infection by vascular colonization and this leads to top die-back. Late-seasonal basal stalk infections are likely the consequence of root infections (presumably through contact of the roots with infected maize residues). **Saprophytic phase**: *C. graminicola* survives as a saprophyte on the infected maize residues on the soil surface. Fungi surviving in the stalk tissues from overwinter will proceed with a sporulation period during spring (Bergstrom and Nicholson, 1999).
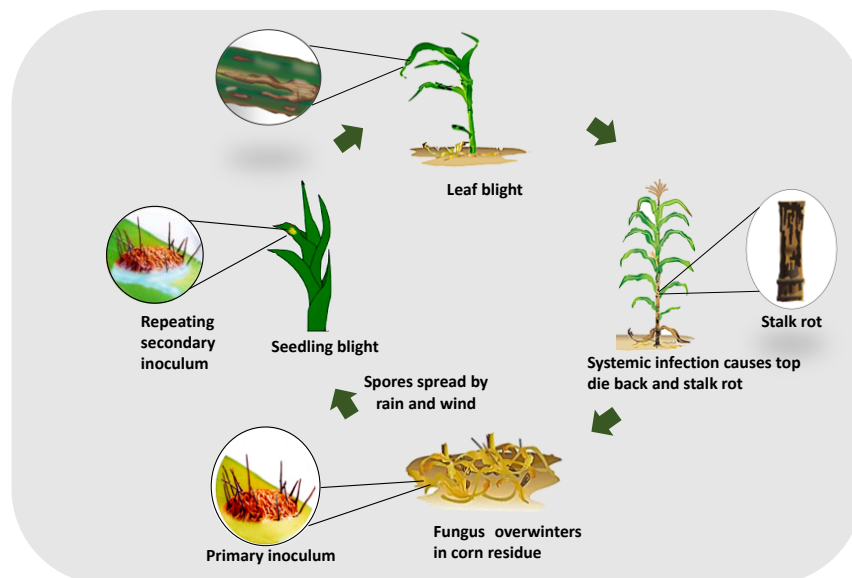
Figure 3: Maize anthracnose disease cycle. (Picture modified from Bergstrom and Nicholson (1999))

1.2.3 Infection and colonization

Anthracnose is a polycyclic disease, which implies that infection can occur several times throughout the season. During the early stages of infection, the fungus establishes a biotrophic relationship with its host, which is crucial for the success of the interaction (Muencha et al., 2008). It takes 6 to 8 hours for spores to germinate. As soon as the conidia germinate, germ tubes are produced. Such tubes secrete materials that act as adhesives binding the fungal germling to the plant surface and prevent it from being moved from the site of infection by wind or water. Initially, melanin is pumped into the appressorium to build high turgor pressure, which helps the fungus to penetrate into the cell wall by a burst directed towards the leaf surface. The resultant structure is called penetration peg which then grows, expands through the cell and deprives nutrients. Further on, the hyphae migrate from the epidermal cells to the mesophyll cells. As a defensive reaction, the plant cells produce papillae to prevent penetration into the cell, but this is typically

Figure 4: *C. graminicola* invasion process (Picture from Bergstrom and Nicholson (1999))

not successful. It is anticipated that *C. graminicola* has a biotrophic phase since the plasma membrane of the epidermal cells are not immediately penetrated after invasion into the epidermal cell wall. By contrast, during necrotrophy, secondary hyphae penetrate through both the cell walls and intercellular space (Bergstrom and Nicholson, 1999). Infection and colonization is depicted in Figure 4.

1.2.4 Approaches for anthracnose disease management and its limitations

Several agronomic strategies are used to control the disease. Tillage generally helps to reduce the amount of disease inoculum, while the data on the role of tillage in reducing the anthracnose stalk rot varies. Cultivation of non-host crops or a crop rotation contributes to the reduction of inoculum (Lipps, 1985). Furthermore, the introduction of resistant varieties is an essential measure to control anthracnose. Few fungicides were characterized as contributing to the control of the leaf blight phase of anthracnose. Foliar fungicides do not act directly on the anthracnose pathogen, but there may be some indirect effects. Application of foliar fungicides at the time of grain filling period limits the incidence of stalk rot (Shriver and Robertson, 2009) and top die-back (Robertson et al., 2010). However, there was no proof of any impact on yield.

1.3 Corn smut

Corn smut disease is caused by the heterobasidiomycetes biotrophic (feeds on living host tissue) fungal pathogen *Ustilago maydis* which additionally infects teosinte (*Zea mexicana*) (Christensen, 1963). In general, smuts are pathogens which mainly infect members of the grass family (Poaceae) and sedges (Cyperaceae). The most economically important hosts beside maize are barley (*U. hordei*), wheat (*U. tritici*), oats (*U. avenae)*, sugarcane (*U. scitaminea*), and forage grasses. Corn smut is clearly distinguished by tumor-like galls that are formed on aerial parts of the plant. Corn smut is considered as a particularly troublesome disease all around the globe. In central Mexico, on the other hand, galls growing on corn cobs are found to be an edible delicacy known as huitlacoche or cuitlacoche (Juarez-Montiel et al., 2011). Infection in the early developmental stages of the plant typically causes death. Severe infection of the mature plant leads to infertility (Kostandi and Geisler, 1989). Christensen (1963) stated that, on average, the yield penalty can be 25% for a single gall. Furthermore, Kostandi and Geisler (1989) reported that big galls located on the cob of corn could reduce yield up to 40-100%. In addition to this, *U. maydis* has been used by researchers as a model organism to study a variety of interesting biological phenomena, such as genetic recombination and repair, plant-pathogen interactions, fungal dimorphism and fungal mating type. It exhibits a fascinating feature of a life cycle that includes both biotrophic and saprophytic stages.

1.3.1 Symptoms

The maize plants that were infected by *U. maydis* display chlorotic lesions, anthocyanin pigment formation and necrosis while the most apparent symptom is tumor-like gall formation (Figure 5A) on the above-ground parts of the plants. The disease symptoms strongly depend on the disease severity. The size of the galls can be less than 1 cm up to more than 30 cm in diameter. Smut galls contain both fungal and host tissues. Young galls are white, firm and coated with a semi-glossy periderm. As galls start to mature, the inner tissue turns into semi-fleshy and streaks of black tissues appear as teliospores begin to form. While the galls are further matured, a mass of powdery teliospores are grown and released once the periderm ruptures (Figure 5B). The size, location, and the number of galls rely on the age of plants at the time of infection.
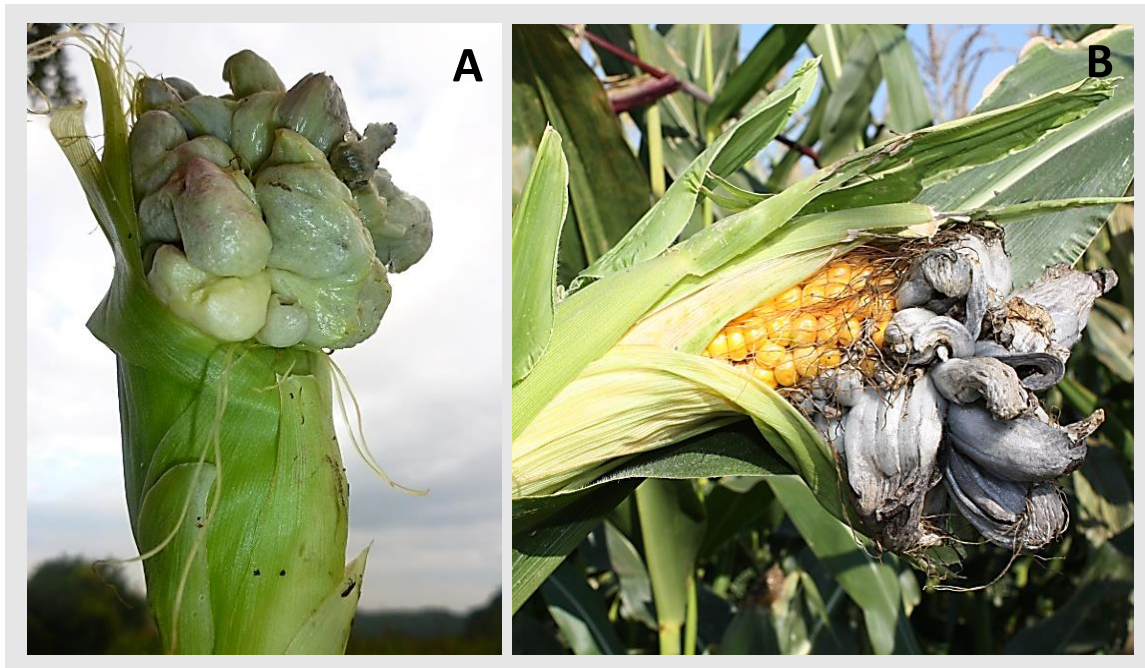
Figure 5: Galls caused by *U. maydis* on field-grown maize plants. (A) gall formation on a cob. (B) matured galls with a mass of powdery teliospores (pictures kindly provided by Armin Djamei)

1.3.2 *U. maydis* life cycle

U. maydis is a facultative biotrophic fungus and its pathogenic character is closely associated with sexual development. The *U. maydis* life cycle starts with haploid, saprophytic sporidia, which reproduce asexually through yeast-like budding. Spores are dispersed by wind or water splash on young plants. They can also be spread by the dung of animals after having consumed infected maize. *U. maydis* has two mating-type loci, the multi-allelic *b* locus, and the bi-allelic *a* locus. Pathogenic development of *U. maydis* is initiated once the fusion of two sporidia of different mating-type loci has taken place (Rowell, 1954; 1955). This fusion is controlled by the bi-allelic *a* locus that encodes a pheromone/pheromone-receptor system, which allows partner recognition and cell fusion (Bolker et al., 1992). Pheromone perception leads to the formation of non-septate conjugation hyphae which grow towards each other directed by the pheromone gradient and fuse at their tips (Snetselaar and Mims, 1992).

The dikaryotic filament shows tip growth, while segments of the distal hyphae are separated from the cytoplasm-filled tip cell by septation (Christensen, 1963; Freitag et al., 2011). The contact with the plant surface plays a crucial role in the early differentiation processes of *U. maydis* (Apoga et al., 2004). Appressoria of *U. maydis* are characterized by swelling of the tip of the hyphae. Compared to many other phytopathogenic fungi (i.e. *C. graminicola*), *U. maydis* appressoria are not melanized (Bell and Wheeler, 1986; Tucker and Talbot, 2001). This implies that the penetration into the plant surface is due to the local secretion of lytic enzymes rather than based on mechanical pressure (Heiler et al., 1993; Kämper et al., 2006). The penetrating

hypha becomes encased by the cytoplasmic membrane of the host cell. The result is a so-called biotrophic interaction zone which facilitates the communication between fungus and the plant, thus providing nutrients to *U. maydis*. By secreting effectors in the apoplastic space, *U. maydis* can suppress the plant's immune responses, which is triggered by molecular pattern associated with the plant, in order to establish a biotrophic interaction (Doehlemann et al., 2008). After the initial penetration, *U. maydis* grows intracellularly in epidermal cells. In the later stages of infection, the hyphae penetrate the deeper cell layers of the mesophyll, where massive proliferation occurs. During the whole cycle of infection, plant tissue remains intact. Initial gall formation can be found approximately 4 days after the infection under greenhouse conditions (Callow, 1975). Karyogamy occurs in the tumor tissue. Hyphae fragments mature into diploid teliospores embedded in a mucilaginous matrix (Banuett and Herskowitz, 1996). After the galls have opened, the spores are released and dispersed by wind, rain, or animals. Under favourable conditions, they germinate to form a probasidium in which meiosis takes place to form haploid cells (Christensen, 1963). The formation of haploid sporidia completes the life cycle of *U. maydis* which is depicted in Figure 6.
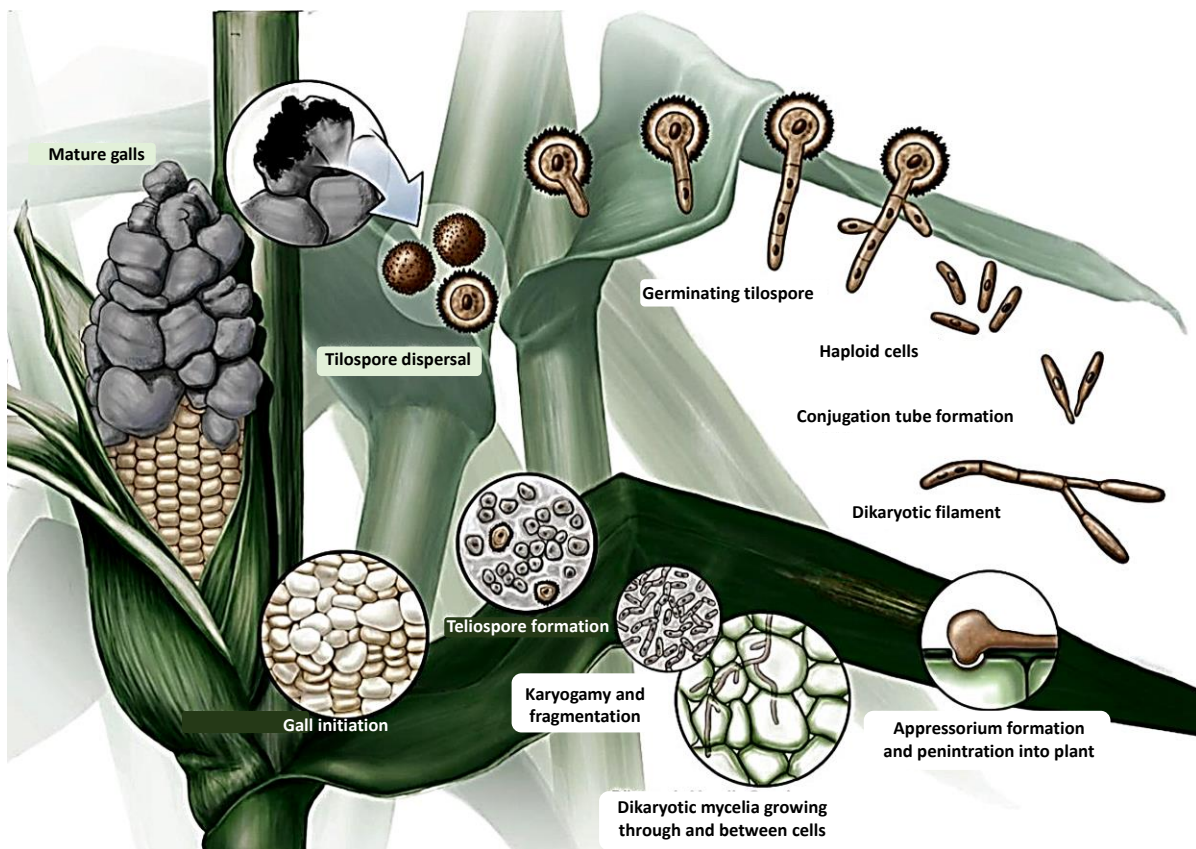
Figure 6: Life cycle of the *U. maydis* (Picture source from the book Molecular Mechanisms and Cytogenetic Diversity by open access publisher Intech Open Saville (2012)

1.3.3 Approaches to control the corn smut disease

Various measures have been recommended to control corn smut, for example crop rotation, seed treatments, and application of foliar fungicides. However, once the galls are formed, the aforementioned methods are ineffective. Regardless of the control procedures referenced above, host resistance is the only practical means of managing corn smut in areas where *U. maydis* is prevalent. Nevertheless, no corn line is immune to infection by *U. maydis*.

1.4 Plant immunity

Plants are constantly exposed to attack by a variety of biological agents such as bacteria, fungi, oomycetes, viruses, and insects. These pathogens and pests can then extract nutrients from the plants that will enable them to establish and grow, which leads to disease and damage to the host plant. In most of the cases, plants can counteract and prevent colonization by pests/pathogens. The outcome of the interplay between plant and pest/pathogen is largely determined by preformed constitutive defence mechanisms in combination with specific defence mechanisms against specific invaders. Plants react to infection by employing a two-branched innate immune system. Its first defense layer perceives and reacts to molecules that are common in many classes of microbes, whereas the second one responds to pathogen-derived virulence factors (effectors) (Jones and Dangl, 2006).

1.4.1 Pattern-triggered immunity (PTI)

The pathogen produces elicitors such as peptides, metabolites, cell wall components, enzymes, and toxins. Pathogen elicitors are recognized by transmembrane pattern recognition receptors (PRRs) which is the first, and the foremost aspect of plant defense leading to an immune response coined pattern (Pathogen-Associated Molecular Patterns (PAMPs))-triggered immunity (Andolfo and Ercolano, 2015). The recognition of PAMPs by plant pattern recognition receptors leads to the activation of characterized downstream signaling events that are regulated by salicylic acid (SA), jasmonic acid (JA) and ethylene (ET), which leads to basal resistance or PAMP-triggered immunity (PTI) (Glazebrook, 2005; Chisholm et al., 2006; Jones and Dangl, 2006).

1.4.2 Effector-triggered immunity (ETI)

During the co-evolution of host and pathogen, plants have developed a further defense layer based on the detection of effector proteins (Chisholm et al., 2006; Jones and Dangl, 2006). When the invading microorganism is able to overcome the basal resistance by suppressing PTI of the plant, a secondary and more efficient resistance is initiated by plants. This secondary resistance is called effector-triggered immunity which occurs mostly within the cell and consists of activation of a specific set of resistance (R) genes (Martin et al., 2003; Nimchuk et al., 2003). R proteins are polymorphic, and the majority of them is represented by NB-LRR proteins (Dangl and Jones, 2001). These proteins recognize a wide variety of pathogen effectors and activate

resistance mechanisms in plants. In case of an incompatible reaction between the pathogen and the host, the recognition of effector molecules by the plant R proteins activate a robust defense response resulting in a hypersensitive response (HR). This is characterized by an apoptotic and localized cell death which controls the spread of the pathogen and leads to plant resistance.

1.4.3 Pattern- and effector-triggered immune response

The immune responses triggered by PRRs and R-gene products are similar (Hammond-Kosack and Parker, 2003; Navarro et al., 2004; Tsuda et al., 2009). Nonetheless, constitutive defense components and related signaling events playing major roles in these two immunity barriers might differ (Navarro et al., 2004; Thilmony et al., 2006; Truman et al., 2006; Zipfel, 2008). Overall, these responses are involved in the generation of reactive oxygen species (ROS), deposition of callose and transcription of numerous defense genes.

1.4.3.1 Production of reactive oxygen species (ROS)

One of the most rapid and strong reaction of plants to pathogen infestation is the accumulation of reactive oxygen species whereby the molecular oxygen can be converted by various reactions into different ROS products, namely superoxide (O_2^-), hydrogen peroxide (H_2O_2), hydroxyl radical (OH.) and singlet oxygen ($^1O_2$) (Jabs et al., 1997; Apel and Hirt, 2004; Torres et al., 2006). The defense reactions related to the generation of ROS include the direct killing of the pathogen, activation of host cell death and cell wall strengthening. ROS production during pathogen attack is initiated by an increased enzymatic activity of plasma membrane-bound NADPH oxidases, cell wall-bound peroxidases and amine oxidases within the apoplast (Grant and Loake, 2000). A biphasic generation of hydrogen peroxide occurs during an incompatible interaction leading to the activation of programmed cell death in order to restrict the pathogen (Bolwell, 1999). Both plants and pathogens have developed efficient scavenging systems to modulate ROS homeostasis, which ultimately determine the occurrence, development and consequences of diseases in the plants (Aguirre et al., 2005; Heller and Tudzynski, 2011).

1.4.3.2 Deposition of callose

During the early stages of pathogen attack, plants can induce the formation of physical barriers known as papillae that mainly consist of callose which is an amorphous high molecular weight β-(1,3)-glucan polymer (Brown et al., 1998; Ellinger et al., 2013). Numerous studies on plant-pathogen interactions have observed callose deposition in the host tissue as a defence response (Bergstrom and Nicholson, 1999; Luna et al., 2011; Seitner et al., 2018). For instance, *Arabidopsis* cotyledons are shown to induce callose formation upon treatment with a bacterial peptide (Luna et al., 2011). Bergstrom and Nicholson (1999) have reported the formation of papillae in maize leaves during infection by *C. graminicola*.

1.4.3.3 Phytohormones and corresponding genes in plant defence

Phytohormones are small molecules that play crucial roles in plant growth development. These mechanisms can be manipulated by pathogen attack. Several studies demonstrated the significant role of phytohormones such as SA, JA and ET in regulating plant defense responses against various pathogens, pests and wounding (del Pozo et al., 2004; Glazebrook, 2005; van Loon et al., 2006; Loake and Grant, 2007). SA is involved in providing systemic acquired resistance (SAR) which is a long-lasting and broad-spectrum induced resistance. It is characterized by an activation of a set of pathogenesis-related (PR) genes that encode proteins with anti-microbial activity (van Loon et al., 2006). Typically, SA plays a crucial role in the activation of defence responses against hemi-biotrophic and biotrophic plant pathogens (van Loon et al., 2006). Studies demonstrated that maize plants can respond to pathogen infection with enhanced accumulation of PR proteins (Nasser et al., 1988; Murillo et al., 1997; Murillo et al., 1999; Majumdar et al., 2017b). In the case of barley, Al daoude et al. (2020) reported activation of the *PR1* and *PR5* genes in resistant plants to fungal infection. On the contrary, JA and ET play vital roles in the defence response against necrotrophic pathogens and herbivorous insects. They act synergistically to activate the expression of defense-relevant genes after pathogen attack (Penninckx et al., 1996; Thomma et al., 2001). Several genes putatively involved in the JA/ ET pathway proved differentially activated during pathogen infection, e.g. *LOXs* (Shivaji et al., 2010; Christensen et al., 2013; Christensen et al., 2014; Nalam et al., 2015), *ALLENE OXIDE SYNTHASE (AOS)* (Shivaji et al., 2010), *ALLENE OXIDE CYCLASE* (*AOC*) (Borrego and Kolomiets, 2016), *12-OXOPHYTODIENOIC ACID* (*OPR*) (Zhang et al., 2005; Shivaji et al., 2010), *P450* (Xu et al., 2015), *CORN CYSTATIN-9* (*CC9*) (Pinter et al., 2019), *ACYL-COA OXIDASE* (*ACX*) (Schilmiller et al., 2007; Xin et al., 2019), HYDROLASE (*HYD*) (Huffaker et al., 2013; Christensen et al., 2015) and *PHENYLALANINE AMMONIA LYASE* (*PAL*) (Diallinas and Kanellis, 1994; Kato et al., 2000; Shoresh et al., 2005). Ethylene response factors (ERF) act as positive regulators of JA and ET signaling. Members of the ERF family were shown to play a significant role in mediating plant defence responses (McGrath et al., 2005). Studies indicated a complex crosstalk between these hormones (Bari and Jones, 2009). Plants regulate the levels of each phytohormone in order to activate an effective defense response against pathogen attacks (Robert-Seilaniantz et al., 2011).

1.5 Microbial manipulation of plant immunity

During co-evolution, plant pathogens have evolved several strategies in order to overcome plant immunity. Research on biotrophic fungal pathogens demonstrated that they vigorously suppress plant defenses. In line with this statement, Doehlemann et al. (2008) reported that *U. maydis* can suppress plant-associated molecular pattern-triggered plant immune responses to establish a biotrophic relation. In the case of *C. graminicola*, plant tissue is killed before being colonized, which probably facililtates the avoidance of plant immunity (Vargas et al., 2012). Furthermore, pathogens secrete effector molecules that can suppress plant immunity pathways

and promote susceptibility factors. Several effector molecules are known to manipulate the plant phytohormone system (Jones and Dangl, 2006; Dangl et al., 2013; Lo Presti et al., 2015; Uhse and Djamei, 2018).

1.5.1 Host susceptibility factors

In addition to suppressing or evading plant immunity, most pathogens require the cooperation of host genes (susceptibility genes) to establish a compatible interaction. Based on these interactions, susceptibility genes are associated with some molecular mechanisms, which is described below (van Schie and Takken, 2014).

1.5.1.1 Basic compatibility susceptibility factors

Once the pathogen comes into the first contact with the host surface or rhizosphere, thus far inactive pathogen genes are activated. The activation of those genes requires recognition of host cues that trigger pathogen development. For instance, plant cutins and epicuticular waxes represent such signals for germination and formation of appressoria. Accordingly, plant mutants that exhibit changes in the wax composition of the leaves are less susceptible to fungal invasion (Hansjakob et al., 2012; Uppalapati et al., 2012; Wang et al., 2012; Weidenbach et al., 2014; Weis et al., 2014; Li et al., 2018).

1.5.1.2 Support of pathogen demands

The cellular processes in the host support specific requirements of pathogens that feed on living tissue. The components of these processes can be susceptibility (S) factors. Several obligate biotrophs may have lost specific biosynthetic pathways while relying on the supply of host metabolites for primary or secondary metabolite biosynthesis. For instance, SWEET proteins are sugar transporters that transport sucrose out of plant cells for redistribution of sugars. *SWEET* genes are considered as S factors, since they can be overexpressed during interactions and are used to provide nutrients to pathogens (Chandran, 2015).

1.5.1.3 Control of plant defense responses

Several S genes encode negative regulators of plant defense responses. Accordingly, loss-of-function-mutants are compromised in the respective defense responses. Notable examples are *LESION-SIMULATING DISEASE 1* (*LSD1*) or the constitutive expression of *PR* genes (*CPR*) such as *CPR1* or *CPR5*. These mutants are generally less susceptible to biotrophic pathogens. In some cases, such mutants exhibit resistance to necrotrophic pathogens or broad-spectrum resistance (Lorrain et al., 2003).

1.6 Lipoxygenases

There is compelling evidence that plant oxylipins play a role as host susceptibility factors (Burow et al., 1997; Wilson et al., 2001; Gao et al., 2007; Nalam et al., 2015). In general, lipoxygenases

are widely distributed in plants (Feussner and Wasternack, 2002). They belong to a family of (non-heme) iron-containing enzymes. Most of which catalyze the dioxygenation of polyunsaturated fatty acids into oxidized fatty acids called Oxylipins. The plant lipoxygenases (LOXs) catalyze the oxygenation of the polyunsaturated fatty acids linoleic acid (C18:2) and linolenic acid (C18:3) which are common substrates for LOXs (Feussner and Wasternack, 2002). Plant lipoxygenases are classified into two types according to the position in which they oxygenate linoleic acid, namely, 9-LIPOXYGENASE (9-LOX) and 13-LIPOXYGENASE (13-LOX) which incorporate molecular oxygen at carbon positions 9- and 13- of the fatty acids' hydrocarbon backbone. This oxygenation process leads to two corresponding groups of compounds, 9-hydroperoxy and 13-hydroperoxy derivatives of linoleic acid (Liavonchanka and Feussner, 2006).

The 9-LOX enzymes catalyze the conversion of 18:2 linoleic acid (LA) and 18:3 linolenic acid, respectively, to 9-hydroperoxide octadecadi(tri)enoic acids (9-HPOD/T) Further, ALLENE OXIDE SYNTHASE (AOS) converts 9-HPOD/T to 9,10-epoxy octadecadienoic acid (9,10-EOD), which is followed by the formation of either 10-OPDA (oxo-phytodienoic acid) or ketols (Figure 7) (Upadhyay et al., 2019).

The 13-LOX pathway catalyzes the conversion of 18:2 linoleic acid (LA) and 18:3 linolenic acid into 13-hydroperoxide octadecatrienoic acid (13-HPOT), which is supplementarily metabolized to plant signaling compounds, namely jasmonates and green leaf volatiles (GLVs) (Figure 7). Numerous downstream pathway branches utilize the products of 13-LOXs; however, currently, the best-characterized enzymes are members of the CYP74 family such as AOS, HPL, DES, and ALLENE OXIDE CYCLASE (AOC) (Brash, 2009), and these enzymes have a close relationship with each other (Wasternack and Feussner, 2018).

Some LOXs possess dual substrate specificity by catalyzing 9- as well as 13(S)-hydroperoxy-9Z, 11E-octadecadienoic acid (13-HPOD)s. For instance, Kim et al. (2003) demonstrated that maize *LOX1* which predominantly is a 9-LOX producing 13-hydroperoxylinolenic acid and 9-hydroperoxylinolenic acid in a 6-to-4 ratio. In the case of pea *LOX3*, a mixture of 9- and 13-hydroperoxides from linoleic acid is formed (Hughes et al., 1998; Feussner and Wasternack, 2002; Santino et al., 2003; Liavonchanka and Feussner, 2006).
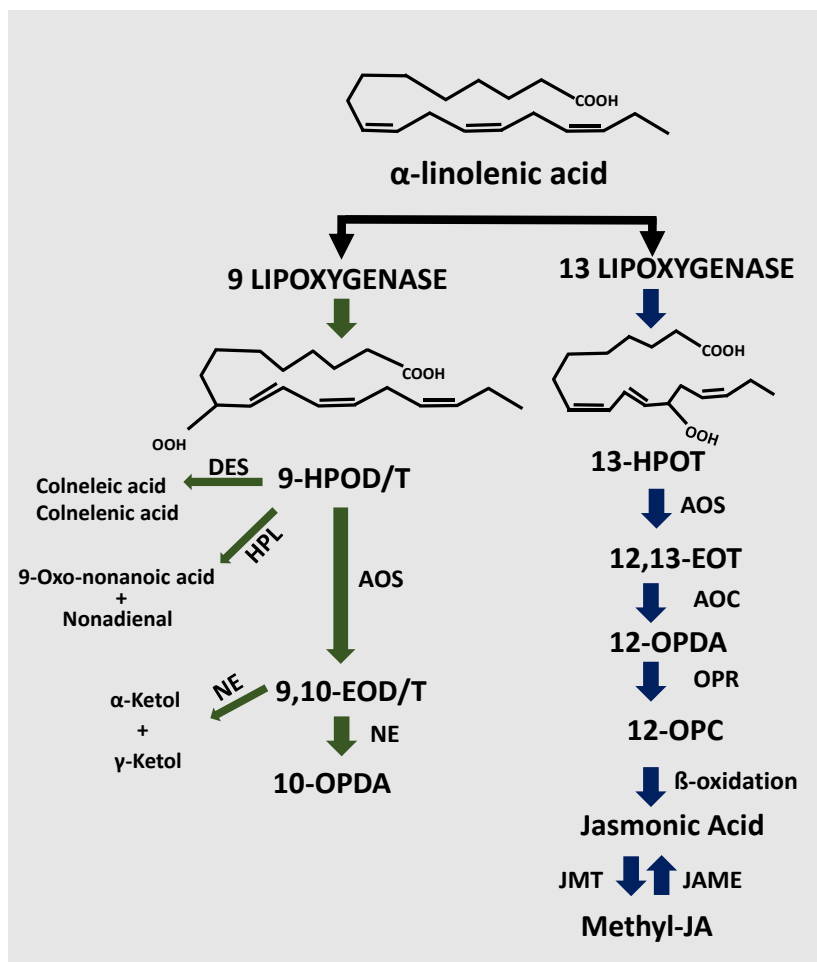
Figure 7: Representation of 9-LOX and 13-LOX pathways in plants. Abbreviations: HPOD: 9 or 13-hydroperoxide linolenic acid; 13(S) or 9(S)-hydroperoxylinolenic acid; OPDA: 12-oxo-phytodienoic acid; LOX: Lipoxygenase; AOS: Allene oxide synthase; AOC: Allene oxide cyclase; OPR: Oxo-phytodienoic acid reductase. JMT: Jasmonic acid carboxyl methyltransferase; JAME: methyl Jasmonate esterase; HPL: Hydroperoxide lyase; DES: Divinyl ether synthase; NE: non-enzymatic (Picture modified from Porta and Rocha-Sosa (2002))

1.6.1 Physiological functions of plant lipoxygenases

LOXs have been identified in various cellular processes involving signaling molecules with diverse functions (Wasternack and Feussner, 2018). For instance, LOXs function as vegetative storage proteins in the seeds. They perform a crucial role in seed growth and maturation (Siedow, 1991). During the early stages of seedling growth, maize and almond *9-LOX* expressions were particularly high (Jensen et al., 1997; Santino et al., 2005). Studies indicated that LOXs have a role in abiotic stress. In agreement with this, the pepper 9-lipoxygenase gene *LOX1* plays a crucial role in drought, high salinity and osmotic stress (Lim et al., 2015). *LOX*s expression is also modulated in association with the occurrence of signaling molecules nitric oxide (NO) and plant hormones, abscisic acid (ABA), SA and JA. Maize *9-LOXs*, *LOX4* and *LOX5* were induced by JA and

SA. Similarly, *13-LOXs*, *LOX10* and *LOX11* were preferentially expressed in response to wounding, JA, SA, ABA and cold stress. At the same time, *LOX11* was induced only by ABA (Nemchenko et al., 2006; Park et al., 2010; Shu et al., 2017). Phytohormones can also suppress the activity of *LOXs*. For instance, maize *LOX6* was shown to be induced by JA, but repressed by SA, ET and ABA (Gao et al., 2008b). Studies further suggested that LOX is a major regulator of lipid peroxidation, and it likely contributes to the membrane damage at the time of senescence. A comparative proteome analysis in maize showed that *LOX* levels were elevated during initial leaf senescence (Wu et al., 2018). A *lox3* knockout mutant exhibited advanced senescence and reduction in root length and plant height (Gao et al., 2008a).

1.6.2 Role(s) of lipoxygenases in pathogen interaction

LOX pathways play an essential role in the defensive response to pathogen attacks (Weber et al., 1999; Kolomiets et al., 2000; Gobel et al., 2001; Gobel et al., 2002; Gobel et al., 2003; Hamberg et al., 2003). The phytohormone JA derived from lipoxygenase is particularly well-known for its role in wound reactions, and the plant defence against insect and pathogens (Creelman and Mulpuri, 2002). Transcripts of maize *LOX10*, *LOX8*, *LOX5* were induced to herbivory and wounding (Nemchenko et al., 2006; Christensen et al., 2013) (Park et al., 2010). In the case of biting-chewing herbivores, it has been suggested that the LOX signaling pathway plays a significant role in plant defense via important oxylipins, namely 10-oxo-11-phytoenoic acid (10-OPEA) through the action of 9-LOXs, 13-LOXs and 12-OPDA (Bruinsma et al., 2010; Viswanath et al., 2020). Following herbivory, LOXs leads to an anti-herbivorous oxidative shift, which causes both direct and indirect oxidative damage to the herbivore (Kaur et al., 2014). Maize *LOX10* was induced during the compatible interaction with *C. carbonum* (Nemchenko et al., 2006; Gao et al., 2008b). The function of *9-LOX* genes was studied in *Arabidopsis* against *Pseudomonas syringae*, by which it was found that the 9- hydroxyoctadeca- trienoic acid (9-HOT)-induced changes in the cell wall reduce pathogen infection (Vellosillo et al., 2013). In potato, 9-LOX-oxylipins are involved in the early stage of the defence process against *P. infestans* (Kolomiets et al., 2000). Hwang and Hwang (2010) reported that upon pathogen attack, the *Capsicum 9-LOX* gene *LOX1* is upregulated in the leaves. Activity levels of *CaLOX1* were faster in non-silenced pepper leaves than those of *CaLOX1*-silenced pepper leaves when infected with *Xanthomonas campestris* or *C. cocci*. The ectopic expression of *CaLOX1* in *Arabidopsis* caused increased resistance to *P. syringae*, *Hyaloperonospora arabidopsis* and *Alternaria brassicicola*. Rice *LOX3* transcripts were increased in leaves after infection with the blast fungus *M. grisea* (Ohta et al., 1991).

Hypersensitive responses (HR) rapidly kill the plant cells localized around sites of infection, which would limit the further spread of pathogens and damage to the plant cells. Therefore, LOX products, mainly of 9-LOXs, play an essential role in this process. In tobacco leaves, HR was examined via the production of oxylipin-reactive electrophilic species (RES) adducts to GLUTATHIONE (GSH) (Davoine et al., 2006). In *Arabidopsis*, *LOX1* was associated with anti-

microbial activity against *P. syringae pv.* tomato (Pst) infection. Furthermore, pretreatment of *lox1* mutant plants with 9-LOX produced 9-KOT, which protected the plant tissue from bacterial infection (Vicente et al., 2012).

The maize genome encodes thirteen LOX genes. They were classified into two categories, that is, 9-type and 13-type *LOX*s based on the respective enzyme activity. *LOX1, LOX2, LOX3, LOX4* and *LOX5* are classified as 9-type, whereas *LOX7, LOX8, LOX9, LOX10, LOX11* and *LOX13* fall into the 13-type category. *LOX12* and *LOX6* are independent of this classification (Nemchenko et al., 2006; Gao et al., 2008b; Park et al., 2010; Borrego and Kolomiets, 2016).

Maize 10-OPEA together with 12- and 14-carbon cyclopente(a)nones, which are collectively referred to as death acids, play important roles in the provision of JA against the fungal pathogen *C. heterostrophus* infection (Christensen et al., 2015). The maize *9-LOX* genes *LOX4* and *LOX5* (segmentally duplicated) were shown to be induced by the fungal pathogens *C. carbonum* and *F. verticillioides*, which was associated with a unique resistance mechanism (Park et al., 2010). Similarly, feeding of *Spodoptera exigua* larvae induced the expression of maize *9-LOXs* to a greater extent than *13-LOXs*. *LOX3* expression is induced upon *Fusarium verticillioides* and *Aspergillus flavus* inoculation (Woldemariam et al., 2018). A *9-LOX* mutant, *lox3-4* of maize, exhibited fewer root and mesocotyl necrosis caused by *Exserohilum pedicellatum* compared with the wild-type *LOX3* (Isakeit et al., 2007).

1.7 Strategies to control the plant diseases

Plant protection is predominantly based on two main aspects, chemical plant protection and plant breeding. Fungicides are plant protection agents employed in agriculture to control or inhibit fungal growth (Gullino et al., 2000). However, some fungicides that were mostly introduced as solo-formulations were broken after various periods of application (Deising et al., 2008). Besides this, the widespread use of these products to control fungal disease in plants led to the emergence of new strains of pathogens that are resistant to commercial products (Garcia et al., 2003). For instance, single mutations confer fungicide insensitivity. In the case of benomyl and carbendazim, fungicides became ineffective due to single mutations in tubulin. Similarly, succinate dehydrogenase mutants are no longer susceptible to boscalid (Malandrakis et al., 2012; Chatzidimopoulos et al., 2014). In addition to mutation-based fungicide resistance, phytopathogenic fungi can acquire resistance to fungicides by activating efflux transporters extruding drugs and maintaining intracellular fungicide concentrations below a critical threshold (Reimann and Deising, 2005; Kretschmer et al., 2009). Furthermore, the toxicity of fungicides is not necessarily limited to the target organism, which has also been reported in mammals (Belpoggi et al., 2002), including humans (Mendes et al., 2005). The large-scale utilization of fungicides for protection against plant fungal diseases produces long-lasting residues in food and the environment (Petit et al., 2008).

On the other hand, breeding of resistant varieties as been considered as being crucial for the development of sustainable agriculture. However, breeding for resistant varieties is not a

universally viable approach. In many crops, the ability to discover new R genes is limited by the available gene pools. It is important to note that new disease-resistant varieties take long time to produce. Unfortunately, pathogen are capable of breaking down specific resistances based upon (R) genes within a few years. For instance, the R-genes *Mildew resistance locus a* (*Mla*)*12* in cv. Sultan, *Mla7* and *Mixed lineage kinases* (*Mlk)1* in cv. Wing, Ml(Ab) and *Mla7* in cv. Triumph, Mlka9 and *Mlk1* in cv. Kym, and *Mla13* in cv. Pipkin integrated into barley, conferring resistance to the powdery mildew fungus *Blumeria graminis* f. sp. hordei, showed signs of decay after three to four years only.

1.8 Approaches pursued in this study

In the present investigation, two approaches were used to control the maize anthracnose disease. The first approach is host-induced gene silencing, by which plant-made small RNAs down-regulate fungal gene-specific transcripts that are indispensable for pathogenicity and fungal growth.

The second strategy is mutational breeding for disease resistance. This method aims to knockout the maize 9-lipoxygenase *LOX3* which is a susceptibility factor for *C. graminicola* infections (Gao et al., 2007) by using Cas endonuclease technology. Furthermore, transcriptional time course analyses from Doehlemann et al. (2008) demonstrated that *LOX3* transcripts are increased upon *U. maydis* infection, suggesting that knocking out *LOX3* would likely result in improved resistance of maize.

1.8.1 Host-induced gene silencing (HIGS)

HIGS is an RNA-interference (RNAi)-based process. RNAi itself is an essential gene regulation process being conserved across most eukaryotes (Fire, 2007). It is initiated by DICER that is an RNase III enzyme cleaving dsRNA into small interfering RNAs (siRNAs) of 20-25 nucleotides in length (Papp et al., 2003; Borges and Martienssen, 2015). These siRNAs are each comprised of an anti-sense and a sense strand. The anti-sense strand is complementary to the target mRNA. The sense strand, which is identical to the target mRNA, has no function and will be degraded in the next steps. The anti-sense strand is loaded onto ARGONAUTE (AGO) proteins, together with other proteins, to form an active RNA-induced silencing complex (RISC). The anti-sense strand can then bind to the target mRNA by sequence complementarity. In case of sufficient sequence identity, this results in degradation of the target mRNA so that it cannot be implemented via translation (Figure 8) (Pratt and MacRae, 2009; Borges and Martienssen, 2015; Majumdar et al., 2017a). RNAi is a crucial pathway to study functional genomics in many different organisms such as humans, animals, fungi, worms and plants (Harborth et al., 2001; Li et al., 2010; Zhu et al., 2017a).
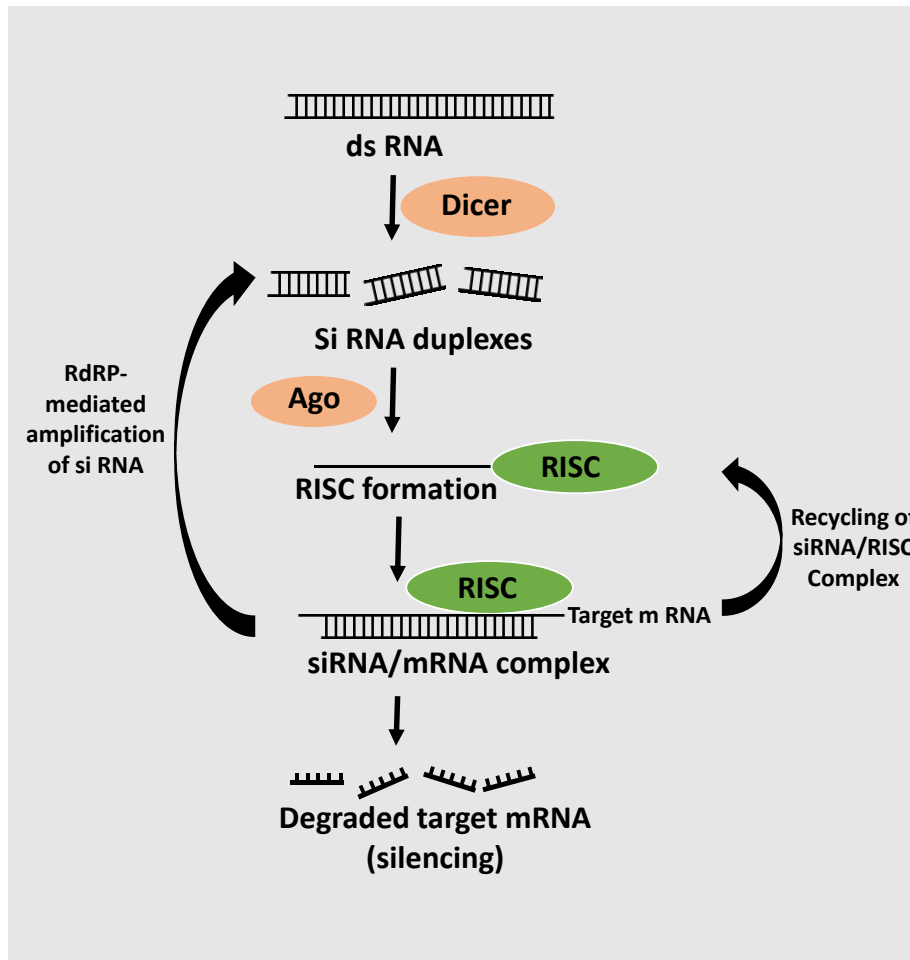
Figure 8: Schematic of RNAi-mediated gene silencing in eukaryotes. Double-stranded RNAs generate small siRNA duplexes by the action of DICER. The guide RNA strand binds with Argonaute (Ago) and other proteins to form an RNA-induced silencing complex (RISC). The siRNA/RISC complex then binds the complementary sequence of the target mRNA resulting in the degradation of the target transcript or mRNA-RISC complex-mediated inhibition of translation. The components of siRNA/mRNA complex can be recycled to the RISC complex or generate siRNA duplexes by the action of RNA-dependent RNA-polymerase (RdRP) (picture modified from Majumdar et al. (2017a)).

In the context of host-induced gene silencing, transgene-derived dsRNA is processed into small interfering RNA by DICER activity. siRNAs are taken up by the interacting pathogen, and interfer with the targeted transcripts, which leads to their cleavage and thus entails the reduction of fungal growth. The transfer mechanism for siRNAs from plant to fungus remains elusive. However, recent literature indicated that siRNAs can be transferred via extracellular vesicles called exosomes (Cai et al., 2018a; Cai et al., 2019; Koch et al., 2020). Numerous studies indicated that RNAi technology could be used in plant protection strategies (Nunes and Dean, 2012; Vinay et al., 2016). In agreement with this, Nowara et al. (2010) first time demonstrated

HIGS-based protection against pathogenic fungus *B. graminis.* Furthermore, this method has proved to be successful in silencing the transcripts of numerous pathogenic fungi such as *B. graminis* (Pliego et al., 2013), *Puccinia striiformis f. sp. tritici* (Yin et al., 2011; Zhang et al., 2012), *P. triticina* (Panwar et al., 2013), *F. culmorum* (Chen et al., 2016), *F. graminearum* (Koch et al., 2013; Cheng et al., 2015), *Bremia lactucae* (Govindarajulu et al., 2015), *Botrytis cinerea* (Wang et al., 2016b) and *F. oxysporum f. sp. Cubense* (Ghag et al., 2014). In addition to fungal pathogens, RNAi has been utilized to develop virus-resistant plants by expressing virus-specific anti-sense transgenes (Frizzi and Huang, 2010). In recent times, a new RNAi-based plant protection has emerged called spray-induced gene silencing (SIGS). This approach relies on spraying of artificially synthesized double-stranded RNAs (dsRNAs) to control pathogens. Few studies were successful in silencing the pathogen genes by using SIGS. (Safarova et al., 2014; Koch et al., 2016). However, in-vitro production of dsRNAs is expensive and sprayed dsRNAs are unstable, and therefore the practical implementation of SIGS to control pathogens is has not been achieved yet.

The major advantage of HIGS is that it operates at the RNA level, thereby the plant protection could be achieved without requirement of any proteinaceous gene product that may cause undesirable, hardly predictable side effects. HIGS was shown to be effective in plants that are interacting with fungi, nematodes and insects (Yadav et al., 2006; Baum et al., 2007; Chen et al., 2010; Nowara et al., 2010; Pitino et al., 2011; Zhang et al., 2015; Chen et al., 2016). Fungicide-resistant pathovars can still be addressed by HIGS, since resistance to fungicides are usually based on small mutations in the fungus target gene sequence. These mutations would not significantly affect the complementarity of the interfering RNAs, which cover a larger part of the target mRNA.

Candidate gene selection plays a vital role for the success of HIGS approaches. Particularly useful genes include those that are indispensable for fungal growth and pathogenicity. Previous studies by plant reproductive biology (PRB) group and of others have shown that for some reason, only a few of the pre-selected candidate genes have been proved effective in HIGS approaches (Baum et al., 2007). One problem was that the level of resistance achieved through HIGS was often insufficient for practical implementation. In the present investigation, fungicide target genes were used for HIGS approaches. Fungicide targets had been comprehensively pre-evaluated as being indispensable for pathogenicity. In particular, *β-Tubulin* and *Succinate dehydrogenase* are being considered as potential HIGS targets in the present study.

1.8.1.1 β-Tubulin

Fungal β-Tubulins are the molecular targets for benzimidazole fungicides that are effective in controlling many plant diseases caused by the fungus (Zhou et al., 2016). Benzimidazole fungicides are a family of fungicides, which include Fuberidazole, Thiabendazole, Thiophanate-methyl, Carbendazim and Benomyl (Hollomon et al., 1998; Ma and Michailides, 2005; Zou et al., 2006). The above-mentioned fungicides bind to β-Tubulins and inhibit microtubule assembly.

Typically, many eukaryotes have α- and β-Tubulins that are encoded by multigene families and are usually assembled into head-to-tail heterodimers to form the basic microtubule building block (Raff, 1984; Cleveland, 1987) (Figure 9). Microtubules play a crucial role in a variety of essential cellular processes. They are involved in the maintenance of cell structure, cell division and intracellular transport (Nogales, 2001; Garnham and Roll-Mecak, 2012; Janke and Bulinski, 2012; Meunier and Vernos, 2012).
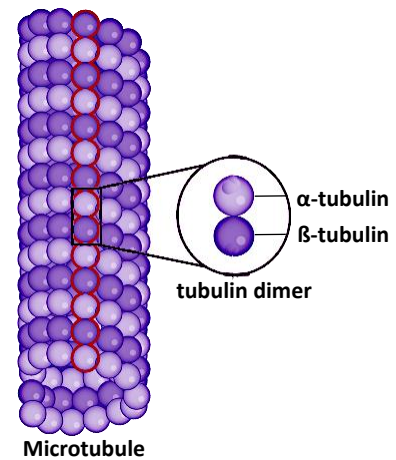
Figure 9: Microtubules are formed from dimer subunits of alpha (α)- and beta (β)-Tubulin that arrange themselves into a hollow tube (picture modified from Muroyama and Lechler (2017)).

1.8.1.2 Succinate dehydrogenase (SDH)

Succinate dehydrogenase (SDH) proved to be a promising target for fungicide discovery. SDH inhibitors (SDHIs) have demonstrated broad-spectrum activity against various fungal species (Xiong et al., 2015). In recent years, several new succinate dehydrogenase (SDH)-inhibiting fungicides were launched. They are collectively referred to as SDHIs. Fungicide resistance action committee (FRAC) currently lists 17 SDHI compounds comprising Thifluzamide, Sedaxane, Penthioprbpyrad, Penflufen, Oxycarboxin, Mepronil, Isopyrazam, Furametpyr, Fluxapyroxad, Flutolanil, Fluopyram, Fenfuram, Carboxin, Boscalid, Bixafen, Benzovindiflupyr and Benodanil (Sierotzki and Scalliet, 2013). Above-mentioned commercially available SDHI fungicides typically bind to the ubiquinone-binding site of the SDH enzyme. The primary biochemical mode of action is the blockage of the tricarboxylic acid (TCA) cycle at the level of succinic acid oxidation to fumaric acid, which results in respiratory inhibition.

Succinic acid dehydrogenase is the only enzyme involved in both TCA cycle and electron transport chain which oxidize succinate to fumarate with the reduction of ubiquinone to ubiquinol. Eukaryotic succinate dehydrogenase is composed of the four subunits SDH 1-4 (also referred to as SDH A-D). The flavoprotein SDH-1 covalently binds flavin adenine dinucleotide (FAD) cofactor to the succinate-binding site. SDH-2 contains iron-sulfur clusters. The catalytic domains of SDH1 and SDH2 are present at the matrix side, while SDH-3 and SDH-4 are the

hydrophobic membrane-anchoring subunits that enable the transfer of electrons from succinate in the mitochondrial matrix to ubiquinone in the inner membrane (Dibrov et al., 1998; Cecchini, 2003; Yankovskaya et al., 2003; Sun et al., 2005) (Figure 10).
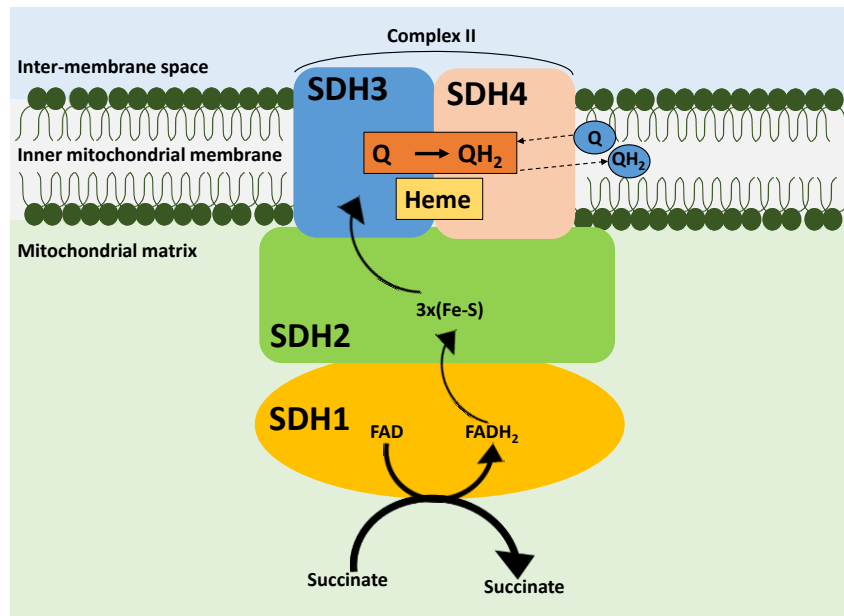
Figure 10: The structure of succinate dehydrogenase (SDH). SDH is composed of the four subunits 1, 2, 3, and 4. Succinate is oxidized to fumarate in the TCA cycle, while the electrons given up are provided for the oxidative phosphorylation of subunits 1, 2, 3, and 4 to eventually form complex III. (Picture modified from Moosavi et al. (2020))

1.9 Site-directed mutagenesis

Site-directed mutagenesis is a biotechnological approach that is used to alter (nucleotide insertion, deletion or replacement) the DNA sequence at a predefined location of the host's genome. Site-directed mutagenesis is an efficient, flexible and reliable method to rapidly produce new plant varieties with improved gene variants and traits, to cope with the serious challenges agricultural production is facing. Furthermore, these techniques will enable the possibility to study the gene function and its regulation, which creates a big impact on basic science (Gurushidze et al., 2017). The main tools for site-directed mutagenesis that have been used in the last three decades are based on engineered nucleases. Those are meganucleases, zinc-finger nucleases (ZFNs), transcription activator-like effector nucleases (TALENs), and clustered, regularly interspaced, short palindromic repeats (CRISPR)-associated (Cas) endonucleases (Koeppel et al., 2019) (Fig 11). The above-mentioned endonucleases can be customized to cleave a specific DNA sequence motif in live cells that is then processed by the cellular DNA repair machinery.

1.9.1 Cellular repair mechanisms for DNA double-strand breaks

The mechanisms of cellular DNA repair are either non-homologous end-joining (NHEJ) or homology-directed repair (HDR).

1.9.1.1 Non-homologous end-joining (NHEJ)

Studies on DNA repair mechanisms have shown that NHEJ is preferably used in DSBs repair mechanism in somatic plant cells (Waterworth et al., 2011). In the context of NHEJ, the two ends of broken double-stranded DNA are religated, which may accidentally result in nucleotide insertions or deletions (Lieber, 1999) (Fig 11).

1.9.1.2 Homology-directed repair

Homology-directed repair (HDR) is the dominant DSBs repair mechanism in yeast and bacteria. It plays a minor role in somatic plant cells. HDR mainly occurs during the S and G2 phases of the cell cycle by using homologous sequences, that is, from the sister chromatid that acts as a template for repair. The two best-known mechanisms of HDR in somatic cells are single-strand annealing (SSA) and synthesis-dependent strand annealing (SDSA) (Puchta and Fauser, 2014). In both mechanisms, the double-stranded DNA ends are first 3'-resected, which leads to 5'-overhangs. In the SSA mechanism, these strands then hybridize with complementary regions, digesting non-homologous overhangs and filling gaps by repair synthesis (Siebert and Puchta, 2002). The SSA mechanism only works when DSBs involve two homologous sequences and leads to loss of sequence information (Puchta and Fauser, 2014). In comparison, the repair of DSBs by the SDSA does not result in the loss of sequences, but there may be changes in the information content owing to recombination. In this mechanism, one of the generated 3'-ends forms a D-loop structure with the homologous, double-stranded repair template. After elongation, this strand is released and hybridizes with the 3'-homologous strand to eventually fill the break (Puchta and Fauser, 2014). In the context of genome editing experiments, HDR is stimulated by homologous donor templates that are delivered in the form of single-stranded oligodeoxynucleotides (ssODNs) or double-stranded DNA (dsDNA) donors. The HDR of these DSBs enables precise editing of the genome by introducing defined genomic changes, for instance, sequence insertions, deletions and defined base substitutions.

On the other hand, micro-homology-mediated end-joining (MMEJ), which involves the alignment of micro-homologous sequences that are internal to the broken ends before joining (Sfeir and Symington, 2015). MMEJ could result in larger deletion, consequently in the loss of comparatively a large amount of genetic information. MMEJ based genome engineering provides the possibility to predict the outcome to some extent (Bae et al., 2014).
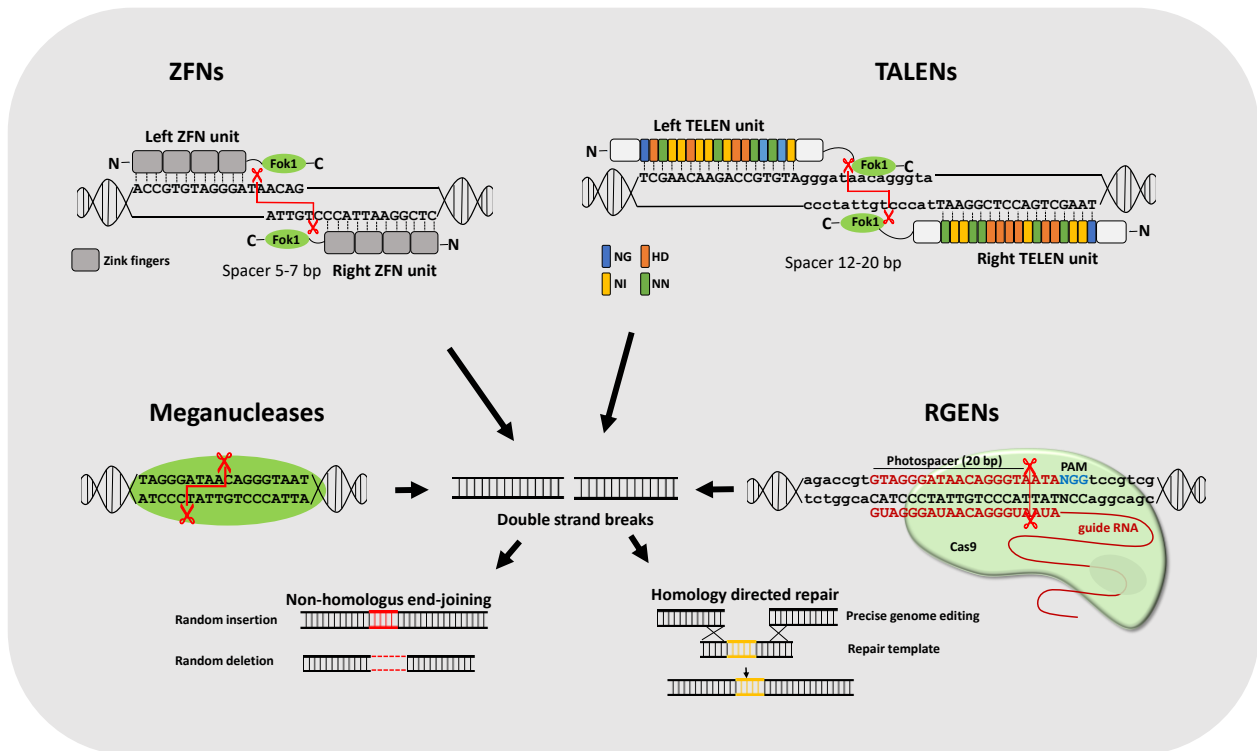
Figure 11: Four platforms of target sequence-specific endonucleases and possible alterations by cellular DNA double-strand break repair mechanisms in plant genomes. The DNA-binding domains of meganucleases, zinc finger nucleases (ZFNs) and transcription activator-like effector nucleases (TALENs) are proteinaceous, while the RNA-guided endonucleases (RGENs) bind to the target sequence by complementary nucleotide pairing. The target sequence-specific double-strand breaks generated by the endonucleases are subsequently repaired by the cells' own repair machinery. Non-homologous end-joining may lead to error prone repair, resulting in random insertions or deletions. In contrast, homology-dependent repair in combination with a repair template can be used to integrate, remove, correct or exchange genes at predefined sites in the genome. RVDs, repeat variable diresidues; PAM, protospacer-associated motif. Picture modified from (Hiekel et al., 2015).

1.9.2 Meganucleases

One of the earliest attempts of genome engineering was based on meganucleases. These are naturally occurring endonucleases capable of recognizing long stretches of nucleotides (12 to 40) and of producing double-strand breaks (DBS) (Silva et al., 2011). The most commonly used meganuclease is the I-SceI from *Saccharomyces cerevisiae* (Plessis et al., 1992; Pauwels et al., 2014). Meganucleases have mainly been used to study DNA repair mechanisms (Daboussi et al., 2015). For instance, meganuclease I-SceI-induced DSBs in tobacco protoplast has resulted in a significantly increased frequency integration of co-transformed construct by HDR (Puchta et al., 1996). A similar approach was demonstrated with the enzyme I-CeuI from *Chlamydomonas eugametos*, with comparable results (Chilton and Que, 2003). Further modification of these

endonucleases to other target sequences is very complex, expensive, and limits routine genomic engineering (Prieto et al., 2007).

1.9.3 Zinc finger nucleases

Zinc finger nucleases (ZFNs) are a class of artificial restriction enzymes. ZFNs were developed by the fusion of zinc finger-based DNA binding domains with the cleavage domain of the FokI endonuclease (Kim et al., 1996). Each zinc-finger particularly interacts with three base pairs (bp) of the genomic target sequence and multiple zinc-fingers can be assembled consecutively to recognize and bind to a total of 9 to 12 bp of DNA (Voytas, 2013). ZFNs should always be used in pairs, since the FokI endonuclease domain is only catalytically activated when it is present as a dimer (Kim et al., 1996). The target motif on the DNA are selected in such a way, that the two zinc finger nuclease monomers bind to the target DNA in anti-parallel manner, with an appropriate distance from each other. Subsequently, DNA double-strand breaks (DSB) are created in the space between the two binding sites (Smith et al., 1999; Doyon et al., 2008). ZFNs were expressed in *Arabidopsis* plants, which induced DSBs that were repaired by NHEJ and which resulted in indels (Lloyd et al., 2005). Wright et al. (2005) demonstrated an increased gene targeting efficiency in tobacco protoplasts by using ZFNs. Further examples followed for *Arabidopsis* (Tovkach et al., 2009; Osakabe et al., 2010; Zhang et al., 2010; de Pater et al., 2013), tobacco (Maeder et al., 2008; Cai et al., 2009; Townsend et al., 2009; Marton et al., 2010), maize (Shukla et al., 2009) and petunia (Marton et al., 2010), which showed either target sequence-specific mutations after ZFN-induced DSBs by NHEJ or targeted DNA integration via HDR.

Despite the advantages of ZFN-based genome editing, there are several potential drawbacks. The use of ZFNs is often associated with toxic effects which can be explained by off-target DSBs that are hardly avoidable (Szczepek et al., 2007). Furthermore, the binding specificity of zinc fingers can be unpredictably affected by other zinc fingers that are part of the same synthetic binding domain.

1.9.4 Transcription activator-like effector nucleases

Transcription activator-like effector nucleases (TALENs) are similar to ZFNs, as they are chimeric proteins formed by the fusion of a modular DNA-binding domain with the FokI endonuclease cleavage domain. However, in contrast to ZFNs, their customizable DNA binding domains are derived from transcription activator-like effectors of plant pathogenic bacteria of the genus *Xanthomonas* (Christian et al., 2010). A cocktail of these effector proteins secreted by the bacterium migrates into the nuclei of infected plant cells, where they particularly bind to the promoter region of target genes and manipulate their expression to the benefit of the pathogen (Boch and Bonas, 2010). The binding domain comprises a variable number (13-28) of near-identical tandem repeats with each repeat consisting of 33 to 35 amino acids. The various types of these repeats are characterized by preferential binding to one of the four nucleotide bases present in the DNA (Boch et al., 2009; Moscou and Bogdanove, 2009). These specificities are

defined by specific amino acids in positions 12 and 13, which have been referred to as repeat-variable diresidues (RVDs). The four predominantly occurring RVDs are NI, NG, HD and NN, which preferentially bind to adenine, thymine, cytosine and guanine, respectively (Joung and Sander, 2013). This principle allows the generation of customized expression units for binding domains in which the RVDs are sorted according to predefined DNA target sequences, provided the bound motifs are preceded by a thymine. Those synthetic DNA-binding domains coupled with FokIR constitute universal tools for the sequence-specific induction of DSBs (Christian et al., 2010). The first successes of TALEN-based mutagenesis in plants were achieved in *Arabidopsis* protoplasts (Cermak et al., 2011) and *N. benthamiana* leaves (Mahfouz et al., 2011). After that, TALEN-induced mutations were produced in rice plants and demonstrated to be heritable (Li et al., 2012). In the following years, several plants species' genomes were altered by using TALENs such as soybean (Haun et al., 2014), tomato (Lor et al., 2014), barley (Gurushidze et al., 2014), wheat (Wang et al., 2014) and maize (Char et al., 2015). In addition to these NHEJ-mediated mutations, it has also been demonstrated that TALEN-induced DSBs, can be used for HDR-mediated gene exchange and targeted insertion in plants when repair templates are provided (Zhang et al., 2013; Budhagatapalli et al., 2015). Due to the modularity of the DBD of the TALE proteins, it is possible that functional domains of other enzymes such as methylases, activators or repressors of transcription can be fused to the C-terminus in addition to endonucleases in order to modify gene expression in plants (Fichtner et al., 2014). The biggest disadvantage of the TALENs is their size. For researches, it is practically difficult to assemble TALEN-coding expression units (Cermak et al., 2011). Furthermore, the delivery and expression of the TALENs into target cells are more challenging.

1.9.5 RNA-guided Cas endonucleases

A new platform has emerged based on RNA-guided Cas endonucleases which derive from the CRISPR/Cas (clustered regularly interspaced short palindromic repeats/CRISPR-associated protein) adaptive immune system of microbes (Jinek et al., 2012). Bacteria and archaea have developed such an adaptive defense mechanism to defend against invading viruses (Wiedenheft et al., 2012). The RNA-guided endonuclease used for genome engineering is the Type II Cas9 from *Streptococcus pyogenes*. The Cas endonuclease platform consists of two components; a synthetic guide RNA (gRNA) and the Cas protein. The gRNA is designed to specifically bind with its 5'-end to a user-defined DNA sequence and guides the Cas9 endonuclease towards this target that is to be cleaved (Figure 12). The recognition of ca. 20 nucleotides of the target motif (called protospacer) is brought about by the principle of complementary base pairing, which allows producing gRNAs for any sequence of choice. In addition to this, the target motif also includes few nucleobases downstream of the target motif which is called protospacer-adjacent motif (PAM) and is bound by the Cas9 protein. For the case of SpCas9, the PAM sequence is NGG (where N stands for any nucleobase and the Gs for two guanines). The DSB occurs between the

third and fourth nucleotide in 5'-direction from the PAM (Jinek et al., 2012; Sander and Joung, 2014).
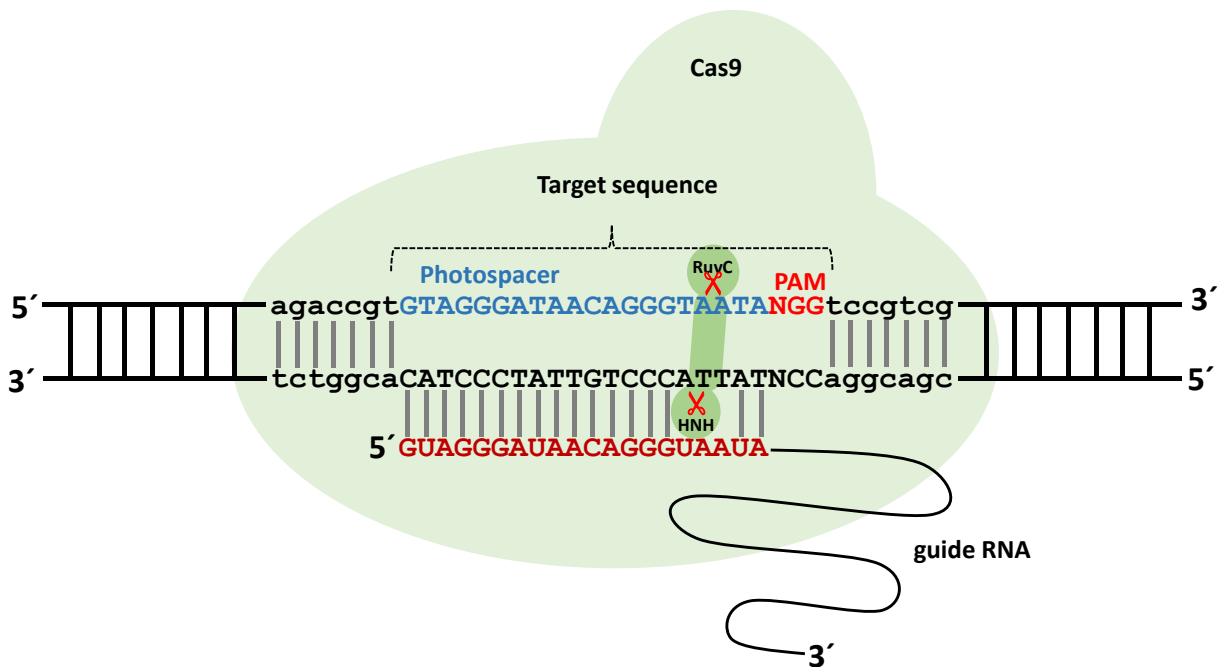
Figure 12: Representation of gRNA-mediated Cas9 in assembly with the target motif. The Cas9 endonuclease is guided by a chimeric guide RNA (gRNA) to the target motif, where it generates double-strand breaks 3 to 4 bp upstream of the PAM. This target motif consists of the protospacer, a ca. 20 bp long sequence to which the gRNA binds by complementary base pairing. Secondly, the target sequence is defined by the protospacer-adjacent motif (PAM) which consists of NGG nucleotides located at the 3'-end. Cas9 recognizes a specific PAM sequence on the DNA, which is subsequently cleaved by the two nuclease domains RuvC and HNH (Picture modified from Mahfouz et al. (2014)).

1.9.5.1 Methodological aspects of Cas endonuclease technology

1.9.5.1.1 System components

The application of Cas endonuclease technology in plants offers several possibilities and certain specific requirements for the construction of transformation vectors. Several modifications were made in Cas9 endonucleases in order to use them in plants. Notably, the coding sequences were complemented by one or two nuclear localization signals (NLS) and the codon usage was optimized for various plant species (Shan et al., 2013; Lawrenson et al., 2015; Liu et al., 2017b). In addition to this, various promotors have been used to drive endonuclease expression, depending on the host organism. A doubled-enhanced cauliflower mosaic virus (2x35S) promoter has been used in crop plants for test systems (Shan et al., 2013; Shan et al., 2014; Upadhyay et al., 2019). To generate heritable mutations, UBIQUITIN promoters are

preferentially used. Consequently, the maize *POLYUBIQUITIN 1* promoter (*ZmUBI1*) has commonly been used for *cas9* expression to produce heritable mutations in monocots (Shi et al., 2017; Upadhyay et al., 2019).

The expression cassette for a gRNA generally consists of plant origin RNA polymerase III (Pol III) processed promoters and terminators. A comparative test in maize protoplasts had shown that U3 promoters from wheat and rice were more efficient than the U6 promoter from *Arabidopsis* which was preferentially used in dicots (Xing et al., 2014). In the case of barley and wheat, the wheat U6 promoter is so far mostly used (Wang et al., 2014; Holme et al., 2017; Upadhyay et al., 2019). More recently, a study by Kumar et al. (2018) indicated that the barley U3 promoter might be more efficient in generating mutants of barley than the rice U3 promoter. Various systems have been developed for the expression of multiple gRNAs (Xing et al., 2014; Lowder et al., 2015; Ma et al., 2015). In most cases, each gRNA is expressed by a separate Pol III promoter.

1.9.5.1.2 Criteria for target motif selection and in silico gRNA design

The target sequence-specific part of the gRNA typically has a length of 20 nucleotides (Jinek et al., 2012; Cong et al., 2013). High performance was shown in *Arabidopsis* and barley when the target sequence-specific gRNA is less than 20 nucleobases long. In contrast, an extension of gRNA at 5'- part over 20 nucleotides led to reduced cleavage efficiency (Cho et al., 2014). Several online platforms were developed for the selection of target motifs and corresponding gRNAs. For instance, CRISPR-Plant (Lei et al., 2014; Liu et al., 2017a), Benchling (Naim et al., 2020), WU-CRISPR (Wong et al., 2015), CRISPOR (Haeussler et al., 2016; Concordet and Haeussler, 2018). All the above-mentioned online platforms have pros and cons. This is supposed to be one of the reasons that the reliability of their results is still limited. Studies which were focused on the gRNA secondary structure, Liang et al. (2016) found that three of the common stem-loops in the gRNA 3'-part are essential for appropriate binding to the Cas9 protein, thereby it is critical to the overall functionality of the gRNA/Cas complex. In order to increase the efficacy, it is recommended to investigate the secondary structure of candidate gRNAs thoroughly. Online platforms such as mfold (Zuker and Jacobson, 1998; Waugh et al., 2002; Zuker, 2003) or RNAfold (Gruber et al., 2008; Lorenz et al., 2011) are available for the prediction of secondary RNA structures. Pre-validation of the gRNA/*cas* construct is essential for its functionality prior to stable transformation. To this end, few transient expression systems have also been established (Budhagatapalli et al., 2016; Feng et al., 2016). The most commonly used transient expression method is based on the transfection of isolated mesophyll protoplasts, whose plasma membrane is rendered porous by application of polyethylene glycol. This enables the gRNA/Cas construct to be taken up by the protoplasts, which has been exemplified in several studies (Wang et al., 2014; Feng et al., 2016; Liang et al., 2016; Gerasimova et al., 2019). The functionality of the transferred components can be verified after amplification of the genomic target regions using T7E1 assay, by Sanger or deep sequencing methods.

In recent years, several Cas variants have emerged with unique features. For instance, Cas12a (Cpf1) recognizes the PAM NTT located at the 5'- end of the protospacer and generates DSBs. The T-dependent PAM of Cpf1 extends the range of possible target sequences of RGENs (Zetsche et al., 2016). Cas14a is used as a genome engineering tool for the cleavage of single-stranded DNA (ssDNA)(Khan et al., 2019). This tool was successfully used to engineering resistance against economically important plant ssDNA viruses because of its sequence-independent and unrestricted cleavage (Khan et al., 2019). Several Cas variants and their usages were reviewed by Manghwar et al. (2019). Advancement in genome engineering has led to an ambitious approach called basic editing. This approach would help to specifically modify a single nucleotide into another so that no more than one amino acid of the encoded protein is altered at a time (Zong et al., 2017). Cytidine deaminases can convert C/G base-pairs to T/A in the target region, whereas adenosine deaminases induce A/T to G/C conversions (Komor et al., 2016; Gaudelli et al., 2017). The functionality of cytidine and adenosine deaminases has already been demonstrated in several plant species (Zong et al., 2017; Zong et al., 2018).

By the utilization of Cas endonuclease technology, any genomic target of choice can be modified, which offers novel opportunities for genetic improvement. This technology has successfully been used in mono-and dicotyledonous plants by using single gRNA expression systems for instance in barley (Gerasimova et al., 2020), wheat (Budhagatapalli et al., 2020), rice (Wang et al., 2016a), tobacco (Schedel et al., 2017) and poplar (Fan et al., 2015). A single cleavage site typically results in short deletions and/ or insertions, whereas simultaneously addressed pairs of target motifs can result in accordingly large and precisely predictable deletions. Targeting more than one genomic target site simultaneously resulted in the deletion of large fragments (Li et al., 2013; Mao et al., 2013) up to whole genes and chromosomal regions (Zhou et al., 2014). Several studies demonstrated multiplex genome editing in plants (Brooks et al., 2014; Zhou et al., 2014; Char et al., 2017; Kapusi et al., 2017; Srivastava et al., 2017; Pathak et al., 2019). Current utilization of Cas endonuclease technology is still mainly limited to random mutagenesis caused by non-homologues end-joining (NHEJ) based repair mechanism. Meanwhile, the targeted insertion or exchange of genes using HDR has only been demonstrated in few situations, with examples in the model plants *Arabidopsis* (Hahn et al., 2018) and *N. benthamiana* (Li et al., 2013), but also in crops such as soybean (Li et al., 2015) and rice (Sun et al., 2016).

2. Objectives of the study

The main objective of the current study is to develop resistant maize plants against yield loss-causing fungal pathogens. Studies on maize diseases have indicated that anthracnose, and common smut of corn are important maize diseases that cause yield losses up to 40% and 15%, respectively.

The standard agricultural strategies are inadequate to control diseases. For instance, the application of fungicides does not control the stalk rot phase anthracnose. Similarly, fungicide application does not help to control the corn smut fungus once the galls are formed. In addition to this, the fungicides are in the form of solo formulations. Within a short period fungus can develop resistance to such fungicides by undergoing point mutations. Furthermore, fungi tolerate a certain concentration of fungicides by activating efflux transporters. On the other hand, resistant maize cultivars are hardly available for both fungal pathogens and therefore, to develop new resistant varieties through breeding is a time-consuming process.

To address the maize anthracnose disease, two approaches were pursued. Host-induced gene silencing to knock-down fungal essential genes. The rational of this approach is to use fungicide target genes as HIGS targets, since these genes are essential for fungal growth and pathogenicity. *C. graminicola* β-Tubulin (target for the benzimidazole group of fungicides) and Succinate dehydrogenase (SDH is a significant target for boscalid) are used as HIGS targets.

During the co-evolution, several fungi have taken advantage of using plant genes and derived products for its development and successful colonization. Plant Lipoxygenases (LOXs) are proven for their role in plant-pathogen interaction. Most strikingly, Gao et al. (2007) reported that maize *9-LIPOXYGENASE LOX3* acts as a susceptibility factor for *C. graminicola* infections. Intriguingly, transcriptional time-course experiments in *U. maydis*-infected maize revealed a large number of maize genes being upregulated upon the establishment of biotrophy (Doehlemann et al., 2008). Among these genes is the maize *LIPOXYGENASE-3* (*LOX3*) that has previously been shown to be a susceptibility factor for *C. graminicola* as well. Given this information, maize *LOX3* was chosen to be knocked out, which may provide resistance to both fungal pathogens. Prior to knocking out target gene, it is essential to establish the genome engineering platform in maize. To this end, Cas endonuclease technology was opted, since it was proven to be one of the best available methods to knockout target gene (Kumlehn et al., 2018).

Objectives
1. Develop anthracnose disease-resistant maize by knock-down of essential fungal genes
2. Establishment of Cas endonuclease technology in maize
3. Knockout of a susceptibility factor for fungal infection in maize (*LOX3*)

3. Materials and Methods

3.1 Chemicals and consumables

The chemicals and consumables were purchased from the following suppliers: Ambion (Waltham, MA, USA), BD (Becton, Dickinson and Company, Franklin Lakes, NJ, USA), Biozym Scientific GmbH (Hessisch Oldendorf, Germany), BRAND GmbH + Co KG (Wertheim, Germany), Carl Roth GmbH + Co. KG (Karlsruhe, Germany), Duchefa Biochemie B.V (Haarlem, Netherlands), Eppendorf (Hamburg, Germany), Greiner Bio-One GmbH (Frickenhausen, Germany), Roche (Mannheim, Germany), Serva Electrophoresis GmbH (Heidelberg, Germany) and Sigma-Aldrich (St. Louis, MO, USA). Individual chemicals or materials purchased from other companies are specifically noted in the text.

3.2 Enzymes

The restriction enzymes used were either conventional or fast digest enzymes from Thermo Fisher Scientific (Waltham, MA, USA). They were used according to the manufacturer's instructions.

3.3 Antibiotics

Stock solutions of antibiotics were prepared with ddH_2O and filter-sterilized using 0.2 μm syringe filters. Deviations from this procedure are indicated with stars. The wide range of antibiotics used in this study were listed in Supplemental Table 1.

3.4 Oligonucleotides

The oligonucleotides used in this study were designed by using Clone Manager 9 Professional Edition (Scientific & Educational Software, Morrisville. NC. USA). The RT-qPCR/qPCR-specific primer sequences were downloaded from the literature and respective oligonucleotides synthesized by the companies Metabion (Planegg, Germany) and Biolegio (Netherlands). The primers used in this study are listed in Supplemental Table 2.

3.5 Software

The software packages used in this study are listed in the Supplemental Table 3.

3.6 Generation of maize transformation vectors
3.6.1 RNAi (hairpin) vectors

To validate the RNAi target gene sequences, primers were designed for full-length genes of *β-Tub2* (GenBank accession number M34492.1) and *Sdh1-4* (GenBank accession numbers XM_008092321.1, XM_008092320.1, XM_008101415.1, XM_008091315.1). To this end, *C. graminicola* genomic DNA was used as template and the PCR-amplified sequences were subsequently confirmed by Sanger sequencing. The Gateway cloning method was used to produce RNAi vectors for the generation of stable transgenic maize plants. To this end, pTA38

was used as an entry vector (Himmelbach et al., 2007). The selected target regions (5'-UTRs and 5'-ends of the coding sequences) were introduced into the entry vectors named as pIPKTA38-Sdh1 and pIPKTA38-Tub2. IPKb009 and IPKb027 were used as the final destination vectors (Himmelbach et al., 2007; Kumlehn, 2008). The destination vectors contain doubled-enhanced Cauliflower Mosaic Virus 35S (IPKb009) and maize *POLYUBIQUITIN 1* (IPKb027) promoters to drive transcription of the chosen sense and anti-sense sequences. These sequences were oriented in opposite direction to one another and connected by the wheat RGA2 intron. The selected target fragments from pIPKTA38 (*Sdh-1, Tub-2*) were cloned into the RNAi destination vector IPKb009 and IPKb027 by a single LR recombination reaction. Correct orientation concerning sense and anti-sense sequences were confirmed by Sanger sequencing and restriction analyses. The verified constructs were introduced into the hypervirulent AGL1 strain of *Agrobacterium tumefaciens* using electroporation. The positive constructs were named as pNB96, pNB97, pNB98, and pNB99.

3.6.2 Vectors for RNA-guided Cas9

The sequence of the target gene *ZmLOX3* was obtained from the maize genome database (https://www.maizegdb.org/). The obtained sequences were further verified by browsing other available databases. The target motifs for site-directed mutagenesis were selected within the first exon. For the selection of target motifs, the online tools WU-CRISPR (Wong et al., 2015), and DESKGEN (Doench et al., 2016) were chosen, which resulted in five best-scoring gRNAs (sequences are listed in Supplemental Table 4). The secondary structures of the gRNAs were modeled with the web-based tool RNAfold described by (Gruber et al., 2008). pSH121 was used as a generic vector (Gerasimova et al., 2020). This vector harbors a maize codon-optimized *cas9* coding sequence under control of the maize *POLYUBIQUITIN 1* promoter, and a guide-RNA scaffold preceded by the RNA polymerase III-processed rice *U3* promoter. A synthetic, double-stranded oligonucleotide carrying the target-specific part of the gRNA was annealed and integrated between the Os*U3* promoter and the upstream gRNA scaffold using *BsaI* restriction and ligation. Subsequently, the *SfiI*-produced vector fragment containing the expression cassettes of gRNA and *cas9* was transferred to the binary vector p6i-d35S-TE9 (DNA CLONING SERVICE e.K., Hamburg, Germany). Finally, the cloned vector sequences were verified by Sanger sequencing and the verified construct was introduced into the virulent AGL1 strain of *Agrobacterium tumefaciens* using electroporation.

3.7 *Agrobacterium*-mediated maize transformation

Stable genetic transformation of maize was conducted using Hi-II A x B F_1 immature embryos (Hi-II A used as female and Hi-II B used as male) as previously described (Hensel et al., 2009) with 100 mg L^{-1} hygromycin as plant selective agent. Parents of Hi-II A and Hi-II B originated from an F_2 population of A188 X B73 accessions.

3.8 Molecular analysis

3.8.1 Genomic DNA isolation

Genomic DNA isolation for DNA gel blot analysis was performed as previously desribed by Pallotta et al. (2000). For the case of genotyping analysis (to confirm the presence of T-DNA by PCR and characterize Cas9/gRNA induced mutations), DNA isolation was conducted according to Milner et al. (2019). Genomic DNA was isolated from protoplast samples by the method described by Wang et al. (2016c).

3.8.2 DNA gel blot

DNA gel blot analysis was performed by the method of Southern (1975). In brief, 25 µg genomic DNA were digested with *HinDIII*, separated by agarose gel electrophoresis and blotted onto a Hybond N membrane. A gene-specific probe for *hpt* was labeled with DIG as recommended by the supplier (Roche, Mannheim, Germany).

3.8.3 Polymerase chain reaction

In all performed Polymerase Chain Reactions (PCR), the GoTaq Polymerase (Promega, Madison, WI, USA) and the corresponding buffer were used in a 20 µL reaction. Depending on the length of the PCR product and the nature of the primers, the elongation time, the annealing temperature and the number of cycles were adjusted to obtain maximum yield. The annealing temperature was optimized by gradient PCR. All standard PCR programs were derived from the following scheme and were performed in the Mastercycler® ep (Eppendorf, Hamburg, Germany).

3.8.4 DNA gel electrophoresis

For the electrophoretic separation of DNA, 0.8-1.5% (w/v) agarose gels were used. The agarose was weighed out and boiled with 0.5x TBE buffer until the agarose was completely dissolved. For DNA visualization, 12-15 µL Stain Clear G (Serva Electrophoresis GmbH, Heidelberg, Germany) was added to 400 mL liquid agarose gel. Solidification was done by using an appropriate comb. Electrophoresis was performed at 200 V, with 0.5x TBE as electrophoresis buffer. The documentation of the results was performed using a gel documentation system.

3.8.5 Restriction digestion

All restrictions using one or two enzymes were carried out at 37 °C for at least 30 min unless otherwise indicated. The buffers recommended by the manufacturer were used and the enzyme activity was then inactivated according to the time and temperature specifications.

3.8.6 Purification of DNA from agarose gel

The extraction and purification of DNA from an agarose gel was performed using the QIAquick Gel Extraction Kit (QIAGEN, Hilden, Germany). The DNA fragment with the expected size was

cut from the agarose gel with a clean scalpel and then eluted according to the manufacturer's instructions. The eluted DNA was promptly used for ligation.

3.8.7 DNA ligation
The ligation of vector and insertion was performed in a molar ratio between 1:3 and 1:7, depending on the size and concentration of the insert thus using the T4 DNA ligase from Thermo Fisher Scientific (Waltham, MA, USA) for the ligation reaction. All components were incubated in a 10 µL ligation kit for 2 hours at RT or overnight at 4 °C.

3.8.8 *Escherichia coli* transformation (heat shock method)
For the transformation of chemically competent *E. coli* cells, 3 µL ligation preparations were mixed with 50 µL cells and incubated on ice for 30 min. Subsequently, a heat shock for 1 min at 42 °C followed by an incubation of 2 min on ice was performed. 450 µL sterile SOC medium was added to the DNA-bacteria mixture and the transformed cells were shaken for 60 min at 37 °C and 550 rpm. Afterwards, 50-100 µL of the transformed cells were spread out on Petri dishes with LB-medium and appropriate antibiotics using a sterile spreader and were incubated overnight at 37 °C. The next day, individual colonies were picked up with a sterile wooden toothpick and transferred to liquid LB medium (including antibiotics). The cells were propagated at 37 °C and 180 rpm overnight.

3.8.9 Transformation of electro-competent Agrobacteria
For each transformation, 50 µL of competent cells were put on ice, mixed with 100-200 ng of binary vector (1-2 µL) and incubated for 2 min, then the mixture was transferred to the pre-cooled electroporation chamber. An electric shock was performed at 25 µF, 400 Ω, 2.5 kV on the Bio-Rad electroporator. One mL of SOC medium was immediately added to transformed cells and incubated at 28 °C with shaking for 2 h. Finally, 50 µL and 150 µL of the bacterial culture was placed on selection plates with appropriate antibiotics and incubated at 28 °C. Positive clones were analyzed using plasmid-specific primers by colony PCR within 2 days after incubation.

3.8.10 Colony PCR
For colony PCR, individual colonies of *E. coli* were swabbed off the plate using a sterile wooden toothpick and placed in a PCR reaction tube. 20 µL of each PCR reaction mixture were added and the PCR was started.

3.8.11 Isolation of plasmid DNA
The isolation of pDNA from transformed *E. coli* or *A. tumefaciens* cells was performed using the QIAprep Spin Miniprep Kit from QIAGEN (Hilden, Germany) according to the manufacturer's instructions.

3.8.12 Purification of PCR products

The purification of PCR products was performed using the QIAquick PCR Purification Kit (QIAGEN, Hilden, Germany) according to the manufacturer's specifications. The purified products were stored at 4 °C for a short period of time or at -20 °C for a more extended period.

3.8.13 Sequencing

To verify the vector sequences or to characterize induced mutations, Sanger sequencing of extracted pDNA or purified PCR products was performed by the company LGC Genomics GmbH (Berlin, Germany). The sequencing results obtained were evaluated using the programs APE, Clone Manager 9. Amplicons derived from protoplast DNA were subjected for NGS-based sequencing with GENEWIZ (Leipzig) and the analysis of the resulting samples was done by using an R script developed in the PRB (working) group.

3.9 Plant material and growth conditions

Plants were grown in peat-based substrate (Substrat 2, Klasmann-Deilmann, Geeste, Germany) in climate chambers under controlled environmental conditions using a 25/20 °C and 16/8 h light/dark regime with a light intensity of 240 µmol photons m^{-2} s^{-1} and a relative humidity of 60%.

3.10 *C. graminicola* culture and plant inoculation

Detached leaf assay was used to examine the *C. graminicola* infection potency towards maize *lox3* mutants and RNAi plants. Fourteen days after seeding, segments (~8 cm) of third leaves were collected and kept onto wet filter paper in square plastic Petri dishes of 14 cm diameter. The wild-type (WT) *C. graminicola* strain CgM2 of (Ces.) (Wilson, 1914) (teleomorph *Glomereella graminicola* D. J. Politis) (Bergstrom and Nicholson, 1999) used in this study was obtained from Prof. H. B. Deising's lab (Halle University, Germany). In order to collect conidia for infection assays, the WT strain was grown on oatmeal agar (OMA) (Werner et al., 2007). Conidia were collected from 2 to 4 weeks-old OMA plates by rinsing with 0.02% (v/v) Tween 20. After washing three times, the conidia suspensions were adjusted to specific concentrations with a haemocytometer (LO-Laboroptik, Friedrichsdorf, Germany). 10 µL droplets of a conidial suspension adjusted to 10^6 conidia/mL were inoculated (no conidia as mock). The inoculation drop was placed on the epidermis directly above the midrib, where it remained until observation. Subsequently, the Petri dishes were sealed with Parafilm and incubated at 23 °C in the dark for up to 120 h. The symptoms on maize leaves were photographed 4 days after inoculation.

3.11 Quantification of *C. graminicola* fungal DNA

Quantitative PCR (qPCR) was employed for quantifying fungal mass as described by Weihmann et al. (2016). Briefly, infected areas were collected at 4 days post inoculation (dpi) using a cork borer (8 mm in diameter). Samples were homogenized using a mixer mill (MM400, Retsch, Haan, Germany) for 1 minute at 30 Hz. DNA was extracted by following the manufacturer's protocol and using the pegGOLD Fungal DNA Mini Kit (PEQLAB Biotechnologie GmbH, Erlangen, Germany). Plasmid pUC18 (50 pg; Fermentas, St. Leon-Rot, Germany) was added at the beginning of DNA isolation as an external normalization reference. qPCR was performed with a Mastercycler Realplex (Eppendorf, Hamburg, Germany) and the iQ SYBR Green Supermix (Bio-Rad Laboratories, Hercules, CA, USA) using the primers Cg-ITS2-qPCR-Fw and Cg-ITS2-qPCR-Rv specific to the internal transcribed space region of ribosomal RNA-coding DNA (rDNA) of *C. graminicola*. The pUC18 concentration was measured using the primers M13-qPCR-Fw and M13-qPCR-Rv.

3.12 Infections of *Z. mays* with *U. maydis*

An experiment was carried out to determine whether maize *lox3* mutant plants are resistant to *U. maydis* infection. Infection assays were performed with the wild-type strains FB1, FB2 and the solo-pathogenic SG200 *U. maydis* strains. These strains were grown overnight in YEPS light medium (0.4% yeast extract, 0.4% peptone, and 2% sucrose) at 28 °C on a rotary shaker. The culture was then diluted using fresh medium to a cell density of $OD_{600\ nm}$ of 0.2. After incubation at 28 °C for about 4 to 6 h, the cells were harvested by centrifugation (10 min at 2,400 g) and resuspended in sterile water so that $OD_{600\ nm}$ of 1.0 was obtained. Syringe infections were made with 300 to 500 µL of the cell suspension into the interior of the leaf whorl of 7 days-old maize seedlings of wild-type and *lox*3 mutants were either generated by Cas9/gRNA-triggered mutagenesis or derived from transposon insertional mutagenesis (Gao et al., 2007). Three independent infections, each with about 40 plants were performed for every experiment.

3.13 Visual quantification of the *U. maydis* infection symptoms

For quantification of disease symptoms in seedlings, a classification scheme was used according to the severity of symptoms for 8 days post-inoculation comprising seven different symptom subcategories as previously described (Kämper et al., 2006).

3.14 Quantification of *U. maydis* fungal DNA

Biomass quantification was carried out as previously described (Brefort et al., 2014) to determine the differences between wild-type and maize *lox3* mutants. Seven days-old maize seedlings were infected with SG200. Six days post-inoculation, a 2-cm section from the tip of the 3rd leaf was used for analysis. Similarly, the same region of the 4th leaf was used 12 days post-inoculation. Ten leaf segments were pooled per each of the indicated points in time and the experiment was performed using 4 biological replicates. For genomic DNA extraction, leaf material was frozen in liquid nitrogen, ground to powder, and extracted using a phenol-based

protocol (Pallotta et al., 2000). The quantitative PCR (qPCR) analysis was performed using a LightCycler® 480 (Roche Life Science, Basel, Switzerland) in combination with the SYBR Premix Ex Taq (TII RNase H Plus) (Takara Bio Europe SAS, Saint Germain en Laye, France). *U. maydis* biomass was quantified using primers specific for the fungal *Peptidyl-prolyl isomerase* (*Ppi*) gene. The maize *GLYCERALDEHYDE 3-PHOSPHATE DEHYDROGENASE (GAPDH)* gene served as reference gene for normalization. Relative amounts of fungal DNA represented by amplified *Ppi* were then calculated relative to the amount of maize-derived *GAPDH* DNA using the cycle threshold (Ct) 2^{-2Ct} method.

3.15 RNA isolation and reverse transcriptase quantitative PCR

Leaf material was collected 4 and 8 days post-inoculation. Each biological replicate consisted of leaf material pooled from ten leaves directly frozen in liquid nitrogen and stored at -80 °C. In addition, three technical replicates of each biological replicate were used for RNA isolation, cDNA preparation and reverse transcriptase quantitative PCR (RT-qPCR) analysis. Total RNA was isolated from plant tissue by using Trizol reagent (Invitrogen, California, USA) according to the manufacturer's instructions and stored at -80 °C. The RNA quality was determined electrophoretically using a 2% non-denaturating agarose gel, and fluorometrically using a NanoDrop ND-1000 photometer (company, affiliation). Reverse transcription was performed using the Revert Aid™ H Minus First Strand cDNA Synthesis Kit (Fermentas, St. Leon-Rot, Germany, K1632) with RNA (1 µg/reaction), oligo(dT)-primer (0.25 µg/reaction) and random hexamer primer (0.25 µg/reaction) according to the manufacturer's guidelines for GC-rich templates. A total of 50 ng cDNA was used as template in a 10-µL reaction mix of the TB Green Premix Ex Taq II (TII RNase H Plus; Takara Bio Europe SAS, Saint Germain en Laye, France, RR820W) together with 0.2 µM each of forward and reverse primer. The RT-qPCR experiments were designed and conducted according to the MIQE guidelines. The reactions were performed in a LightCycler® 480 (Roche Life Science, Basel, Switzerland) using the following program: 95 °C, 30 s; 95 °C, 5s, 50/60 °C, 30 s 72 °C, 30 s (40 cycles) followed by a final melting curve with stepwise increments of 0.5 °C from 65 to 95 °C. Gene-specific primer sequences were retrieved from the literature. Maize *POLYUBIQUITIN 1* and *18S* ribosomal RNA were used as reference genes due to their reliability under various conditions according to previous findings (Shivaji et al., 2010; Manoli et al., 2012). Every primer combination was checked for its sensitivity by a primer efficacy tests using 5-fold dilutions starting with 100 ng cDNA and by a melt curve to confirm the presence of no more than one transcript. The geometric means of the Cq values of the two reference genes were calculated (Vandesompele et al., 2002). RT-qPCR experiments were conducted using three biological replicates, with three technical replicates per biological replicate. Raw Cq values were statistically examined using a linear mixed model described in detail by Steibel et al. (2009) and adapted in the R-Macro' qpcrmix' (https://github.com/daniel-gerhard/qpcrmix) by calculation of log-differences of normalized gene expression data based on the $2^{-\Delta\Delta Cq}$ method (Livak and Schmittgen, 2001). Briefly, raw Cq data were normalized by the

geometric means of two housekeeping genes (*POLYUBIQUITIN 1* and *18S*) with regard to possible random effects caused by pipetting or sampling, which resulted in ΔCq data for each treatment of each gene as well as in p-values (α<0.05) with six degrees of freedom. A linear model was applied on the ΔCq values to quantify deviations from the two competing hypotheses that either there are no, or there are differences among the pairwise compared treatments.

3.16 WGA staining, confocal microscopy and image processing
To evaluate fungal proliferation in infected tissue, confocal microscopy was carried out as described previously (Doehlemann et al., 2009). In brief, maize plant leaves were analyzed for 8 d after infection using the third outer leaf 1 cm below the infection site. Plant leaves were destained for at least 12 h in ethanol and incubated for 16 h at room temperature in 1M KOH. Further, the samples were gently washed 3 times with 50 mM Tris (pH 7.5). Fungal hyphae were stained with 10 mg/mL wheat germ agglutinin (WGA)-Alexa Fluor 488 conjugate (Molecular Probes, Oregon, United States), while plant cell walls were visualized using 1 mg/mL propidium iodide (Sigma-Aldrich, Missouri, United States)/0.02% Tween 20 for 30 min, followed by washing with 50 mM Tris at pH 7.5. The resulting samples were carefully analyzed using a Zeiss LSM780 confocal laser scanning microscope (Carl Zeiss, Jena, Germany). The plant cell wall was visualized by a 561 nm laser with an emission spectrum of 584-651 nm. Fungal hyphae were visualized by WGA-Alexa Fluor signal using a 488 nm laser and an emission spectrum of 493-541 nm. Fluorescence induction was obtained by means of sequential scanning. Pictures represent maximal z-stack projections. Captured images were further processed using the ImageJ freeware.

3.17 Protoplast isolation and PEG-mediated transfection
Maize protoplast isolation and transformation was established in our own research group by modification of the procedures described by Sheen (1991); Cao et al. (2014); Zhu et al. (2016). In brief, maize plants were grown under standard glasshouse conditions in the dark (or semi-dark by covering with cardboard boxes). The middle part of the 2nd leave (when the length was about 5 to 7 cm) was chopped into 0.5 mm strips with a sharp razor blade. Subsequently, the strips were soaked into 20 mL cell wall digestion enzyme (macerozyme). Vacuum pressure (600 mbar) was applied for approximately 30 to 60 min and the digestion was continued with gentle shaking (40 rpm) for 3 hours in the dark at room temperature. Protoplasts were filtered through a 75-µm nylon mesh and centrifuged for 2 min at 100 *g*. Depending upon the pellet size, protoplasts were resuspended in 2 to 5 mL W5 solution. Protoplast density was calculated by using a hemocytometer. The W5 solution was discarded and the protoplasts were resuspended in MMG solution. For PEG transformation, 15 ng plasmid DNA was mixed gently with 200 µl protoplasts and 220 mL PEG solution, incubated at room temperature for 18 min, and then the reaction was stopped by adding 800 mL of W5 solution. Centrifugation was conducted at 100 *g*

for 2 min to remove the supernatant. Further, the transfection mixture was diluted with 1 mL W1 solution at room temperature and mixed well by gently rocking or inverting the tube to stop the transfection process. Subsequently, 250 µl protoplasts were added in BSA-coated wells and incubated at room temperature in the dark. The GFP-expressing construct pGH215 (Hensel et al., 2017) was used as a control to quantify the proportion of transfected protoplasts. Chemicals used for protoplast isolation were listed in Supplemental Table 5.

3.18 Quantification of PAMP-triggered ROS accumulation

ROS accumulation was measured in maize plants using a luminol-based bioassay as described previously (Hilbert et al., 2013; Hückelhoven and Seidl, 2016; Navarrete et al., 2019; Samira et al., 2019). This assay is relying on the detection of luminescence released by excited luminol molecules produced after horseradish peroxidase (HRP)-catalyzed oxidation of luminol in the presence of plant-derived ROS. The emitted light directly correlates to the amount of H_2O_2 produced upon PAMP treatment of the plant. Maize plants were grown in a climate chamber at 16/8 hours light/dark cycles at 25/18 °C in peat moss-based substrate. Six days after germination, plants were infected with the solo-pathogenic *U. maydis* strain SG200. Four days post-inoculation, eight leaf discs were collected from the midrib of the third leaf using a biopsy punch, and incubated in a black 96-well polystyrene plate containing 100 µL of deionized water. The plates were then covered with aluminum foil and incubated overnight at room temperature. Water was removed and flagellin (flg22) solution was added which comprised Horseradish peroxidase (HRP 10 µg/mL, Sigma-Aldrich cat# P8375), L-012 (34 µg/mL Fujifilm WAKO cat# 120-04891) and flg22 (100 nM) in H_2O. ROS production was monitored by luminescence over 30 to 40 min in a microplate reader (Spark, Tecan). At least three plants per mutant were used in each experiment. All experiments were performed at least 4 times.

3.19 Measuring of callose deposition in *U. maydis*-infected plant leaves

Aniline blue-staining for callose detection was performed accoding to Seitner et al. (2018). Twenty-four hours post-inoculation, maize leaves (2 cm above the infection site of the third leaf) were destained using 100% ethanol. After de-staining, samples were incubated in 1x PBS for 30 min. The leaves were covered with staining solution (10 µg/mL WGA-AF488, 0.02% Tween 20 in 1x PBS (pH 7.4)) and incubated for 30 min. Samples were washed with 1x PBS and incubated in sodium phosphate buffer (0.07 M, pH 9) for 30 min followed by incubation with 0.005% Aniline blue solution (in sodium phosphate buffer 0.07 M, pH 9) for one hour. Leaves were washed with sodium phosphate buffer and visualized by confocal microscopy. The captured images were processed by Image J freeware.

4. Results

4.1 Host-induced silencing
4.1.1 Design and cloning of RNAi expression vectors

C. graminicola genes *β-Tubulin2* (*β-Tub2*)*, Succinate dehydrogenase* (*Sdh1-4*) were blasted against the maize genome database (http://www.maizegdb.org/) to avoid any possible potential off-targets. Which resulted in sequence homology in the genome of maize (nucleotide level) for *β-Tub2, Sdh1*, and *Sdh2* 82, 81, 85% respectively. No homology was found for *Sdh3, 4*. Designing RNAi vectors against the target regions of the fungus species turned out not to be possible due to its sequence homology to maize genes, therefore, the highly conserved 5'-untranslated region (UTR) and the 5'-end of the gene were used for *Cg β-Tub2* (89+11=100 nucleotides) and *Cg Sdh1* ((71+46=117 nucleotides). The 5'-UTR of this fungal region showed the most sufficient sequence diversity from the host.

To produce a sufficient amount of siRNA, three repeats of the selected target sequence were artificially synthesized into the entry vectors pIPKTA38-Sdh1 and pIPKTA38-β-Tub2. By using Gateway recombination, the target sequences were cloned into the modular binary vectors IPKb009, IPKb027. Essentially, these vectors were developed for cereal transformation to achieve RNA-interference (RNAi)-mediated gene knock-down (Himmelbach et al., 2007). Restriction digestion and Sanger sequencing confirmed the desired orientation of the sense and anti-sense sequences in the destination vector. The resulting clones were named pNB96, pNB96, pNB97, pNB98, pNB99 (Figure 13).
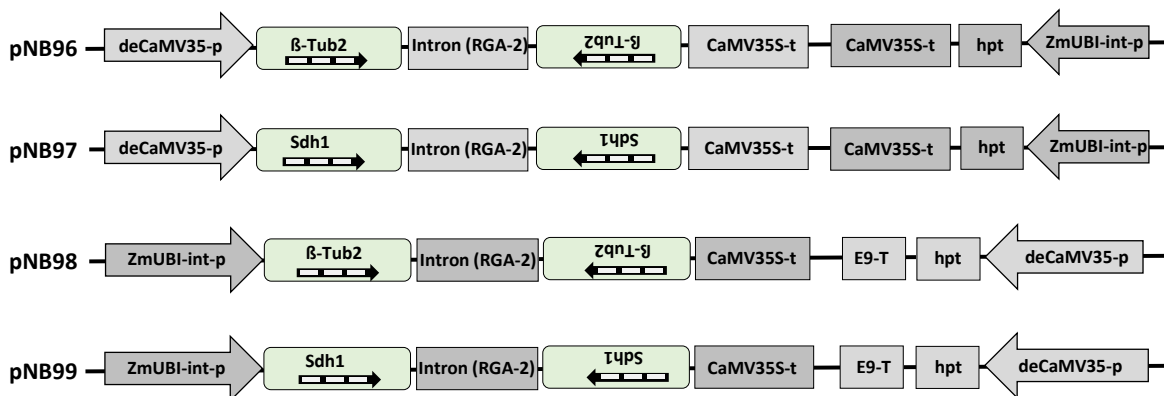
Figure 13: Schematic of the binary RNAi vectors generated for the transformation of maize. pNB96 and 97 are derivatives of pIPKb009 in which a doubled enhanced *CaMV35S* (deCaMV35S) promoter drives the expression of the hairpin construct consisting of target sequences of the *Cg β-Tub2* (pNB96) and *Cg Sdh1* (pNB97) gene sequences and a *CaMV35S* termination signal (T). The *hygromycin hosphotransferase (hpt)* gene is used as a plant selection marker controlled by the maize *Ubi-1* promoter and CaMV35S termination signal (T). pNB98 and 99 are derivatives of pIPKb027 in which the maize *Ubi-1* promoter drives the hairpin construct.

4.2 Production of transgenic maize plants

For the transformation studies, Hi-II (A x B) hybrid is used due to its amenability to genetic transformation studies, as described in Hensel et al. (2009). Immature embryos used as explants for the transformation experiment (Figure 14A), resulted in rapidly growing type-2 hygromycin resistant callus (Figure 14, C), a series of sub cultivation of the selected callus with somatic embryos matured into plantlets (Figure 14D). The regenerated shoots established the roots in the rooting medium (Figure 14 E), which helped for the successful acclimatization in the green house.

A	B	C	D	E
Co-cultivation of immature embryos with *A. tumefaciens*	Rapidly growing Type-II callus with somatic embryos	Series of developmental stages of somatic embryogenesis	Multiple shoot formation from a single embryo explant	Regenerated plantlet ready for transfer to soil

13 weeks time span
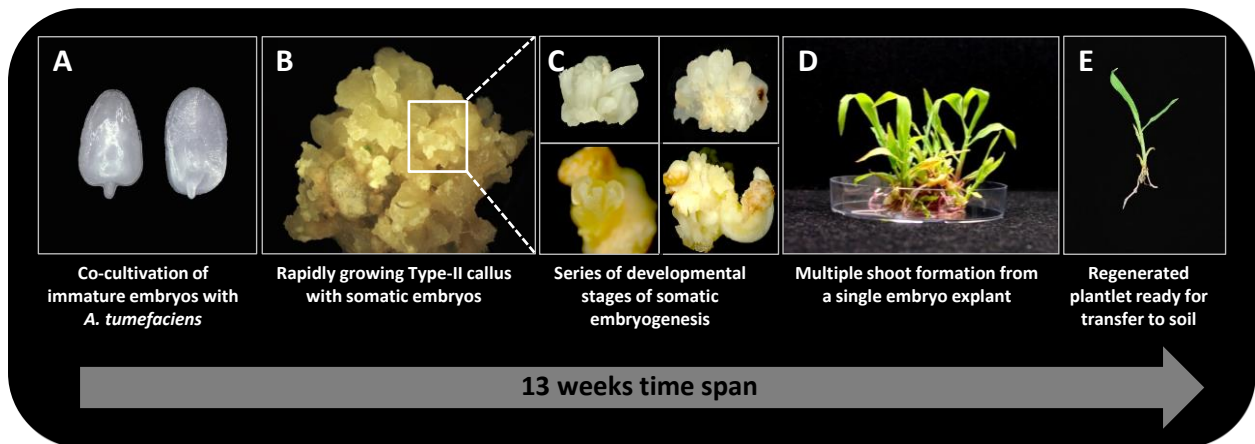
Figure 14: Production of transgenic maize plants via *Agrobacterium*-mediated transformation of immature embryos. (A) Immature embryos used as explants. (B) hygromycin-resistant calli growing on the selection medium (with somatic embryos). (C) Somatic embryo formation. (D) Multiple shoot formation from embryo-derived callus. (E) Plantlet with roots.

4.3 Molecular analyses of transgenic plants

PCR analysis was performed with isolated genomic DNA of young maize leaves to confirm the presence of T-DNA. Vectors pNB96, 97, 98 produced regenerates, whereas vector pNB99 failed to produce regenerants, due to poor embryo quality. Thereby, the transformation for the vector pNB99 were repeated. Regeneration and transformation efficiencies were listed in Table 1.

Table 1: Generation of transgenic maize using RNAi vectors. Regeneration and transformation efficiencies refer to the number of processed embryos.

Vector	Target genes	No. of agro infected embryos	No. of plants produced	Regeneration efficiency (%)	Transformation efficiency (%) (PCR for HPT)	(PCR for inverted repeats)
pNB96	*ß-Tub2*	107	5	4.6	4.6	4.6
pNB97	*Sdh1*	145	34	23.4	22.7	6.8
pNB98	*ß-Tub2*	87	28	32.1	32.1	11.4
pNB99	*Sdh1*	220	13	6.5	6.5	6.5

For the host-induced gene silencing approach, the copy number of the integrated T-DNAs can be crucial. The transgene copy number may affect transgene expression positively or negatively,

and multiple copy integration may cause gene silencing. To this end, DNA gel blot analysis was performed with the PCR-confirmed T_0 (pNB99) and T_1 (pNB96, 97, 98) plants.

For the transformation construct of pNB96, only five T_0 plants were produced. Selected T_1 plants (from self-pollinated T_0) were subjected to DNA gel blot analysis. Four T_1 siblings per each primary transgenic plant were used for analysis. Figure 15 represents a diverse integration pattern of T-DNA. Progeny shown #MH46E1a (#MH46E1a T_1-1, #MH46E1a T_1-2, #MH46E1a T_1-3, #MH46E1a T_1-4) and plant #MH46E1b (#MH46E1b T_1-1, #MH46E1b T_1-2, #MH46E1b T_1-3, #MH46E1b T_1-6) are likely to carry an identical T-DNA copy. These two plants derived from same embryo, could have the common origin from the same transformation event. Similarly, plant #MH46E2a (#MH46E2a T_1-2, #MH46E2a T_1-3, #MH46E2a T_1-4, #MH46E2a T_1-8) and #MH46E2b (#MH46E2b T_1-2,#MH46E2b T_1-3, #MH46E2b T_1-4, #MH46E2b T_1-5) carry identical T-DNA copies. For plant #MH46E3 (#MH46E3-T_1-2,#MH46E3-T_1-4, #MH46E3-T_1-5, #MH46E3-T_1-6) contains 4 copy number. T-DNA-free plants (segregated out in progeny via self-fertilization) were used as azygous control plants for the infection assays. For each independent event three plants were selected to produce homozygous progeny.
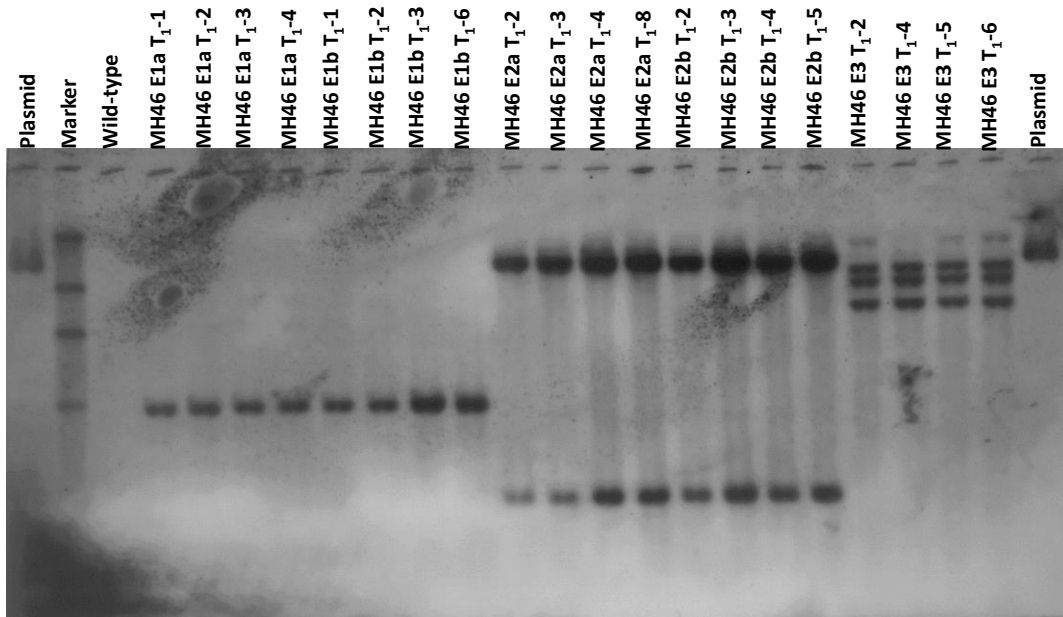
Figure 15: DNA gel blot analysis of transgenic segregants of T_1 (from self-pollinated T_0) transgenic plants from the transformation experiment with pNB96 carrying an RNAi unit addressing the *C. graminicola β-Tub2*. 20 µg genomic DNA each were digested with *HinDIII* and the fragments were separated into 0.8% (w/v) agarose gel. Hybridization of the specific DNA sequences was performed with a *hygromycin hosphotransferase (hpt)* specific probe. The names of the individual plants belonging to three T_1 families are given above the picture. Wild-type used as a negative control, plasmid as a positive control. MH46 indicates maize transformation experiment number. Alphabets a, b indicates transgenic siblings.

Other transformation experiments comprising RNAi vectors (i.e. pNB97, 98 and 99) resulted in similar results. All PCR-positive plants tested proved also DNA gel blot-positive indicating stable T-DNA integration. Range and average of copy numbers of T_0 plants tested, proportion of T_0 plants with consistently co-segregating copies indicating a shared genomic insertion site. The detailed copy numbers are listed in the Table 2. And the respective pictures depicted in supplemental Figure 1, 2, 3.

Table 2: Summary of the transgene copy number of transformation experiment pNB97, 98, 99.

Vector	Target genes	Plant identifiers	Number of copies (DNA gel blot analysis)
pNB97	*Sdh1*	#MH47E1 (#MH47 E1 T1-1, #MH47 E1 T1-3, #MH47 E1 T1-5, #MH47 E1 T1-9)	1
		#MH47E5a (#MH47 E5a T1-2, #MH47 E5a T1-3, #MH47 E5a T1-4, #MH47 E5a T1-5)	2
		#MH47E14 (#MH47 E14 T1-1, #MH47 E14 T1-2, #MH47 E14 T1-3, #MH47 E14 T1-6)	2
		#MH47E25 (#MH47 E25 T1-1, #MH47 E25 T1-2, #MH47 E25 T1-4, #MH47 E25 T1-6)	Multiple
		#MH47E6 (#MH47 E6 T1-1, #MH47 E6 T1-2, #MH47 E6 T1-3, #MH47 E6 T1-6)	2
pNB98	*ß-Tub2*	#MH47 E101 (# MH47 E101 T1-2, MH47 E101 T1-5, MH47 E101 T1-6, MH47 E101 T1-10)	1
		#MH47 E103 (# MH47 E103 T1-1, MH47 E103 T1-2, MH47 E103 T1-5, MH47 E103 T1-6)	Multiple
		#MH47 E118 (# MH47 E118 T1-2, MH47 E118 T1-3, MH47 E118 T1-4, MH47 E118 T1-6)	3
		#MH47 E119 (# MH47 E119 T1-1, MH47 E119 T1-2, MH47 E119 T1-4, MH47 E119 T1-5)	1
		#MH47 E125 (# MH47 E125 T1-1, MH47 E125 T1-2, MH47 E125 T1-4, MH47 E125 T1-5)	2
pNB99*	*Sdh1*	#MH55E1a, #MH55E3, #MH55E5, #MH55E6, #MH55E10,#MH55E12a,#MH55E12b	2
		#MH55E1b, #MH55E13	1
		#MH55E2, #MH55E8a, #MH55E8b, #MH55E9, #MH55L8b	3
		#MH55E4a, #MH55E4b	Multiple

DNA gel blot analysis of transgenic segregants of PNB97, 98, 99. 20 µg genomic DNA each were digested with *HinDIII* and the fragments were separated into 0.8% (w/v) agarose gel. Hybridization of the specific DNA sequences was performed with a *hygromycin hosphotransferase (hpt)* specific probe. * indicates Primary transgenic (T_0) plants subjected to DNA gel blot analysis.

4.4 Determination of plant resistance by infection of leaf segments with *C. graminicola*
4.4.1 Hi-II A x B susceptible to *C. graminicola* infections
Hi-II A x B genetic background was used to generate transgenic maize plants expressing RNAi vectors, since this hybrid has a high capability of producing embryogenic callus (i.e. rapidly growing type 2 callus), which makes it an excellent explant source for plant genetic transformation studies. Hi-II (A x B) recombinant between A188 and B73. A screening of maize varieties for their susceptibility to *C. graminicola* unveiled that the B73 is resistant to *C. graminicola* infection (Weihmann et al., 2016). Therefore, it is very crucial to determine the infection potency of *C. graminicola* towards Hi-II (A x B) hybrid material before examining the RNAi plants. To this end, an experiment was conducted by which Hi-II (A x B) was compared with the cultivars Golden Jubilee (highly susceptible) and Mikado (susceptible) using quantitative PCR (qPCR) assays to assess the amount of fungal DNA. Leaf disks containing the infection spot were excised at 4 dpi, and primers were used that bind in the Internal transcribed spacer (ITS2) region

which is highly specific for fungi. Under the assumption that the amount of fungal DNA is highly correlated with the amount of fungal biomass, the qPCR results allow concluding the infection success of *C. graminicola*. The qPCR data illustrated that the fungal biomass of *C. graminicola* was reduced to the level of the standard susceptibility cultivar Mikado (Figure 16A). This observation is also in line with the occurrence of visual symptoms on the leaf surface (Figure 16B). In accordance with these results, Hi-II A x B further used as a wild-type control to assess the RNAi-expressing plants as to their resistance towards *C. graminicola*.
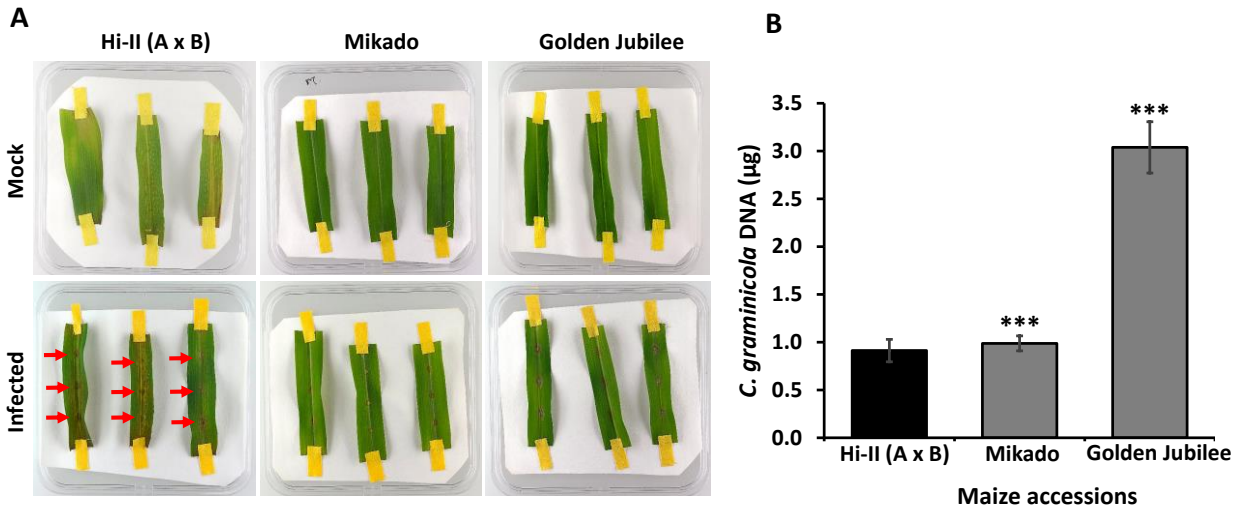
Figure 16: Susceptibility test towards *C. graminicola*. (A) Symptom development on the leaf surface at 4 dpi (red arrows indicate infection lesions). (B) Quantification of *C. graminicola* biomass by using qPCR (using 10 ng of total DNA as template). Three asterisks indicate a significant difference as compared with the wild-type control at P < 0.001 (one-way ANOVA with post-hoc Tukey honestly significant difference). Bars represent standard deviations.

4.4.2 HIGS confers quantitative resistance towards *C. graminicola*

To assess whether HIGS of two target genes confers resistance to *C. graminicola,* homozygous lines expressing different RNAi vectors were used for infection assays with *C. graminicola* wild-type strain M001. Azygous Hi-II (A x B) plants were used as wild-type. The pictures were photographed 4 days post-inoculation to see any visual effects. The photographs indicate that RNAi expressing transgenic event 25-2 show a visibly reduced fungal growth as compared with wild-type (Figure 17A). Further, the fungal biomass was quantified using the amount of fungal DNA as a proxy. Plant #E-25-2 exhibited a significant reduction of fungal DNA, whereas other transgenic plants showed only a tendency of reduction (Figure 17B). Based on the reduced fungal biomass in the RNAi plants, it is proposed that host-induced RNAi confers quantitative resistance against *C. graminicola*.
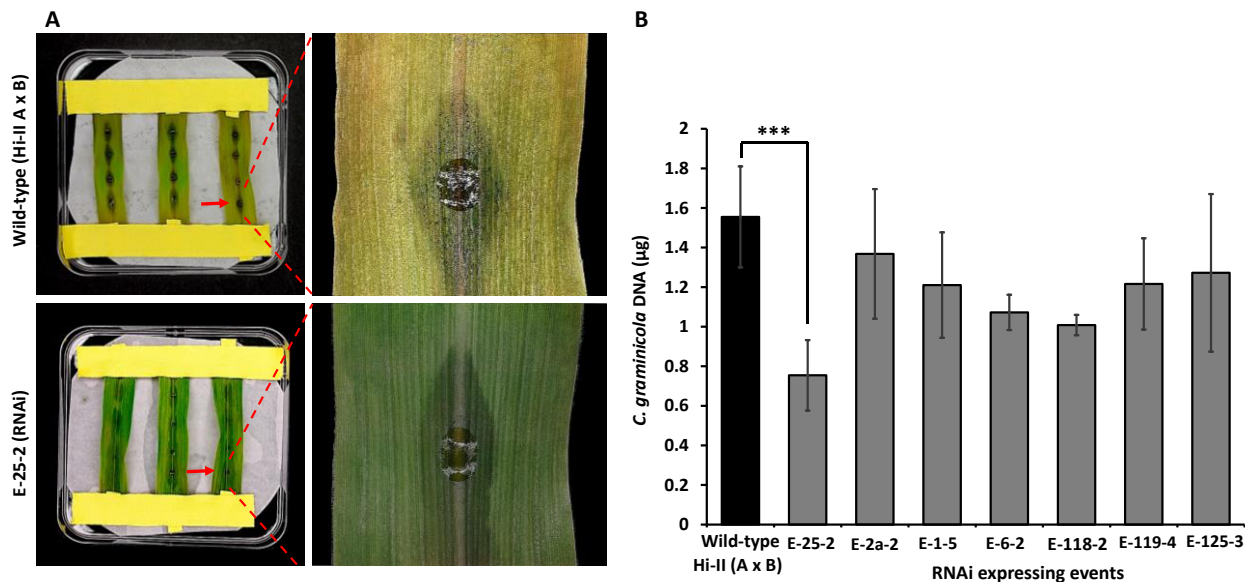
Figure 17: Quantitative protection from *C. graminicola* leaf infection of transgenic maize events expressing *Cg β-Tub2* HIGS constructs. (A) Detached-leaf assay with *C. graminicola* showing symptoms occurring at 4 dpi. Transgenic maize events expressing HIGS constructs show visual quantitative protection against *C. graminicola* in comparison to azygous wild-type. (B) Results of qPCR using 10 ng of total DNA as template. Columns represent means of three independent experiments. Each pool comprised twelve leaf discs excised from individual leaves carrying a single inoculation site at their middle. Event 2-a-2 carrying pIPKb009_β-Tub2, Event-1-5, E-25-2, E-6-2 carrying pIPKb009_Sdh-1 Event 118-2, E-119-4,125-3 carrying pIPKb027_β-Tub2. Three asterisks indicate a significant difference as compared with the wild-type control at P < 0.001 (one-way ANOVA with post-hoc Tukey honestly significant difference). Bars indicate standard deviation.

4.5 Knockout of maize *LOX3* by Cas9-triggered mutagenesis

4.5.1 Preparation of a *LOX3* knockout construct

Targeted mutagenesis approach, aimed to mutate the first exon region (Figure 18), To design gRNAs targeting *LOX3*, full length gene information retrieved from maize genome database (Maize GDB). The websites www.deskgen.com, http://crispr.wustl.edu were used to predict potential target motifs within this gene sequence. The motifs suggested are then compared with the organism's whole genome sequence. Based on the activity score from both online platforms and the gRNA predicted secondary structures, selected 5 target motifs residing within the first exon of *LOX3*.
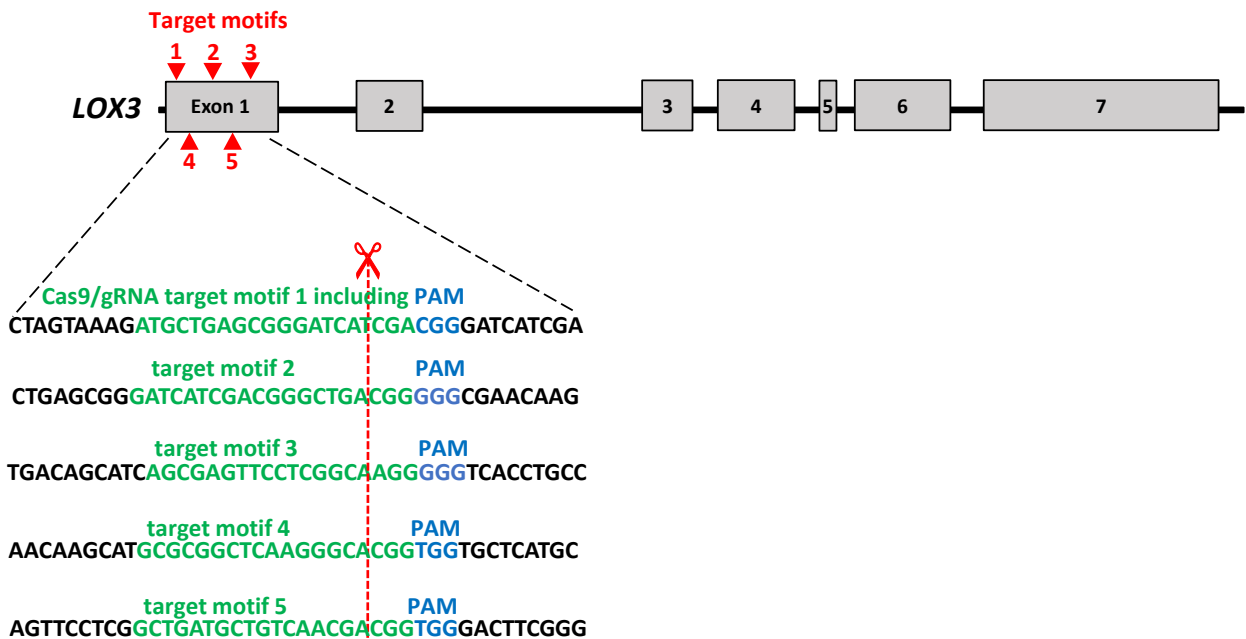
Figure 18: Schematic of *LOX3* (based on B73 RefGen_v3 GRMZM2G109130) gene structure and Cas9/gRNA target motif. Maize *LOX3* contains seven exons, represented by light grey rectangles, while introns are represented by lines. Cas9/gRNA target motif specifically addressed by the gRNA are illustrated in green, and the protospacer-adjacent motif (PAM, bound by the Cas9 enzyme) in blue. The scissors indicate the expected cleavage site.

The respective sequences of gRNAs corresponding to the target sites were inserted in between the rice u3 promotor and the gRNA scaffold (Figure 19). The resulting vectors were confirmed by Sanger-sequencing and named as pKP1, pKP2, pNB103, pNB104, pNB105 (Table 3).

Table 3: gRNA target motifs with respective sequences.

Vector	Target motif	Target motif sequence	PAM
pKP1	1	ATGCTGAGCGGGATCATCGA	CGG
pNB103	2	GATCATCGACGGGCTGACGG	GGG
pNB104	3	CAGCGAGTTCCTCGGCAAGG	GGG
pNB105	4	TGCGCGGCTCAAGGGCACGG	TGG
pKP2	5	GCTGATGCTGTCAACGACGG	TGG
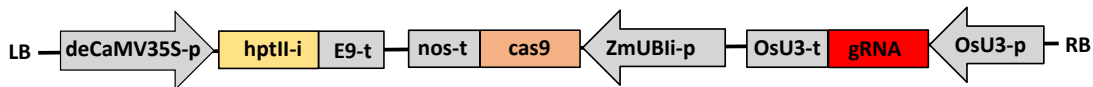
Figure 19: Schematic of the T-DNA used for plant transformation. Expression of *cas9* is driven by the maize *POLYUBIQUITIN 1* promoter with first intron that resides in the 5'-UTR (UBIi). Expression of the gRNA is driven by the rice U3 Polymerase III-processed promoter (OsU3-p). Expression of the *hygromycin phosphotransferase II* selectable marker gene including the potato LS1 intron (hptIIi) is driven by the doubled enhanced *CaMV35S* (deCaMV35S) promoter. E9-t, nos-t, OsU3-t: terminators; LB and RB: left and right borders.

4.5.2 Validation of gRNAs via protoplast transformation

The functionality of *cas9* and gRNA expression units as well as of their products was validated prior to the stable transformation by transfection of maize protoplasts using the generated plasmids. To assess the transfection success, a vector harboring a GFP expression unit was simultaneously used as control. The transformation efficacy was calculated based on the proportion of green fluorescing protoplasts (Figure 20). As a result, transformation efficacies of over 90% was achieved. Sequencing analysis resulted with the mutation efficiency of 7%, 24%, 12% for target motif 2, 3 and 4 respectively, target motif 5 resulted poor mutation efficiency such as 0.05%, and target motif 1 resulted no mutations.

| Etiolated maize seedling used for protoplast isolation | Cut leaf strips subjected to enzymatic digestion | Freshly isolated mesophyll protoplasts | PEG-mediated transfection | GFP-derived fluorescence in protoplasts |
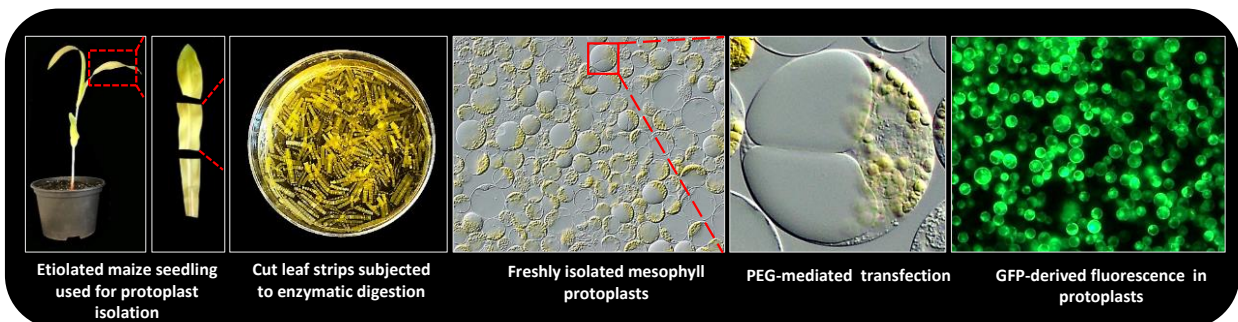
Figure 20: Schematic of mesophyll protoplast isolation from maize and peg mediated transfection. Etiolated maize seeding, enzymatic digested leaf strips, isolated protoplast with the high efficient PEG mediated transformation.

4.5.3 Maize transformation using single gRNAs

Based on the results of the protoplast assays, stable maize transformation was performed with constructs pNB103 (target motif 2), pNB104 (target motif 3), (pNB105) target motif 4, single Cas9/gRNA-containing vectors were independently used for stable transformation. Summary of the transformation results are illustrated in the Table 4.

Table 4: Summary of stable maize transformation using Cas9/gRNA constructs.

	target motif 2	target motif 3	target motif 4
No. of I.E inoculated	118	140	116
Regenerant plants produced	6	88	43
Regenerants tested for the presence of T-DNA	6	88	43
PCR-positive plants	6	88	43
Plants used to sequence the target	6	88	43
Plants with conclusive target sequence	6	85	42
Plants without mutated target	0	0	0
Mutated plants	6	85	42
No. of independent mutational events	3	6	4

4.5.3.1 Detection of mutations

To detect mutations, amplified PCR product of relevant target regions of all the regenerated plants were subjected to Sanger-sequencing. The resulting sequencing files were analyzed by aligning them with the wild-type sequences. The sequencing analysis was performed by using the Clone Manager software (Morrisville, NC, USA), and the Plasmid Editor software. Mutations were detected in all the regenerated plants 3 bp upstream of PAM. The majority of mutations were insertion/deletions. For target motif 2 transformation experiment, detected mutations were, one nucleotide insertion (#1a), a combination mutation which was 16 nucleotides deletion/2 nucleotides insertion (Figure 21A). Target motif 3, a large portion of deletion as many as 34 bp deletion is detected in plant #10c. A combination of mutation were detected, such as deletion of 24 bp with insertion of 6bp (#13a), and deletion of 2 bp and 1 bp insertion (#10j) (Figure 21B). Target motif 4 a deletion of 29 bp is detected (#6). Remarkably, all plants were efficiently mutated. The detailed description of the detected mutations are depicted in Figure 21A, Figure 21B, and Figure 21C for target motif 2, 3, 4 respectively.

```
     Plant code        target motif 2         ✂    PAM                    InDels
  A    WT  TGCTGAGCGGGATCATCGACGGGCTGACGGGGGCGAACAAGCA
       1a  TGCTGAGCGGGATCATCGACGGGCTGTACGGGGGCGAACAAGC           +1
       1d  TGCTGAGCGGGATCA-----------------CTCGAACAAGCA         -16/+2
       4a  TGCTGAGCGGGATCATCGACGGGCTGGACGGGGGCGAACAGCA          +1

                        target motif 3         ✂    PAM
  B    WT  TGACAGCATCAGCGAGTTCCTCGGCAAGGGGGTCACCTGCCA
       10a TGACAGCATCAGCGAGTTCCTCGGCAAAGGGGGTCACCTGCC           +1
       10c TGACAG-------------------------------CA              -34
       10j TGACAGCATCAGCGAGTTCCTC--AAAGGGGGTCACCTGCCA          -2/+1
       11b TGACAGCATCAGCGAGTTCCTCGGC-AGGGGGTCACCTGCCA           -1
       13a TGACAGCATCAGCGAGTTCCTC------------ATGTCG           -24/+6
       15d TGACAGCATCAGCGAGTTCCTCGGCAAAAGGGGGTCACCTGC           +2

                        target motif 4         ✂    PAM
  C    WT  GAACAAGCATGCGCGGCTCAAGGGCACGGTGGTGCTCATGCG
        6  GAACAAG----------------------------CATGCG           -29
       21a GAACAAGCATGCGCGGCTCAAGGGCAACGGTGGTGCTCATGC           +1
       23a GAACAAGCATGCGCGGCTCAAGGG--CGGTGGTGCTCATGCG           -2
       24e GAACAAGCATGCGCGGCTCAAGGGCATCGGTGGTGCTCATGC           +1
```

Figure 21: Mutations detected in primary transgenic plants. Sequencing results of selected primary transgenic plants for target motif 2 (A), 3(B) and 4(C). The sequence marked in green represents the gRNA-specific part of the targeted motif, the blue color indicates the protospacer-adjacent motif (PAM) which is bound by the Cas endonuclease. Plant identifiers given at the left-hand side, deletions are highlighted with red hyphens and inserted nucleotides with red letters, numbers of modified nucleotides (in bp) are given on the right side of the sequences.

4.5.3.2 Inheritance of detected mutations

In order to analyze inheritance and segregation of mutations and to produce homozygous progeny, selected plants were further grown to maturity. For genotyping of T_1 plants (self-pollinated from T_0), 10 grains per cob were grown in the glasshouse. DNA was extracted from leaf material, the target region was amplified and purified PCR product was Sanger-sequenced. Most T_1 siblings exhibited the same mutations that were present in respected T_0 plants. However, very few progeny of (T_0) carried mutations which had not been detected in their mother plants. This indicates that Sanger-sequencing is not sensitive enough to reveal allelic variants residing in comparatively small sectors of chimeric T_0 plants and/or Cas9/gRNA is still capable of triggering further mutations in residual wild-type alleles of such sectors after the T_0 leaf samples had been collected. Further investigation carried out to check the presence of T-DNA and their segregation in T_1 plants by performing PCR with transgene-specific primers.

About 25% of the T_1 plants tested proved to be T-DNA-free, which corresponds to Mendelian segregation in case of a single insertion site.

4.5.3.3 Progeny analysis of T_0 plant #4a

To provide a representative example for a heterozygous primary mutant, the progeny analysis of plant #4a, mutated in target motif 2, is presented. Eight plants carried a 1 bp insertion (+G) as had been detected in the T_0, whereas two plants (#4a_5 and #4a_6) displayed newly found mutations. #4a_6 did not contain T-DNA. To produce T-DNA free plants, plant #4a-2 continued further generations. T_2 plants of # 4a_2 was analyzed. 10 plants represented identical mutation (+G insertion) as detected in T_1, which confirms that the mutation was homozygous in T_1. The complete segregation pattern is illustrated in Figure 22.

```
Generation  Plant code              target motif 2        PAM         InDels  T-DNA
  T0         WT    TGCTGAGCGGGATCATCGACGGGCTGACGGGGGCGAACAAGCA
             4a    TGCTGAGCGGGATCATCGACGGGCTGGACGGGGGCGAACAAGC    +1      +

             4a_1  TGCTGAGCGGGATCATCGACGGGCTGGACGGGGGCGAACAAGC    +1      –
             4a_2  TGCTGAGCGGGATCATCGACGGGCTGGACGGGGGCGAACAAGC    +1      –
             4a_3  TGCTGAGCGGGATCATCGACGGGCTGGACGGGGGCGAACAAGC    +1      +
             4a_4  TGCTGAGCGGGATCATCGACGGGCTGGACGGGGGCGAACAAGC    +1      +
             4a_5  TGCTGAGCGGGATCATCGACGGGC---ACGGGGGCGAACAAGC    -3      +
  T1         4a_6  TGCTGAGCGGGATCATCGACGGGCTGCACGGGGGCGAACAAGC    +1      –
             4a_7  TGCTGAGCGGGATCATCGACGGGCTGGACGGGGGCGAACAAGC    +1      +
             4a_8  TGCTGAGCGGGATCATCGACGGGCTGGACGGGGGCGAACAAGC    +1      +
             4a_9  TGCTGAGCGGGATCATCGACGGGCTGGACGGGGGCGAACAAGC    +1      +
            4a_10  TGCTGAGCGGGATCATCGACGGGCTGGCGGGGGCGAACAAGCA    +1      +

  T2  4a_2_1to10  TGCTGAGCGGGATCATCGACGGGCTGGACGGGGGCGAACAAGC    +1      –
```

Figure 22: Inheritance of induced mutations of T_0 plant #4a. The upper part represents the mutation detected in T_0, and below, the sequencing results of T_1 and T_2 are depicted. The individual plant identifiers are given at the left-hand side. The green marked sequence represents the gRNA-specific part of the targeted motif, the blue color indicates the protospacer-adjacent motif (PAM) bound by the Cas endonuclease. Deletions are highlighted with red hyphens, and inserted nucleotides with red letters. The respective numbers of modified nucleotides (in bp) and information on transgenicity are given to the right of the mutant sequences.

4.5.3.4 Progeny analysis of T_0 plant #17a

Mutation segregation pattern of plant #17a was different from the plant # 4a. Sequencing results of plant #17a shown to be +A in T_0, none of the selected T_1 plants detected +A mutation, they shown completely new mutations such as six plants exhibited –A, one plant +AG, one plant –C, one plant +GAAA, one plant –GGCAA. The mutation pattern indicates it is likely that T_0 plant was chimeric. Only a few plants produced very few grains. T_2 individuals (self-pollinated fromT_1) of Plants #17a_10 were analyzed. Five plants shown the same mutation as observed in the T_1, three plants exhibited new mutation, such as +AA. The conceivable explanation is that the plants were heterozygous in T_1 and Sangers sequencing might not detected the +AA mutation in the T_1. The complete segregation pattern is illustrated Figure 23.

Generation	Plant code	target motif 3 — PAM	InDels	T-DNA
T_0	WT	TGACAGCATCAGCGAGTTCCTCGGCAAGGGGGTCACCTGCCA		
	17a	TGACAGCATCAGCGAGTTCCTCGGCAAAGGGGGTCACCTGCC	+1	+
T_1	17a_1	TGACAGCATCAGCGAGTTCCTCGGCAAGAGGGGGTCACCTGCC	+2	+
	17a_2	TGCTGAGCGGGATCATCGACGGGCTG–ACGGGGCGAACAAGC	−1	+
	17a_3	TGCTGAGCGGGATCATCGACGGGCTG–ACGGGGCGAACAAGC	−1	+
	17a_4	TGCTGAGCGGGATCATCGACGGGCTG–ACGGGGCGAACAAGC	−1	–
	17a_5	TGCTGAGCGGGATCATCGACGGGCTG–ACGGGGCGAACAAGC	−1	+
	17a_6	TGCTGAGCGGGATCATCGACGGGCTG–ACGGGGCGAACAAGC	−1	+
	17a_7	TGCTGAGCGGGATCATCGACGGGCTGGAAAACGGGGCGAACA	+4	+
	17a_8	TGACAGCATCAGCGAGTTCCTC-----GGGGGTCACCTGCCAG	−5	+
	17a_9	TGCTGAGCGGGATCATCGACGGGCTG–ACGGGGCGAACAAGC	−1	–
	17a_10	TGCTGAGCGGGATCATCGACGGGCTG–ACGGGGCGAACAAGC	−1	–
T_2	17a_10_1,2,4,5,10	TGCTGAGCGGGATCATCGACGGGCTG–ACGGGGCGAACAAGC	−1	–
	17a_10_3,6,7	TGCTGAGCGGGATCATCGACGGGCTGAAACGGGGCGAACAAG	+2	–

Figure 23: Inheritance of induced mutations of T_0 plant #17a. The upper part represents the mutation detected in T_0, and below, the sequencing results of T_1 and T_2 are depicted. The individual plant identifiers are given at the left-hand side. The green marked sequence represents the gRNA-specific part of the targeted motif, the blue color indicates the protospacer-adjacent motif (PAM) bound by the Cas endonuclease. Deletions are highlighted with red hyphens, and inserted nucleotides with red letters. The respective numbers of modified nucleotides (in bp) and information on transgenicity are given to the right of the mutant sequences.

4.5.3.5 Progeny analysis of (homozygous) T_0 plant #21A

T_0 plant #21A detected as one nucleotide insertion, which is +A. The randomly selected ten T_1 plants displayed the same mutation was seen in their T_0 mother plant (Figure 24), which indicates the homogenous state already in T_0.

| Generation | Plant code | | target motif 4 | | PAM | | InDels | T-DNA |

```
Generation  Plant code                target motif 4        ✂        PAM              InDels  T-DNA
   T₀        WT   GAACAAGCATGCGCGGCTCAAGGGCACGGTGGTGCTCATGCG
             21a  GAACAAGCATGCGCGGCTCAAGGGCAACGGTGGTGCTCATGC           +1       +

   T₁   21a_1to10 GAACAAGCATGCGCGGCTCAAGGGCAACGGTGGTGCTCATGC           +1       +
```

Figure 24: Inheritance of induced mutations of T_0 plant #21a. The upper part represents the mutation detected in T_0, and below, the sequencing results of T_1. The individual plant identifiers are given at the left-hand side. The green marked sequence represents the gRNA-specific part of the targeted motif, the blue color indicates the protospacer-adjacent motif (PAM) bound by the Cas endonuclease. Inserted nucleotides are highlighted with red letters. The respective numbers of modified nucleotides (in bp) and information on transgenicity are given to the right of the mutant sequences.

4.5.3.6 Summary of the progeny analysis

Majority of the plants followed a similar trend of T_0 plant #4a with regards to mutation. However, few plants exhibited another trend. For instance, Plant #06 detected as 30 BP deletion in T_0, the progeny analysis reveals that 50% of the plants contain the same mutation as shown in T_0, reaming 50 % plants exhibited wild-type alleles. Summary of the progeny analysis is listed in table 5.

Table 5: Overview of mutations patterns obtained.

		T_0			T_1		T_2
Target motif	Plant code	Mutation detected			Mutation detected	PCR for T-DNA	Mutation detected
2	1a	+1	+T		1P (+A); 1P (+G)	2+	
2	1d	-16/+2	-TCGACGGGCTGACGGG/+CT		1P -16,+2	1+	
2	1e	+1	+T		1P (+G) *	1-	10P +G *
2	4a	+1	+G		8P (+G); 1P (+C),1P (-TGA)	3-; 7+	
3	10a	+1	+A		7P (+A); 1P (+AA); 2P (-AA)	1-; 9+	10P +A*
3	10c	-34	-CATCAGCGAGTTCCTCGGCAAGGGGGTCACCTGC	8P (-35) ; 2P (-A)	1-; 9+	10P -35 BP*, 10 -A*
3	11b	-1	-A		8P (-A); 2P (-GGCAA)	3-; 7+	10P -GGCAA*, 10P -A*
3	13a	-24/+6	-		5P (-24/+6); 2P (+A); 3P (-18/+7);	3-; 7+	40P -24, +6*
3	15d	+2	+AA		9P(+AA);1P(+A)	1-; 9+	20P +AA*
3	17a	+1	+A		GGCAA)	3-; 7+	
4	21a*	+1	+A *		10 +A*	10+	10P +A*
4	23a	-2	-CA		7P(-CA); 2P(+A)	2-; 8+	10P -CA*
4	26b	+1	+T		9P(+T);1P(-A)	3-; 8+	20P +T*
4	6	-29	-CATGCGCGGCTCAAGGGCACGGTGGTGCT	5P(-30); 5(WT)	2-; 8+	

P= plants, (8P means 8 plants);

* =homozygote;

+/- = T-DNA positive/negative (PCR analysis).

4.5.4 Maize transformation using combined gRNAs

Cas9/gRNA transformation using the gRNAs individually resulted in efficiently mutated plants. In addition, the feasibility of mutating two target motifs by simultaneous expression of gRNAs was explored. To this end, the transformation procedure was performed by mixing

51

Agrobacterium strains harboring different gRNA constructs at 1:1 ratio for co-transformation. In particular, vectors with target motif 2 and target motif 3, target motif 3 and target motif 4, as well as target motif 2 and target motif 4 were considered. Co-transformation experiment has resulted in less mutagenesis efficiency in comparison to individual Cas9/gRNA expression system. Overview of the transformation is listed in Table 6.

Table 6: Summary of stable maize co-transformation using Cas9/gRNA constructs.

	target motif 2 and 3 (pNB103 and pNB104)	target motif 3 and 4 (pNB104 and pNB105)	target motif 2 and 4 (pNB103 and pNB105)
No. of I.E agro infected	186	143	129
Regenerent plants produced	48	30	16
Regeneration effiency (%)	26%	21%	12%
Regenerants tested for the presence of T-DNA	48	30	16
PCR positive plants for cas9	44	28	15
HPT positive plants	45	28	15
gRNA2 positive plants	31	NA	11
gRNA3 positive plants	19	14	NA
gRNA4 positive plants	NA	21	4
Plants used to sequence the target	48	30	30
Plants with conclusive target sequence	41	27	27
No. of plants contain mutations for both target motifs	1	1	1
Total no. of plants mutated	37	24	15

4.5.4.1 Detection of mutations in primary T_0 transgenic plants of co-transformation experiment

The mutations were detected in the respective target motives for the co-transformation experiment of target motif 2 and target motif 3. In one plant (#18) mutations were detected in both target motives, with a deletion of 8 nucleotides at target motif 2 and one nucleotide insertion at target motif 3 (Figure 25A).

Co-transformation experiment for target motif 4 and target motif 3 also resulted mutations at individual target motives and mutations for both target motives (4 and 3). Particularly one plant (#114), with a mutation of one nucleotide insertion at target motif 4 and 39 nucleotides deletion at target motif 3 (Figure 25B).

Co-transformation experiment for target motif 2 and target motif 4 produced only few plants and the mutations were detected at individual target motives. The mutations for both target motives were detected in one plant (#216a) which was the deletion of 33 nucleotides and the insertion of 10 nucleotides. Detected T_0 mutation for the co-transformation experiments were described in detail in Figure 25C.

A Plant code   target motif 2   ✂ PAM   target motif 3   ✂ PAM   InDels

```
A  Plant code    target motif 2      ✂   PAM        target motif 3        ✂   PAM     InDels
        WT  GGGATCATCGACGGGCTGACGGGGGC (91BP) ATCAGCGAGTTCCTCGGCAAGGGGGT
         1  GGGATCATCGACGGGCTGACGGGGGC (91BP) ATCAGCGAGTTCCTCGGCA--GGGGT    -2
         2  GGGATCATCGACGGGCTGTACGGGGG (91BP) ATCAGCGAGTTCCTCGGCAAGGGGGT    +1
        11  GGGATCATCGACGGGCT--CGGGGGC (91BP) ATCAGCGAGTTCCTCGGCAAGGGGGT    -2
        18  GGGATCATCGA-------CGGGGGC (91BP) ATCAGCGAGTTCCTCGGCAAAGGGGG    -8/+1
        19  GGGATCATCGACGGGCTGAACGGGGG (91BP) ATCAGCGAGTTCCTCGGCAAGGGGGT    +1
        23  GGATCATCGACGGGCTGATGCGGGGG (91BP) ATCAGCGAGTTCCTCGGCAAGGGGGT    +2
        31  GGGATCATCGACGGGCTGACGGGGGC (91BP) ATCAGCGAGTTCCTC----GGGGT       -5
        35  GGGATCATCGACGGGCTGACGGGGGC (91BP) A---------------------T      -24
        36  GGGATCATCGACGGG----GGGGGC (91BP) ATCAGCGAGTTCCTCGGCAAGGGGGT    -5

B              target motif 4      ✂   PAM        target motif 3        ✂   PAM     InDels
        WT  ATGCGCGGCTCAAGGGCACGGTGGT (58BP) ATCAGCGAGTTCCTCGGCAAGGGGGT
       101  ATGCGCGGCTCAAGGGCTACGGTGG (58BP) ATCAGCGAGTTCCTCGGCAAGGGGGT    +1
       102  ATGCGCGGCTCAAGGGCAACGGTGG (58BP) ATCAGCGAGTTCCTCGGCAAGGGGGT    +1
       107  ATGCGCGGCT-----------GCTG (58BP) ATCAGCGAGTTCCTCGGCAAGGGGGT    -44/+13
       111  ATGCGCGGCTCAAGGG--CGGTGGT (58BP) ATCAGCGAGTTCCTCGGCAAGGGGGT    -2
       114  ATGCGCGGCTCAAGGGCATCGGTGG (58BP) ATCAGCGAGTTCCTC----------    +1/-39
       126  ATGCGCGGCTCAAGGGCACGGTGGT (58BP) ATCAGCGAGTTCCTCGGC-AGGGGGT    -1
       128  ATGCGCGGCTCAAGGGCACGGTGGT (58BP) ATCAGCGAGTTCCTCGGCTAAGGGGG    +1
       129  ATGCGCGGCTCAAGGGCACGGTGGT (58BP) ATCAGCGAGTTCCTCGGCAAGGGGGTC   +1

C              target motif 2      ✂   PAM        target motif 4        ✂   PAM     InDels
        WT  GGATCATCGACGGGCTGACGGGGGGCGAACAAGCATGCGCGGCTCAAGGGCACGGTGGT
       201  GGATCATCGACGGGCTGAACGGGGGGCGAACAAGCATGCGCGGCTCAAGGGCACGGTGG   +1
       202  GGATCATCGACGGGCTGTACGGGGGGCGAACAAGCATGCGCGGCTCAAGGGCACGGTGG   +1
       209  GGATCATCGACGGGCTGACGGGGGCGAACAAGCATGCGCGGCTCAAGGGCAACGGTGG   +1
       210  GGATCATCGACGGGCTGACGGGGGCGAACAAGCATGCGCGGCTCAAGGGC-CGGTGGT   -1
      216a  GGATCATCGACGGGCTGA--------------------------------ACGGGGG   -33/+10
```

Figure 25: Mutations detected in primary transgenic plants of co-transformation experiment. Sequencing results of selected primary transgenic plants for target motif 2 and 3(A), 4 and3 (B), 2 and 4 (C). The sequence marked in green represents the gRNA-specific part of the targeted motif, the blue color indicates the protospacer-adjacent motif (PAM) which is bound by the Cas endonuclease. Plant identifiers given at the left-hand side, deletions are highlighted with red hyphens and inserted nucleotides with red letters, numbers of modified nucleotides (in bp) are given on the right side of the sequences.

4.5.4.2 Analysis of T_1 siblings derived from T_0 plants mutated in two target motifs

T_1 plants were obtained by self-pollinating the mutated primary transformants #18, #35, #43 and #114 to examine inheritance and segregation pattern of mutations. To this end, twelve plants per cob were analyzed.

For the case of plant #18 the detected mutation in T_0 was small fragment deletion (-8) for target motif 2 and insertion (+1) at target motif 3. The detected mutation in T_0 was inherited into the analyzed progeny. Plants do not display any wild-type and new mutation, which indicates that the plant was homozygous for the mutation. The PCR analysis of T-DNA (*cas9/hpt*) unveils four among twelve plants were negative. This indicates that the transgenes (*cas9, hpt*) segregated

independently from the mutations. The T0 plant #35 detected 23 nucleotides deletion at the target motif 3, no mutation at target motif 2. Progeny analysis revealed that 8 plants exhibited the same mutation as detected in T0, four plants turned out to be a new mutation at the targetmotif3 position such as (-35/+14). Four plants lost T-DNA during segregation. No new mutations were detected for the target motif 2 (Figure 26A). For plant #43 no mutation detected in primary T0 plant, but the plant was T-DNA (Cas9, gRNA2, gRNA3, HPT), therefore the plant continued further generation with the assumption of producing mutations in the next generation. Among 12 grains potted, only five plants were germinated. Interestingly all the five plants were efficiently mutated in both g RNA positions. For the target motif 2 one nucleotide insertion (+T) and for the case of target motive 3, two nucleotides deletions were detected. Detailed mutation sequences were listed in Figure 26B.

For T0 plant #114 detected mutation is one nucleotide insertion at target motive 4, 39 nucleotides deletions for target motif 3. The progeny analysis revealed that 7 plants among 12exhibited same mutations as detected in T0. Five plants exhibited new mutation such as one base insertion at target motif 4, two nucleotides deletions at target motif 3 sequences were listed in Figure 26C.

Figure 26: Inheritance of induced mutations of co-transformation experiment. The upper part represents the mutation detected in T0, and below, the sequencing results of T1 are depicted. The individual plant identifiers are given at the left-hand side. The green marked sequence represents the gRNA-specific part of the targeted motif, the blue color indicates the protospacer-adjacent motif (PAM) bound by the Cas endonuclease. Deletions are highlighted with red hyphens, and inserted nucleotides with red letters. The respective numbers of modified nucleotides (in bp) and information on transgenicity are given to the right of the mutant sequences.

4.6 Determination of plant resistance by infection with *C. graminicola*

4.6.1 *lox3* mutants are more resistant to *C. graminicola* than wild-type plants

An experiment was carried out to determine how maize *lox3* mutant plants behave in terms of defense against *C. graminicola* infection. Several homozygous mutant T_2 lines (each derived from a homozygous T1 line) with different types of allelic mutations were infected. WT and *lox3* mutant leaves were inoculated by drop inoculation. Disease symptom development such as lesion area was monitored. Figure 27A shows a clear difference in the severity of *C. graminicola* infection between WT and *lox3* mutant plants. This observation was further corroborated by quantification of fungal biomass using qPCR as is shown in Figure 27B. There was significantly less fungal biomass in the *lox3* mutants in comparison to the wild-type control. The alleles of the tested mutants are depicted in the Figure 27C.
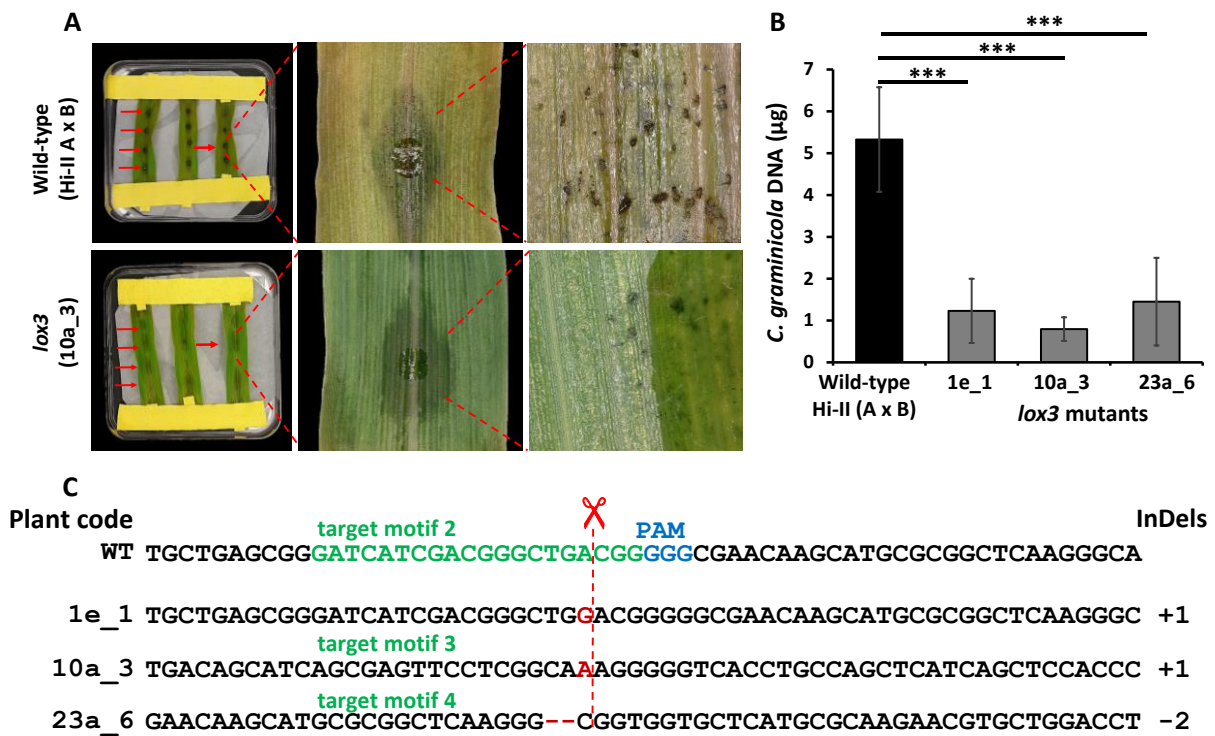
Figure 27: Quantitative protection from *C. graminicola* leaf infection of *lox3* mutants. (A) Detached leaf assays with *C. graminicola* Symptoms occurring at 4 dpi. Red arrow marks indicate infected area. (B) Results of qPCR using 10 ng of total DNA as template. Columns represent means of three independent experiments. Each pool comprised twelve leaf discs excised from individual leaves carrying a single inoculation site. Three asterisks correspond to a significant difference to the wild-type control at P < 0.001 (one-way ANOVA with post-hoc Tukey honestly significant difference). Bars represent standard deviation. (C) Mutant genotypes of resistant plants comprising independent knockout alleles which lead to quantitative resistance to *C. graminicola* infections.

4.7 *U. maydis* infection disease symptoms quantification

Few infection experiments were carried out with a mixture of *U. maydis* FB1 and FB2 strains and several others with the solo-pathogenic fungus SG200. For all these strains, the disease symptoms were scored 8 days post inoculation as described by Kämper et al. (2006). Symptoms were illustrated and described in Figure 28.
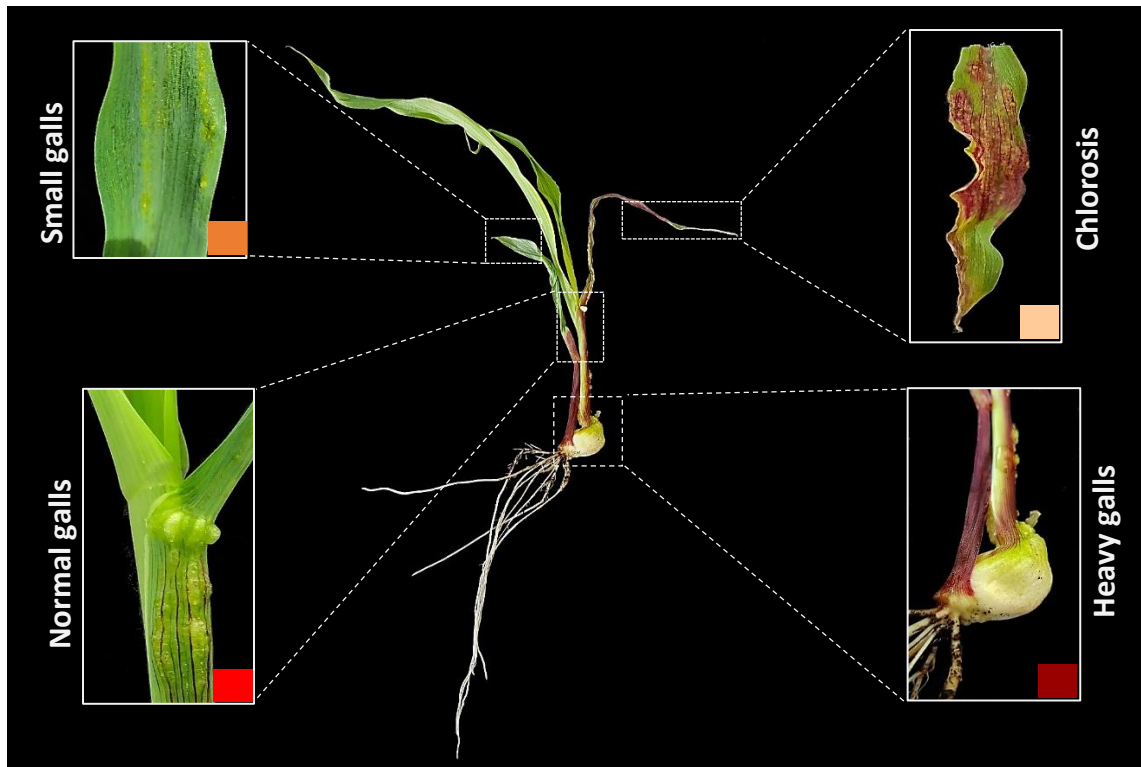
Figure 28: Visual disease symptoms caused by *U. maydis and* scoring at 8 days post-inoculation

No symptom: The plant shows no signs of infection

Chlorosis: The plant shows chlorotic discoloration of the infected leaves

Small galls: The largest galls of the plant are <1.5 mm

Normal galls: Galls of the plant are 2-4 mm in diameter

Heavy galls: Very strong galls associated curvature of the stem axis

Stunted: Stunted growth of stem

Dead plant: The plant is dead and looks necrotic after infection with *U. maydis*

4.7.1 Hi-II A x B is susceptible to *U. maydis* infection

Before using *lox3* mutants for the analysis of their effect on the interaction of maize with *U. maydis*, it was crucial to examine the infection potency of this fungus towards the Hi-II (A x B) hybrid, because the mutations had been generated in this genetic background. To this end, Hi-II (A x B) was compared with the B73 which is an often-used standard line for infection studies. Hi-II (A x B) consistently displayed more severe disease symptoms in comparison to B73 as is illustrated in Figure 29A. Quantification of the disease symptoms confirmed these phenotypic observations (Figure 29B). These results demonstrates that Hi-II (A x B) is susceptible to the *U. maydis* infections. Consequently, it was considered suitable for infection studies using *U. maydis*.
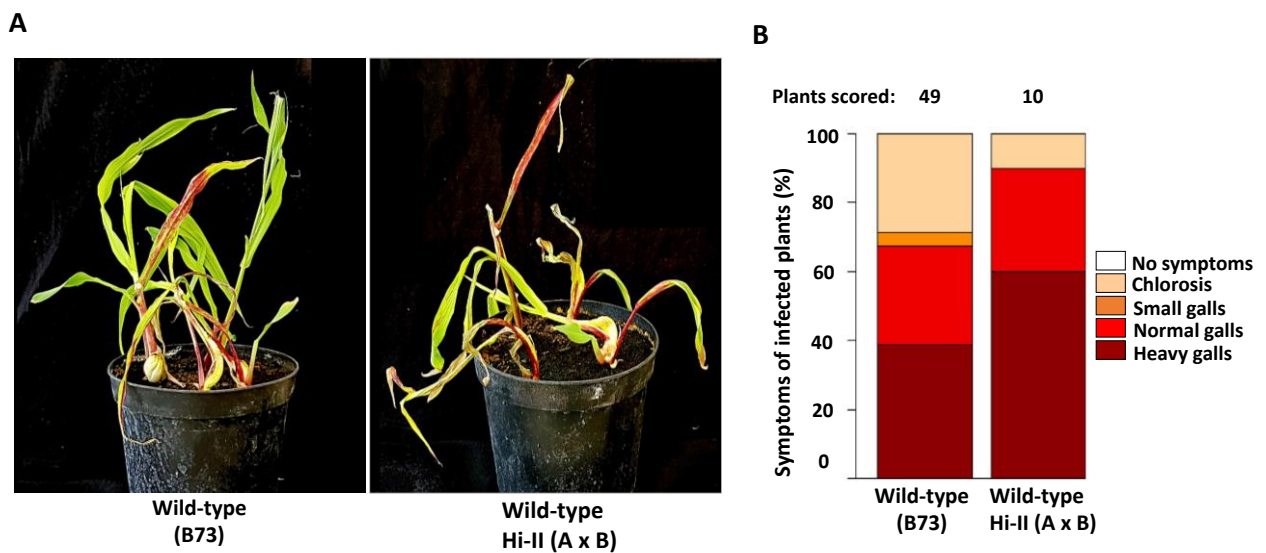
Figure 29: Comparison of wild-type Hi-II hybrid and B73 inbred susceptibility towards *U. maydis*. (A) Typical symptom development 8 dpi. (B) Quantification of infection symptoms on maize seedlings at 8 dpi.

4.7.2 Cas9/gRNA-induced *lox3* mutants show moderate resistance to *U. maydis* infection

An experiment was carried out to determine whether maize *lox3* mutant plants are more susceptible to *U. maydis* infection than their wild-type counterparts. For this purpose, several independent, homozygous T_2 lines (each derived from a homozygous T_1 line) were used. The infection studies usually required a large number of siblings. Therefore, a preliminary experiment was conducted with small scale, which indicated the visual and quantifiable differences between wild-type and mutant (Supplemental Figure 4). For the first large scale experiment, line #13a_8 tested, which is carrying an in/del mutation involving a 24-nucleotide deletion and a 6-nucleotide insertion. The plants were infected with engineered solo-pathogenic *U. maydis* strain SG200. One week after injection of the fungal cell suspension, disease symptoms ranged from chlorosis, light swelling up to heavy gall formation on all aerial parts of the maize plants. Disease symptoms were scored at 8 days post-inoculation (dpi). The size and shape of the galls remarkably varied between the wild-type and mutant plant (Figure 30A). Mutant siblings were less susceptible to *U. maydis* infections than the wild-type, as is shown by the quantification of symptoms in (Figure 30B), while the *lox3* allele of the used knockout line is depicted in Figure 30C.
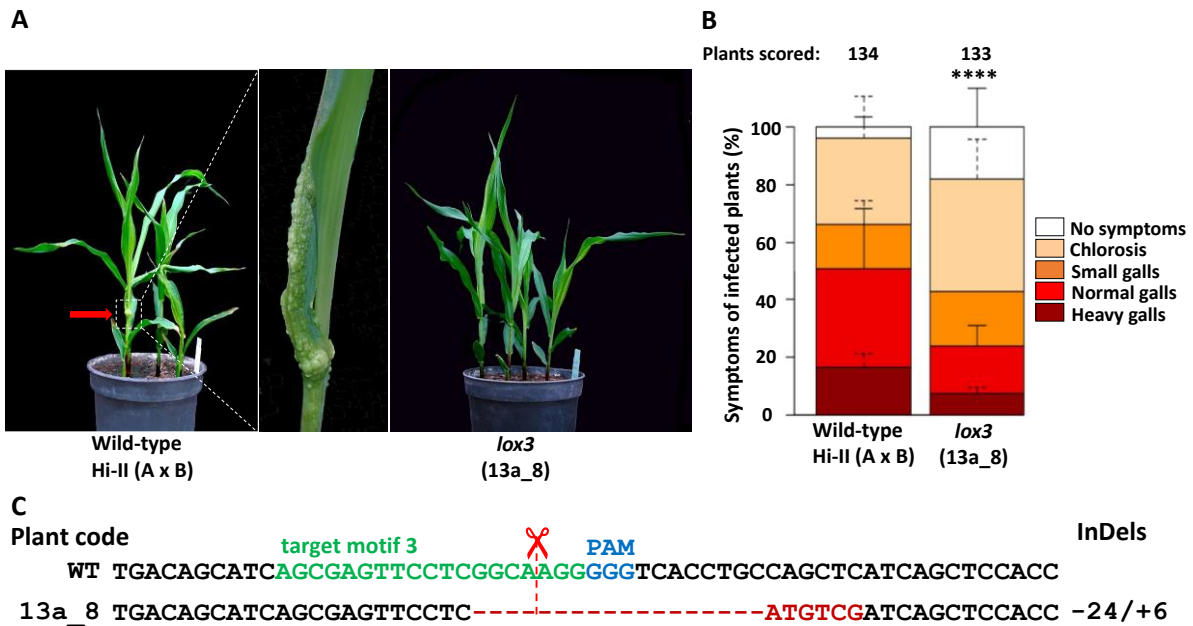
Figure 30: Disease rating of plants infected with *U. maydis*. (A) Phenotype of *lox3* mutants and WT plants in response to *U. maydis* infection. Heavy gall formation, as indicated by a red arrow, was observed significantly more frequently on wild-type than on *lox3* mutant plants. (B) Corn smut disease rating on wild-type vs. *lox3* mutant maize as scored 8 dpi. Mean standard deviation of relative counts from 3 replicates are displayed. *P-values* were calculated by Fishers exact test. Multiple testing correction was done by the Benjamini-Hochberg algorithm. **** indicate significant differences as compared with wild-type at the level of p<0.0001. (C) Mutation in *lox3* of the maize line used for the disease rating assays.

4.7.3 Screening of further *lox3* (Cas9/gRNA-induced) mutants for resistance against *U. maydis*

Given the results from only one *lox3* knockout line, further different types of mutations (Figure 31A) were subjected for *U. maydis* infections to access their response. All the tested mutant plants exhibited similar and significant decrease in disease severity (Figure 31B). According to the disease scoring, Cas9/gRNA-induced *lox3* mutants with different allelic variations were considered as moderate resistant to *U. maydis* infections.

A

```
Plant code                                      ✂                              InDels
                  target motif 3            PAM
        WT TGACAGCATCAGCGAGTTCCTCGGCAAGGGGGTCACCTGCCAGCTCATCAGCTCC
     10c_1 TGACAG----------------------------------CAGCTCATCAGCTCC    -34
     11b_9 TGACAGCATCAGCGAGTTCCTCGGC-AGGGGGTCACCTGCCAGCTCATCAGCTCC    -1
     15d_8 TGACAGCATCAGCGAGTTCCTCGGCAAAAGGGGGTCACCTGCCAGCTCATCAGCT    +2
```

B
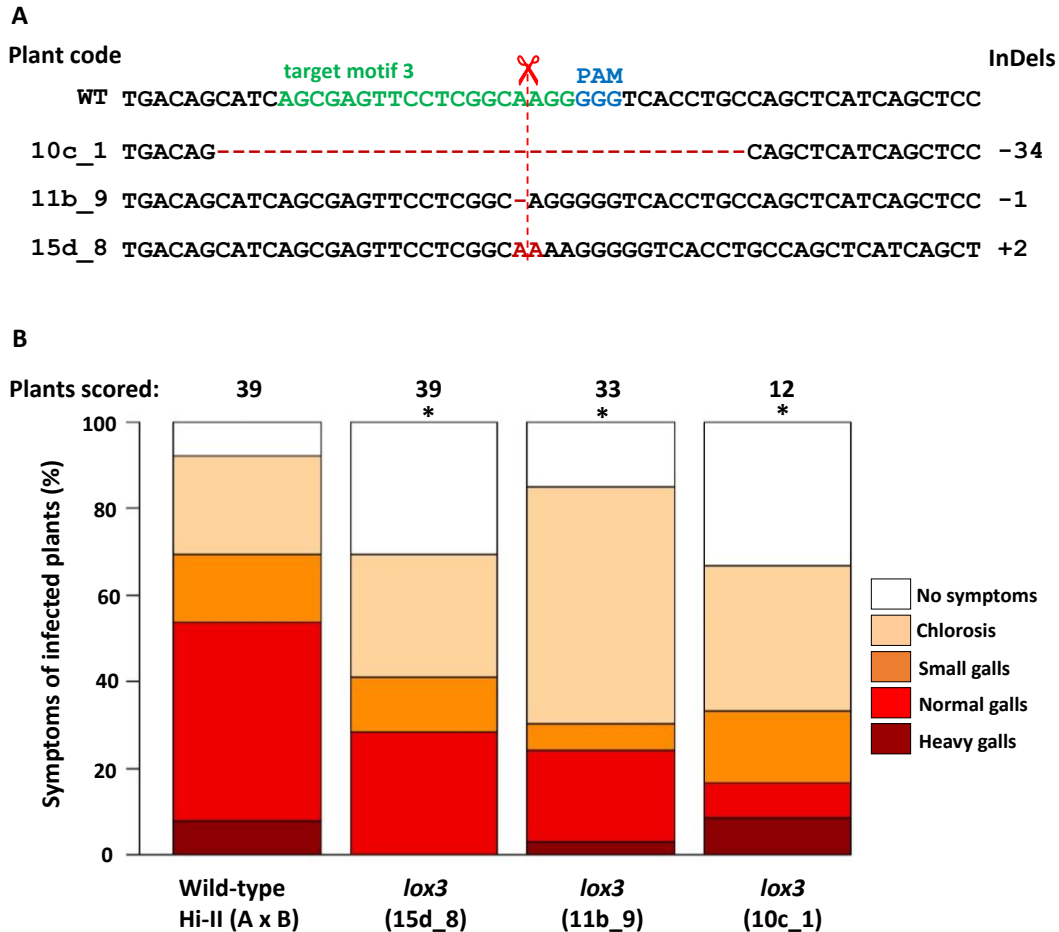
Figure 31: Disease rating of three independent mutant plants infected with the solo-pathogenic *U. maydis* strain SG200 eight days post-inoculation (dpi). (A) Maize mutant lines used for the disease rating assays. (B) Corn smut disease rating on wild-type vs. Cas9/gRNA-induced *lox3* mutant maize as scored at 8 dpi. *P-values* were calculated by Wilcoxon rank-sum test. Multiple testing correction was done by the Benjamini-Hochberg algorithm. * indicates significant differences as compared with wild-type at the level of p<0.05.

4.7.4 Confirmation of moderate resistance of maize *lox3* mutants to *U. maydis* by analysis of a transposon insertion line

Given the resistance of the Cas9/gRNA-induced *lox3* mutants, infection carried out with a transposon insertion maize *lox3* knockout mutant line with *U. maydis* (Figure 32A). The generation of maize insertional mutants was previously described by Gao et al. (2007). B73 was used as a wild-type control since the mutant had been generated in this background. Infection assays were performed with the solo-pathogenic fungus SG200. Eight days post-inoculation, the disease scoring was performed. Disease symptoms were notably different between wild-type and mutant as is represented in Figure 32B. The scoring results unveiled that heavy symptoms did occur significantly less frequent in the mutant plants as compared to wild-type. In comparison to wild-type, mutant plants were also significantly more asymptomatic. Briefly, mutant plants exhibited significantly less disease symptoms in contrast to wild-type (Figure 32C). According to disease scoring, *lox3* mutants can be considered as moderate resistant to *U. maydis* infections. The analysis of the transposon insertional mutant provided convergent evidence for significant disease resistance of *lox3* mutants.
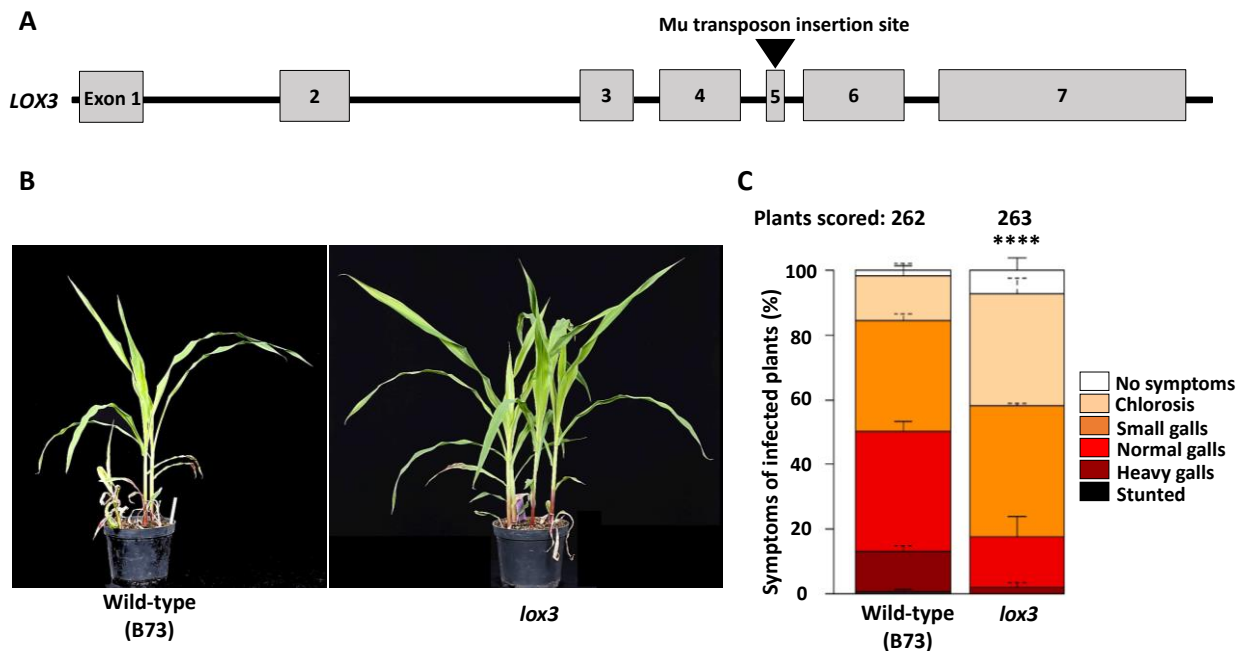
Figure 32: Disease rating of wild-type and transposon insertion *lox3* mutant lines infected with the solo-pathogenic *U. maydis* strain SG200 8 days post-inoculation. (A) Schematic of the *Mutator* transposon insertion site in *LOX3* (adapted from Gao et al. 2007). (B) Phenotype of *lox3* mutants and WT plants in response to *U. maydis* infection. (C) Corn smut disease rating on wild-type vs. *lox3* mutant (generated via transposon insertional mutation) in maize as scored 8 dpi. Mean standard deviation of relative counts from 3 replicates are displayed. P-values were calculated by Fishers exact test. Multiple testing correction was done by the Benjamini-Hochberg algorithm. **** indicate significant differences as compared with wild-type at the level of p<0.0001.

4.7.5 Comparison of inter- and intracellular fungal development in wild-type and *lox3* mutant

Confocal microscopy was used to visualize inter- and intracellularly growing fungal hyphae comparing wild-type and *lox*3 mutant plants infected with *U. maydis* (Figure 33). Plant cell walls were stained with propidium iodide (magenta color), and *U. maydis* hyphae were stained with WGA-AF 488 (green colour). Whereas disease symptom scoring shows quantitative differences, microscopy did not reveal any obvious differences in the hyphal structure or the infected tissues when comparing wild-type with *lox3* mutant plants.
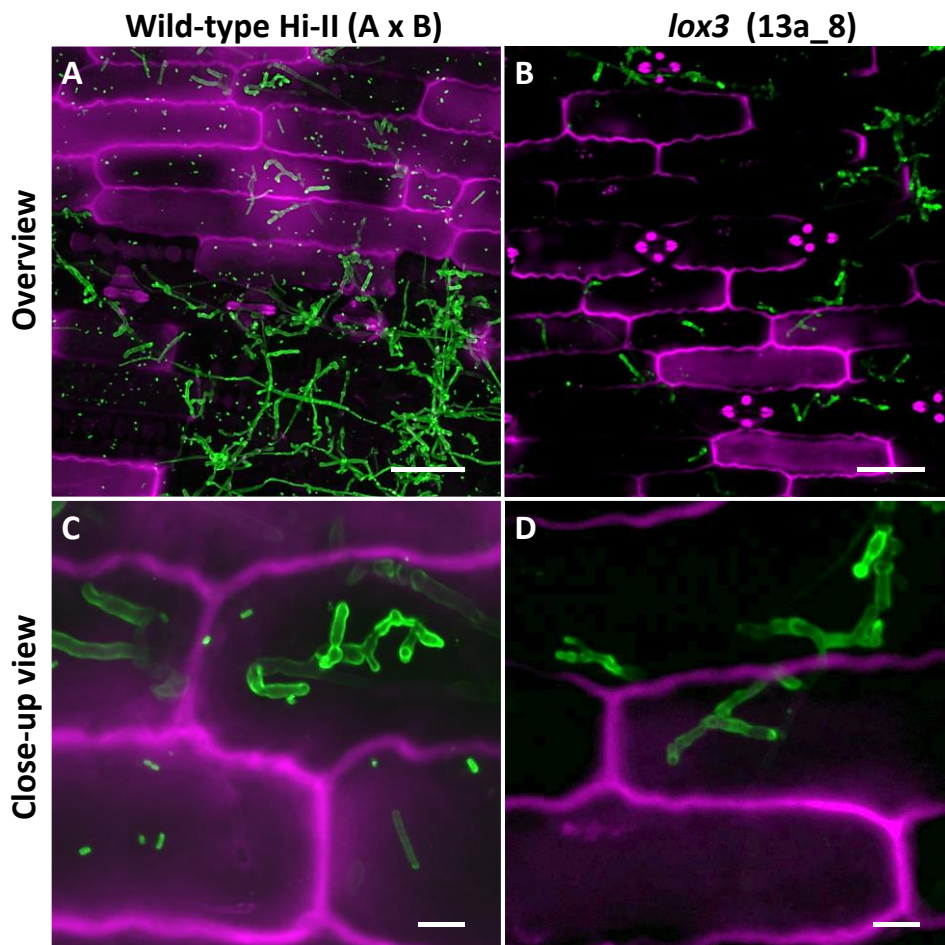
Figure 33: Confocal microscopic examination of *U. maydis*-infected tissue in wild-type (A, C) and *lox*3 mutant (B, D) maize 8 dpi. *U. maydis* invasive inter- and intracellular growth and formation of branching hyphae. Infected plant tissue was stained with propidium iodide (purple) and fungal hyphae with lectin binding WGA-AF488 (green). Scale bars in A, B = 50 µm; scale bars in C and D = 10 µm.

4.7.6 *lox3* mutants exhibit reduced fungal biomass

To test if the observed differences in symptom formation upon *U. maydis* infection of wildtype and *lox3* mutant plants are indeed due to lower colonization by the fungus, a fungal biomass quantification was performed by a qPCR and the amount of fungal genomic DNA is defined in the infected plant tissue. The fungal biomass is significantly less in the *lox3* mutants at 6 and 12 days post inoculation in comparison to wild-type infected maize (Figure 34).
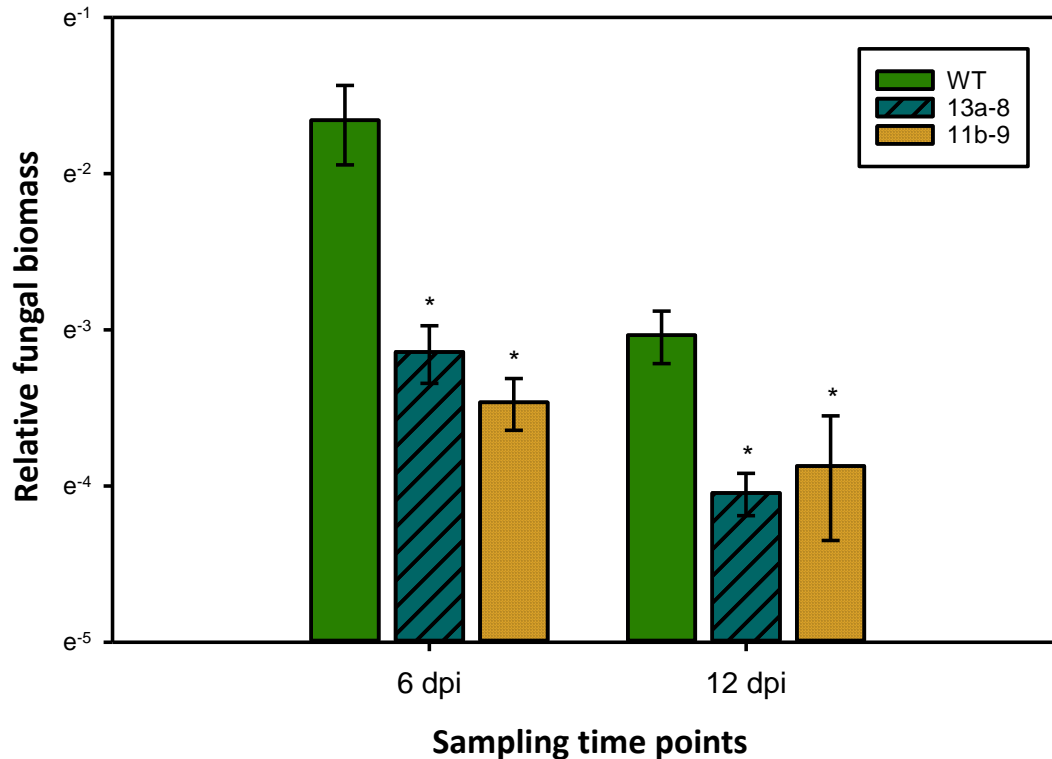
Figure 34: Genomic DNA was extracted from the maize leaves infected with SG200, at 6 and 12 dpi and used for qPCR. Relative fungal biomass was calculated by the comparison between *U. maydis Peptidylprolyl isomerase gene (Ppi)* and *Z. mays GLYCERALDEHYDE 3-PHOSPHATE DEHYDROGENASE GENE (GAPDH)*. Bars indicate standard error. * indicate significant differences between treatments at $p < 0.05$. p-values were calculated by Student's t-test.

4.7.7 *lox3* mutant maize responds with increased ROS accumulation to PAMPs

To find an explanation for the moderate resistance of *lox3* mutant maize towards *U. maydis*, various early host defense responses were tested upon infection with *U. maydis*. One of the first signaling and defense responses that plants activate upon recognition of invading microbes is the accumulation of ROS in the apoplastic space, a process that is usually suppressed by effectors from virulent pathogens (Jones and Dangl, 2006; Dodds and Rathjen, 2010). We assessed the ROS abundance in wild-type and *lox3* mutants in response to the standard PAMP flagellin and *U. maydis* infection. To this end, leaf disks of plants were treated with the PAMP flg22 and ROS production was monitored over 30 to 40 minutes using a luminol-based assay. A clear difference was observed in ROS production; *lox3* mutants exhibited an enhanced PAMP-triggered ROS burst in comparison to the wild-type maize plants. This was observed upon flagellin treatment alone (Figure 35A) and, even more pronounced, in response to additional infection by *U. maydis* (Figure 35B). The enhanced ROS-accumulation in *lox3* mutant maize and the corresponding PTI responses might be the basis of the reduced colonization success of *U. maydis*.
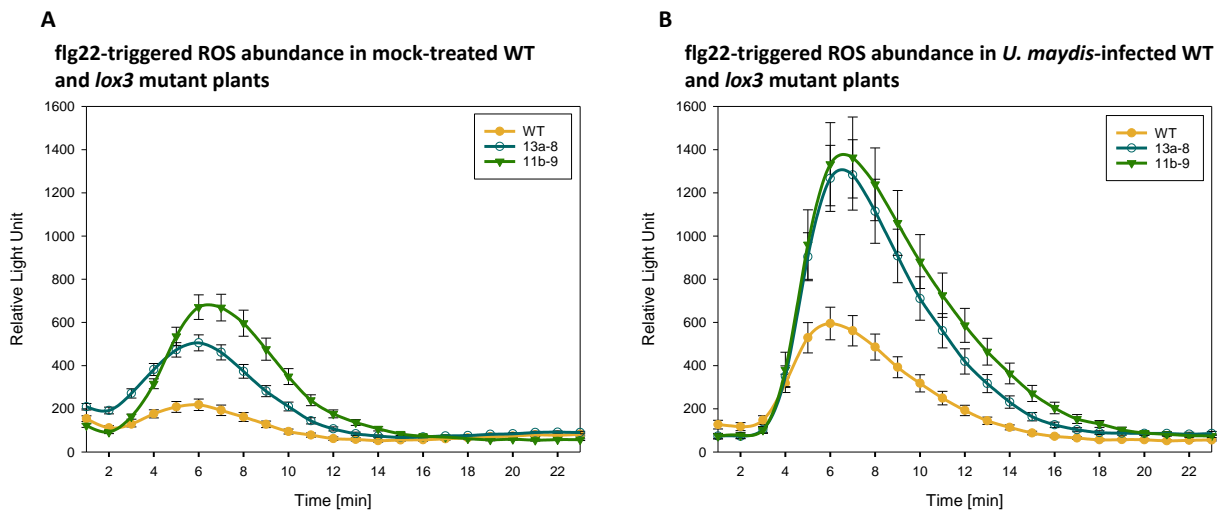
Figure 35: PAMP-triggered ROS accumulation. Figure (A) Curves corresponding to mock. 13a-8, 11b-9 lines show higher ROS burst upon flg22-treatment compared to wild-type. Figure B curves corresponding to *U. maydis* infected 13a-8, 11b-9 lines show higher ROS burst upon flg22-treatment compared to wild-type. Both *lox3* mutants contribute to the flg22-triggered ROS burst response. Shown are the average values of 4 independent experiments, ± standard error of the mean (SEM).

4.7.8 Infection-dependent regulation of selected maize gene expression

To understand the potential cause of the increased resistance to *U. maydis*, expression of *PATHOGENESIS-RELATED* (*PR*) genes were studied since they are induced upon infection. In particular, *LOX*, *12-OXOPHYTODIENOATE REDUCTASE* (*OPR*) and other genes were selected based on the RNA sequencing data from Lanver et al. (2018). The maize *POLYUBIQUITIN 1* gene and the *18S RIBOSOMAL RNA* were used as endogenous controls to normalize the expression values. To understand the transcriptional differences between *lox3* mutant (#13a_8, generated with Cas endonuclease technology) and wild-type, plants were infected with the solo-pathogenic fungus SG200 and water was injected for the case of mock treatment. Plant leaf material was harvested at two time points i.e at 4 days and 8 days post inoculation. At 4 days post inoculation, two leaves (i.e. the 2nd, 3rd) were harvested independently to observe the differential regulation across the leaves. Four independent experiments were performed and for each experiment 20 plants were infected. Usually, *U. maydis* infection varies to some extent even across genetically identical plants. Therefore, ten siblings were pooled into one sample and used for RNA extraction.

4.7.8.1 Infection-dependent regulation of selected maize *PR* gene expression

Many *PATHOGENESIS-RELATED* (PR) genes are induced upon pathogen attack. Hence, they are widely used as marker genes for defense responses in plant-pathogen interactions. To this end, expression of *PR* genes such as *PR1*, *PR3*, *PR4, and PR5* were quantified in response to *U. maydis* infections. Selected four *PR* genes were upregulated in two different leaves upon *U. maydis* infection in comparison to the mock-inoculated wild-type. Transcripts of *PR3*, *PR4* were significantly upregulated in two different leaves, whereas in the case of *PR1* it was significant only in the second leaf in comparison to the wild-type (Figure 36A).

Given the transcript upregulation results from infected wild-type plants, the comparative data of wild- type mock versus mutant mock treatments were further generated in order to investigate the mutant background for infection-independent particularities. The selected *PR* genes were downregulated in the mock-inoculated lox3 mutant. Transcripts of *PR4*, *PR3* were significantly downregulated in the second and third leaf respectively (Figure 36B).

To examine the behavior of *PR* transcripts in the *lox3* mutant plants upon *U. maydis* infection, transcripts were measured and compared with the wild-type-infected plants. *PR1*, *PR4*, *PR3* transcripts were upregulated in third leaf and *PR3* was significant (Figure 36C). For 8 dpi *PR1*, *PR3*, *PR4* transcripts were down-regulated and *PR1* was significant. *PR5* transcripts were upregulated (Figure 36D).
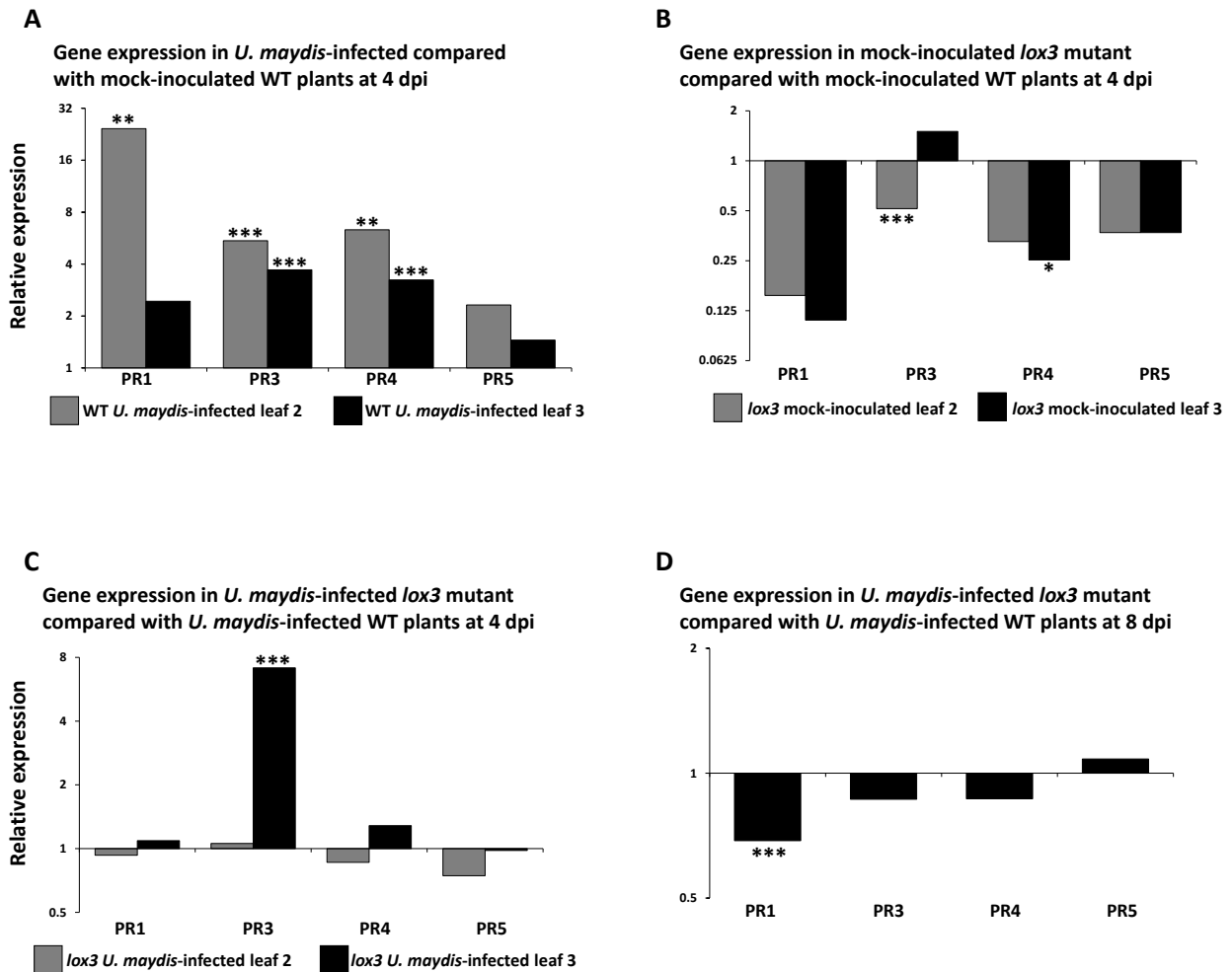
Figure 36: Differential expression of selected pathogenesis-related genes. (A) Gene expression in *U. maydis*-infected compared with mock-inoculated WT maize, with the expression level of the latter being set to 1 (4 dpi). (B) Gene expression in mock-inoculated *lox3* compared with mock-inoculated WT maize (4 dpi), (C) Gene expression in *U. maydis*-infected *lox3* compared with *U. maydis*-infected WT maize (4 dpi). (D) Gene expression in *U. maydis*-infected *lox3* compared with *U. maydis*-infected WT maize (8 dpi). Gray color indicates second leaf transcripts, black color indicates third leaf transcripts. Asterisks indicate significant differences from the corresponding control (***, P < 0.001, **p<0.01,*p<0.5), Statistical analysis of RT-qPCR was performed using the R-Macro (Steibel et al., 2009).

4.7.8.2 Infection-dependent regulation of selected maize *LOX* gene expression

Several *9LOX* genes, namely *LOX1*, *LOX2*, *LOX3* and *LOX5*, were shown to be upregulated in response to *U. maydis* infection by transcriptional time course data ((Doehlemann et al., 2008). Given the expression of these genes, further looked at the expression of all *9-LOX* genes which comprise *LOX1*, *LOX2*, *LOX3*, *LOX4*, *LOX5*, *LOX6* and *LOX12* as well as the 13*LOX* members *LOX8*, *LOX9*, *LOX10* and *LOX11* in mutant and wild-type plants responding to *U. maydis* infection.

Transcripts of *LOX1*, *LOX2*, *LOX3*, *LOX4* and *LOX9* were significantly upregulated in two different leaves of *U. maydis* infected, in comparison to the mock-inoculated wild-type. Transcripts of *LOX8 is* significantly upregulated in second leaf. Transcripts of *LOX6* is significantly down regulated in third leaf. Transcripts of *LOX5* and *LOX12* exhibited a similar tendency of upregulation in two different leaves, which was however not significant. These results indicate, predominant *LOX*s were upregulated with the *U. maydis* infection (Figure 37A).

Transcripts of *LOX2*, *LOX3*, and *LOX11* were significantly down-regulated in two different leaf tissues of mock-inoculated *lox3* mutants in comparison to mock-inoculated wild-type. Furthermore *LOX10, LOX12* transcripts were down regulated in third leaf. These results indicate the majority of the lox transcripts were down-regulated in the mutant background (Figure 37B). Transcripts of *LOX1*, *LOX8*, and *LOX9* were induced in two different *U. maydis* infected leaves, but only the second leaf demonstrated significant upregulation of the transcripts. Transcripts of *LOX4, LOX6* significantly upregulated in third leaf (Figure 37C). For 8DPI, transcripts of *LOX1, LOX2, LOX3, LOX11* significantly down-regulated) in comparison to the wild-type infected (Figure 37D).

A

Gene expression in *U. maydis*-infected compared with mock-inoculated WT plants at 4 dpi

WT *U. maydis*-infected leaf 2
WT *U. maydis*-infected leaf 3

B

Gene expression in mock-inoculated *lox3* mutant compared with mock-inoculated WT plants at 4 dpi

lox3 mock-inoculated leaf 2
lox3 mock-inoculated leaf 3

C

Gene expression in *U. maydis*-infected *lox3* mutant compared with *U. maydis*-infected WT plants at 4 dpi

lox3 U. maydis-infected leaf 2
lox3 U. maydis-infected leaf 3

D

Gene expression in *U. maydis*-infected *lox3* mutant compared with *U. maydis*-infected WT plants at 8 dpi

Figure 37: Differential expression of *LOX* genes. (A) Gene expression in *U. maydis*-infected compared with mock-inoculated WT maize, with the expression level of the latter being set to 1 (4 dpi). (B) Gene expression in mock-inoculated *lox3* compared with mock-inoculated WT maize (4 dpi), (C) Gene expression in *U. maydis*-infected *lox3* compared with *U. maydis*-infected WT maize (4 dpi). (D) Gene expression in *U. maydis*-infected *lox3* compared with *U. maydis*-infected WT maize (8 dpi). Gray color indicates second leaf transcripts, black color indicates third leaf transcripts. Asterisks indicate significant differences from the corresponding control (***, P < 0.001, **p<0.01,*p<0.5), Statistical analysis of RT-qPCR was performed using the R-Macro (Steibel et al., 2009).

4.7.8.3 Infection-dependent regulation of selected maize *12-OXOPHYTODIENOATE REDUCTASE (OPR)* gene expression

Given the differential expression of *LOXs*, the downstream genes Of *LOXs* such as *OPR* (*12-oxo-phytodienoic acid reductases*) were further studied. Literature indicates that *LOXs* were also involved in jasmonic acid (JA) biosynthesis. Besides this some *OPR* have the substrate specificity and are part of the octadecanoid pathway which converts linolenic acid to the phytohormone JA. Given this information, the transcriptional behavior of selected *OPR* genes were further studied (i.e. *OPR2*, *OPR5*, *OPR6*, *OPR7*, and *OPR8*).

Transcripts of *OPR2*, *OPR8* were significantly upregulated in two different leaves of *U. maydis* infected wild-type in comparison to mock-inoculated wild-type. *OPR5*, *OPR7* were also upregulated in both leaf tissues but this was not significant. *OPR6* transcripts were down regulated and this was significant in the third leaf. Results indicate that the majority of *OPRs* (except *OPR6*) were upregulated with the infection of *U. maydis* (Figure 38A).

Transcripts of *OPR2*, *OPR5* were downregulated, *OPR5* was significant in the third leaf of mock-inoculated mutant compared to mock-inoculated wild-type. *OPR6*, *OPR7* have exhibited the same trend of transcriptional behavior such as upregulation in the third leaf and down-regulation in the second leaf, *OPR6* was significant in the third leaf. Transcripts of *OPR8* were upregulated in two different leaves and the third leaf was significant (Figure 38B).

Transcripts of *OPR2*, *OPR5* and *OPR7* were upregulated in the mutant infected plants in comparison to the infected wild-type and *OPR5*, *OPR7* were significant in the second leaf. *OPR6*, *OPR8* exhibited the same trend of transcriptional behavior i.e. downregulation in the second leaf and upregulation in the third leaf and both were not significant. Results indicate that the selected *OPRs* were upregulated in the third leaf of a mutant plant at 4dpi (Figure 38C). For 8 dpi transcripts of *OPR2*, *OPR5*, *OPR8* were downregulated and *OPR2* was significant (Figure 38D).
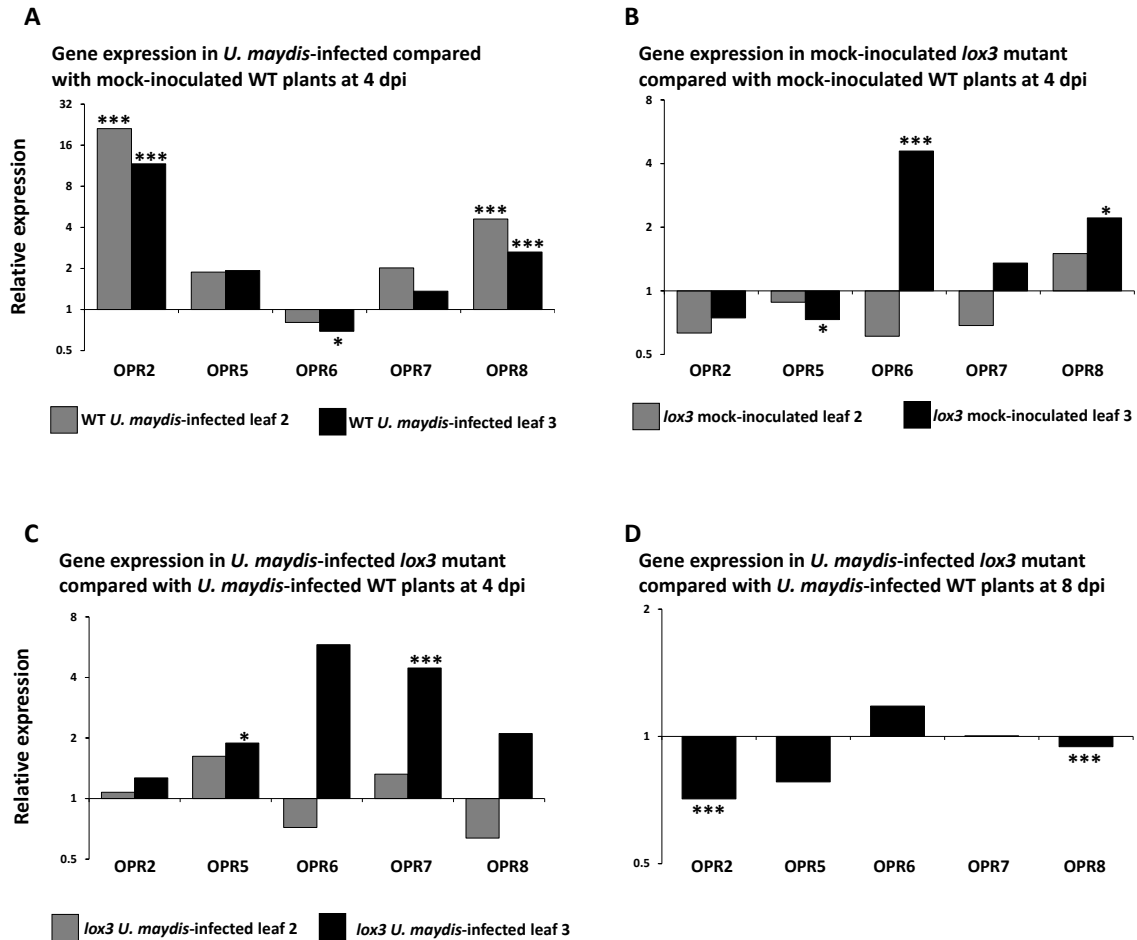
Figure 38: Differential expression of selected *12-OXOPHYTODIENOATE REDUCTASE (OPR)* genes. (A) Gene expression in *U. maydis*-infected compared with mock-inoculated WT maize, with the expression level of the latter being set to 1 (4 dpi). (B) Gene expression in mock-inoculated *lox3* compared with mock-inoculated WT maize (4 dpi), (C) Gene expression in *U. maydis*-infected *lox3* compared with *U. maydis*-infected WT maize (4 dpi). (D) Gene expression in *U. maydis*-infected *lox3* compared with *U. maydis*-infected WT maize (8 dpi). Gray color indicates second leaf transcripts, black color indicates third leaf transcripts. Asterisks indicate significant differences from the corresponding control (***, P < 0.001, **p<0.01,*p<0.5), Statistical analysis of RT-qPCR was performed using the R-Macro (Steibel et al., 2009).

4.7.8.4 Infection-dependent regulation of selected maize gene expression

Transcripts of *CORN CYSTAIN9 (CC9), PHENYLALANINE AMMONIA-LYASE (PAL), PATHOGENESIS-RELATED MAIZE PROTEIN (PRM3), MAIZE PROTEINASE INHIBITOR (MPI), ALLENE OXIDE SYNTHASE (AOS), GLUTATHIONE S-TRANSFERASE (GST), CYTOCHROME P450* and *HYDROLASE (HYD)*, were measured since these genes have the putative association to JA or induced upon pathogen.

Transcripts of *p450, PAL1, PRM3, CC9, GST2, HYD* were significantly upregulated in two different leaf tissues of *U. maydis* infected in comparison to the mock-inoculated wildtype. Transcripts *ACX* were upregulated third leaf. Results indicate that the majority of the selected gene transcripts were induced with *Ustilago* infection (Figure 39A).

P450, PRM3 transcripts were significantly down-regulated in two different leaf tissues of mock-inoculated mutant in comparison to the mock-inoculated wild-type. *PAL, CC9, GST2* downregulated in third leaf, but not significant. Transcripts of *ACX, HYD* significantly upregulate in second leaf of mock-inoculated mutant in comparison to the mock-inoculated wildtype (Figure 39B).

Transcripts of *PAL, MPI, CC9*, and *HYD* were significantly upregulated in the mutant-infected second leaf in comparison to the infected wild-type. Transcripts of ACX were upregulated in second leaf, and downregulated in third leaf significantly (Figure 39C). For the 8 dpi transcripts of *MPI* is upregulated and all other transcripts were down-regulated, none of them were significant (Figure 39D).

A

Gene expression in *U. maydis*-infected compared with mock-inoculated WT plants at 4 dpi

P450 PAL1 PRM3 MPI ACX AOS CC9 GST2 HYD

■ WT *U. maydis*-infected leaf 2   ■ WT *U. maydis*-infected leaf 3

B

Gene expression in mock-inoculated *lox3* mutant compared with mock-inoculated WT plants at 4 dpi

P450 PAL1 PRM3 MPI ACX AOS CC9 GST2 HYD

■ *lox3* mock-inoculated leaf 2   ■ *lox3* mock-inoculated leaf 3

C

Gene expression in *U. maydis*-infected *lox3* mutant compared with *U. maydis*-infected WT plants at 4 dpi

P450 PAL1 PRM3 MPI ACX AOS CC9 GST2 HYD

■ *lox3 U. maydis*-infected leaf 2   ■ *lox3 U. maydis*-infected leaf 3

D

Gene expression in *U. maydis*-infected *lox3* mutant compared with *U. maydis*-infected WT plants at 8 dpi
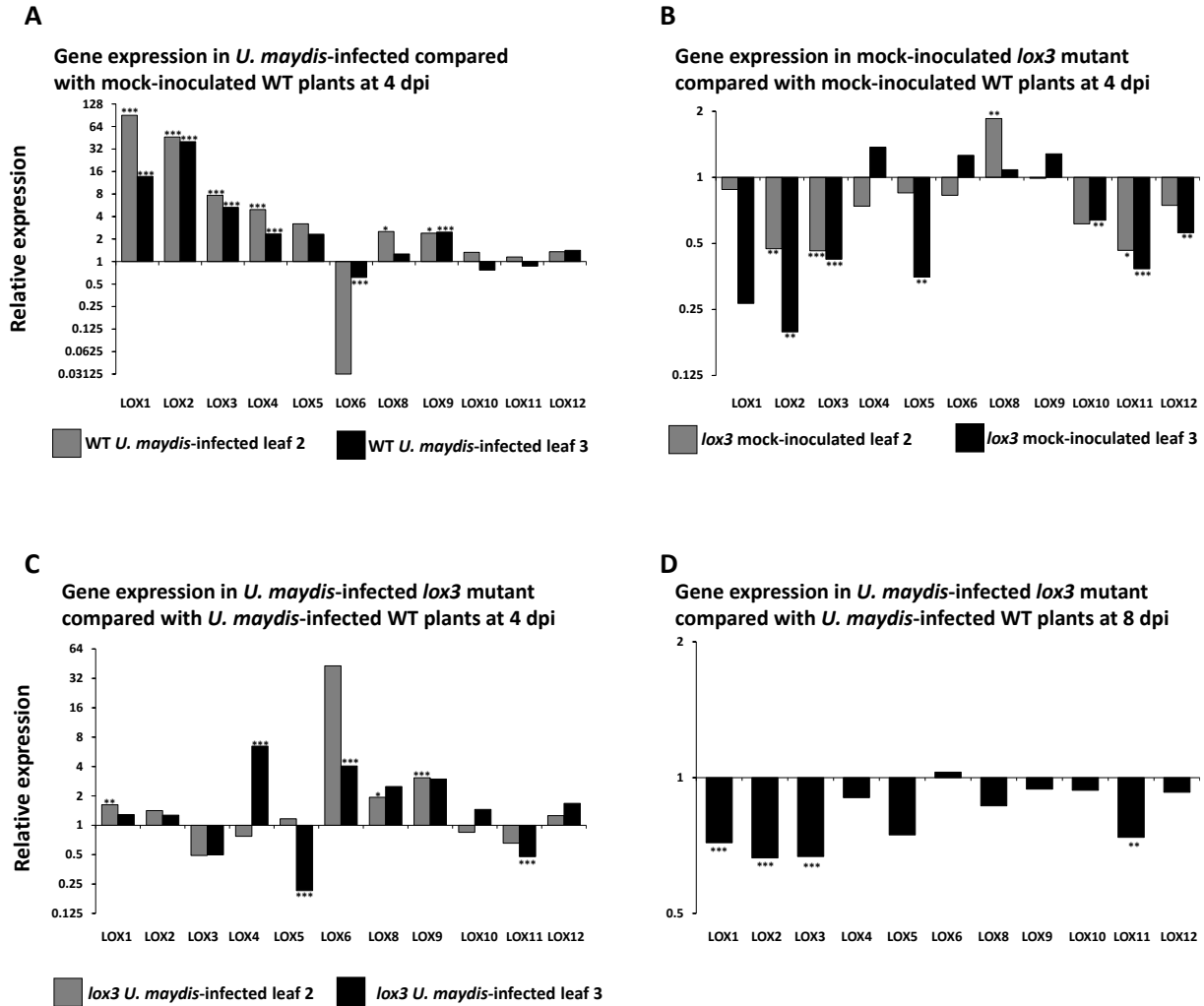
P450 PAL1 PRM3 MPI ACX AOS CC9 GST2 HYD

Figure 39: Differential expression of selected genes. (A) Gene expression in *U. maydis*-infected compared with mock-inoculated WT maize, with the expression level of the latter being set to 1 (4 dpi). (B) Gene expression in mock-inoculated *lox3* compared with mock-inoculated WT maize (4 dpi), (C) Gene expression in *U. maydis*-infected *lox3* compared with *U. maydis*-infected WT maize (4 dpi). (D) Gene expression in *U. maydis*-infected *lox3* compared with *U. maydis*-infected WT maize (8 dpi). Gray color indicates second leaf transcripts, black color indicates third leaf transcripts. Asterisks indicate significant differences from the corresponding control (***, $P < 0.001$, **$p<0.01$,*$p<0.5$), Statistical analysis of RT-qPCR was performed using the R-Macro (Steibel et al., 2009).

4.7.9 Callose deposition investigation in wild-type and *lox3* mutants in response to *U. maydis* infection

Given the results from PAMP triggered ROS burst assay, further investigation was carried out to assess callose deposition in the maize *lox3* mutants. Typically callose formation is an important aspect of development and plant response to stress conditions (Verma and Hong, 2001). Callose deposition does not seem to be enhanced in *U. maydis* infected *lox3* mutants in comparison to wild-type counterpart. One day after *U. maydis* infection, leaf segments from wild type and *lox3* mutant maize lines were stained with aniline blue for detection of callose deposition events (Figure 40).
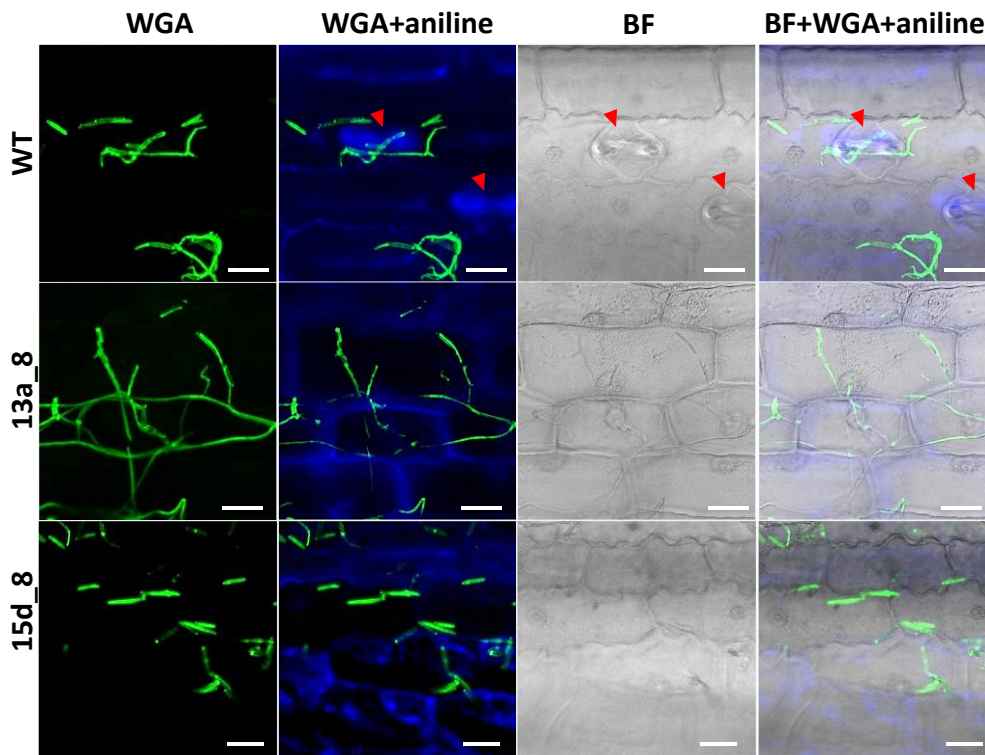
Figure 40: Fungal hyphae were visualized by Alexa Flour WGA treatment. Pictures of WGA and aniline blue channels represent projections of confocal z-stacks. Brightfield (BF) pictures are single optical sections from the same respective z-stacks. Scale bars represent 20 µm. Extensive aniline blue staining of callose depots in vascular tissue (asterisks) and stomata (arrowheads) are marked exemplary.

5. Discussion

5.1 Host-induced gene silencing-based resistance to maize anthracnose

Plant pathogenic fungi are a constant and major threat to global food security; they represent the largest group of disease-causing and the most devastating agents for crop plants on our planet. Thus, protection of plants against pathogenic fungi is one of the major challenges. Maize is one of the most cultivated crops in the world. On a worldwide scale, pathogen causes approximately 75 million metric tons yield losses annually. Most notable diseases are maize anthracnose and corn smut. Given the information, the present investigation was aim to establish disease resistance in maize plants by using host-induced gene silencing (HIGS) and Cas endonuclease technology.

HIGS is an RNAi-based mechanism. In this process, small RNAs are produced by the transgenic plants. The resulting small RNAs silence the gene-specific transcripts of the pathogen that attack.

Plants have evolutionarily acquired an immune system based on their gene silencing machinery to defend themselves against invading viruses (Csorba et al., 2009; Harvey et al., 2011; Hu et al., 2011). Based on this feature, HIGS was developed (Huang et al., 2006). The principle of HIGS has been intensively used to control the fungal pathogens of wheat and barley *Puccinia species, Blumeria graminis,* and *Fusarium species* (Nowara et al., 2010; Koch et al., 2013; Pliego et al., 2013; Cheng et al., 2015; Chen et al., 2016; Zhu et al., 2017b; Panwar et al., 2018; Qi et al., 2018). In rice, it was showed against *Magnaporthe oryzae* (Zhu et al., 2017a). Further, this technology has been used in other plants species such as banana, tomato, and potato (Dou et al.; Jahan et al., 2015; Song and Thomma, 2018). Remarkably, this technology is well proven in maize against the fungal pathogen *Aspergillus flavus* that causes aflatoxin contamination. Therefore, millions of tons of maize are lost globally, and the consumption of contaminated food and feed constitutes a critical health issue for humans and livestock (Wu, 2006; Thakare et al., 2017).

The selection of candidate genes is very crucial for the success of HIGS approaches. In theory, any essential gene of the pathogen can be used to produce plants that show resistance. However, previous work of PRB (working group) and others has shown that for some reason, only a few of the pre-selected candidate genes eventually prove useful (Baum et al., 2007). The rational of the present project is that fungicide targets have been comprehensively pre-evaluated as being indispensable for pathogenicity. Therefore, in the present investigation, fungicide targets genes were used as prime candidates for particularly effective HIGS approaches. To this end, *C. graminicola β-Tubulin* (*β-Tub*) and *Succinate dehydrogenase* (*Sdh*) were used as potential candidate genes, since they are the targets of fungicides such as benzimidazoles and boscalid respectively (Hollomon et al., 1998; Ma and Michailides, 2005; Zou et al., 2006; Xiong et al., 2015). Typically, orthologues of these genes do exist in maize as well, which is why it is essential to find target regions showing sufficient sequence diversity as

compared to their hosts' counterparts to avoid off-target effects. To find out the sequence diversity, NCBI-blast analysis was performed and revealed sequence similarity at the nucleotide level of 82% for β-Tub2, 81% for Sdh1, 85% for Sdh2. By contrast, no hits were found for Sdh3 and 4. Similarly, blast-based sequence analysis performed by Govindarajulu et al. (2015) for the case of developing downy mildew resistance in lettuce plants. Downy mildew in lettuce is caused by *Bremia lactucae*, a biotrophic oomycete. In this approach, several vital genes from the pathogen were selected and the absence of stretches of 14 nucleotides or more in the lettuce genome was confirmed to minimize off-target effects. For the case of developing aflatoxin resistance in maize, Thakare et al. (2017) targeted *A. flavus Polyketide synthase* (*PksA*) by an HIGS approach. To this end, a detailed bioinformatics analysis was performed to confirm that *A. flavus* do not have any notable DNA sequence homology with the maize genome. Furthermore, Yin et al. (2011) selected an RNAi target region specific to the rust fungus *Puccinia striiformis* to avoid unspecific silencing of wheat genes for developing stripe rust-resistant in wheat plants. Given the sequence homology, in the present study, 5'-untranslated regions (UTR) and 5'-ends of the coding sequence were targeted, to take advantage of their diversity to the respective host sequences. Several RNAi-based studies used UTR regions to control diseases in mammalian systems, for instance, Hepatitis C virus (HCV), the major causative agent of liver associated diseases. To this end, siRNAs were designed to target the 5'-UTR region, which resulted in 80% suppression of HCV replication (Yokota et al., 2003). Khaliq et al. (2011) demonstrated a dramatic reduction of mRNA and protein levels by targeting the HCV 5'-UTR. A study from Raheel and Zaidi (2014) showed that targeting the 5'-UTR region with siRNAs is a promising strategy to control the dengue disease. Similar results were reported by Deng et al. (2012) for the case of Enterovirus 71 (EV71). In the present research, to increase the formation of siRNAs, the target sequences were cloned three times into the IPKb vectors. The IPKb vectors were developed in the PRB group of IPK to facilitate RNAi-based studies (Himmelbach et al., 2007; Kumlehn, 2008). They were tailored for cereal transformation. A detailed description of the vectors can be found by Kumlehn (2008). These vectors were used in several studies, notably to control fungal diseases in barley and wheat (Nowara et al., 2010; Chen et al., 2016). Selected 5'-UTR regions were synthesized into entry vectors and cloned into IPKb (destination) vectors via LR Gateway cloning reaction. Nowara et al. (2010) used IPKb based vectors for *B. graminis* target gene *Avra10*. Later, Chen et al. (2016) used fragments of the *F. culmorum β-1,3-Glucan synthase* gene (*Gls1*) in IPKb vectors.

To achieve the transgenic plants in order to expressing hairpin expression units, it is very important to select the maize genotype that is amenable to genetic transformation studies. For this purpose, the Hi-II A x B hybrid is used. It has the ability to produce type-2 rapidly growing callus, which is an excellent explant source for maize transformation studies (Armstrong et al., 1991; Jones, 2009; Que et al., 2014). Given the information, stable maize genetic transformation was performed with Hi-II A x B F_1 embryos (Hi-II A used as female and Hi-II B used as male) as

described by Hensel et al. (2009). In a similar HIGS approach for developing aflatoxin resistance of maize, Thakare et al. (2017) used the same Hi-II A x B hybrid.

The level of resistance varies between genotypes (Weihmann et al., 2016). Therefore, it is essential to screen the genotypes for its susceptibility. To this end, an infection test was carried out with *C. graminicola* comparing Hi-II A x B, Golden Jubilee (super susceptible) and Mikado (standard susceptible cultivar) (Weihmann et al., 2016) by quantified fungal biomass with qPCR (Weihmann et al., 2016). The results indicated that the Hi-II A x B susceptibility levels are similar to Mikado. It is a standard method to quantify the fungal biomass with qPCR in maize-*Colletotrichum* infection studies, since it is difficult to judge the infection symptoms on a visual basis. A detailed explanation of the methodology is very well described by Weihmann et al. (2016) by comparing several maize accessions. Several other studies also used qPCR-based assays to access the infection rate (Brouwer et al., 2003; Gachon and Saindrenan, 2004; Silvar et al., 2005). For instance, it has been shown that the quantification of fungal DNA is an accurate measure of the disease severity of *Pyrenophora tritici-repentis* (See et al., 2016) and *Stagonospora nodorum* (Oliver et al., 2008). In maize, Mitema et al. (2019) quantified *A. flavus* biomass with a qPCR-based assay.

In the present investigation, homozygous plants were produced for single, double and multiple T-DNA copies. The number of transgene copies can be positively or negatively associated with transgene expression (Hobbs et al., 1993), thus T-DNA copy numbers were assessed in transgenic plants using DNA gel blot analysis. In this study, infection tests were conducted with several homozygous RNAi events to access its resistance towards *C. graminicola*. To this end Hi-II A x B azygous wild-type plants (derived from the same tissue culture procedure) being used as control.

The results illustrate that a few RNAi transgenic events exhibited lower fungal biomass as compared to the azygous wild-type control. For instance, #E-25-2 exhibited significantly reduced fungal biomass, whilst events #E-118-2, #E-6-2, #E-1-5 showed only a tendency of less fungal growth. Events #E-1-5, #E-6-2, #E-25-2 were derived from the transformation using the vector pNB97. This vector targets the fungal *Sdh1*, and the sense and antisense sequences are driven by double enhanced CaMV 35S promoter. Events #E-1-5, #E-6-2 and #E-25-2 had one, two and three T-DNA copies, respectively. Quantification results indicated that plants with three copies had a significantly stronger resistance that those with one or two copies. More copies likely provide more abundant siRNAs which down-regulated Sdh efficiently in *C. graminicola.* In agreement with this speculation, Ku et al. (1999) experimentally achieved higher transcript abundance with a high copy number. Besides this, Zuo et al. (2016) reported gene dosage-dependent expression pattern of small RNA transcripts in maize. HIGS based quantitative resistance was demonstrated by several authors in several plant species. For instance, *B. graminis* is the powdery mildew fungus that infects cereal crops and thereby causes significant yield losses. Transgenic barley and wheat engineered to express dsRNA targeting *Glucanosyltransferase* genes, which resulted in reduced disease symptoms (Nowara et al.,

2010). Further, the HIGS strategy was also used to silence the fungal effector gene *Avra10* in *Mla10* mutant lines of barley which showed reduced fungal development. Later, Koch et al. (2013) reported HIGS directed to the fungal *Cytochrome P450 lanosterol C-14α-demethylase* (*Cyp51*) gene to limit the growth and development of *F. graminearum* on barley plants. In maize, the HIGS strategy was used to knock-down transcription factor (*AflR*) and polyketide synthase (*PksA*) of *A. flavus*, which are regulators of the aflatoxin biosynthetic pathway (Masanga et al., 2015; Thakare et al., 2017). The expression of the hairpin construct directed against *AflR* in transgenic maize plants resulted in 14-fold reduced aflatoxin levels when the *A. flavus* strain colonized the plants (Masanga et al., 2015). Thakare et al. (2017) also produced transgenic maize lines carrying RNAi cassettes that simultaneously targeted three regions of *AflC*. The transgenic lines infected with an *A. flavus* strain displayed no aflatoxin production. In addition, *Alpha-amylase* gene expression (*Amy1*) in *A. flavus* was suppressed in maize by expressing an RNAi construct against *Amy1*, resulting in reduced fungal colonization and decreased aflatoxin production (Gilbert et al., 2018).

Event #E-2a-3 derived from transformation using pNB96 which targets fungal *β-Tub*2, with the hairpin construct being driven by a doubled enhanced CaMV 35S promoter. This event does not show any difference compared to the wild-type. Transgenic events #E-119-4, #E118-2 and #E-125-3 derived from transformation using pNB98 targeting *β-Tub*2, with the hairpin construct being driven by maize Ubi-1 promoter. Event #E-118-2 exhibited less fungal growth compared to the wild-type, but not significant. Events #E-119-4 and # E125-2 exhibited similar fungal biomass like wild-type. These results co-inside with the those of Govindarajulu et al. (2015) who targeted several fungal genes with RNAi to provide resistance to downy mildew of lettuce, caused by *Bremia lactucae.* One of these target genes as *β-Tub* which was not effective in causing resistance. The maize transformation experiment using with pNB99 vectors initially failed to produce regenerants, thereby, RNAi expressing events derived from pNB99 will be used in future infection experiments.

To our knowledge, this is the first report to demonstrate that silencing of *C. graminicola Sdh1* leads to quantitative resistance of maize towards the anthracnose disease. Selected transgenic events will be tested in field-like conditions to access the durability of the resistance. According to the EU law,
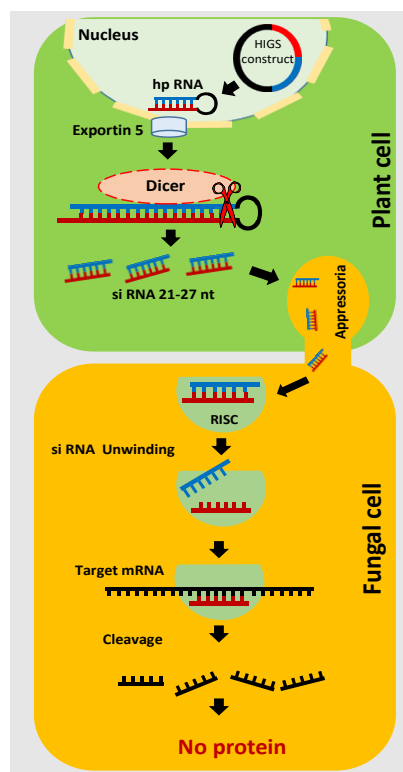
Figure 41: Proposed working model. Plant-made small RNAs silence gene-specific products of *C. graminicola* transcripts.

the developed transgenic material falls into the category of genetically modified organisms (GMOs), whereas validated candidate genes and target sequences can be used in the spraying induced gene silencing (SIGS) approach which may not fall in GMO category.

5.2 RNA guided Cas endonuclease - the new era of genome engineering

In addition to the HIGS approach, another strategy was pursued, which is site-directed mutagenesis. As a part of this strategy, the current study aim to knock out the host susceptibility factor maize *9-LIPOXYGENASE* (*LOX3*) by Cas endonuclease technology. This technology has evolved as a particularly powerful means to improve crop plants through site-directed genome modification (Kumlehn et al., 2018). This method has been successfully employed in almost all important crop species, for instance, wheat, rice, cassava, maize (Connorton et al., 2017; Nieves-Cordones et al., 2017; Odipio et al., 2017; Shi et al., 2017; Wang et al., 2017; Mao et al., 2018).

5.2.1 Knock out of *LOX3*

Maize *LOX3* is proven to be a susceptibility factor for *C. graminicola* infections (Gao et al., 2007). Therefore it was targeted in the present study by Cas endonuclease technology, which may provide resistance. Theoretically, any part of the gene can be potentially used as a target region for site-directed mutagenesis approaches. In the current investigation, first exon region was targeted. In several other reports, the first exon was chosen as target site to mutate (Jansing et al., 2019). The success of the mutation rate is depended of the gRNA. In the present investigation, the DESKGEN online platform knock-in panel (Chandrasekaran et al., 2016; Doench et al., 2016; Gomez et al., 2019) was used to select the gRNAs. This included a detailed off-target analysis, which revealed potential off-targets with a least three base pair mismatches. However, off-target cleavage is very unlikely in motifs with three base pair mismatches. The five gRNAs selected were further validated using the WU-CRISPR (Wong et al., 2015) online tool for the activity score. The selected gRNAs were also compared with each other using the "sgRNA design tool" of the Broad Institute (http://portals.broadinstitute.org/gpp/public/analysis-tools/sgrna-design). This prediction model for gRNA activities was developed based on the investigation of several thousand gRNAs and should improve the selection of these for a specific target sequence (Doench et al., 2016).

5.2.2 Cas9/gRNA transient test system in protoplasts

It is advisable to pre-validate the selected gRNAs to test their efficiency prior to stable genetic transformation, which provides the possibility to choose truly functional and the most efficient gRNAs. To this end, a protoplast transient expression test system was adapted with modifications according to Sheen (1991); Cao et al. (2014); Zhu et al. (2016) in the PRB (working) group. GFP was used as an internal control to validate the incidence of the transformation. High transformation efficiency (more than 90%) was achieved, which is consistent with results from Cao et al. (2014) for maize. Mutations were detected for gRNA target motifs 2, 3 and 4. By

contrast, low and no mutations were detected for target motif 1 and 5 respectively. Zhu et al. (2016) demonstrated the validation of gRNAs in maize protoplasts. Besides this, Lin et al. (2018) defined potential applications of protoplast technology and its validation in several plant species such as *N. tabacum*, bamboo, millet, rice, maize, *Arabidopsis*, broccoli and rapeseed. Given the result from the protoplast assay, gRNA target motif 1 and 5 were not continued further for the stable transformation studies in the present investigation.

5.2.3 Molecular characterization of maize *lox3* mutations

Stable genetic transformation resulted with the mutation efficiency more than 95% for all the target motifs. The achieved efficiencies are on par with the best results reported thus far in maize (Shi et al., 2017). The predominant occurrence of small insertions and deletions amongst the mutations obtained is in accordance with previous work on crop species of the *Poaceae* family as well (Shi et al., 2017; Gerasimova et al., 2020). In general, Cas endonuclease technology could result five genotypes. Namely, homozygous (the two alleles have the same mutation), bi-allele (the two alleles have different mutations), heterozygote (only one allele is mutated), chimera (more than two different mutations exist), and Wild-type (no mutation) (Yang et al., 2017).

5.2.4 Heritability of gRNA/Cas9-induced mutations

Several primary transgenic plants (T_0) with mutations were further grown to next generations to produce homozygous mutations. The progeny analysis of T_0 plants revealed that vast majority of the mutations detected in T_0 were heritable to T_1 (and further) generations. For instance, progeny analysis of plant #21a revealed that, all T_1 siblings contained the same mutation as their mother plant. Progeny analysis indicated that the T_0 mutation was homozygous. A conceivable interpretation for this result is, that, after double-strand break induction, one mutated allele likely served as repair template for the other. A similar phenomenon was reported by Schedel et al. (2017). In the present investigation, new mutation pattern also observed within T_1 siblings. For instance, in plant 4a#, a +G insertion was detected in T_0. Out of 10 analyzed T_1 siblings, eight contained the same mutation. However, the two plants #4a_6, #4a_5 exhibited newly occurring mutations, namely a C insertion and a deletion of 3 nucleotides, respectively. Based on a comparison of plants of T_0 and T_1, the primary T_0 Cas9/gRNA edited line #4a was interpreted as heterozygous. However, heterozygotes carry the wild-type alleles which can still be mutated, as Cas9/gRNA transgenes stay active over generations. These results coincide with findings in *A. thaliana* (Ma et al., 2015), tomato (Pan et al., 2017) and rice (Zhang et al., 2014). In the present investigation, progeny analysis of plant #17a resulted in vast variety of new mutations. In T_0, a +A mutation was detected, whereas the majority of T_1 siblings (7) exhibited a -A, while a +A mutations was found in only one plant and three plants carried mutations (+2, +4, -5) which were not found in T_0. The analysis of T_2 plants of selected self-pollinated T_1 17a_10 mutants showed that new mutations also occurred in the T_2 generation, but the number was lower

compared to the T_1 generation. This is consistent with the results from a progeny analysis in *Arabidopsis* (Feng et al., 2014). This phenomenon speculated, that new mutations were derived from chimeric tissue of T_0 plants which was not represented in the leaf sample used for genotyping of the T_0. Cas9/gRNA can simultaneously or successively produce a number of independent mutation events in different cells of a developing individual as long as the wild-type target region is present in any of the two corresponding gene copies of a diploid species in the G1 phase of the cell cycle or in any of the 4 copies in G2. Coincide with previous work of Yang et al. (2017); Zhang et al. (2020). T-DNA-free mutants were generated by self-pollination, by which valuable material can be provided for crop improvement (Pan et al., 2017). Independent segregation of mutations and T-DNA insertion loci has also been observed in previous investigations in maize and other plants (Schedel et al., 2017; Lee et al., 2019; Li et al., 2019).

5.2.5 Dual gRNA-induced mutations

Genomic deletions have been playing an essential role in plant evolution (Soltis et al., 2014; De Smet et al., 2017). For instance, the spontaneous mutation in the rice *DENSE AND ERECT PANICLE1* (*DEP1)* gene has a 625 bp deletion, which results in upright panicles and increased grain yield (Huang et al., 2009). Likewise, spontaneous deletions in the maize *WAXY* gene alter the starch composition of the grains (Wessler et al., 1990). Therefore, targeted genomic deletions could serve as useful means in modern plant breeding. A single cleavage site typically results in short deletions and/ or insertions, whereas simultaneously addressed pairs of target motifs can result in accordingly large and precisely predictable deletions. For instance, expression of dual gRNAs in soybean resulted in large fragment deletions (Cai et al., 2018b). In each genetic transformation of the present investigation, two gRNAs were combined for a particular target region. Dual gRNA expression resulted in lower mutation frequency (including mutations at the individual cut sites), as compared to individually expressed gRNAs. One possible explanation for this low efficiency is that the DNA cut at each target must be performed simultaneously, and the probability of this occurrence is much lower than asynchronous cuts and repairs at each site. In the present investigation, each of the transformation experiment resulted mutations for only one plant for both target motifs. For instance, plant #18a was mutated at both target motifs at target motif 2 eight bp deletion detected, at target motif 3 one bp insertion detected. A progeny analysis revealed that all T_1 siblings contained the same mutation as their mother plant, indicating its homozygous state for detected mutations. Dual gRNA expression resulted in large deletions. For instance, in plant #216a, a 33 bp deletion was detected which exactly represents the region between the cleavage sites of the two target motifs, while an insertion of 10 bp occurred in addition. These results are consistent with Srivastava et al. (2017), who demonstrated a deletion of the *gus* marker gene in rice by expressing dual gRNAs. Dual gRNA-based deletions were also reported in other plant species,

for instance in barley (Kapusi et al., 2017), tomato (Brooks et al., 2014), *Arabidopsis* (Pauwels et al., 2019) and *Nicotiana tabacum* (Mercx et al., 2017).

5.2.6 *lox3* mutants are more resistant to *C. graminicola*

lox3 mutant plants derived from all 3 gRNAs were tested for their response to *C. graminicola* infections. The selected mutant plants #1e_1, #10a_3 and # 23a_6 contain the mutations +G, +A and -CA. *In silico* analysis revealed a premature stop. The infection assays revealed that the fungal biomass is significantly reduced in the *lox3* mutant plants. A study from Gao et al. (2007) demonstrated similar resistance in maize by mutating *lox3* pursuing a transposon insertional mutation approach. Furthermore, several studies reported *LOX*-based resistance in several plants species such as tobacco (Rance et al., 1998; Cacas et al., 2005), pepper (Hwang and Hwang, 2010) *Arabidopsis* and wheat (Nalam et al., 2012; Nalam et al., 2015).

5.2.7 *lox3* mutants show moderate resistance to *U. maydis*

In the present investigation, a preliminary test revealed that Hi-II-A x B is susceptible to *U. maydis* infections. This test and all further infection and scoring experiments followed the principles established by Kämper et al. (2006), since these are standard in the maize-*Ustilago* pathosystem community. Notably, the test is necessary, since several studies have shown that different *Z. mays* varieties display varying susceptibility to *U. maydis* infection (Stirnberg and Djamei, 2016). For example, Early Golden Bantam (EGB) sweet corn is reportedly more susceptible than field corn to *U. maydis* (Laplace, 1989; Parry, 1990; White, 1999). In the present study, infection assays with *lox3* maize mutants challenged by *U. maydis* revealed that the mutants exhibited moderate resistance, as was seen by comparing the symptom profiles of the mutant plants in comparison to wild-type. Both in-frame and frameshift mutations caused moderate resistance to *U. maydis.* Furthermore, *lox3* transposon insertional mutants also exhibited moderate resistance to *U. maydis*, which provided convergent evidence that *lox3* mutants with different allelic variation and genetic background exhibit the same phenotype. The present investigation confirms the expectation that, *lox3* plants generated by site-directed mutagenesis show moderate disease resistance to *U. maydis* infections as well.

An advantage of using Cas endonuclease technology over former approaches is that background mutations can be ruled out to a great extent. Similarly, Zhang et al. (2017) reported enhanced powdery mildew resistance in wheat by simultaneously targeting the three homoeologs of wheat *ENHANCED DISEASE RESISTANCE1* (*EDR1)*. Nekrasov et al. (2017) demonstrated the knockout of *MILDEW RESISTANT LOCUS O* (*MLO),* which conferred resistance to powdery mildew resistance in tomato. Resistance to powdery mildew was also achieved by targeted mutagenesis of *POWDERY MILDEW RESISTANCE4* (*PMR4*) in tomato (Koseoglou, 2017). Targeted mutagenesis of rice *ETHYLENE RESPONSIVE FACTORS* (*ERF922*) resulted in enhanced resistance against *Magnaporthe oryzae* infections (Wang et al., 2016a). Furthermore, targeting grape transcription factor *WRKY52* demonstrated enhanced resistance to *Botrytis cinerea*

(Wang et al., 2018). In a similar manner, virus resistance was achieved in several plant species by using Cas endonuclease technology (Chandrasekaran et al., 2016; Pyott et al., 2016; Tashkandi et al., 2018; Gomez et al., 2019).

5.2.8 *U. maydis* growth is hampered in the *lox3* mutants

Give the resistance, further investigation was carried out to measure the fungal biomass by qPCR at two time points namely 6 and 12 dpi. The results revealed that the fungal biomass is less in the *lox3* mutant plants in comparison to the wild-type. Decreased fungal biomass correlated with the less symptoms observed in the *lox3* mutants, suggesting that the fungus invasion does not impaired whereas colonization is likely hampered in the *lox3* mutant plants.

5.2.9 *lox3* mutants do not affect the morphology and Inter-intracellular growth of *U. maydis*

Confocal microscopy was used to visualize the fungal growth at the cellular level. The results revealed that the fungal hyphae were growing inter- and intracellularly in both wild-type and *lox3* mutant plants. Therefore, it is postulated that fungal invasion is not hampered in *lox3* mutants and wild-type.

5.2.10 *lox3* mutant plants respond to *U. maydis* by increased production of ROS

Reactive oxygen species (ROS) act as cellular signaling molecules to implement plant immune responses, such as pathogen-associated molecular pattern (PAMP)-triggered immunity (PTI) and effector-triggered immunity (ETI) (Jwa and Hwang, 2017). To stop the fungal spread, the plant accumulates reactive oxygen species (ROS) which promote localized cell death. Plants use this defence strategy against biotrophs and hemi-biotrophs (Constantino et al., 2013; McCormick, 2017). In the present investigation, infected mutant plants exhibited more ROS accumulation as compared to the infected wild-type. This suggests that PAMP-triggered immunity is activated against *U. maydis.* Constantino et al. (2013) reported *lox3* maize mutants (generated via transposon insertional mutagenesis) which accumulated higher levels of ROS in comparison to wild-type at 24 hours post-inoculation with *C. graminicola.* They proposed that the higher accumulation of ROS likely limit the duration of the biotrophic stage of the fungal life cycle during the disease development. This suggests a decisive role of lipoxygenases in the regulation of ROS levels, and that *U. maydis* inhibits the plant ROS accumulation to establish the biotrophic interaction (Molina and Kahmann, 2007; Hemetsberger et al., 2012). Molina and Kahmann (2007) speculated that virulence of *U. maydis* depends on its ability to detoxify ROS. Furthermore, Hemetsberger et al. (2012) experimentally proved that *U. maydis* effector PEP1 (Protein essential during penetration-1) suppresses plant immunity by inhibition of host peroxidase activity. Based on the above-discussed results, it is postulated that the higher accumulation of ROS in *lox3* mutants is the major reason of limited growth of *U. maydis* and the achieved resistance.

5.2.11 Callose deposition is not affected in maize *lox3* mutants

Host deposit the callose as a physical barrier to prevent invading pathogens (Bergstrom and Nicholson, 1999; Luna et al., 2011; Seitner et al., 2018). Given this information, callose deposition was examined. The results revealed that *lox3* mutants doesn't exhibited distinguable differences in callose deposition around the fungal hyphae in comparison to wild-type. This could be due to maize *lox3* mutants may provide the resistance to the *U. maydis* by another mechanism, or aniline blue based callose deposition staining may not sensitive enough to distinguish the little amount of callose deposition.

5.2.12 Infection-dependent regulation of selected genes

Transcriptional time course data from Doehlemann et al. (2008) revealed that several *LOX* genes are upregulated upon *Ustilago maydis* infection. Considering this information, in the present investigation, several *LOX* and other related plant genes that were influenced by *U. maydis* were measured. RNA sequencing data from Lanver et al. (2018) served as a basis to select some candidate genes and to compare the results. These data indicated that transcriptional changes were already induced as early as 24 hours post-inoculation. Inoculations were carried out in a maize variety called Early Golden Bantam with *U. maydis* wild-type strains FB1 and FB2 which are more virulent in comparison to solo-pathogenic SG 200 (Kämper et al., 2006; Djamei et al., 2011; Lanver et al., 2018). In the present investigation, plants were analyzed 4 days post-inoculation, since the solo-pathogenic haploid strain SG200 was used for infection. Transcripts were analyzed in leaf 2 and leaf 3. Transcriptional changes that were analyzed in leaf 3 explained in the discussion, since it is the leaf emerging after inoculation. This may have the appropriate transcriptional changes in response to infection. Using the 8 dpi samples, the study focused only on the transcripts of *U. maydis*-infected *lox3* vs. *U. maydis* infected WT plants.

Pathogenesis-related (PR) proteins are plant proteins that are induced in response to an infection by pathogens (Murillo et al., 1997). Therefore these genes can be used as markers of plant defense responses. To understand transcriptional regulation in *lox3* mutants, transcripts of selected *PR* genes were analysed. In the present investigation, upon *U. maydis* infection, transcripts of *PR1, PR3, PR4 and PR5* were shown to be upregulated. This observation is consistent with the results published by Doehlemann et al. (2008). Maschietto et al. (2016) also demonstrated the upregulation of several *PR* genes after plants had been infected with *F. verticillioides.* Furthermore, pathogen-induced upregulation of *PR* genes was reported in several plant species namely, rice (Mitsuhara et al., 2008) and tobacco (Kim et al., 2015). However, in the non-infected mutant maize plants, all (selected) *PR* genes were down-regulated except *PR3*, while the transcripts of *PR1*, *PR3* and *PR4* were upregulated in infected *lox3* mutants. Gao et al. (2008a) reported expression of *PR1* as a response of a maize *lox3* mutant to infection with the root-knot nematode *Meloidogyne incognita*. However, this

upregulation phenomenon was not seen at 8 dpi in the present study. *LOX3* likely interferes with *PR* genes by an as yet unknown mechanism.

Little is known about the biosynthesis and perception of jasmonic acid in maize. In this context, the best-characterized enzyme family is the *LOX* family, where it has been shown that mutants with loss of function exhibit striking phenotypes such as feminized tassel structures (Acosta et al., 2009) and altered responses to fungal pathogens (Christensen et al., 2013; Christensen et al., 2014). In order to establish the biotrophic relationship *U. maydis* induce JA signaling (Doehlemann et al., 2008; Martínez-Soto and Ruiz-Herrera, 2016). Furthermore, upregulation of *LOX* genes upon infections by several pathogen is very well described in the literature, for instance in maize by Doehlemann et al. (2008) and in *Arabidopsis* and wheat by Nalam et al. (2015). Maize carries 13 *LOX* genes (Ogunola et al., 2017). In this study, except *LOX13* and *LOX7* other transcripts were analyzed. Upon *U. maydis* infection, the majority of the LOX genes were upregulated. However, *LOX6, LOX10 and LOX11* proved to be down-regulated. Maschietto et al. (2015) reported a strong induction of the maize *LOX* genes after *F. verticillioides* infection, indicating their significant role in pathogen interaction. In agreement with this, data from Woldemariam et al. (2018) showed that maize *LOX* genes are induced in feeding experiments using *Spodoptera exigua* (beet armyworm) larvae on maize. A study from Shivaji et al. (2010) reported maize *LOX1* and *LOX3* transcript upregulation upon herbivore feeding. In the present Investigation, transcript measurements of mock-inoculated *lox3* mutants revealed that several *LOX* genes were down-regulated, except *LOX4, LOX6, LOX8 and LOX9*. Given this result, it is speculated that *LOX3* likely regulates other *LOX* genes. In the present investigation, infected *lox3* mutant plants exhibited a down-regulation of *LOX3, LOX5 and LOX11* and an upregulation of *LOX1, LOX2, LOX4, LOX6, LOX8, LOX9, LOX10 and LOX12* at 4 dpi. At 8 dpi, the majority of the *LOX* transcripts were down-regulated in the mutant plants except for *LOX6*. Some of the down-regulated genes were consistent with the previous observation of Battilani et al. (2018) that *LOX1, LOX2, LOX5* were down-regulated in maize *lox3* mutant kernels inoculated with *F. verticillioides.* This indicates that reduced transcript accumulation or limited downstream product formation of the respective genes might resulted in increased resistance.

Lipoxygenases (LOXs) are very well known for their role in JA biosynthesis (Porta and Rocha-Sosa, 2002). 12-oxo-phytodienoic acid reductases (OPRs) catalyze the production of JA from its precursor 12-oxo-phytodienoic acid (OPDA) which is 13-LOX–derived compound (Lyons et al., 2013). *OPR* genes are differentially regulated in response to pathogen infection (Zhang et al., 2005), which is in agreement with the statement that differential regulation of *OPR*s are observed upon *U. maydis* infection. In the present study, transcripts of *OPR2, OPR5, OPR7* and *OPR8* were upregulated, while *OPR6* was down-regulated in *U. maydis* infected maize. Zhang et al. (2005) reported a strong induction of the *OPR2* transcripts when plants had been infected with *F. verticillioides* or *Cochliobolus heterostrophus*. Furthermore, these authors reported that *OPR6, OPR7* and *OPR8* were induced by wounding. Shivaji et al. (2010) experimentally demonstrated the upregulation of *OPR2, OPR6,* and *OPR7* on larval feeding experiments,

postulating their role in JA regulation. *OPR2* and *OPR5* were down-regulated in the mock-inoculated mutants at 4 dpi and in infected mutants at 8 dpi. In the present study, infected maize *lox3* mutant plants exhibited induction of all *OPR* genes at 4 dpi. Based on these results, it is concluded that *LOX3* might have role in the regulation of these genes.

CYTOCHROMES P450 s (P450s) participate in the regulation of jasmonic acid (JA) biosynthesis for plant defense (Xu et al., 2015). In the present investigation, upregulation of *p450* was observed upon *U. maydis* infection. These results are consistent with previous work of Doehlemann et al. (2008). Smigocki and Wilson (2004) reported that antisense-suppression of *Nicotiana* cytochrome *P450* resulted in increased resistance to *Manduca sexta*. In agreement with this, in the present study, transcripts of *P450* were down-regulated in both mock-inoculated and infected mutant plants at 8 dpi. However, the down-regulated transcripts might have an only indirect effect on the observed resistance. Doehlemann et al. (2008) demonstrated that *PHENYLALANINE AMMONIUMLYASE* (*PAL*) transcript levels were strongly increased in *U. maydis* infected maize gall tissues at 8 dpi. Similarly, a significant transcript upregulation was observed in wild-type plants 4 dpi in the present study. By contrast, a tendency of reduced *PAL* transcription was observed in mock-inoculated mutants at 4 dpi. A similar trend was observed in infected mutant plants in comparison to the wild-type at 8 dpi. Under consideration that *PAL* was reported as being activated by the JA/ET signaling pathway (Diallinas and Kanellis, 1994; Kato et al., 2000; Shoresh et al., 2005), the reduced transcript abundance at 8 dpi suggests that JA/ET signaling is compromised in the *lox3* mutants.

Transcript levels of *PRm3 (PATHOGENESIS-RELATED MAIZE SEED)*, which encodes a maize chitinase, were increased in infected maize plants in response to fall armyworm feeding (Shivaji et al., 2010). In the present investigation, mock-inoculated *lox3* mutants at 4 dpi and infected mutants at 8 dpi exhibited lower transcript accumulation. *MAIZE PROTEINASE INHIBITOR* (*MPI*) transcript accumulation was reported in response to fungal (*Fusarium moniliforme*, *Penicillium* ssp. and *Trichoderma* ssp.) infection by Cordero et al. (1994) and fall armyworm feeding by Shivaji et al. (2010). Indicating its role in plant defence. Ectopic expression of *MPI* in rice resulted in enhanced resistance to the striped stem borer (*Chilo suppressalis*). In the present investigation, *MPI* transcripts were induced in *U. maydis* infected *lox3* mutants at 4 and 8dpi.

In the present investigation, the transcripts of *ACYL-COENZYME A OXIDASE* (*ACX*) were upregulated upon *U. maydis* infection of wild-type plants, whereas infected mutants exhibited reduced transcripts. It was previously known that ACX action is required for the biosynthesis of jasmonic acid (JA) in plant peroxisomes (Schilmiller et al., 2007). Xin et al. (2019) experimentally proved induction of *Arabidopsis ACX* transcripts upon JA treatment. More strikingly, Lanver et al. (2018) reported that *U. maydis* induces jasmonate signaling. Given the results of the present study and the literature, it is suggested that *U. maydis* likely profits from *ACX* transcripts, and that the reduced expression in infected *lox3* mutant plants may have contributed to improved resistance. ALLENE OXIDE SYNTHASE (AOS), a key enzyme involved in the JA pathway (Shivaji et al., 2010). In the present investigation, reduced levels of AOS transcripts were detected in

infected wild-type plants. Gao et al. (2008a) previously reported reduced *AOS* transcript levels in maize upon infection by the root-knot nematode *Meloidogyne incognita*. *CORN CYSTATIN-9* (*CC9)* is a known compatibility factor for the biotrophic interaction of maize with *U. maydis*, as *CC9*-silenced maize plants featured penetration resistance (van der Linde et al., 2012). Consequently, *CC9* can be used as a marker gene for JA-related responses (Pinter et al., 2019). However, neither 4 nor 8 days post-inoculation, the comparison between wild-type and *lox3* mutant plants infected with *U. maydis* showed significant differences in *CC9* transcript levels, which suggests either that JA signaling induction upon *U. maydis* is not hampered or that *U. maydis* induces host *CC9* transcripts in JA-independent manner. *GLUTATHIONE S-TRANSFERASES* (*GST2*) transcripts were upregulated in *U. maydis* infected wild-type plants. The late blight oomycete *Phytophthora infestans* was shown to activate *GST* expression and increasing accumulation of the resultant gene product in potato leaves after fungal infection (Hahn and Strittmatter, 1994). Chacon et al. (2009) reported high induction of *GST* in tobacco during the interaction with *Phytophthora parasitica.* Later, Hernandez et al. (2009) demonstrated that antisense suppression of *GST* caused increased resistance to *Phytophthora parasitica* and postulated that *GST* acts as a negative regulator of defence response. In the present investigation, mock-inoculated mutant plants exhibited down-regulated *GST* transcripts, suggesting this gene might be susceptibility factor. Upon *U. maydis* infection, *HYDROLASE (HYD)* transcripts were upregulated in the current study. In general *HYD* expression was shown to be induced by both insect and fungal pathogens (Huffaker et al., 2013; Christensen et al., 2015). Later, Dowd et al. (2019) suggested that *HYD* might play a role against pests in an unknown resistance mechanism. Christensen et al. (2015) reported a significant upregulation of *HYD* upon treating maize plants with 10-oxo-11-phytoenoic acid (10-OPEA).

5.2.13 The role of *lox3* in plant defense

The specific chemical functions of the *9-LOX* genes are largely unknown. On the other hand, literature indicates that 9-oxylipins likely regulate JA production in maize (Borrego and Kolomiets, 2016). This was corroborated by the observation that some 9-LOXs possess dual substrate specificity by catalyzing 9- as well as 13(S)-hydroperoxy-9Z, 11E-octadecadienoic acid (13-HPOD). Kim et al. (2003) demonstrated that maize *LOX1* produces 13-hydroperoxylinolenic acid and 9-hydroperoxylinolenic acid in a 6-to-4 ratio. 13-hydroperoxylinolenic acid is an intermediate substrate in the JA biosynthesis pathway. For maize *LOX1*, this suggests a role in JA regulation. As another predominant 9-LOX, maize LOX12 appears to act as a positive regulator of JA production (Christensen et al., 2014). The most compelling indications for a role of maize *LOX3* in JA biosynthesis come from Gao et al. (2008a) who have demonstrated that maize *lox3* mutant plants show a tendency to have lower JA levels in the leaves and a corresponding increase of salicylic acid. This correlation could explain why *U. maydis* is hampered in establishing biotrophy in maize *lox3* mutants, since elevated SA levels have been shown previously to inhibit fungal colonization (Djamei et al., 2011). On the other hand,

Vellosillo et al. (2007) showed that, *Arabidopsis* 9-LOX products involvement in ROS, in agreement with this idea, in the present study, ROS accumulation was more in *lox3* mutants in comparison to wild-type in response to pathogen. Given the results, it is speculated that PAMP triggered immunity (PTI) likely activated against *U. maydis* which could be the reason for the achieved resistance.

The biological role of maize *LOX3* and its products is only poorly understood. Thereby, several further studies are required to elucidate the underlying resistance mechanism. This is the first study which revealed that *lox3* mutants can exhibit moderate resistance to *U. maydis.* Given these results, it is suggested that *lox3* is a susceptibility factor for *Ustilago maydis* as well. In addition, *LOX* genes have their role in the abiotic stress response as well, which provides further options in plant research and breeding to take advantage of the mutant plants generated in the present work.
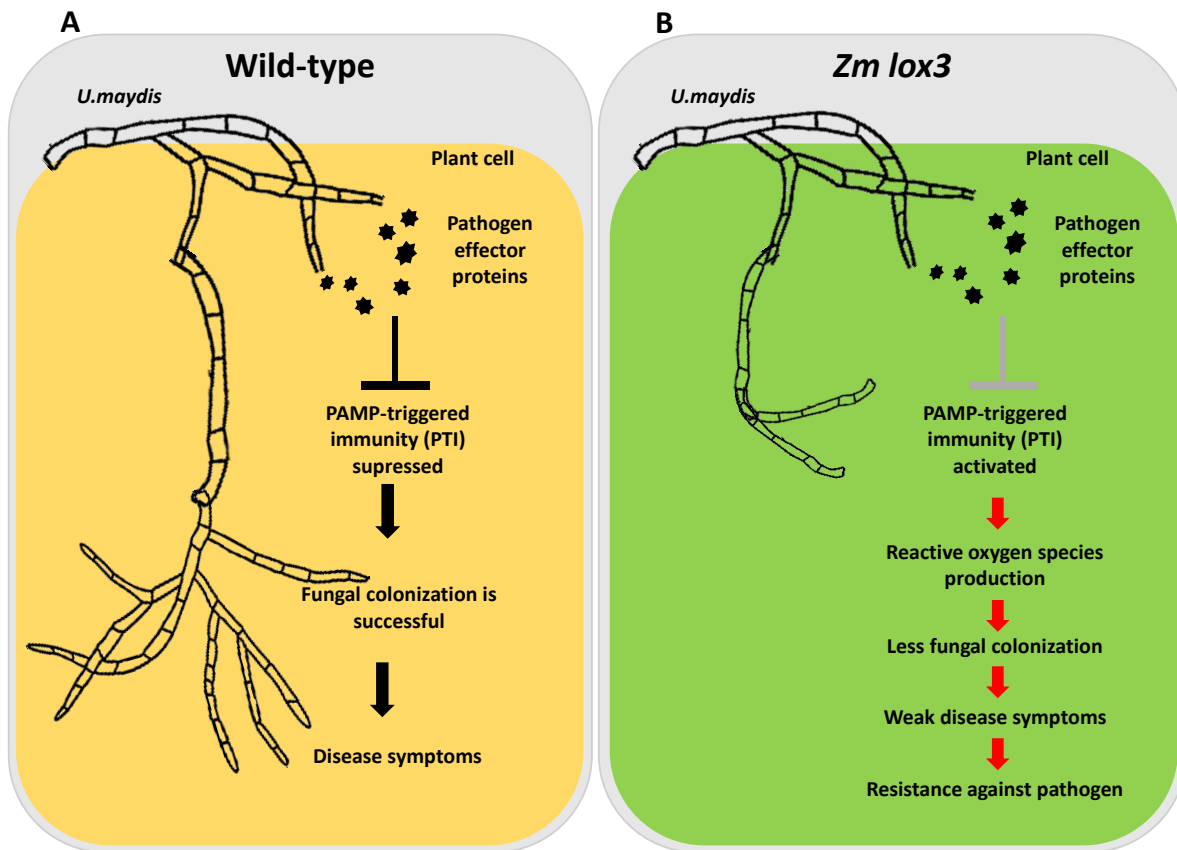

Figure 42: Proposed working model (A) Typically *U. maydis* suppress plant PTI to establish the biotrophic interaction. (B) PAMP triggered immunity (PTI) is activated in the *lox3* mutant which results the production of ROS, likely reduce the *U. maydis* colonization.

6. References

Acosta, I.F., Laparra, H., Romero, S.P., Schmelz, E., Hamberg, M., Mottinger, J.P., Moreno, M.A., and Dellaporta, S.L. (2009). tasselseed1 is a lipoxygenase affecting jasmonic acid signaling in sex determination of maize. *Science* 323**,** 262-265. DOI: 10.1126/science.1164645.

Aguirre, J., Ríos-Momberg, M., Hewitt, D., and Hansberg, W. (2005). Reactive oxygen species and development in microbial eukaryotes. *Trends Microbiol* 13**,** 111-118. DOI: 10.1016/j.tim.2005.01.007.

Al Daoude, A., Shoaib, A., Al-Shehadah, E., Jawhar, M., and Arabi, M.I.E. (2020). Pathogenesis-related genes responses in barley plants challenged with pathogenic fungi with different lifestyles. *Cereal Research Communications* 48**,** 341-346. DOI: 10.1007/s42976-020-00047-8.

Ali, F., and Yan, J.B. (2012). Disease resistance in maize and the role of molecular breeding in defending against global threat. *Journal of Integrative Plant Biology* 54**,** 134-151. DOI: 10.1111/j.1744-7909.2012.01105.x.

Andolfo, G., and Ercolano, M.R. (2015). Plant innate immunity multicomponent model. *Frontiers in Plant Science* 6. DOI: 10.3389/fpls.2015.00987.

Apel, K., and Hirt, H. (2004). Reactive oxygen species: metabolism, oxidative stress, and signal transduction. *Annu Rev Plant Biol* 55**,** 373-399. DOI: 10.1146/annurev.arplant.55.031903.141701.

Apoga, D., Barnard, J., Craighead, H.G., and Hoch, H.C. (2004). Quantification of substratum contact required for initiation of *Colletotrichum graminicola* appressoria. *Fungal Genetics and Biology* 41**,** 1-12. DOI: 10.1016/j.fgb.2003.10.001.

Armstrong, C.L., Green, C., and Phillips, R.L. (1991). Development and availability of germplasm with high type-II culture formation response. *Maize genetics cooperation news letter* 65**,** 92-93.

Bae, S., Kweon, J., Kim, H.S., and Kim, J.S. (2014). Microhomology-based choice of Cas9 nuclease target sites. *Nat Methods* 11**,** 705-706. DOI: 10.1038/nmeth.3015.

Balint-Kurti, P.J., and Johal, G.S. (2009). "Maize disease resistance," in *Handbook of Maize: Its Biology,* eds. J.L. Bennetzen & S.C. Hake. (New York, NY: Springer New York), 229-250. DOI: 10.1007/978-0-387-79418-1_12.

Banuett, F., and Herskowitz, I. (1996). Discrete developmental stages during teliospore formation in the corn smut fungus, *Ustilago maydis*. *Development* 122**,** 2965-2976.

Bari, R., and Jones, J.D. (2009). Role of plant hormones in plant defence responses. *Plant Mol Biol* 69**,** 473-488. DOI: 10.1007/s11103-008-9435-0.

Battilani, P., Lanubile, A., Scala, V., Reverberi, M., Gregori, R., Falavigna, C., Dall'asta, C., Park, Y.S., Bennett, J., Borrego, E.J., and Kolomiets, M.V. (2018). Oxylipins from both pathogen and host antagonize jasmonic acid-mediated defence via the 9-lipoxygenase pathway in *Fusarium verticillioides* infection of maize. *Mol Plant Pathol* 19**,** 2162-2176. DOI: 10.1111/mpp.12690.

Baum, J.A., Bogaert, T., Clinton, W., Heck, G.R., Feldmann, P., Ilagan, O., Johnson, S., Plaetinck, G., Munyikwa, T., Pleau, M., Vaughn, T., and Roberts, J. (2007). Control of coleopteran insect pests through RNA interference. *Nature Biotechnology* 25**,** 1322-1326. DOI: 10.1038/nbt1359.

Bell, A.A., and Wheeler, M.H. (1986). Biosynthesis and functions of fungal melanins. *Annual Review of Phytopathology* 24**,** 411-451. DOI: 10.1146/annurev.py.24.090186.002211.

Belpoggi, F., Soffritti, M., Guarino, M., Lambertini, L., Cevolani, D., and Maltoni, C. (2002). "Results of long-term experimental studies on the carcinogenicity of ethylene-bis-dithiocarbamate (Mancozeb) in rats," in *Carcinogenesis Bioassays and Protecting Public Health: Commemorating the Lifework of Cesare Maltoni and Colleagues,* eds. M.A. Mehlman, E. Bingham, P.J. Landrigan, M. Soffritti, F. Belpoggi & R.L. Melnick. (New York: New York Acad Sciences), 123-136.

Benz, B.F. (2001). Archaeological evidence of teosinte domestication from Guilá Naquitz, Oaxaca. *Proceedings of the National Academy of Sciences* 98**,** 2104-2106. DOI: 10.1073/pnas.98.4.2104.

Bergstrom, G.C., and Nicholson, R.L. (1999). The biology of corn anthracnose - Knowledge to exploit for improved management. *Plant Disease* 83**,** 596-608. DOI: 10.1094/pdis.1999.83.7.596.

Boa, E. (2001). Compendium of corn diseases, 3rd Edition. Edited by Donald G. White. 81/2 × 11 inches, 78 pp. St Paul, USA: American Phytopathological Society Press (http://www.scisoc.org), 1999. US$42. ISBN 089054 234 1 (soft covers).Compendium of strawberry diseases, 2nd Edition. Edited by J L Maas. 81/2×11 inches, 98 pp. St Paul, USA: American Phytopathological Society (http://www.scisoc.org), 1998. US$42. ISBN 089053 194 9 (soft covers). *Plant Pathology* 50**,** 138-138. DOI: 10.1046/j.1365-3059.2001.00529-3.x.

Boch, J., and Bonas, U. (2010). "*Xanthomonas* AvrBs3 family-type III effectors: discovery and function," in *Annual Review of Phytopathology, Vol 48,* eds. N.K. Vanalfen, G. Bruening & J.E. Leach. (Palo Alto: Annual Reviews), 419-436. DOI: 10.1146/annurev-phyto-080508-081936.

Boch, J., Scholze, H., Schornack, S., Landgraf, A., Hahn, S., Kay, S., Lahaye, T., Nickstadt, A., and Bonas, U. (2009). Breaking the code of DNA binding specificity of TAL-type III effectors. *Science* 326**,** 1509-1512. DOI: 10.1126/science.1178811.

Bolker, M., Urban, M., and Kahmann, R. (1992). The a mating type locus of *U. maydis* specifies cell signaling components. *Cell* 68**,** 441-450. DOI: 10.1016/0092-8674(92)90182-c.

Bolwell, G.P. (1999). Role of active oxygen species and NO in plant defence responses. *Curr Opin Plant Biol* 2**,** 287-294. DOI: 10.1016/s1369-5266(99)80051-x.

Borges, F., and Martienssen, R.A. (2015). The expanding world of small RNAs in plants. *Nature Reviews Molecular Cell Biology* 16**,** 727-741. DOI: 10.1038/nrm4085.

Borrego, E.J., and Kolomiets, M.V. (2016). Synthesis and functions of jasmonates in maize. *Plants-Basel* 5**,** 25. DOI: 10.3390/plants5040041.

Brash, A.R. (2009). Mechanistic aspects of CYP74 allene oxide synthases and related cytochrome P450 enzymes. *Phytochemistry* 70**,** 1522-1531. DOI: 10.1016/j.phytochem.2009.08.005.

Brefort, T., Tanaka, S., Neidig, N., Doehlemann, G., Vincon, V., and Kahmann, R. (2014). Characterization of the largest effector gene cluster of *Ustilago maydis. PLoS Pathog* 10**,** e1003866. DOI: 10.1371/journal.ppat.1003866.

Brooks, C., Nekrasov, V., Lippman, Z.B., and Van Eck, J. (2014). Efficient gene editing in tomato in the first generation using the clustered regularly interspaced short palindromic repeats/CRISPR-associated9 system. *Plant Physiology* 166**,** 1292-1297. DOI: 10.1104/pp.114.247577.

Brouwer, M., Lievens, B., Van Hemelrijck, W., Van Den Ackerveken, G., Cammue, B.P.A., and Thomma, B. (2003). Quantification of disease progression of several microbial pathogens on *Arabidopsis thaliana* using real-time fluorescence PCR. *Fems Microbiology Letters* 228**,** 241-248. DOI: 10.1016/s0378-1097(03)00759-6.

Brown, I., Trethowan, J., Kerry, M., Mansfield, J., and Bolwell, G.P. (1998). Localization of components of the oxidative cross-linking of glycoproteins and of callose synthesis in papillae formed during the interaction between non-pathogenic strains of *Xanthomonas campestris* and French bean mesophyll cells. *The Plant Journal* 15**,** 333-343. DOI: 10.1046/j.1365-313X.1998.00215.x.

Bruinsma, M., Van Broekhoven, S., Poelman, E.H., Posthumus, M.A., Muller, M.J., Van Loon, J.J.A., and Dicke, M. (2010). Inhibition of lipoxygenase affects induction of both direct and indirect plant defences against herbivorous insects. *Oecologia* 162**,** 393-404. DOI: 10.1007/s00442-009-1459-x.

Budhagatapalli, N., Halbach, T., Hiekel, S., Büchner, H., Müller, A.E., and Kumlehn, J. (2020). Site-directed mutagenesis in bread and durum wheat via pollination by cas9/guide RNA-transgenic maize used as haploidy inducer. *Plant Biotechnol J*. DOI: 10.1111/pbi.13415.

Budhagatapalli, N., Rutten, T., Gurushidze, M., Kumlehn, J., and Hensel, G. (2015). Targeted modification of gene function exploiting homology-directed repair of TALEN-mediated double-strand breaks in barley. *G3-Genes Genomes Genetics* 5**,** 1857-1863. DOI: 10.1534/g3.115.018762.

Budhagatapalli, N., Schedel, S., Gurushidze, M., Pencs, S., Hiekel, S., Rutten, T., Kusch, S., Morbitzer, R., Lahaye, T., Panstruga, R., Kumlehn, J., and Hensel, G. (2016). A simple test for the cleavage activity of customized endonucleases in plants. *Plant Methods* 12**,** 18. DOI: 10.1186/s13007-016-0118-6.

Burow, G.B., Nesbitt, T.C., Dunlap, J., and Keller, N.P. (1997). Seed lipoxygenase products modulate *Aspergillus* mycotoxin biosynthesis. *Molecular Plant-Microbe Interactions* 10**,** 380-387. DOI: 10.1094/mpmi.1997.10.3.380.

Cacas, J.L., Vailleau, F., Davoine, C., Ennar, N., Agnel, J.P., Tronchet, M., Ponchet, M., Blein, J.P., Roby, D., Triantaphylides, C., and Montillet, J.L. (2005). The combined action of 9 lipoxygenase and galactolipase is sufficient to bring about programmed cell death during tobacco hypersensitive response. *Plant Cell and Environment* 28**,** 1367-1378. DOI: 10.1111/j.1365-3040.2005.01369.x.

Cai, C.Q., Doyon, Y., Ainley, W.M., Miller, J.C., Dekelver, R.C., Moehle, E.A., Rock, J.M., Lee, Y.L., Garrison, R., Schulenberg, L., Blue, R., Worden, A., Baker, L., Faraji, F., Zhang, L., Holmes, M.C., Rebar, E.J., Collingwood, T.N., Rubin-Wilson, B., Gregory, P.D., Urnov, F.D., and Petolino, J.F. (2009). Targeted transgene integration in plant cells using designed zinc finger nucleases. *Plant Molecular Biology* 69**,** 699-709. DOI: 10.1007/s11103-008-9449-7.

Cai, Q., He, B., Weiberg, A., Buck, A.H., and Jin, H. (2019). Small RNAs and extracellular vesicles: new mechanisms of cross-species communication and innovative tools for disease control. *PLoS Pathog* 15**,** e1008090. DOI: 10.1371/journal.ppat.1008090.

Cai, Q., Qiao, L., Wang, M., He, B., Lin, F.M., Palmquist, J., Huang, S.D., and Jin, H. (2018a). Plants send small RNAs in extracellular vesicles to fungal pathogen to silence virulence genes. *Science* 360**,** 1126-1129. DOI: 10.1126/science.aar4142.

Cai, Y.P., Chen, L., Sun, S., Wu, C.X., Yao, W.W., Jiang, B.J., Han, T.F., and Hou, W.S. (2018b). CRISPR/Cas9-mediated deletion of large genomic fragments in soybean. *International Journal of Molecular Sciences* 19**,** 13. DOI: 10.3390/ijms19123835.

Callow, J.A. (1975). Endopolyploidy in maize smut neoplasms induced by the maize smut fungus, *Ustilago maydis*. *New Phytologist* 75**,** 253-257. DOI: 10.1111/j.1469-8137.1975.tb01394.x.

Cao, J.M., Yao, D.M., Lin, F., and Jiang, M.Y. (2014). PEG-mediated transient gene expression and silencing system in maize mesophyll protoplasts: a valuable tool for signal transduction study in maize. *Acta Physiologiae Plantarum* 36**,** 1271-1281. DOI: 10.1007/s11738-014-1508-x.

Cecchini, G. (2003). Function and structure of complex II of the respiratory chain. *Annu. Rev. Biochem.* 72**,** 77.

Cermak, T., Doyle, E.L., Christian, M., Wang, L., Zhang, Y., Schmidt, C., Baller, J.A., Somia, N.V., Bogdanove, A.J., and Voytas, D.F. (2011). Efficient design and assembly of custom TALEN and other TAL effector-based constructs for DNA targeting (vol 39, pg e82, 2011). *Nucleic Acids Research* 39**,** 7879-7879. DOI: 10.1093/nar/gkr739.

Chacon, O., Hernandez, I., Portieles, R., Lopez, Y., Pujol, M., and Borras-Hidalgo, O. (2009). Identification of defense-related genes in tobacco responding to black shank disease. *Plant Science* 177**,** 175-180. DOI: 10.1016/j.plantsci.2009.05.009.

Chandran, D. (2015). Co-option of developmentally regulated plant SWEET transporters for pathogen nutrition and abiotic stress tolerance. *Iubmb Life* 67**,** 461-471. DOI: 10.1002/iub.1394.

Chandrasekaran, J., Brumin, M., Wolf, D., Leibman, D., Klap, C., Pearlsman, M., Sherman, A., Arazi, T., and Gal-On, A. (2016). Development of broad virus resistance in non-transgenic cucumber using CRISPR/Cas9 technology. *Molecular Plant Pathology* 17**,** 1140-1153. DOI: 10.1111/mpp.12375.

Char, S.N., Neelakandan, A.K., Nahampun, H., Frame, B., Main, M., Spalding, M.H., Becraft, P.W., Meyers, B.C., Walbot, V., Wang, K., and Yang, B. (2017). An *Agrobacterium*-delivered CRISPR/Cas9 system for high-frequency targeted mutagenesis in maize. *Plant Biotechnol J* 15**,** 257-268. DOI: 10.1111/pbi.12611.

Char, S.N., Unger-Wallace, E., Frame, B., Briggs, S.A., Main, M., Spalding, M.H., Vollbrecht, E., Wang, K., and Yang, B. (2015). Heritable site-specific mutagenesis using TALENs in maize. *Plant Biotechnology Journal* 13**,** 1002-1010. DOI: 10.1111/pbi.12344.

Chatzidimopoulos, M., Ganopoulos, I., Madesis, P., Vellios, E., Tsaftaris, A., and Pappas, A.C. (2014). High-resolution melting analysis for rapid detection and characterization of *Botrytis cinerea* phenotypes resistant to fenhexamid and boscalid. *Plant Pathology* 63**,** 1336-1343. DOI: 10.1111/ppa.12210.

Chen, J., Zhang, D., Yao, Q., Zhang, J., Dong, X., Tian, H., Chen, J., and Zhang, W. (2010). Feeding-based RNA interference of a *trehalose phosphate synthase gene* in the brown planthopper, *Nilaparvata lugens*. *Insect Molecular Biology* 19**,** 777-786. DOI: 10.1111/j.1365-2583.2010.01038.x.

Chen, W.X., Kastner, C., Nowara, D., Oliveira-Garcia, E., Rutten, T., Zhao, Y.S., Deising, H.B., Kumlehn, J., and Schweizer, P. (2016). Host-induced silencing of *Fusarium culmorum* genes protects wheat from infection. *Journal of Experimental Botany* 67**,** 4979-4991. DOI: 10.1093/jxb/erw263.

Cheng, W., Song, X.S., Li, H.P., Cao, L.H., Sun, K., Qiu, X.L., Xu, Y.B., Yang, P., Huang, T., Zhang, J.B., Qu, B., and Liao, Y.C. (2015). Host-induced gene silencing of an essential *Chitin synthase* gene confers durable resistance to Fusarium head blight and seedling blight in wheat. *Plant Biotechnology Journal* 13**,** 1335-1345. DOI: 10.1111/pbi.12352.

Chilton, M.D.M., and Que, Q.D. (2003). Targeted integration of T-DNA into the tobacco genome at double-stranded breaks: new insights on the mechanism of T-DNA integration. *Plant Physiology* 133**,** 956-965. DOI: 10.1104/pp.103.026104.

Chisholm, S.T., Coaker, G., Day, B., and Staskawicz, B.J. (2006). Host-microbe interactions: shaping the evolution of the plant immune response. *Cell* 124**,** 803-814. DOI: 10.1016/j.cell.2006.02.008.

Cho, S.W., Kim, S., Kim, Y., Kweon, J., Kim, H.S., Bae, S., and Kim, J.S. (2014). Analysis of off-target effects of CRISPR/Cas-derived RNA-guided endonucleases and nickases. *Genome Res* 24**,** 132-141. DOI: 10.1101/gr.162339.113.

Christensen, J.J. (1963). Corn smut caused by *Ustilago maydis*. *American Phytopathological Society***,** 35-41.

Christensen, S.A., Huffaker, A., Kaplan, F., Sims, J., Ziemann, S., Doehlemann, G., Ji, L., Schmitz, R.J., Kolomiets, M.V., Alborn, H.T., Mori, N., Jander, G., Ni, X., Sartor, R.C., Byers, S., Abdo, Z., and Schmelz, E.A. (2015). Maize death acids, 9-lipoxygenase-derived cyclopente(a)nones, display activity as cytotoxic phytoalexins and transcriptional mediators. *Proc Natl Acad Sci U S A* 112**,** 11407-11412. DOI: 10.1073/pnas.1511131112.

Christensen, S.A., Nemchenko, A., Borrego, E., Murray, I., Sobhy, I.S., Bosak, L., Deblasio, S., Erb, M., Robert, C.A., Vaughn, K.A., Herrfurth, C., Tumlinson, J., Feussner, I., Jackson, D., Turlings, T.C., Engelberth, J., Nansen, C., Meeley, R., and Kolomiets, M.V. (2013). The maize lipoxygenase, *ZmLOX10*, mediates green leaf volatile, jasmonate and herbivore-induced plant volatile production for defense against insect attack. *Plant J* 74**,** 59-73. DOI: 10.1111/tpj.12101.

Christensen, S.A., Nemchenko, A., Park, Y.S., Borrego, E., Huang, P.C., Schmelz, E.A., Kunze, S., Feussner, I., Yalpani, N., Meeley, R., and Kolomiets, M.V. (2014). The novel monocot-specific 9-lipoxygenase *ZmLOX12* is required to mount an effective jasmonate-mediated defense against *Fusarium verticillioides* in maize. *Mol Plant Microbe Interact* 27**,** 1263-1276. DOI: 10.1094/MPMI-06-13-0184-R.

Christian, M., Cermak, T., Doyle, E.L., Schmidt, C., Zhang, F., Hummel, A., Bogdanove, A.J., and Voytas, D.F. (2010). Targeting DNA double-strand breaks with TAL effector nucleases. *Genetics* 186**,** 757-U476. DOI: 10.1534/genetics.110.120717.

Cleveland, D.W. (1987). The multitubulin hypothesis revisited - what have we learned. *Journal of Cell Biology* 104**,** 381-383. DOI: 10.1083/jcb.104.3.381.

Concordet, J.P., and Haeussler, M. (2018). CRISPOR: intuitive guide selection for CRISPR/Cas9 genome editing experiments and screens. *Nucleic Acids Res* 46**,** W242-w245. DOI: 10.1093/nar/gky354.

Cong, L., Ran, F.A., Cox, D., Lin, S.L., Barretto, R., Habib, N., Hsu, P.D., Wu, X.B., Jiang, W.Y., Marraffini, L.A., and Zhang, F. (2013). Multiplex genome engineering using CRISPR/Cas systems. *Science* 339**,** 819-823. DOI: 10.1126/science.1231143.

Connorton, J.M., Jones, E.R., Rodríguez-Ramiro, I., Fairweather-Tait, S., Uauy, C., and Balk, J. (2017). Wheat *VACUOLAR IRON TRANSPORTER TaVIT2* transports Fe and Mn and Is effective for biofortification. *Plant Physiology* 174**,** 2434-2444. DOI: 10.1104/pp.17.00672.

Constantino, N.N., Mastouri, F., Damarwinasis, R., Borrego, E.J., Moran-Diez, M.E., Kenerley, C.M., Gao, X., and Kolomiets, M.V. (2013). Root-expressed maize lipoxygenase 3 negatively regulates induced systemic resistance to *Colletotrichum graminicola* in shoots. *Front Plant Sci* 4**,** 510. DOI: 10.3389/fpls.2013.00510.

Cordero, M.J., Raventós, D., and San Segundo, B. (1994). Expression of a maize *PROTEINASE INHIBITOR* gene is induced in response to wounding and fungal infection: systemic wound-response of a monocot gene. *Plant J* 6**,** 141-150. DOI: 10.1046/j.1365-313x.1994.6020141.x.

Creelman, R.A., and Mulpuri, R. (2002). The oxylipin pathway in *Arabidopsis*. *The Arabidopsis book* 1**,** e0012-e0012. DOI: 10.1199/tab.0012.

Crouch, J.A., and Beirn, L.A. (2009). Anthracnose of cereals and grasses. *Fungal Diversity* 39**,** 19-44.

Csorba, T., Pantaleo, V., and Burgyán, J. (2009). RNA silencing: an antiviral mechanism. *Adv Virus Res* 75**,** 35-71. DOI: 10.1016/s0065-3527(09)07502-2.

Daboussi, F., Stoddard, T.J., and Zhang, F. (2015). "Engineering meganuclease for precise plant genome modification," in *Advances in New Technology for Targeted Modification of Plant Genomes,* eds. F. Zhang, H. Puchta & J.G. Thomson. (New York, NY: Springer New York), 21-38. DOI: 10.1007/978-1-4939-2556-8_2.

Dangl, J.L., Horvath, D.M., and Staskawicz, B.J. (2013). Pivoting the plant immune system from dissection to deployment. 341**,** 746-751. DOI: 10.1126/science.

Dangl, J.L., and Jones, J.D. (2001). Plant pathogens and integrated defence responses to infection. *Nature* 411**,** 826-833. DOI: 10.1038/35081161.

Davoine, C., Falletti, O., Douki, T., Iacazio, G., Ennar, N., Montillet, J.L., and Triantaphylides, C. (2006). Adducts of oxylipin electrophiles to glutathione reflect a 13 specificity of the downstream lipoxygenase pathway in the tobacco hypersensitive response. *Plant Physiology* 140**,** 1484-1493. DOI: 10.1104/pp.105.074690.

De Pater, S., Pinas, J.E., Hooykaas, P.J.J., and Van Der Zaal, B.J. (2013). ZFN-mediated gene targeting of the *Arabidopsis PROTOPORPHYRINOGEN OXIDASE* gene through *Agrobacterium*-mediated floral dip transformation. *Plant Biotechnology Journal* 11**,** 510-515. DOI: 10.1111/pbi.12040.

De Smet, R., Sabaghian, E., Li, Z., Saeys, Y., and Van De Peer, Y. (2017). Coordinated functional divergence of genes after genome duplication in *Arabidopsis thaliana*. *Plant Cell* 29**,** 2786-2800. DOI: 10.1105/tpc.17.00531.

Deising, H.B., Reimann, S., and Pascholati, S.F. (2008). Mechanisms and significance of fungicide resistance. *Brazilian Journal of Microbiology* 39**,** 286-295. DOI: 10.1590/s1517-83822008000200017.

Del Pozo, O., Pedley, K.F., and Martin, G.B. (2004). *MAPKKKα* is a positive regulator of cell death associated with both plant immunity and disease. *Embo j* 23**,** 3072-3082. DOI: 10.1038/sj.emboj.7600283.

Deng, J.X., Nie, X.J., Lei, Y.F., Ma, C.F., Xu, D.L., Li, B.A., Xu, Z.K., and Zhang, G.C. (2012). The highly conserved 5' untranslated region as an effective target towards the inhibition of enterovirus 71 replication by unmodified and appropriate 2'-modified siRNAs. *Journal of Biomedical Science* 19**,** 14. DOI: 10.1186/1423-0127-19-73.

Diallinas, G., and Kanellis, A.K. (1994). A *PHENYLALANINE AMMONIA-LYASE* gene from melon fruit: cDNA cloning, sequence and expression in response to development and wounding. *Plant Mol Biol* 26**,** 473-479. DOI: 10.1007/bf00039557.

Dibrov, E., Fu, S., and Lemire, B.D. (1998). The *Saccharomyces cerevisiae TCM62* gene encodes a chaperone necessary for the assembly of the mitochondrial succinate dehydrogenase (Complex II). *Journal of Biological Chemistry* 273**,** 32042-32048. DOI: 10.1074/jbc.273.48.32042.

Djamei, A., Schipper, K., Rabe, F., Ghosh, A., Vincon, V., Kahnt, J., Osorio, S., Tohge, T., Fernie, A.R., Feussner, I., Feussner, K., Meinicke, P., Stierhof, Y.D., Schwarz, H., Macek, B., Mann, M., and Kahmann, R. (2011). Metabolic priming by a secreted fungal effector. *Nature* 478**,** 395-398. DOI: 10.1038/nature10454.

Dodds, P.N., and Rathjen, J.P. (2010). Plant immunity: towards an integrated view of plant-pathogen interactions. *Nature Reviews Genetics* 11**,** 539-548. DOI: 10.1038/nrg2812.

Doehlemann, G., Van Der Linde, K., Amann, D., Schwammbach, D., Hof, A., Mohanty, A., Jackson, D., and Kahmann, R. (2009). PEP1, a Secreted effector protein of *Ustilago maydis*, is required for successful invasion of plant cells. *Plos Pathogens* 5**,** 16. DOI: 10.1371/journal.ppat.1000290.

Doehlemann, G., Wahl, R., Horst, R.J., Voll, L.M., Usadel, B., Poree, F., Stitt, M., Pons-Kuhnemann, J., Sonnewald, U., Kahmann, R., and Kamper, J. (2008). Reprogramming a maize plant: transcriptional and metabolic changes induced by the fungal biotroph *Ustilago maydis*. *Plant Journal* 56**,** 181-195. DOI: 10.1111/j.1365-313X.2008.03590.x.

Doench, J.G., Hartenian, E., Graham, D.B., Tothova, Z., Hegde, M., Smith, I., Sullender, M., Ebert, B.L., Xavier, R.J., and Root, D.E. (2016). Rational design of highly active sgRNAs for CRISPR-Cas9-mediated gene inactivation. *Nature Biotechnology* 32**,** 1262-U1130. DOI: 10.1038/nbt.3026.

Dou, T.X., Shao, X.H., Hu, C.H., Liu, S.W., Sheng, O., Bi, F.C., Deng, G.M., Ding, L.J., Li, C.Y., Dong, T., Gao, H.J., He, W.D., Peng, X.X., Zhang, S., Huo, H.Q., Yang, Q.S., and Yi, G.J. Host-induced gene silencing of Foc *Tr4 Erg6/11* genes exhibits superior resistance to Fusarium wilt of banana. *Plant Biotechnology Journal***,** 3. DOI: 10.1111/pbi.13204.

Dowd, P., Naumann, T., Johnson, E., and Price, N. (2019). A maize hydrolase with activity against maize insect and fungal pests. *Plant Gene* 21**,** 100214. DOI: 10.1016/j.plgene.2019.100214.

Doyon, Y., Mccammon, J.M., Miller, J.C., Faraji, F., Ngo, C., Katibah, G.E., Amora, R., Hocking, T.D., Zhang, L., Rebar, E.J., Gregory, P.D., Urnov, F.D., and Amacher, S.L. (2008). Heritable targeted gene disruption in zebrafish using designed zinc-finger nucleases. *Nature Biotechnology* 26**,** 702-708. DOI: 10.1038/nbt1409.

Ellinger, D., Naumann, M., Falter, C., Zwikowics, C., Jamrow, T., Manisseri, C., Somerville, S.C., and Voigt, C.A. (2013). Elevated early callose deposition results in complete penetration resistance to powdery mildew in *Arabidopsis. Plant Physiol* 161**,** 1433-1444. DOI: 10.1104/pp.112.211011.

Fan, D., Liu, T.T., Li, C.F., Jiao, B., Li, S., Hou, Y.S., and Luo, K.M. (2015). Efficient CRISPR/Cas9-mediated targeted mutagenesis in populus in the first generation. *Scientific Reports* 5**,** 7. DOI: 10.1038/srep12217.

Feng, C., Yuan, J., Wang, R., Liu, Y., Birchler, J.A., and Han, F. (2016). Efficient targeted genome modification in maize using CRISPR/Cas9 system. *J Genet Genomics* 43**,** 37-43. DOI: 10.1016/j.jgg.2015.10.002.

Feng, Z.Y., Mao, Y.F., Xu, N.F., Zhang, B.T., Wei, P.L., Yang, D.L., Wang, Z., Zhang, Z.J., Zheng, R., Yang, L., Zeng, L., Liu, X.D., and Zhu, J.K. (2014). Multigeneration analysis reveals the inheritance, specificity, and patterns of CRISPR/Cas-induced gene modifications in *Arabidopsis*. *Proceedings of the National Academy of Sciences of the United States of America* 111**,** 4632-4637. DOI: 10.1073/pnas.1400822111.

Feussner, I., and Wasternack, C. (2002). The lipoxygenase pathway. *Annual Review of Plant Biology* 53**,** 275-297. DOI: 10.1146/annurev.arplant.53.100301.135248.

Fichtner, F., Castellanos, R.U., and Ulker, B. (2014). Precision genetic modifications: a new era in molecular biology and crop improvement. *Planta* 239**,** 921-939. DOI: 10.1007/s00425-014-2029-y.

Fire, A.Z. (2007). Gene silencing by double-stranded RNA (Nobel lecture). *Angewandte Chemie-International Edition* 46**,** 6967-6984. DOI: 10.1002/anie.200701979.

Freitag, J., Lanver, D., Bohmer, C., Schink, K.O., Bolker, M., and Sandrock, B. (2011). Septation of infectious hyphae is critical for appressoria formation and virulence in the smut fungus *Ustilago maydis*. *Plos Pathogens* 7**,** 15. DOI: 10.1371/journal.ppat.1002044.

Frey, T.J., Weldekidan, T., Colbert, T., Wolters, P., and Hawk, J.A. (2011). Fitness evaluation of *Rcg1*, a locus that confers resistance to *Colletotrichum graminicola* (Ces.) GW Wils. using near-isogenic maize hybrids. *Crop Science* 51**,** 1551-1563. DOI: 10.2135/cropsci2010.10.0613.

Frizzi, A., and Huang, S.S. (2010). Tapping RNA silencing pathways for plant biotechnology. *Plant Biotechnology Journal* 8**,** 655-677. DOI: 10.1111/j.1467-7652.2010.00505.x.

Gachon, C., and Saindrenan, P. (2004). Real-time PCR monitoring of fungal development in *Arabidopsis thaliana* infected by *Alternaria brassicicola* and *Botrytis cinerea*. *Plant Physiology and Biochemistry* 42**,** 367-371. DOI: 10.1016/j.plaphy.2004.04.001.

Gao, X.Q., Shim, W.B., Gobel, C., Kunze, S., Feussner, I., Meeley, R., Balint-Kurti, P., and Kolomiets, M. (2007). Disruption of a maize 9-lipoxygenase results in increased resistance to fungal pathogens and reduced levels of contamination with mycotoxin fumonisin. *Molecular Plant-Microbe Interactions* 20**,** 922-933. DOI: 10.1094/mpmi-20-8-0922.

Gao, X.Q., Starr, J., Gobel, C., Engelberth, J., Feussner, I., Tumlinson, J., and Kolomiets, M. (2008a). Maize 9-lipoxygenase *ZmLOX3* controls development, root-specific expression of defense genes, and resistance to root-knot nematodes. *Molecular Plant-Microbe Interactions* 21**,** 98-109. DOI: 10.1094/mpmi-21-1-0098.

Gao, X.Q., Stumpe, M., Feussner, I., and Kolomiets, M. (2008b). A novel plastidial lipoxygenase of maize (*Zea mays*) *ZmLOX6* encodes for a fatty acid hydroperoxide lyase and is uniquely regulated by phytohormones and pathogen infection. *Planta* 227**,** 491-503. DOI: 10.1007/s00425-007-0634-8.

Garcia, P.C., Rivero, R.M., Ruiz, J.M., and Romero, L. (2003). The role of fungicides in the physiology of higher plants: Implications for defense responses. *Botanical Review* 69**,** 162-172. DOI: 10.1663/0006-8101(2003)069[0162:Trofit]2.0.Co;2.

Garnham, C.P., and Roll-Mecak, A. (2012). The chemical complexity of cellular microtubules: Tubulin post-translational modification enzymes and their roles in tuning microtubule functions. *Cytoskeleton* 69**,** 442-463. DOI: 10.1002/cm.21027.

Gaudelli, N.M., Komor, A.C., Rees, H.A., Packer, M.S., Badran, A.H., Bryson, D.I., and Liu, D.R. (2017). Programmable base editing of A•T to G•C in genomic DNA without DNA cleavage. *Nature* 551**,** 464-471. DOI: 10.1038/nature24644.

Gerasimova, S.V., Hertig, C., Korotkova, A.M., Kolosovskaya, E., Otto, I., Hiekel, S., Kochetov, A.V., Khlestkina, E.K., and Kumlehn, J. (2020). Conversion of hulled into naked barley by Cas endonuclease-mediated knockout of the *NUD* gene. *BMC Plant Biology,accepted*

Gerasimova, S.V., Korotkova, A.M., Hertig, C., Hiekel, S., Hofe, R., Budhagatapalli, N., Otto, I., Hensel, G., Shumny, V.K., Kochetov, A.V., Kumlehn, J., and Khlestkina, E.K. (2019). Targeted genome modifcation in protoplasts of a highly regenerable Siberian barley cultivar using RNA-guided Cas9 endonuclease. *Vavilov Journal of Genetics and Breeding* 22**,** 1033-1039. DOI: 10.18699/vj18.447.

Ghag, S.B., Shekhawat, U.K.S., and Ganapathi, T.R. (2014). Host-induced post-transcriptional hairpin RNA-mediated gene silencing of vital fungal genes confers efficient resistance against Fusarium wilt in banana. *Plant Biotechnology Journal* 12**,** 541-553. DOI: 10.1111/pbi.12158.

Gilbert, M.K., Majumdar, R., Rajasekaran, K., Chen, Z.Y., Wei, Q.J., Sickler, C.M., Lebar, M.D., Cary, J.W., Frame, B.R., and Wang, K. (2018). RNA interference-based silencing of the *Alpha-amylase* (*Amy1*) gene in *Aspergillus flavus* decreases fungal growth and aflatoxin production in maize kernels. *Planta* 247**,** 1465-1473. DOI: 10.1007/s00425-018-2875-0.

Glazebrook, J. (2005). Contrasting mechanisms of defense against biotrophic and necrotrophic pathogens. *Annual Review of Phytopathology* 43**,** 205-227. DOI: 10.1146/annurev.phyto.43.040204.135923.

Gobel, C., Feussner, I., Hamberg, M., and Rosahl, S. (2002). Oxylipin profiling in pathogen-infected potato leaves. *Biochimica Et Biophysica Acta-Molecular and Cell Biology of Lipids* 1584**,** 55-64. DOI: 10.1016/s1388-1981(02)00268-8.

Gobel, C., Feussner, I., and Rosahl, S. (2003). Lipid peroxidation during the hypersensitive response in potato in the absence of 9-lipoxygenases. *Journal of Biological Chemistry* 278**,** 52834-52840. DOI: 10.1074/jbc.M310833200.

Gobel, C., Feussner, I., Schmidt, A., Scheel, D., Sanchez-Serrano, J., Hamberg, M., and Rosahl, S. (2001). Oxylipin profiling reveals the preferential stimulation of the 9-lipoxygenase pathway in elicitor-treated potato cells. *Journal of Biological Chemistry* 276**,** 6267-6273. DOI: 10.1074/jbc.M008606200.

Gomez, M.A., Lin, Z.D., Moll, T., Chauhan, R.D., Hayden, L., Renninger, K., Beyene, G., Taylor, N.J., Carrington, J.C., Staskawicz, B.J., and Bart, R.S. (2019). Simultaneous CRISPR/Cas9-mediated editing of cassava *eIF4E* isoforms *nCBP-1* and *nCBP-2* reduces cassava brown streak disease symptom severity and incidence. *Plant Biotechnol J* 17**,** 421-434. DOI: 10.1111/pbi.12987.

Govindarajulu, M., Epstein, L., Wroblewski, T., and Michelmore, R.W. (2015). Host-induced gene silencing inhibits the biotrophic pathogen causing downy mildew of lettuce. *Plant Biotechnology Journal* 13**,** 875-883. DOI: 10.1111/pbi.12307.

Grant, J.J., and Loake, G.J. (2000). Role of reactive oxygen intermediates and cognate redox signaling in disease resistance. *Plant Physiol* 124**,** 21-29. DOI: 10.1104/pp.124.1.21.

Gruber, A.R., Lorenz, R., Bernhart, S.H., Neuböck, R., and Hofacker, I.L. (2008). The Vienna RNA websuite. *Nucleic Acids Res* 36**,** W70-74. DOI: 10.1093/nar/gkn188.

Gullino, M.L., Leroux, P., and Smith, C.M. (2000). Uses and challenges of novel compounds for plant disease control. *Crop Protection* 19**,** 1-11. DOI: 10.1016/s0261-2194(99)00095-2.

Gurushidze, M., Hensel, G., Hiekel, S., Schedel, S., Valkov, V., and Kumlehn, J. (2014). True-breeding targeted gene knock-out in barley using designer TALE-nuclease in haploid cells. *Plos One* 9**,** 9. DOI: 10.1371/journal.pone.0092046.

Gurushidze, M., Hiekel, S., Otto, I., Hensel, G., and Kumlehn, J. (2017). "Site-directed mutagenesis in barley by expression of TALE nuclease in embryogenic pollen," in *Biotechnologies for Plant Mutation Breeding: Protocols,* eds. J. Jankowicz-Cieslak, T.H. Tai, J. Kumlehn & B.J. Till. (Cham: Springer International Publishing), 113-128. DOI: 10.1007/978-3-319-45021-6_7.

Gwirtz, J.A., and Garcia-Casal, M.N. (2014). "Processing maize flour and corn meal food products," in *technical considerations for maize flour and corn meal fortification in public health,* eds. J.P. Penarosas, M.N. Garciacasal & H. Pachon. (Oxford: Blackwell Science Publ), 66-75. DOI: 10.1111/nyas.12299.

Haeussler, M., Schönig, K., Eckert, H., Eschstruth, A., Mianné, J., Renaud, J.B., Schneider-Maunoury, S., Shkumatava, A., Teboul, L., Kent, J., Joly, J.S., and Concordet, J.P. (2016). Evaluation of off-target and on-target scoring algorithms and integration into the guide RNA selection tool CRISPOR. *Genome Biol* 17**,** 148. DOI: 10.1186/s13059-016-1012-2.

Hahn, F., Eisenhut, M., Mantegazza, O., and Weber, A.P.M. (2018). Homology-directed repair of a defective *GLABROUS* gene in *Arabidopsis* with Cas9-based gene targeting. *Frontiers in Plant Science* 9. DOI: 10.3389/fpls.2018.00424.

Hahn, K., and Strittmatter, G. (1994). Pathogen-defence gene *PRP1-1* from potato encodes an auxin-responsive glutathione S-transferase. *Eur J Biochem* 226**,** 619-626. DOI: 10.1111/j.1432-1033.1994.tb20088.x.

Hamberg, M., Sanz, A., Rodriguez, M.J., Calvo, A.P., and Castresana, C. (2003). Activation of the fatty acid alpha-dioxygenase pathway during bacterial infection of tobacco leaves - formation of oxylipins protecting against cell death. *Journal of Biological Chemistry* 278**,** 51796-51805. DOI: 10.1074/jbc.M310514200.

Hammond-Kosack, K.E., and Parker, J.E. (2003). Deciphering plant-pathogen communication: fresh perspectives for molecular resistance breeding. *Curr Opin Biotechnol* 14**,** 177-193. DOI: 10.1016/s0958-1669(03)00035-1.

Hansjakob, A., Riederer, M., and Hildebrandt, U. (2012). Appressorium morphogenesis and cell cycle progression are linked in the grass powdery mildew fungus *Blumeria graminis*. *Fungal Biology* 116**,** 890-901. DOI: 10.1016/j.funbio.2012.05.006.

Harborth, J., Elbashir, S.M., Bechert, K., Tuschl, T., and Weber, K. (2001). Identification of essential genes in cultured mammalian cells using small interfering RNAs. *Journal of Cell Science* 114**,** 4557-4565.

Harvey, J.J.W., Lewsey, M.G., Patel, K., Westwood, J., Heimstadt, S., Carr, J.P., and Baulcombe, D.C. (2011). An antiviral defense role of AGO2 in plants. *Plos One* 6**,** 6. DOI: 10.1371/journal.pone.0014639.

Haun, W., Coffman, A., Clasen, B.M., Demorest, Z.L., Lowy, A., Ray, E., Retterath, A., Stoddard, T., Juillerat, A., Cedrone, F., Mathis, L., Voytas, D.F., and Zhang, F. (2014). Improved soybean oil quality by targeted mutagenesis of the *FATTY ACID DESATURASE 2* gene family. *Plant Biotechnology Journal* 12**,** 934-940. DOI: 10.1111/pbi.12201.

Heiler, S., Mendgen, K., and Deising, H. (1993). Cellulolytic enzymes of the obligately biotrophic rust fungus *Uromyces viciae-fabae* are regulated differentiation-specifically. *Mycological Research* 97**,** 77-85. DOI: https://doi.org/10.1016/S0953-7562(09)81116-7.

Heller, J., and Tudzynski, P. (2011). Reactive oxygen species in phytopathogenic fungi: signaling, development, and disease. *Annu Rev Phytopathol* 49**,** 369-390. DOI: 10.1146/annurev-phyto-072910-095355.

Hemetsberger, C., Herrberger, C., Zechmann, B., Hillmer, M., and Doehlemann, G. (2012). The *Ustilago maydis* effector PEP1 suppresses plant immunity by inhibition of host peroxidase activity. *Plos Pathogens* 8**,** 14. DOI: 10.1371/journal.ppat.1002684.

Hensel, G., Kastner, C., Oleszczuk, S., Riechen, J., and Kumlehn, J. (2009). *Agrobacterium*-mediated gene transfer to cereal crop plants: current protocols for barley, wheat, triticale, and maize. *Int J Plant Genomics* 2009**,** 835608. DOI: 10.1155/2009/835608.

Hensel, G., Marthe, C., and Kumlehn, J. (2017). "*Agrobacterium*-mediated transformation of wheat using immature embryos," in *Wheat Biotechnology: Methods and Protocols,* eds. P.L. Bhalla & M.B. Singh. (New York, NY: Springer New York), 129-139. DOI: 10.1007/978-1-4939-7337-8_8.

Hernandez, I., Chacon, O., Rodriguez, R., Portieles, R., Lopez, Y., Pujol, M., and Borras-Hidalgo, O. (2009). Black shank resistant tobacco by silencing of glutathione S-transferase. *Biochemical and Biophysical Research Communications* 387**,** 300-304. DOI: 10.1016/j.bbrc.2009.07.003.

Hiekel, S., Schedel, S., Hensel, G., Gurushidze, M., Budhagatapalli, N., and Kumlehn, J. (Year). "Synthetic endonucleases: novel tools for the site-directed genetic modification of plants": International Society for Horticultural Science (ISHS), Leuven, Belgium), 71-81. DOI: 10.17660/ActaHortic.2015.1087.8.

Hilbert, M., Nostadt, R., and Zuccaro, A. (2013). Exogenous auxin affects the oxidative burst in barley roots colonized by *Piriformospora indica*. *Plant Signal Behav* 8**,** e23572. DOI: 10.4161/psb.23572.

Himmelbach, A., Zierold, U., Hensel, G., Riechen, J., Douchkov, D., Schweizer, P., and Kumlehn, J. (2007). A set of modular binary vectors for transformation of cereals. *Plant Physiology* 145**,** 1192-1200. DOI: 10.1104/pp.107.111575.

Hobbs, S.L., Warkentin, T.D., and Delong, C.M. (1993). Transgene copy number can be positively or negatively associated with transgene expression. *Plant Mol Biol* 21**,** 17-26. DOI: 10.1007/bf00039614.

Hoefnagels, M.H. (2005). Biodiversity of fungi: inventory and monitoring methods. *BioScience* 55**,** 282-283. DOI: 10.1641/0006-3568(2005)055[0282:Sftida]2.0.Co;2.

Hollomon, D.W., Butters, J.A., Barker, H., and Hall, L. (1998). Fungal β-Tubulin, expressed as a fusion protein, binds benzimidazole and phenylcarbamate fungicides. *Antimicrobial Agents and Chemotherapy* 42**,** 2171-2173. DOI: 10.1128/aac.42.9.2171.

Holme, I.B., Wendt, T., Gil-Humanes, J., Deleuran, L.C., Starker, C.G., Voytas, D.F., and Brinch-Pedersen, H. (2017). Evaluation of the mature grain phytase candidate *HvPAPhy_a* gene in barley (*Hordeum vulgare* L.) using CRISPR/Cas9 and TALENs. *Plant Mol Biol* 95**,** 111-121. DOI: 10.1007/s11103-017-0640-6.

Hu, Q.O., Niu, Y.B., Zhang, K., Liu, Y., and Zhou, X.P. (2011). Virus-derived transgenes expressing hairpin RNA give immunity to Tobacco mosaic virus and Cucumber mosaic virus. *Virology Journal* 8**,** 11. DOI: 10.1186/1743-422x-8-41.

Huang, G.Z., Allen, R., Davis, E.L., Baum, T.J., and Hussey, R.S. (2006). Engineering broad root-knot resistance in transgenic plants by RNAi silencing of a conserved and essential root-knot nematode parasitism gene. *Proceedings of the National Academy of Sciences of the United States of America* 103**,** 14302-14306. DOI: 10.1073/pnas.0604698103.

Huang, X.Z., Qian, Q., Liu, Z.B., Sun, H.Y., He, S.Y., Luo, D., Xia, G.M., Chu, C.C., Li, J.Y., and Fu, X.D. (2009). Natural variation at the *DEP1* locus enhances grain yield in rice. *Nature Genetics* 41**,** 494-497. DOI: 10.1038/ng.352.

Hückelhoven, R., and Seidl, A. (2016). PAMP-triggered immune responses in barley and susceptibility to powdery mildew. *Plant Signal Behav* 11**,** e1197465. DOI: 10.1080/15592324.2016.1197465.

Huffaker, A., Pearce, G., Veyrat, N., Erb, M., Turlings, T.C.J., Sartor, R., Shen, Z.X., Briggs, S.P., Vaughan, M.M., Alborn, H.T., Teal, P.E.A., and Schmelz, E.A. (2013). Plant elicitor peptides are conserved signals regulating direct and indirect antiherbivore defense. *Proceedings of the National Academy of Sciences of the United States of America* 110**,** 5707-5712. DOI: 10.1073/pnas.1214668110.

Hughes, R.K., Wu, Z.C., Robinson, D.S., Hardy, D., West, S.I., Fairhurst, S.A., and Casey, R. (1998). Characterization of authentic recombinant pea-seed lipoxygenases with distinct properties and reaction mechanisms. *Biochemical Journal* 333**,** 33-43. DOI: 10.1042/bj3330033.

Hwang, I.S., and Hwang, B.K. (2010). The pepper 9-lipoxygenase gene *CaLOX1* functions in defense and cell death responses to microbial pathogens. *Plant Physiol* 152**,** 948-967. DOI: 10.1104/pp.109.147827.

Isakeit, T., Gao, X., and Kolomiets, M. (2007). *Exserohilum pedicellatum* root rot of corn in Texas. *Plant Dis* 91**,** 634. DOI: 10.1094/PDIS-91-5-0634C.

Jabs, T., Tschope, M., Colling, C., Hahlbrock, K., and Scheel, D. (1997). Elicitor-stimulated ion fluxes and O_2- from the oxidative burst are essential components in triggering defense gene activation and phytoalexin synthesis in parsley. *Proc Natl Acad Sci U S A* 94**,** 4800-4805. DOI: 10.1073/pnas.94.9.4800.

Jahan, S.N., Asman, A.K.M., Corcoran, P., Fogelqvist, J., Vetukuri, R.R., and Dixelius, C. (2015). Plant-mediated gene silencing restricts growth of the potato late blight pathogen *Phytophthora infestans*. *Journal of Experimental Botany* 66**,** 2785-2794. DOI: 10.1093/jxb/erv094.

Janke, C., and Bulinski, J.C. (2012). Post-translational regulation of the microtubule cytoskeleton: mechanisms and functions (vol 12, pg 773, 2011). *Nature Reviews Molecular Cell Biology* 13**,** 276-276. DOI: 10.1038/nrm3310.

Jansing, J., Sack, M., Augustine, S.M., Fischer, R., and Bortesi, L. (2019). CRISPR/Cas9-mediated knockout of six *GLYCOSYLTRANSFERASE* genes in *Nicotiana benthamiana* for the production of recombinant proteins lacking β-1,2-xylose and core α-1,3-fucose. *Plant Biotechnol J* 17**,** 350-361. DOI: 10.1111/pbi.12981.

Jeger, M.J., Bailey, J.A., and British Society for Plant, P. (1992). *Colletotrichum : biology, pathology, and control.* Wallingford, Oxon, UK: C.A.B. International.

Jensen, A.B., Poca, E., Rigaud, M., Freyssinet, G., and Pages, M. (1997). Molecular characterization of L2 lipoxygenase from maize embryos. *Plant Molecular Biology* 33**,** 605-614. DOI: 10.1023/a:1005742719019.

Jinek, M., Chylinski, K., Fonfara, I., Hauer, M., Doudna, J.A., and Charpentier, E. (2012). A programmable dual-RNA-guided DNA endonuclease in adaptive bacterial immunity. *Science* 337**,** 816-821. DOI: 10.1126/science.1225829.

Jones, J.D.G., and Dangl, J.L. (2006). The plant immune system. *Nature* 444**,** 323-329. DOI: 10.1038/nature05286.

Jones, T.J. (2009). "Maize tissue culture and transformation: the first 20 years," in *Molecular Genetic Approaches to Maize Improvement,* eds. A.L. Kriz & B.A. Larkins. (Berlin, Heidelberg: Springer Berlin Heidelberg), 7-27. DOI: 10.1007/978-3-540-68922-5_2.

Joung, J.K., and Sander, J.D. (2013). Innovation TALENs: a widely applicable technology for targeted genome editing. *Nature Reviews Molecular Cell Biology* 14**,** 49-55. DOI: 10.1038/nrm3486.

Juarez-Montiel, M., De Leon, S.R., Chavez-Camarillo, G., Hernandez-Rodriguez, C., and Villa-Tanaca, L. (2011). Huitlacoche (corn smut), caused by the phytopathogenic fungus *Ustilago maydis,* as a functional food. *Revista Iberoamericana De Micologia* 28**,** 69-73. DOI: 10.1016/j.riam.2011.01.001.

Jwa, N.S., and Hwang, B.K. (2017). Convergent evolution of pathogen effectors toward reactive oxygen species signaling networks in plants. *Frontiers in Plant Science* 8**,** 12. DOI: 10.3389/fpls.2017.01687.

Kämper, J., Kahmann, R., Bolker, M., Ma, L.J., Brefort, T., Saville, B.J., Banuett, F., Kronstad, J.W., Gold, S.E., Muller, O., Perlin, M.H., Wosten, H.a.B., De Vries, R., Ruiz-Herrera, J., Reynaga-Pena, C.G., Snetselaar, K., Mccann, M., Perez-Martin, J., Feldbrugge, M., Basse, C.W., Steinberg, G., Ibeas, J.I., Holloman, W., Guzman, P., Farman, M., Stajich, J.E., Sentandreu, R., Gonzalez-Prieto, J.M., Kennell, J.C., Molina, L., Schirawski, J., Mendoza-Mendoza, A., Greilinger, D., Munch, K., Rossel, N., Scherer, M., Vranes, M., Ladendorf, O., Vincon, V., Fuchs, U., Sandrock, B., Meng, S., Ho, E.C.H., Cahill, M.J., Boyce, K.J., Klose, J., Klosterman, S.J., Deelstra, H.J., Ortiz-Castellanos, L., Li, W.X., Sanchez-Alonso, P., Schreier, P.H., Hauser-Hahn, I., Vaupel, M., Koopmann, E., Friedrich, G., Voss, H., Schluter, T., Margolis, J., Platt, D., Swimmer, C., Gnirke, A., Chen, F., Vysotskaia, V., Mannhaupt, G., Guldener, U., Munsterkotter, M., Haase, D., Oesterheld, M., Mewes, H.W., Mauceli, E.W., Decaprio, D., Wade, C.M., Butler, J., Young, S., Jaffe, D.B., Calvo, S., Nusbaum, C., Galagan, J., and Birren, B.W. (2006). Insights from the genome of the biotrophic fungal plant pathogen *Ustilago maydis*. *Nature* 444**,** 97-101. DOI: 10.1038/nature05248.

Kapusi, E., Corcuera-Gomez, M., Melnik, S., and Stoger, E. (2017). Heritable genomic fragment deletions and small indels in the putative ENGase gene induced by CRISPR/Cas9 in barley. *Frontiers in Plant Science* 8**,** 11. DOI: 10.3389/fpls.2017.00540.

Kato, M., Hayakawa, Y., Hyodo, H., Ikoma, Y., and Yano, M. (2000). Wound-induced ethylene synthesis and expression and formation of 1-aminocyclopropane-1-carboxylate (ACC) synthase, ACC oxidase, phenylalanine ammonia-lyase, and peroxidase in wounded mesocarp tissue of *Cucurbita maxima*. *Plant and Cell Physiology* 41**,** 440-447. DOI: 10.1093/pcp/41.4.440.

Kaur, K.D., Jha, A., Sabikhi, L., and Singh, A.K. (2014). Significance of coarse cereals in health and nutrition: a review. *Journal of Food Science and Technology-Mysore* 51**,** 1429-1441. DOI: 10.1007/s13197-011-0612-9.

Khaliq, S., Jahan, S., Pervaiz, A., Ashfaq, U.A., and Hassan, S. (2011). Down-regulation of IRES containing 5' UTR of HCV genotype 3a using siRNAs. *Virology Journal* 8**,** 9. DOI: 10.1186/1743-422x-8-221.

Khan, M.Z., Haider, S., Mansoor, S., and Amin, I. (2019). Targeting plant ssDNA viruses with engineered miniature CRISPR-Cas14a. *Trends in Biotechnology* 37**,** 800-804. DOI: 10.1016/j.tibtech.2019.03.015.

Kim, E.S., Choi, E., Kim, Y., Cho, K.W., Lee, A., Shim, J., Rakwal, R., Agrawal, G.K., and Han, O.S. (2003). Dual positional specificity and expression of non-traditional lipoxygenase induced by wounding and methyl jasmonate in maize seedlings. *Plant Molecular Biology* 52**,** 1203-1213. DOI: 10.1023/B:PLAN.0000004331.94803.b0.

Kim, J.S., Lee, J., Lee, C.H., Woo, S.Y., Kang, H., Seo, S.G., and Kim, S.H. (2015). Activation of *PATHOGENESIS-RELATED* genes by the *Rhizobacterium*, *Bacillus* sp JS, which induces systemic resistance in tobacco plants. *Plant Pathology Journal* 31**,** 195-201. DOI: 10.5423/ppj.Nt.11.2014.0122.

Kim, Y.G., Cha, J., and Chandrasegaran, S. (1996). Hybrid restriction enzymes: Zinc finger fusions to Fok I cleavage domain. *Proceedings of the National Academy of Sciences of the United States of America* 93**,** 1156-1160. DOI: 10.1073/pnas.93.3.1156.

Koch, A., Biedenkopf, D., Furch, A., Weber, L., Rossbach, O., Abdellatef, E., Linicus, L., Johannsmeier, J., Jelonek, L., Goesmann, A., Cardoza, V., Mcmillan, J., Mentzel, T., and Kogel, K.H. (2016). An RNAi-based control of *Fusarium graminearum* infections through spraying of long dsRNAs involves a plant passage and is controlled by the fungal silencing machinery. *Plos Pathogens* 12**,** 22. DOI: 10.1371/journal.ppat.1005901.

Koch, A., Kumar, N., Weber, L., Keller, H., Imani, J., and Kogel, K.-H. (2013). Host-induced gene silencing of cytochrome P450 lanosterol C14α-demethylase–encoding genes confers strong resistance to *Fusarium* species. *Proceedings of the National Academy of Sciences* 110**,** 19324. DOI: 10.1073/pnas.1306373110.

Koch, A., Schlemmer, T., Höfle, L., Werner, B., Preußer, C., Hardt, M., Möbus, A., Biedenkopf, D., Claar, M., Perlet, C., Jelonek, L., Goesmann, A., Garikapati, V., Spengler, B., Busche, T., Kalinowski, J., and Kogel, K. (2020). Host-induced gene silencing involves transfer of dsRNA-derived siRNA via extracellular vesicles. *bioRxiv*, 2020.2002.2012.945154. DOI: 10.1101/2020.02.12.945154.

Koeppel, I., Hertig, C., Hoffie, R., and Kumlehn, J. (2019). Cas endonuclease technology a quantum leap in the advancement of barley and wheat genetic engineering. *International Journal of Molecular Sciences* 20**,** 24. DOI: 10.3390/ijms20112647.

Kolomiets, M.V., Chen, H., Gladon, R.J., Braun, E.J., and Hannapel, D.J. (2000). A leaf lipoxygenase of potato induced specifically by pathogen infection. *Plant Physiology* 124**,** 1121-1130. DOI: 10.1104/pp.124.3.1121.

Komor, A.C., Kim, Y.B., Packer, M.S., Zuris, J.A., and Liu, D.R. (2016). Programmable editing of a target base in genomic DNA without double-stranded DNA cleavage. *Nature* 533**,** 420-424. DOI: 10.1038/nature17946.

Koseoglou, E. (2017). The study of *SlPMR4* CRISPR/Cas9-mediated tomato allelic series for resistance against powdery mildew. *Department of Plant BreedingWageningen University and Research* 34.

Kostandi, S.F., and Geisler, G. (1989). Maize smut induced by *Ustilago maydis* (d-c) corda - specific effect of smut intensity and location of galls on yield losses. *Journal of Agronomy and Crop Science-Zeitschrift Fur Acker Und Pflanzenbau* 163**,** 62-68. DOI: 10.1111/j.1439-037X.1989.tb00738.x.

Kretschmer, M., Leroch, M., Mosbach, A., Walker, A.S., Fillinger, S., Mernke, D., Schoonbeek, H.J., Pradier, J.M., Leroux, P., De Waard, M.A., and Hahn, M. (2009). Fungicide-driven evolution and molecular basis of multidrug resistance in field populations of the grey mould fungus *Botrytis cinerea*. *Plos Pathogens* 5**,** 13. DOI: 10.1371/journal.ppat.1000696.

Ku, M.S.B., Agarie, S., Nomura, M., Fukayama, H., Tsuchida, H., Ono, K., Hirose, S., Toki, S., Miyao, M., and Matsuoka, M. (1999). High-level expression of maize *PHOSPHOENOLPYRUVATE CARBOXYLASE* in transgenic rice plants. *Nature Biotechnology* 17**,** 76-80. DOI: 10.1038/5256.

Kumar, N., Galli, M., Ordon, J., Stuttmann, J., Kogel, K.H., and Imani, J. (2018). Further analysis of barley MORC1 using a highly efficient RNA-guided Cas9 gene-editing system. *Plant Biotechnol J* 16**,** 1892-1903. DOI: 10.1111/pbi.12924.

Kumlehn, J. (2008). The IPKb vector set: modular binary plasmids for cereal transformation. *Information Systems for Biotechnology News Report, Virginia Tech, Blacksburg,* **,** 3-6.

Kumlehn, J., Pietralla, J., Hensel, G., Pacher, M., and Puchta, H. (2018). The CRISPR/Cas revolution continues: from efficient gene editing for crop breeding to plant synthetic biology. *Journal of Integrative Plant Biology* 60**,** 1127-1153. DOI: 10.1111/jipb.12734.

Kynast, R.G. (2012). Handbook of maize: genetics and genomics. *Annals of Botany* 109**,** viii-ix. DOI: 10.1093/aob/mcs080.

Lanver, D., Muller, A.N., Happel, P., Schweizer, G., Haas, F.B., Franitza, M., Pellegrin, C., Reissmann, S., Altmuller, J., Rensing, S.A., and Kahmann, R. (2018). The biotrophic development of *Ustilago maydis* studied by RNA-seq analysis. *Plant Cell* 30**,** 300-323. DOI: 10.1105/tpc.17.00764.

Laplace, F. (1989). G. N. Agrios, Plant Pathology (3rd Edition). XVI + 803 S., 265 Abb. San Diego–New York–Berkeley–Boston–London–Sydney–Tokyo–Toronto 1988. Academic Press Inc. $ 45.00. ISBN: 0-12-044563-8. *Journal of Basic Microbiology* 29**,** 500-500. DOI: 10.1002/jobm.3620290804.

Lawrenson, T., Shorinola, O., Stacey, N., Li, C.D., Ostergaard, L., Patron, N., Uauy, C., and Harwood, W. (2015). Induction of targeted, heritable mutations in barley and *Brassica oleracea* using RNA-guided Cas9 nuclease. *Genome Biology* 16**,** 13. DOI: 10.1186/s13059-015-0826-7.

Lee, K., Zhang, Y.X., Kleinstiver, B.P., Guo, J.A., Aryee, M.J., Miller, J., Malzahn, A., Zarecor, S., Lawrence-Dill, C.J., Joung, J.K., Qi, Y.P., and Wang, K. (2019). Activities and specificities of CRISPR/Cas9 and Cas12a nucleases for targeted mutagenesis in maize. *Plant Biotechnology Journal* 17**,** 362-372. DOI: 10.1111/pbi.12982.

Lei, Y., Lu, L., Liu, H.Y., Li, S., Xing, F., and Chen, L.L. (2014). CRISPR-P: a web tool for synthetic single-guide RNA design of CRISPR-system in plants. *Mol Plant* 7**,** 1494-1496. DOI: 10.1093/mp/ssu044.

Li, C., Haslam, T.M., Kruger, A., Schneider, L.M., Mishina, K., Samuels, L., Yan, H.X., Kunst, L., Schaffrath, U., Nawrath, C., Chen, G.X., Komatsuda, T., and Von Wettstein-Knowles, P. (2018). The β-ketoacyl-CoA synthase HvKCS1, Encoded by Cer-zh, plays a key role in synthesis of barley leaf wax and germination of barley powdery mildew. *Plant and Cell Physiology* 59**,** 811-827. DOI: 10.1093/pcp/pcy020.

Li, J.-F., Norville, J.E., Aach, J., Mccormack, M., Zhang, D., Bush, J., Church, G.M., and Sheen, J. (2013). Multiplex and homologous recombination–mediated genome editing in *Arabidopsis* and *Nicotiana benthamiana* using guide RNA and Cas9. *Nature Biotechnology* 31**,** 688-691. DOI: 10.1038/nbt.2654.

Li, L.D., Chang, S.S., and Liu, Y. (2010). RNA interference pathways in filamentous fungi. *Cellular and Molecular Life Sciences* 67**,** 3849-3863. DOI: 10.1007/s00018-010-0471-y.

Li, M., Hensel, G., Mascher, M., Melzer, M., Budhagatapalli, N., Rutten, T., Himmelbach, A., Beier, S., Korzun, V., Kumlehn, J., Borner, T., and Stein, N. (2019). Leaf variegation and impaired chloroplast development caused by a truncated CCT domain gene in *albostrians* barley. *Plant Cell* 31**,** 1430-1445. DOI: 10.1105/tpc.19.00132.

Li, T., Liu, B., Spalding, M.H., Weeks, D.P., and Yang, B. (2012). High-efficiency TALEN-based gene editing produces disease-resistant rice. *Nature Biotechnology* 30**,** 390-392. DOI: 10.1038/nbt.2199.

Li, Z.S., Liu, Z.B., Xing, A.Q., Moon, B.P., Koellhoffer, J.P., Huang, L.X., Ward, R.T., Clifton, E., Falco, S.C., and Cigan, A.M. (2015). Cas9-Guide RNA directed genome editing in soybean. *Plant Physiology* 169**,** 960-+. DOI: 10.1104/pp.15.00783.

Liang, G., Zhang, H., Lou, D., and Yu, D. (2016). Selection of highly efficient sgRNAs for CRISPR/Cas9-based plant genome editing. *Sci Rep* 6**,** 21451. DOI: 10.1038/srep21451.

Liavonchanka, A., and Feussner, N. (2006). Lipoxygenases: Occurrence, functions and catalysis. *Journal of Plant Physiology* 163**,** 348-357. DOI: 10.1016/j.jplph.2005.11.006.

Lieber, M.R. (1999). The biochemistry and biological significance of nonhomologous DNA end joining: an essential repair process in multicellular eukaryotes. *Genes to Cells* 4**,** 77-85. DOI: 10.1046/j.1365-2443.1999.00245.x.

Lim, C.W., Han, S.W., Hwang, I.S., Kim, D.S., Hwang, B.K., and Lee, S.C. (2015). The pepper lipoxygenase *CaLOX1* plays a role in osmotic, drought and high salinity stress response. *Plant and Cell Physiology* 56**,** 930-942. DOI: 10.1093/pcp/pcv020.

Lin, C.S., Hsu, C.T., Yang, L.H., Lee, L.Y., Fu, J.Y., Cheng, Q.W., Wu, F.H., Hsiao, H.C.W., Zhang, Y.S., Zhang, R., Chang, W.J., Yu, C.T., Wang, W., Liao, L.J., Gelvin, S.B., and Shih, M.C. (2018). Application of protoplast technology to CRISPR/Cas9 mutagenesis: from single-cell mutation detection to mutant plant regeneration. *Plant Biotechnology Journal* 16**,** 1295-1310. DOI: 10.1111/pbi.12870.

Lipps, P.E. (1985). Influence of inoculum from buried and surface corn residues on the incidence of corn anthracnose. *Phytopathology* 75**,** 1212-1216. DOI: 10.1094/Phyto-75-1212.

Liu, H., Ding, Y., Zhou, Y., Jin, W., Xie, K., and Chen, L.L. (2017a). CRISPR-P 2.0: An improved CRISPR-Cas9 tool for genome editing in plants. *Mol Plant* 10**,** 530-532. DOI: 10.1016/j.molp.2017.01.003.

Liu, X., Wu, S., Xu, J., Sui, C., and Wei, J. (2017b). Application of CRISPR/Cas9 in plant biology. *Acta Pharm Sin B* 7**,** 292-302. DOI: 10.1016/j.apsb.2017.01.002.

Livak, K.J., and Schmittgen, T.D. (2001). Analysis of relative gene expression data using real-time quantitative PCR and the $2^{-\Delta\Delta CT}$ method. *Methods* 25**,** 402-408. DOI: 10.1006/meth.2001.1262.

Lloyd, A., Plaisier, C.L., Carroll, D., and Drews, G.N. (2005). Targeted mutagenesis using zinc-finger nucleases in *Arabidopsis*. *Proceedings of the National Academy of Sciences of the United States of America* 102**,** 2232-2237. DOI: 10.1073/pnas.0409339102.

Lo Presti, L., Lanver, D., Schweizer, G., Tanaka, S., Liang, L., Tollot, M., Zuccaro, A., Reissmann, S., and Kahmann, R. (2015). "Fungal effectors and plant susceptibility," in *Annual Review of Plant Biology, Vol 66,* ed. S.S. Merchant. (Palo Alto: Annual Reviews), 513-545. DOI: 10.1146/annurev-arplant-043014-114623.

Loake, G., and Grant, M. (2007). Salicylic acid in plant defence-the players and protagonists. *Curr Opin Plant Biol* 10**,** 466-472. DOI: 10.1016/j.pbi.2007.08.008.

Lor, V.S., Starker, C.G., Voytas, D.F., Weiss, D., and Olszewski, N.E. (2014). Targeted mutagenesis of the tomato *PROCERA* gene using transcription activator-like effector nucleases. *Plant Physiology* 166**,** 1288-+. DOI: 10.1104/pp.114.247593.

Lorenz, R., Bernhart, S.H., Höner Zu Siederdissen, C., Tafer, H., Flamm, C., Stadler, P.F., and Hofacker, I.L. (2011). ViennaRNA Package 2.0. *Algorithms Mol Biol* 6**,** 26. DOI: 10.1186/1748-7188-6-26.

Lorrain, S., Vailleau, F., Balaque, C., and Roby, D. (2003). Lesion mimic mutants: keys for deciphering cell death and defense pathways in plants? *Trends in Plant Science* 8**,** 263-271. DOI: 10.1016/s1360-1385(03)00108-0.

Lowder, L.G., Zhang, D., Baltes, N.J., Paul, J.W., 3rd, Tang, X., Zheng, X., Voytas, D.F., Hsieh, T.F., Zhang, Y., and Qi, Y. (2015). A CRISPR/Cas9 toolbox for multiplexed plant genome editing and transcriptional regulation. *Plant Physiol* 169**,** 971-985. DOI: 10.1104/pp.15.00636.

Luna, E., Pastor, V., Robert, J., Flors, V., Mauch-Mani, B., and Ton, J. (2011). Callose deposition: a multifaceted plant defense response. *Mol Plant Microbe Interact* 24**,** 183-193. DOI: 10.1094/mpmi-07-10-0149.

Lyons, R., Manners, J.M., and Kazan, K. (2013). Jasmonate biosynthesis and signaling in monocots: a comparative overview. *Plant Cell Rep* 32**,** 815-827. DOI: 10.1007/s00299-013-1400-y.

Ma, X.L., Zhang, Q.Y., Zhu, Q.L., Liu, W., Chen, Y., Qiu, R., Wang, B., Yang, Z.F., Li, H.Y., Lin, Y.R., Xie, Y.Y., Shen, R.X., Chen, S.F., Wang, Z., Chen, Y.L., Guo, J.X., Chen, L.T., Zhao, X.C., Dong, Z.C., and Liu, Y.G. (2015). A robust CRISPR/Cas9 system for convenient, high-efficiency multiplex genome editing in monocot and dicot plants. *Molecular Plant* 8**,** 1274-1284. DOI: 10.1016/j.molp.2015.04.007.

Ma, Z.H., and Michailides, T.J. (2005). Advances in understanding molecular mechanisms of fungicide resistance and molecular detection of resistant genotypes in phytopathogenic fungi. *Crop Protection* 24**,** 853-863. DOI: 10.1016/j.cropro.2005.01.011.

Maeder, M.L., Thibodeau-Beganny, S., Osiak, A., Wright, D.A., Anthony, R.M., Eichtinger, M., Jiang, T., Foley, J.E., Winfrey, R.J., Townsend, J.A., Unger-Wallace, E., Sander, J.D., Muller-Lerch, F., Fu, F.L., Pearlberg, J., Gobel, C., Dassie, J.P., Pruett-Miller, S.M., Porteus, M.H., Sgroi, D.C., Iafrate, A.J., Dobbs, D., Mccray, P.B., Cathomen, T., Voytas, D.F., and Joung, J.K. (2008). Rapid "open-source" engineering of customized zinc-finger nucleases for highly efficient gene modification. *Molecular Cell* 31**,** 294-301. DOI: 10.1016/j.molcel.2008.06.016.

Mahfouz, M.M., Li, L.X., Shamimuzzaman, M., Wibowo, A., Fang, X.Y., and Zhu, J.K. (2011). De novo-engineered transcription activator-like effector (TALE) hybrid nuclease with novel DNA binding specificity creates double-strand breaks. *Proceedings of the National Academy of Sciences of the United States of America* 108**,** 2623-2628. DOI: 10.1073/pnas.1019533108.

Mahfouz, M.M., Piatek, A., and Stewart, C.N. (2014). Genome engineering via TALENs and CRISPR/Cas9 systems: challenges and perspectives. *Plant Biotechnology Journal* 12**,** 1006-1014. DOI: 10.1111/pbi.12256.

Majumdar, R., Rajasekaran, K., and Cary, J.W. (2017a). RNA interference (RNAi) as a potential tool for control of mycotoxin contamination in crop plants: concepts and considerations. *Frontiers in Plant Science* 8**,** 14. DOI: 10.3389/fpls.2017.00200.

Majumdar, R., Rajasekaran, K., Sickler, C., Lebar, M., Musungu, B.M., Fakhoury, A.M., Payne, G.A., Geisler, M., Carter-Wientjes, C., Wei, Q., Bhatnagar, D., and Cary, J.W. (2017b). The *PATHOGENESIS-RELATED MAIZE SEED* (*PRMS*) gene plays a role in resistance to *Aspergillus flavus* infection and aflatoxin contamination. *Frontiers in Plant Science* 8. DOI: 10.3389/fpls.2017.01758.

Malandrakis, A.A., Markoglou, A.N., and Ziogas, B.N. (2012). PCR-RFLP detection of the E198A mutation conferring resistance to benzimidazoles in field isolates of *Monilinia laxa* from Greece. *Crop Protection* 39**,** 11-17. DOI: 10.1016/j.cropro.2012.04.001.

Manghwar, H., Lindsey, K., Zhang, X.L., and Jin, S.X. (2019). CRISPR/Cas system: recent advances and future prospects for genome editing. *Trends in Plant Science* 24**,** 1102-1125. DOI: 10.1016/j.tplants.2019.09.006.

Manoli, A., Sturaro, A., Trevisan, S., Quaggiotti, S., and Nonis, A. (2012). Evaluation of candidate reference genes for qPCR in maize. *Journal of Plant Physiology* 169**,** 807-815. DOI: 10.1016/j.jplph.2012.01.019.

Mao, X.H., Zheng, Y.M., Xiao, K.Z., Wei, Y.D., Zhu, Y.S., Cai, Q.H., Chen, L.P., Xie, H.A., and Zhang, J.F. (2018). *OsPRX2* contributes to stomatal closure and improves potassium deficiency tolerance

in rice. *Biochemical and Biophysical Research Communications* 495**,** 461-467. DOI: 10.1016/j.bbrc.2017.11.045.

Mao, Y.F., Zhang, H., Xu, N.F., Zhang, B.T., Gou, F., and Zhu, J.K. (2013). Application of the CRISPRCas system for efficient genome engineering in plants. *Molecular Plant* 6**,** 2008-2011. DOI: 10.1093/mp/sst121.

Martin, G.B., Bogdanove, A.J., and Sessa, G. (2003). Understanding the functions of plant disease resistance proteins. *Annu Rev Plant Biol* 54**,** 23-61. DOI: 10.1146/annurev.arplant.54.031902.135035.

Martínez-Soto, D., and Ruiz-Herrera, J. (2016). Infection of *Zea mays* by haploid strains of *Ustilago maydis*. *Fungal Genomics & Biology* 06. DOI: 10.4172/2165-8056.1000141.

Marton, I., Zuker, A., Shklarman, E., Zeevi, V., Tovkach, A., Roffe, S., Ovadis, M., Tzfira, T., and Vainstein, A. (2010). Nontransgenic genome modification in plant cells. *Plant Physiology* 154**,** 1079-1087. DOI: 10.1104/pp.110.164806.

Masanga, J.O., Matheka, J.M., Omer, R.A., Ommeh, S.C., Monda, E.O., and Alakonya, A.E. (2015). Downregulation of transcription factor *AflR* in *Aspergillus flavus* confers reduction to aflatoxin accumulation in transgenic maize with alteration of host plant architecture. *Plant Cell Reports* 34**,** 1379-1387. DOI: 10.1007/s00299-015-1794-9.

Maschietto, V., Lanubile, A., De Leonardis, S., Marocco, A., and Paciollaba, C. (2016). Constitutive expression of PATHOGENESIS-RELATED proteins and antioxydant enzyme activities triggers maize resistance towards *Fusarium verticillioides*. *Journal of Plant Physiology* 200**,** 53-61. DOI: 10.1016/j.jplph.2016.06.006.

Maschietto, V., Marocco, A., Malachova, A., and Lanubile, A. (2015). Resistance to *Fusarium verticillioides* and fumonisin accumulation in maize inbred lines involves an earlier and enhanced expression of *LIPOXYGENASE* (*LOX*) genes. *Journal of Plant Physiology* 188**,** 9-18. DOI: 10.1016/j.jplph.2015.09.003.

Mccormick, S. (2017). Chloroplast-targeted antioxidant protein protects against necrotrophic fungal attack. *Plant Journal* 92**,** 759-760. DOI: 10.1111/tpj.13762.

Mcgrath, K.C., Dombrecht, B., Manners, J.M., Schenk, P.M., Edgar, C.I., Maclean, D.J., Scheible, W.R., Udvardi, M.K., and Kazan, K. (2005). Repressor- and activator-type ethylene response factors functioning in jasmonate signaling and disease resistance identified via a genome-wide screen of *Arabidopsis* transcription factor gene expression. *Plant Physiol* 139**,** 949-959. DOI: 10.1104/pp.105.068544.

Mendes, C.a.C., Mendes, G.E., Cipullo, J.P., and Burdmann, E.A. (2005). Acute intoxication due to ingestion of vegetables contaminated with aldicarb. *Clinical Toxicology* 43**,** 117-118. DOI: 10.1081/clt-200050392.

Mercx, S., Smargiasso, N., Chaumont, F., De Pauw, E., Boutry, M., and Navarre, C. (2017). Inactivation of the *β(1,2)-XYLOSYLTRANSFERASE* and the *α(1,3)-FUCOSYLTRANSFERASE* genes in *Nicotiana tabacum* BY-2 cells by a multiplex CRISPR/Cas9 strategy results in glycoproteins without plant-specific glycans. *Frontiers in Plant Science* 8. DOI: 10.3389/fpls.2017.00403.

Meunier, S., and Vernos, I. (2012). Microtubule assembly during mitosis - from distinct origins to distinct functions? *Journal of Cell Science* 125**,** 2805-2814. DOI: 10.1242/jcs.092429.

Milner, S.G., Jost, M., Taketa, S., Mazón, E.R., Himmelbach, A., Oppermann, M., Weise, S., Knüpffer, H., Basterrechea, M., König, P., Schüler, D., Sharma, R., Pasam, R.K., Rutten, T., Guo, G., Xu, D., Zhang, J., Herren, G., Müller, T., Krattinger, S.G., Keller, B., Jiang, Y., González, M.Y., Zhao, Y., Habekuß, A., Färber, S., Ordon, F., Lange, M., Börner, A., Graner, A., Reif, J.C., Scholz, U., Mascher, M., and Stein, N. (2019). Genebank genomics highlights the diversity of a global barley collection. *Nat Genet* 51**,** 319-326. DOI: 10.1038/s41588-018-0266-x.

Mitema, A., Okoth, S., and Rafudeen, S.M. (2019). The development of a qPCR assay to measure *Aspergillus flavus* biomass in maize and the use of a biocontrol strategy to limit aflatoxin production (vol 11, 179, 2019). *Toxins* 11**,** 1. DOI: 10.3390/toxins11070384.

Mitsuhara, I., Iwai, T., Seo, S., Yanagawa, Y., Kawahigasi, H., Hirose, S., Ohkawa, Y., and Ohashi, Y. (2008). Characteristic expression of twelve rice *PRI* family genes in response to pathogen infection, wounding, and defense-related signal compounds (121/180). *Molecular Genetics and Genomics* 279**,** 415-427. DOI: 10.1007/s00438-008-0322-9.

Molina, L., and Kahmann, R. (2007). An *Ustilago maydis* gene involved in H_2O_2 detoxification is required for virulence. *Plant Cell* 19**,** 2293-2309. DOI: 10.1105/tpc.107.052332.

Moosavi, B., Zhu, X.L., Yang, W.C., and Yang, G.F. (2020). Genetic, epigenetic and biochemical regulation of succinate dehydrogenase function. *Biological Chemistry* 401**,** 319-330. DOI: 10.1515/hsz-2019-0264.

Moscou, M.J., and Bogdanove, A.J. (2009). A Simple cipher governs DNA recognition by TAL effectors. *Science* 326**,** 1501-1501. DOI: 10.1126/science.1178817.

Muencha, S., Lingner, U., Floss, D.S., Ludwig, N., Sauer, N., and Deising, H.B. (2008). The hemibiotrophic lifestyle of *Colletotrichum* species. *Journal of Plant Physiology* 165**,** 41-51. DOI: 10.1016/j.jplph.2007.06.008.

Murillo, I., Cavallarin, L., and Sansegundo, B. (1997). The maize pathogenesis-related PRMS protein localizes to plasmodesmata in maize radicles. *Plant Cell* 9**,** 145-156.

Murillo, I., Cavallarin, L., and Segundo, B.S. (1999). Cytology of infection of maize seedlings by *fusarium moniliforme* and immunolocalization of the pathogenesis-related PRMS protein. *Phytopathology* 89**,** 737-747. DOI: 10.1094/phyto.1999.89.9.737.

Muroyama, A., and Lechler, T. (2017). Microtubule organization, dynamics and functions in differentiated cells. *Development* 144**,** 3012-3021. DOI: 10.1242/dev.153171.

Naim, F., Shand, K., Hayashi, S., O'brien, M., Mcgree, J., Johnson, A.a.T., Dugdale, B., and Waterhouse, P.M. (2020). Are the current gRNA ranking prediction algorithms useful for genome editing in plants? *PLoS One* 15**,** e0227994. DOI: 10.1371/journal.pone.0227994.

Nalam, V.J., Alam, S., Keereetaweep, J., Venables, B., Burdan, D., Lee, H., Trick, H.N., Sarowar, S., Makandar, R., and Shah, J. (2015). Facilitation of *Fusarium graminearum* infection by 9-lipoxygenases in *Arabidopsis* and Wheat. *Mol Plant Microbe Interact* 28**,** 1142-1152. DOI: 10.1094/mpmi-04-15-0096-r.

Nalam, V.J., Keeretaweep, J., Sarowar, S., and Shah, J. (2012). Root-derived oxylipins promote green peach aphid performance on *Arabidopsis* foliage. *Plant Cell* 24**,** 1643-1653. DOI: 10.1105/tpc.111.094110.

Nasser, W., De Tapia, M., Kauffmann, S., Montasser-Kouhsari, S., and Burkard, G. (1988). Identification and characterization of maize PATHOGENESIS-RELATED proteins. Four maize PR proteins are chitinases. *Plant Mol Biol* 11**,** 529-538. DOI: 10.1007/bf00039033.

Navarrete, F., Grujic, N., Stirnberg, A., Aleksza, D., Gallei, M., Adi, H., Bindics, J., Trujillo, M., and Djamei, A. (2019). The Pleiades cluster of fungal effector genes inhibit host defenses. *bioRxiv***,** 827600. DOI: 10.1101/827600.

Navarro, L., Zipfel, C., Rowland, O., Keller, I., Robatzek, S., Boller, T., and Jones, J.D. (2004). The transcriptional innate immune response to *flg22*. Interplay and overlap with *avr* gene-dependent defense responses and bacterial pathogenesis. *Plant Physiol* 135**,** 1113-1128. DOI: 10.1104/pp.103.036749.

Nekrasov, V., Wang, C., Win, J., Lanz, C., Weigel, D., and Kamoun, S. (2017). Rapid generation of a transgene-free powdery mildew resistant tomato by genome deletion. *Scientific Reports* 7**,** 482. DOI: 10.1038/s41598-017-00578-x.

Nemchenko, A., Kunze, S., Feussner, I., and Kolomiets, M. (2006). Duplicate maize 13-lipoxygenase genes are differentially regulated by circadian rhythm, cold stress, wounding, pathogen infection, and hormonal treatments. *J Exp Bot* 57**,** 3767-3779. DOI: 10.1093/jxb/erl137.

Nieves-Cordones, M., Mohamed, S., Tanoi, K., Kobayashi, N.I., Takagi, K., Vernet, A., Guiderdoni, E., Périn, C., Sentenac, H., and Véry, A.-A. (2017). Production of low-Cs+ rice plants by inactivation of the K+ transporter OsHAK1 with the CRISPR-Cas system. *The Plant Journal* 92**,** 43-56. DOI: 10.1111/tpj.13632.

Nimchuk, Z., Eulgem, T., Holt, B.F., 3rd, and Dangl, J.L. (2003). Recognition and response in the plant immune system. *Annu Rev Genet* 37**,** 579-609. DOI: 10.1146/annurev.genet.37.110801.142628.

Nogales, E. (2001). Structural insights into microtubule function. *Annual Review of Biophysics and Biomolecular Structure* 30**,** 397-420. DOI: 10.1146/annurev.biophys.30.1.397.

Nowara, D., Gay, A., Lacomme, C., Shaw, J., Ridout, C., Douchkov, D., Hensel, G., Kumlehn, J., and Schweizer, P. (2010). HIGS: host-induced gene silencing in the obligate biotrophic fungal pathogen *Blumeria graminis*. *Plant Cell* 22**,** 3130-3141. DOI: 10.1105/tpc.110.077040.

Nunes, C.C., and Dean, R.A. (2012). Host-induced gene silencing: a tool for understanding fungal host interaction and for developing novel disease control strategies. *Molecular Plant Pathology* 13**,** 519-529. DOI: 10.1111/j.1364-3703.2011.00766.x.

Odipio, J., Alicai, T., Ingelbrecht, I., Nusinow, D.A., Bart, R., and Taylor, N.J. (2017). Efficient CRISPR/Cas9 genome editing of phytoene desaturase in cassava. *Frontiers in Plant Science* 8. DOI: 10.3389/fpls.2017.01780.

Ogunola, O.F., Hawkins, L.K., Mylroie, E., Kolomiets, M.V., Borrego, E., Tang, J.D., Williams, W.P., and Warburton, M.L. (2017). Characterization of the maize lipoxygenase gene family in relation to aflatoxin accumulation resistance. *PLoS One* 12**,** e0181265. DOI: 10.1371/journal.pone.0181265.

Ohta, H., Shida, K., Peng, Y.L., Furusawa, I., Shishiyama, J., Aibara, S., and Morita, Y. (1991). A lipoxygenase pathway is activated in rice after infection with the rice blast fungus *Magnaporthe grisea*. *Plant Physiol* 97**,** 94-98. DOI: 10.1104/pp.97.1.94.

Oliver, R.P., Rybak, K., Shankar, M., Loughman, R., Harry, N., and Solomon, P.S. (2008). Quantitative disease resistance assessment by real-time PCR using the *Stagonospora nodorum*-wheat pathosystem as a model. *Plant Pathology* 57**,** 527-532. DOI: 10.1111/j.1365-3059.2007.01787.x.

Osakabe, K., Osakabe, Y., and Toki, S. (2010). Site-directed mutagenesis in *Arabidopsis* using custom-designed zinc finger nucleases. *Proceedings of the National Academy of Sciences of the United States of America* 107**,** 12034-12039. DOI: 10.1073/pnas.1000234107.

Pallotta, M., Graham, R., Langridge, P., Sparrow, D., and Barker, S. (2000). RFLP mapping of manganese efficiency in barley. *Theoretical and Applied Genetics* 101**,** 1100-1108.

Pan, C.T., Ye, L., Qin, L., Liu, X., He, Y.J., Wang, J., Chen, L.F., and Lu, G. (2017). CRISPR/Cas9-mediated efficient and heritable targeted mutagenesis in tomato plants in the first and later generations (vol 6, 24765, 2016). *Scientific Reports* 7**,** 1. DOI: 10.1038/srep46916.

Panwar, V., Jordan, M., Mccallum, B., and Bakkeren, G. (2018). Host-induced silencing of essential genes in *Puccinia triticina* through transgenic expression of RNAi sequences reduces severity of leaf rust infection in wheat. *Plant Biotechnology Journal* 16**,** 1013-1023. DOI: 10.1111/pbi.12845.

Panwar, V., Mccallum, B., and Bakkeren, G. (2013). Host-induced gene silencing of wheat leaf rust fungus *Puccinia triticina* pathogenicity genes mediated by the Barley stripe mosaic virus. *Plant Molecular Biology* 81**,** 595-608. DOI: 10.1007/s11103-013-0022-7.

Papp, I., Mette, M.F., Aufsatz, W., Daxinger, L., Schauer, S.E., Ray, A., Van Der Winden, J., Matzke, M., and Matzke, A.J.M. (2003). Evidence for nuclear processing of plant micro RNA and short interfering RNA precursors. *Plant Physiology* 132**,** 1382-1390. DOI: 10.1104/pp.103.021980.

Park, Y.S., Kunze, S., Ni, X.Z., Feussner, I., and Kolomiets, M.V. (2010). Comparative molecular and biochemical characterization of segmentally duplicated 9-lipoxygenase genes *ZmLOX4* and *ZmLOX5* of maize. *Planta* 231**,** 1425-1437. DOI: 10.1007/s00425-010-1143-8.

Parry, D.W. (1990). *Plant pathology in agriculture.* CUP Archive.

Pathak, B., Zhao, S., Manoharan, M., and Srivastava, V. (2019). Dual-targeting by CRISPR/Cas9 leads to efficient point mutagenesis but only rare targeted deletions in the rice genome. *3 Biotech* 9**,** 158. DOI: 10.1007/s13205-019-1690-z.

Pathi, K.M., Rink, P., Budhagatapalli, N., Betz, R., Saado, I., Hiekel, S., Becker, M., Djamei, A., and Kumlehn, J. (2020). Engineering smut resistance in maize by site-directed mutagenesis of *LIPOXYGENASE 3*. *Frontiers in Plant Science* 11. DOI: 10.3389/fpls.2020.543895.

Pathi, K.M., Tula, S., Huda, K.M., Srivastava, V.K., and Tuteja, N. (2013). An efficient and rapid regeneration via multiple shoot induction from mature seed derived embryogenic and organogenic callus of Indian maize (*Zea mays* L.). *Plant Signal Behav* 8**,** doi: 10.4161/psb.25891. DOI: 10.4161/psb.25891.

Pauwels, K., Podevin, N., Breyer, D., Carroll, D., and Herman, P. (2014). Engineering nucleases for gene targeting: safety and regulatory considerations. *New Biotechnology* 31**,** 18-27. DOI: 10.1016/j.nbt.2013.07.001.

Pauwels, L., De Clercq, R., Goossens, J., Inigo, S., Williams, C., Ron, M., Britt, A., and Goossens, A. (2019). A Dual sgRNA approach for functional genomics in *Arabidopsis thaliana* (vol 8, pg 2603, 2018). *G3-Genes Genomes Genetics* 9**,** 3907-3907. DOI: 10.1534/g3.119.400709.

Pechanova, O., and Pechan, T. (2015). Maize-Pathogen Interactions: An ongoing combat from a proteomics perspective. *International Journal of Molecular Sciences* 16**,** 28429-28448. DOI: 10.3390/ijms161226106.

Penninckx, I.A., Eggermont, K., Terras, F.R., Thomma, B.P., De Samblanx, G.W., Buchala, A., Métraux, J.P., Manners, J.M., and Broekaert, W.F. (1996). Pathogen-induced systemic activation of a plant defensin gene in *Arabidopsis* follows a salicylic acid-independent pathway. *Plant Cell* 8**,** 2309-2323. DOI: 10.1105/tpc.8.12.2309.

Perkins, J.M., and Hooker, A.L. (1979). Effects of anthracnose stalk rot on corn yields in Illinois. *Plant Disease Reporter* 63**,** 26-30.

Petit, A.N., Fontaine, F., Clement, C., and Vaillant-Gaveau, N. (2008). Photosynthesis limitations of grapevine after treatment with the fungicide fludioxonil. *Journal of Agricultural and Food Chemistry* 56**,** 6761-6767. DOI: 10.1021/jf800919u.

Pinter, N., Hach, C.A., Hampel, M., Rekhter, D., Zienkiewicz, K., Feussner, I., Poehlein, A., Daniel, R., Finkernagel, F., and Heimel, K. (2019). Signal peptide peptidase activity connects the unfolded protein response to plant defense suppression by *Ustilago maydis*. *Plos Pathogens* 15**,** 40. DOI: 10.1371/journal.ppat.1007734.

Pitino, M., Coleman, A.D., Maffei, M.E., Ridout, C.J., and Hogenhout, S.A. (2011). Silencing of aphid genes by dsRNA feeding from plants. *Plos One* 6**,** 8. DOI: 10.1371/journal.pone.0025709.

Plessis, A., Perrin, A., Haber, J.E., and Dujon, B. (1992). Site-specific recombination determined by I-SceI, a mitochondrial group-i intron-encoded endonuclease expressed in the yeast nucleus. *Genetics* 130**,** 451-460.

Pliego, C., Nowara, D., Bonciani, G., Gheorghe, D.M., Xu, R., Surana, P., Whigham, E., Nettleton, D., Bogdanove, A.J., Wise, R.P., Schweizer, P., Bindschedler, L.V., and Spanu, P.D. (2013). Host-induced gene silencing in barley powdery mildew reveals a class of ribonuclease-like effectors. *Molecular Plant-Microbe Interactions* 26**,** 633-642. DOI: 10.1094/mpmi-01-13-0005-r.

Porta, H., and Rocha-Sosa, M. (2002). Plant lipoxygenases. Physiological and molecular features. *Plant Physiol* 130**,** 15-21. DOI: 10.1104/pp.010787.

Pratt, A.J., and Macrae, I.J. (2009). The RNA-induced silencing complex: a versatile gene-silencing machine. *Journal of Biological Chemistry* 284**,** 17897-17901. DOI: 10.1074/jbc.R900012200.

Prieto, J., Redondo, P., Padro, D., Arnould, S., Epinat, J.C., Paques, F., Blanco, F.J., and Montoya, G. (2007). The C-terminal loop of the homing endonuclease I-CreI is essential for site recognition, DNA binding and cleavage. *Nucleic Acids Research* 35**,** 3262-3271. DOI: 10.1093/nar/gkm183.

Puchta, H., Dujon, B., and Hohn, B. (1996). Two different but related mechanisms are used in plants for the repair of genomic double-strand breaks by homologous recombination. *Proceedings of the National Academy of Sciences of the United States of America* 93**,** 5055-5060. DOI: 10.1073/pnas.93.10.5055.

Puchta, H., and Fauser, F. (2014). Synthetic nucleases for genome engineering in plants: prospects for a bright future. *Plant Journal* 78**,** 727-741. DOI: 10.1111/tpj.12338.

Pyott, D.E., Sheehan, E., and Molnar, A. (2016). Engineering of CRISPR/Cas9-mediated Potyvirus resistance in transgene-free *Arabidopsis* plants. *Mol Plant Pathol* 17**,** 1276-1288. DOI: 10.1111/mpp.12417.

Qi, T., Zhu, X.G., Tan, C.L., Liu, P., Guo, J., Kang, Z.S., and Guo, J. (2018). Host-induced gene silencing of an important pathogenicity factor *PsCpk1* in *Puccinia striiformis f. sp tritici* enhances resistance of wheat to stripe rust. *Plant Biotechnology Journal* 16**,** 797-807. DOI: 10.1111/pbi.12829.

Que, Q., Elumalai, S., Li, X., Zhong, H., Nalapalli, S., Schweiner, M., Fei, X., Nuccio, M., Kelliher, T., Gu, W., Chen, Z., and Chilton, M.-D.M. (2014). Maize transformation technology development for commercial event generation. *Frontiers in Plant Science* 5. DOI: 10.3389/fpls.2014.00379.

Raff, E.C. (1984). Genetics of microtubule systems. *Journal of Cell Biology* 99**,** 1-10. DOI: 10.1083/jcb.99.1.1.

Raheel, U., and Zaidi, N. (2014). Inhibition of Dengue virus 3 in mammalian cell culture by synthetic small interfering RNAs targeting highly conserved sequences. *Tropical Journal of Pharmaceutical Research* 13**,** 1621-1627. DOI: 10.4314/tjpr.v13i10.8.

Rance, I., Fournier, J., and Esquerre-Tugaye, M.T. (1998). The incompatible interaction between *Phytophthora parasitica* var. nicotianae race 0 and tobacco is suppressed in transgenic plants expressing antisense lipoxygenase sequences. *Proceedings of the National Academy of Sciences of the United States of America* 95**,** 6554-6559. DOI: 10.1073/pnas.95.11.6554.

Reimann, S., and Deising, H.B. (2005). Inhibition of efflux transporter-mediated fungicide resistance in *Pyrenophora tritici*-repentis by a derivative of 4'-hydroxyflavone and enhancement of fungicide activity. *Applied and Environmental Microbiology* 71**,** 3269-3275. DOI: 10.1128/aem.71.6.3269-3275.2005.

Robert-Seilaniantz, A., Grant, M., and Jones, J.D. (2011). Hormone crosstalk in plant disease and defense: more than just jasmonate-salicylate antagonism. *Annu Rev Phytopathol* 49**,** 317-343. DOI: 10.1146/annurev-phyto-073009-114447.

Robertson, A. (2013). *An in-depth look at the Corn-Colletotrichum graminicola (causal organism of anthracnose) pathosystem.*

Robertson, A.E., Pecinovsky, K., and Liu (2010). Effect of fungicides on anthracnose top dieback, frost severity and yield of hybrid corn at Nashua. *Iowa in 2009, Plant Disease Management Reports 4:FC087*. DOI: 10.1094/PDMR04.

Rowell, J.B. (1954). Genetics of *Ustilago zeae* in relation to basic problems of its pathogenicity. *Phytopathology* 44**,** 356-362.

Rowell, J.B. (1955). Functional role of incompatibility factors and an in vitro test for sexual incompatibility with haploid lines of *Ustilago zaes. Phytopathology* 45**,** 370-374.

Safarova, D., Brazda, P., and Navratil, M. (2014). Effect of artificial dsRNA on infection of pea plants by pea seed-borne mosaic virus. *Czech Journal of Genetics and Plant Breeding* 50**,** 105-108. DOI: 10.17221/120/2013-cjgpb.

Samira, R., Zhang, X., Kimball, J., Cui, Y., Stacey, G., and Balint-Kurti, P.J. (2019). Quantifying MAMP-induced production of reactive oxygen species in sorghum and maize. *Bio-protocol* 9**,** e3304. DOI: 10.21769/BioProtoc.3304.

Sander, J.D., and Joung, J.K. (2014). CRISPR-Cas systems for editing, regulating and targeting genomes. *Nature Biotechnology* 32**,** 347-355. DOI: 10.1038/nbt.2842.

Santino, A., De Paolis, A., Gallo, A., Quarta, A., Casey, R., and Mita, G. (2003). Biochemical and molecular characterization of hazelnut (*Corylus avellana*) seed lipoxygenases. *European Journal of Biochemistry* 270**,** 4365-4375. DOI: 10.1046/j.1432-1033.2003.03831.x.

Santino, A., Iannacone, R., Hughes, R., Casey, R., and Mita, G. (2005). Cloning and characterisation of an almond 9-lipoxygenase expressed early during seed development. *Plant Science* 168**,** 699-706. DOI: 10.1016/j.plantsci.2004.10.001.

Saville, B.J. (2012). "Investigating host induced meiosis in a fungal plant pathogen," in *Meiosis,* ed. M.E. Donaldson. (Rijeka: IntechOpen), Ch.-22.

Schedel, S., Pencs, S., Hensel, G., Muller, A., Rutten, T., and Kumlehn, J. (2017). RNA-guided Cas9-induced mutagenesis in tobacco followed by efficient genetic fixation in doubled haploid plants. *Frontiers in Plant Science* 7**,** 14. DOI: 10.3389/fpls.2016.01995.

Schilmiller, A.L., Koo, A.J.K., and Howe, G.A. (2007). Functional diversification of acyl-coenzyme A oxidases in jasmonic acid biosynthesis and action. *Plant Physiology* 143**,** 812-824. DOI: 10.1104/pp.106.092916.

See, P.T., Moffat, C.S., Morina, J., and Oliver, R.P. (2016). Evaluation of a multilocus indel DNA region for the detection of the wheat tan spot pathogen *Pyrenophora tritici-*repentis. *Plant Disease* 100**,** 2215-2225. DOI: 10.1094/pdis-03-16-0262-re.

Seitner, D., Uhse, S., Gallei, M., and Djamei, A. (2018). The core effector CCE1 is required for early infection of maize by *Ustilago maydis*. *Mol Plant Pathol* 19**,** 2277-2287. DOI: 10.1111/mpp.12698.

Sfeir, A., and Symington, L.S. (2015). Microhomology-mediated end joining: a back-up survival mechanism or dedicated pathway? *Trends Biochem Sci* 40**,** 701-714. DOI: 10.1016/j.tibs.2015.08.006.

Shan, Q., Wang, Y., Li, J., and Gao, C. (2014). Genome editing in rice and wheat using the CRISPR/Cas system. *Nature Protocols* 9**,** 2395-2410. DOI: 10.1038/nprot.2014.157.

Shan, Q.W., Wang, Y.P., Li, J., Zhang, Y., Chen, K.L., Liang, Z., Zhang, K., Liu, J.X., Xi, J.J., Qiu, J.L., and Gao, C.X. (2013). Targeted genome modification of crop plants using a CRISPR-Cas system. *Nature Biotechnology* 31**,** 686-688. DOI: 10.1038/nbt.2650.

Sheen, J. (1991). Molecular mechanisms underlying the differential expression of maize *PYRUVATE, ORTHOPHOSPHATE DIKINASE* genes. *Plant Cell* 3**,** 225-245. DOI: 10.1105/tpc.3.3.225.

Shi, J., Gao, H., Wang, H., Lafitte, H.R., Archibald, R.L., Yang, M., Hakimi, S.M., Mo, H., and Habben, J.E. (2017). *ARGOS8* variants generated by CRISPR-Cas9 improve maize grain yield under field drought stress conditions. *Plant Biotechnology Journal* 15**,** 207-216. DOI: 10.1111/pbi.12603.

Shivaji, R., Camas, A., Ankala, A., Engelberth, J., Tumlinson, J.H., Williams, W.P., Wilkinson, J.R., and Luthe, D.S. (2010). Plants on constant alert: elevated levels of jasmonic acid and jasmonate-induced transcripts in caterpillar-resistant maize. *Journal of Chemical Ecology* 36**,** 179-191. DOI: 10.1007/s10886-010-9752-z.

Shoresh, M., Yedidia, I., and Chet, I. (2005). Involvement of jasmonic acid/ethylene signaling pathway in the systemic resistance induced in cucumber by *Trichoderma asperellum* T203. *Phytopathology* 95**,** 76-84. DOI: 10.1094/phyto-95-0076.

Shriver, J.M., and Robertson, A.E. (2009). Comparison of fungicide products for disease control and yield in corn at Crawfordsville. *Iowa 2008, Plant Disease Management Reports 3:FC015.*

Shu, X.M., Livingston, D.P., Woloshuk, C.P., and Payne, G.A. (2017). Comparative histological and transcriptional analysis of maize kernels infected with *Aspergillus flavus* and *Fusarium verticillioides*. *Frontiers in Plant Science* 8**,** 14. DOI: 10.3389/fpls.2017.02075.

Shukla, V.K., Doyon, Y., Miller, J.C., Dekelver, R.C., Moehle, E.A., Worden, S.E., Mitchell, J.C., Arnold, N.L., Gopalan, S., Meng, X.D., Choi, V.M., Rock, J.M., Wu, Y.Y., Katibah, G.E., Zhifang, G.,

Mccaskill, D., Simpson, M.A., Blakeslee, B., Greenwalt, S.A., Butler, H.J., Hinkley, S.J., Zhang, L., Rebar, E.J., Gregory, P.D., and Urnov, F.D. (2009). Precise genome modification in the crop species *Zea mays* using zinc-finger nucleases. *Nature* 459**,** 437-U156. DOI: 10.1038/nature07992.

Siebert, R., and Puchta, H. (2002). Efficient repair of genomic double-strand breaks by homologous recombination between directly repeated sequences in the plant genome. *Plant Cell* 14**,** 1121-1131. DOI: 10.1105/tpc.001727.

Siedow, J.N. (1991). Plant lipoxygenase - structure and function. *Annual Review of Plant Physiology and Plant Molecular Biology* 42**,** 145-188. DOI: 10.1146/annurev.pp.42.060191.001045.

Sierotzki, H., and Scalliet, G. (2013). A review of current knowledge of resistance aspects for the next-generation succinate dehydrogenase inhibitor fungicides. *Phytopathology* 103**,** 880.

Silva, G., Poirot, L., Galetto, R., Smith, J., Montoya, G., Duchateau, P., and Paques, F. (2011). Meganucleases and other tools for targeted genome engineering: perspectives and challenges for gene therapy. *Current Gene Therapy* 11**,** 11-27. DOI: 10.2174/156652311794520111.

Silvar, C., Diaz, J., and Merino, F. (2005). Real-time polymerase chain reaction quantification of *Phytophthora capsici* in different pepper genotype. *Phytopathology* 95**,** 1423-1429. DOI: 10.1094/phyto-95-1423.

Smigocki, A.C., and Wilson, D. (2004). Pest and disease resistance enhanced by heterologous suppression of a *Nicotiana plumbaginifolia* cytochrome P450 gene *CYP72A2*. *Biotechnology Letters* 26**,** 1809-1814. DOI: 10.1007/s10529-004-4615-8.

Smith, J., Berg, J.M., and Chandrasegaran, S. (1999). A detailed study of the substrate specificity of a chimeric restriction enzyme. *Nucleic Acids Research* 27**,** 674-681. DOI: 10.1093/nar/27.2.674.

Snetselaar, K.M., and Mims, C.W. (1992). Sporidial fusion and infection of maize seedlings by the smut fungus *Ustilago maydis*. *Mycologia* 84**,** 193-203. DOI: 10.2307/3760250.

Soltis, D.E., Visger, C.J., and Soltis, P.S. (2014). The polyploidy revolution then…and now: Stebbins revisited. *American Journal of Botany* 101**,** 1057-1078. DOI: 10.3732/ajb.1400178.

Song, Y., and Thomma, B. (2018). Host-induced gene silencing compromises Verticillium wilt in tomato and *Arabidopsis*. *Molecular Plant Pathology* 19**,** 77-89. DOI: 10.1111/mpp.12500.

Southern, E.M. (1975). Detection of specific sequences among DNA fragments separated by gel electrophoresis. *J Mol Biol* 98**,** 503-517. DOI: 10.1016/s0022-2836(75)80083-0.

Srivastava, V., Underwood, J.L., and Zhao, S. (2017). Dual-targeting by CRISPR/Cas9 for precise excision of transgenes from rice genome. *Plant Cell Tissue and Organ Culture* 129**,** 153-160. DOI: 10.1007/s11240-016-1166-3.

Steibel, J.P., Poletto, R., Coussens, P.M., and Rosa, G.J.M. (2009). A powerful and flexible linear mixed model framework for the analysis of relative quantification RT-PCR data. *Genomics* 94**,** 146-152. DOI: 10.1016/j.ygeno.2009.04.008.

Stirnberg, A., and Djamei, A. (2016). Characterization of ApB73, a virulence factor important for colonization of *Zea mays* by the smut *Ustilago maydis*. *Molecular Plant Pathology* 17**,** 1467-1479. DOI: 10.1111/mpp.12442.

Sun, F., Huo, X., Zhai, Y.J., Wang, A.J., Xu, J.X., Su, D., Bartlam, M., and Rao, Z.H. (2005). Crystal structure of mitochondrial respiratory membrane protein complex II. *Cell* 121**,** 1043-1057. DOI: 10.1016/j.cell.2005.05.025.

Sun, Y.W., Zhang, X., Wu, C.Y., He, Y.B., Ma, Y.Z., Hou, H., Guo, X.P., Du, W.M., Zhao, Y.D., and Xia, L.Q. (2016). Engineering herbicide-resistant rice plants through CRISPR/Cas9-mediated homologous recombination of acetolactate synthase. *Molecular Plant* 9**,** 628-631. DOI: 10.1016/j.molp.2016.01.001.

Szczepek, M., Brondani, V., Buchel, J., Serrano, L., Segal, D.J., and Cathomen, T. (2007). Structure-based redesign of the dimerization interface reduces the toxicity of zinc-finger nucleases. *Nature Biotechnology* 25**,** 786-793. DOI: 10.1038/nbt1317.

Tashkandi, M., Ali, Z., Aljedaani, F., Shami, A., and Mahfouz, M.M. (2018). Engineering resistance against Tomato yellow leaf curl virus via the CRISPR/Cas9 system in tomato. *Plant Signaling & Behavior* 13**,** 7. DOI: 10.1080/15592324.2018.1525996.

Thakare, D., Zhang, J.W., Wing, R.A., Cotty, P.J., and Schmidt, M.A. (2017). Aflatoxin-free transgenic maize using host-induced gene silencing. *Science Advances* 3**,** 8. DOI: 10.1126/sciadv.1602382.

Thilmony, R., Underwood, W., and He, S.Y. (2006). Genome-wide transcriptional analysis of the *Arabidopsis thaliana* interaction with the plant pathogen *Pseudomonas syringae* pv. tomato DC3000 and the human pathogen *Escherichia coli* O157:H7. *Plant J* 46**,** 34-53. DOI: 10.1111/j.1365-313X.2006.02725.x.

Thomma, B.P., Penninckx, I.A., Broekaert, W.F., and Cammue, B.P. (2001). The complexity of disease signaling in *Arabidopsis. Curr Opin Immunol* 13**,** 63-68. DOI: 10.1016/s0952-7915(00)00183-7.

Torres, M.A., Jones, J.D., and Dangl, J.L. (2006). Reactive oxygen species signaling in response to pathogens. *Plant Physiol* 141**,** 373-378. DOI: 10.1104/pp.106.079467.

Tovkach, A., Zeevi, V., and Tzfira, T. (2009). A toolbox and procedural notes for characterizing novel zinc finger nucleases for genome editing in plant cells. *Plant Journal* 57**,** 747-757. DOI: 10.1111/j.1365-313X.2008.03718.x.

Townsend, J.A., Wright, D.A., Winfrey, R.J., Fu, F.L., Maeder, M.L., Joung, J.K., and Voytas, D.F. (2009). High-frequency modification of plant genes using engineered zinc-finger nucleases. *Nature* 459**,** 442-U161. DOI: 10.1038/nature07845.

Truman, W., De Zabala, M.T., and Grant, M. (2006). Type III effectors orchestrate a complex interplay between transcriptional networks to modify basal defence responses during pathogenesis and resistance. *Plant J* 46**,** 14-33. DOI: 10.1111/j.1365-313X.2006.02672.x.

Tsror, L., Erlich, O., and Hazanovsky, M. (1999). Effect of *Colletotrichum coccodes* on potato yield, tuber quality, and stem colonization during spring and autumn. *Plant Disease* 83**,** 561-565. DOI: 10.1094/pdis.1999.83.6.561.

Tsuda, K., Sato, M., Stoddard, T., Glazebrook, J., and Katagiri, F. (2009). Network properties of robust immunity in plants. *PLoS Genet* 5**,** e1000772. DOI: 10.1371/journal.pgen.1000772.

Tucker, S.L., and Talbot, N.J. (2001). Surface attachment and pre-penetration stage development by plant pathogenic fungi. *Annual Review of Phytopathology* 39**,** 385-+. DOI: 10.1146/annurev.phyto.39.1.385.

Uhse, S., and Djamei, A. (2018). Effectors of plant-colonizing fungi and beyond. *Plos Pathogens* 14**,** 8. DOI: 10.1371/journal.ppat.1006992.

Upadhyay, R.K., Handa, A.K., and Mattoo, A.K. (2019). Transcript abundance patterns of 9-and 13-lipoxygenase subfamily gene members in response to abiotic stresses (heat, cold, drought or salt) in tomato (*Solanum lycopersicum L.*) highlights member-specific dynamics relevant to each stress. *Genes* 10**,** 15. DOI: 10.3390/genes10090683.

Uppalapati, S.R., Ishiga, Y., Doraiswamy, V., Bedair, M., Mittal, S., Chen, J.H., Nakashima, J., Tang, Y.H., Tadege, M., Ratet, P., Chen, R.J., Schultheiss, H., and Mysore, K.S. (2012). Loss of abaxial leaf epicuticular wax in *Medicago truncatula irg1/palm1* mutants results in reduced spore differentiation of anthracnose and nonhost rust pathogens. *Plant Cell* 24**,** 353-370. DOI: 10.1105/tpc.111.093104.

Van Der Linde, K., Hemetsberger, C., Kastner, C., Kaschani, F., Van Der Hoorn, R.a.L., Kumlehn, J., and Doehlemann, G. (2012). A maize CYSTATIN suppresses host immunity by inhibiting apoplastic cysteine proteases. *Plant Cell* 24**,** 1285-1300. DOI: 10.1105/tpc.111.093732.

Van Loon, L.C., Geraats, B.P., and Linthorst, H.J. (2006). Ethylene as a modulator of disease resistance in plants. *Trends Plant Sci* 11**,** 184-191. DOI: 10.1016/j.tplants.2006.02.005.

Van Schie, C.C.N., and Takken, F.L.W. (2014). "Susceptibility genes 101: how to be a good host," *Annual Review of Phytopathology, Vol 52,* ed. N.K. Vanalfen. (Palo Alto: Annual Reviews), 551-+. DOI: 10.1146/annurev-phyto-102313-045854.

Vandesompele, J., De Preter, K., Pattyn, F., Poppe, B., Van Roy, N., De Paepe, A., and Speleman, F. (2002). Accurate normalization of real-time quantitative RT-PCR data by geometric averaging of multiple internal control genes. *Genome Biology* 3**,** 12. DOI: 10.1186/gb-2002-3-7-research0034.

Vargas, W.A., Martin, J.M.S., Rech, G.E., Rivera, L.P., Benito, E.P., Diaz-Minguez, J.M., Thon, M.R., and Sukno, S.A. (2012). Plant defense mechanisms are activated during biotrophic and necrotrophic development of *Colletotricum graminicola* in maize. *Plant Physiology* 158**,** 1342-1358. DOI: 10.1104/pp.111.190397.

Vellosillo, T., Aguilera, V., Marcos, R., Bartsch, M., Vicente, J., Cascon, T., Hamberg, M., and Castresana, C. (2013). Defense Activated by 9-Lipoxygenase-Derived Oxylipins Requires Specific Mitochondrial Proteins. *Plant Physiology* 161**,** 617-627. DOI: 10.1104/pp.112.207514.

Vellosillo, T., Martinez, M., Lopez, M.A., Vicente, J., Cascon, T., Dolan, L., Hamberg, M., and Castresana, C. (2007). Oxylipins produced by the 9-lipoxygenase pathway in *Arabidopsis* regulate lateral root development and defense responses through a specific signaling cascade. *Plant Cell* 19**,** 831-846. DOI: 10.1105/tpc.106.046052.

Verma, D.P., and Hong, Z. (2001). Plant callose synthase complexes. *Plant Mol Biol* 47**,** 693-701. DOI: 10.1023/a:1013679111111.

Vicente, J., Cascon, T., Vicedo, B., Garcia-Agustin, P., Hamberg, M., and Castresana, C. (2012). Role of 9-lipoxygenase and alpha-dioxygenase oxylipin pathways as modulators of local and systemic defense. *Mol Plant* 5**,** 914-928. DOI: 10.1093/mp/ssr105.

Vinay, P., Mccallum, B., Jordan, M., Loewen, M., Fobert, P., Mccartney, C., and Bakkeren, G. (2016). RNA silencing approaches for identifying pathogenicity and virulence elements towards engineering crop resistance to plant pathogenic fungi. *CAB Reviews* 11**,** 1-13. DOI: 10.1079/PAVSNNR201611027.

Viswanath, K.K., Varakumar, P., Pamuru, R.R., Basha, S.J., Mehta, S., and Rao, A.D. (2020). Plant lipoxygenases and their role in plant physiology. *Journal of Plant Biology* 63**,** 83-95. DOI: 10.1007/s12374-020-09241-x.

Voytas, D.F. (2013). Plant genome engineering with sequence-specific nucleases. 64**,** 327-350. DOI: 10.1146/annurev-arplant-042811-105552.

Wang, E.T., Schornack, S., Marsh, J.F., Gobbato, E., Schwessinger, B., Eastmond, P., Schultze, M., Kamoun, S., and Oldroyd, G.E.D. (2012). A common signaling process that promotes mycorrhizal and oomycete colonization of plants. *Current Biology* 22**,** 2242-2246. DOI: 10.1016/j.cub.2012.09.043.

Wang, F.J., Wang, C.L., Liu, P.Q., Lei, C.L., Hao, W., Gao, Y., Liu, Y.G., and Zhao, K.J. (2016a). Enhanced rice blast resistance by CRISPR/Cas9-targeted mutagenesis of the *ERF* transcription factor gene *OsERF922*. *Plos One* 11**,** 18. DOI: 10.1371/journal.pone.0154027.

Wang, L., Chen, L., Li, R., Zhao, R., Yang, M., Sheng, J., and Shen, L. (2017). Reduced drought tolerance by CRISPR/Cas9-mediated SlMAPK3 mutagenesis in tomato plants. *J Agric Food Chem* 65**,** 8674-8682. DOI: 10.1021/acs.jafc.7b02745.

Wang, M., Weiberg, A., Lin, F.M., Thomma, B., Huang, H.D., and Jin, H.L. (2016b). Bidirectional cross-kingdom RNAi and fungal uptake of external RNAs confer plant protection. *Nature Plants* 2**,** 10. DOI: 10.1038/nplants.2016.151.

Wang, W., Akhunova, A., Chao, S., and Akhunov, E. (2016c). Optimizing multiplex CRISPR/Cas9-based genome editing for wheat. *bioRxiv***,** 051342. DOI: 10.1101/051342.

Wang, X., Tu, M., Wang, D., Liu, J., Li, Y., Li, Z., Wang, Y., and Wang, X. (2018). CRISPR/Cas9-mediated efficient targeted mutagenesis in grape in the first generation. *Plant Biotechnol J* 16**,** 844-855. DOI: 10.1111/pbi.12832.

Wang, Y.P., Cheng, X., Shan, Q.W., Zhang, Y., Liu, J.X., Gao, C.X., and Qiu, J.L. (2014). Simultaneous editing of three homoeoalleles in hexaploid bread wheat confers heritable resistance to powdery mildew. *Nature Biotechnology* 32**,** 947-951. DOI: 10.1038/nbt.2969.

Wasternack, C., and Feussner, I. (2018). "The oxylipin pathways: biochemistry and function," in *Annual Review of Plant Biology, Vol 69,* ed. S.S. Merchant. (Palo Alto: Annual Reviews), 363-386. DOI: 10.1146/annurev-arplant-042817-040440.

Waterworth, W.M., Drury, G.E., Bray, C.M., and West, C.E. (2011). Repairing breaks in the plant genome: the importance of keeping it together. *New Phytol* 192**,** 805-822. DOI: 10.1111/j.1469-8137.2011.03926.x.

Waugh, A., Gendron, P., Altman, R., Brown, J.W., Case, D., Gautheret, D., Harvey, S.C., Leontis, N., Westbrook, J., Westhof, E., Zuker, M., and Major, F. (2002). RNAML: a standard syntax for exchanging RNA information. *RNA* 8**,** 707-717. DOI: 10.1017/s1355838202028017.

Weber, H., Chetelat, A., Caldelari, D., and Farmer, E.E. (1999). Divinyl ether fatty acid synthesis in late blight-diseased potato leaves. *Plant Cell* 11**,** 485-493. DOI: 10.1105/tpc.11.3.485.

Weidenbach, D., Jansen, M., Franke, R.B., Hensel, G., Weissgerber, W., Ulferts, S., Jansen, I., Schreiber, L., Korzun, V., Pontzen, R., Kumlehn, J., Pillen, K., and Schaffrath, U. (2014). Evolutionary conserved function of barley and *Arabidopsis* 3-ketoacyl-CoA synthases in providing wax signals for germination of powdery mildew fungi. *Plant Physiology* 166**,** 1621-+. DOI: 10.1104/pp.114.246348.

Weihmann, F., Eisermann, I., Becher, R., Krijger, J.J., Hubner, K., Deising, H.B., and Wirsel, S.G.R. (2016). Correspondence between symptom development of *Colletotrichum graminicola* and fungal biomass, quantified by a newly developed qPCR assay, depends on the maize variety. *Bmc Microbiology* 16**,** 14. DOI: 10.1186/s12866-016-0709-4.

Weis, C., Hildebrandt, U., Hoffmann, T., Hemetsberger, C., Pfeilmeier, S., Konig, C., Schwab, W., Eichmann, R., and Huckelhoven, R. (2014). CYP83A1 is required for metabolic compatibility of *Arabidopsis* with the adapted powdery mildew fungus *Erysiphe cruciferarum*. *New Phytologist* 202**,** 1310-1319. DOI: 10.1111/nph.12759.

Werner, S., Sugui, J.A., Steinberg, G., and Deising, H.B. (2007). A chitin synthase with a myosin-like motor domain is essential for hyphal growth, appressorium differentiation, and pathogenicity of the maize anthracnose fungus *Colletotrichum graminicola*. *Mol Plant Microbe Interact* 20**,** 1555-1567. DOI: 10.1094/mpmi-20-12-1555.

Wessler, S., Tarpley, A., Purugganan, M., Spell, M., and Okagaki, R. (1990). Filler DNA is associated with spontaneous deletions in maize. *Proceedings of the National Academy of Sciences of the United States of America* 87**,** 8731-8735. DOI: 10.1073/pnas.87.22.8731.

White, D.G. (1999). *Compendium of corn diseases.*

Wiedenheft, B., Sternberg, S.H., and Doudna, J.A. (2012). RNA-guided genetic silencing systems in bacteria and archaea. *Nature* 482**,** 331-338. DOI: 10.1038/nature10886.

Wilson, G.W. (1914). *The Identity of the anthracnose of Grasses in the United States.*

Wilson, R.A., Gardner, H.W., and Keller, N.P. (2001). Cultivar-dependent expression of a maize lipoxygenase responsive to seed infesting fungi. *Molecular Plant-Microbe Interactions* 14**,** 980-987. DOI: 10.1094/mpmi.2001.14.8.980.

Woldemariam, M.G., Ahern, K., Jander, G., and Tzin, V. (2018). A role for 9-lipoxygenases in maize defense against insect herbivory. *Plant Signal Behav* 13**,** e1422462. DOI: 10.1080/15592324.2017.1422462.

Wong, N., Liu, W.J., and Wang, X.W. (2015). WU-CRISPR: characteristics of functional guide RNAs for the CRISPR/Cas9 system. *Genome Biology* 16**,** 8. DOI: 10.1186/s13059-015-0784-0.

Wright, D.A., Townsend, J.A., Winfrey, R.J., Irwin, P.A., Rajagopal, J., Lonosky, P.M., Hall, B.D., Jondle, M.D., and Voytas, D.F. (2005). High-frequency homologous recombination in plants mediated by zinc-finger nucleases. *Plant Journal* 44**,** 693-705. DOI: 10.1111/j.1365-313X.2005.02551.x.

Wu, F. (2006). Mycotoxin reduction in Bt corn: Potential economic, health, and regulatory impacts. *Transgenic Research* 15**,** 277-289. DOI: 10.1007/s11248-005-5237-1.

Wu, L.C., Wang, S.X., Tian, L., Wu, L.J., Li, M.N., Zhang, J., Li, P., Zhang, W.G., and Chen, Y.H. (2018). Comparative proteomic analysis of the maize responses to early leaf senescence induced by preventing pollination. *Journal of Proteomics* 177**,** 75-87. DOI: 10.1016/j.jprot.2018.02.017.

Xin, Z.J., Chen, S.L., Ge, L.G., Li, X.W., and Sun, X.L. (2019). The involvement of a herbivore-induced acyl-CoA oxidase gene, *CsACX1*, in the synthesis of jasmonic acid and its expression in flower opening in tea plant (*Camellia sinensis*). *Plant Physiology and Biochemistry* 135**,** 132-140. DOI: 10.1016/j.plaphy.2018.11.035.

Xing, H.L., Dong, L., Wang, Z.P., Zhang, H.Y., Han, C.Y., Liu, B., Wang, X.C., and Chen, Q.J. (2014). A CRISPR/Cas9 toolkit for multiplex genome editing in plants. *Bmc Plant Biology* 14**,** 12. DOI: 10.1186/s12870-014-0327-y.

Xiong, L., Shen, Y.-Q., Jiang, L.-N., Zhu, X.-L., Yang, W.-C., Huang, W., and Yang, G.-F. (2015). "Succinate dehydrogenase: an ideal target for fungicide discovery," in *Discovery and Synthesis of Crop Protection Products*. American Chemical Society), 175-194.

Xu, J., Wang, X.Y., and Guo, W.Z. (2015). The cytochrome P450 superfamily: key players in plant development and defense. *Journal of Integrative Agriculture* 14**,** 1673-1686. DOI: 10.1016/s2095-3119(14)60980-1.

Yadav, B.C., Veluthambi, K., and Subramaniam, K. (2006). Host-generated double stranded RNA induces RNAi in plant-parasitic nematodes and protects the host from infection. *Molecular and Biochemical Parasitology* 148**,** 219-222. DOI: 10.1016/j.molbiopara.2006.03.013.

Yang, H., Wu, J.J., Tang, T., Liu, K.D., and Dai, C. (2017). CRISPR/Cas9-mediated genome editing efficiently creates specific mutations at multiple loci using one sgRNA in *Brassica napus*. *Scientific Reports* 7**,** 13. DOI: 10.1038/s41598-017-07871-9.

Yankovskaya, V., Horsefield, R., Törnroth, S., Luna-Chavez, C., Miyoshi, H., Léger, C., Byrne, B., Cecchini, G., and Iwata, S. (2003). Architecture of succinate dehydrogenase and reactive oxygen species generation. *Science* 299**,** 700-704. DOI: 10.1126/science.1079605.

Yin, C.T., Jurgenson, J.E., and Hulbert, S.H. (2011). Development of a host-induced RNAi system in the wheat stripe rust fungus *Puccinia striiformis* f. sp tritici. *Molecular Plant-Microbe Interactions* 24**,** 554-561. DOI: 10.1094/mpmi-10-10-0229.

Yokota, T., Sakamoto, N., Enomoto, N., Tanabe, Y., Miyagishi, M., Maekawa, S., Yi, L., Kurosaki, M., Taira, K., Watanabe, M., and Mizusawa, H. (2003). Inhibition of intracellular Hepatitis C virus replication by synthetic and vector-derived small interfering RNAs. *Embo Reports* 4**,** 602-608. DOI: 10.1038/sj.embor.embor840.

Zetsche, B., Gootenberg, J.S., Abudayyeh, O.O., Slaymaker, I.M., Makarova, K.S., Essletzbichler, P., Volz, S., Joung, J., Van Der Oost, J., Regev, A., Koonin, E.V., and Zhang, F. (2016). Cpf1 is a single-RNA-guided endonuclease of a class 2 CRISPR-Cas system. *Transgenic Research* 25**,** 207-207.

Zhang, F., Maeder, M.L., Unger-Wallace, E., Hoshaw, J.P., Reyon, D., Christian, M., Li, X.H., Pierick, C.J., Dobbs, D., Peterson, T., Joung, J.K., and Voytas, D.F. (2010). High frequency targeted mutagenesis in *Arabidopsis thaliana* using zinc finger nucleases. *Proceedings of the National Academy of Sciences of the United States of America* 107**,** 12028-12033. DOI: 10.1073/pnas.0914991107.

Zhang, H., Guo, J., Voegele, R.T., Zhang, J.S., Duan, Y.H., Luo, H.Y., and Kang, Z.S. (2012). Functional characterization of calcineurin homologs *PsCna1/PsCnb1* in *Puccinia striiformis* f. sp tritici using a host-induced RNAi system. *Plos One* 7**,** 8. DOI: 10.1371/journal.pone.0049262.

Zhang, H., Zhang, J.S., Wei, P.L., Zhang, B.T., Gou, F., Feng, Z.Y., Mao, Y.F., Yang, L., Zhang, H., Xu, N.F., and Zhu, J.K. (2014). The CRISPR/Cas9 system produces specific and homozygous targeted gene editing in rice in one generation. *Plant Biotechnology Journal* 12**,** 797-807. DOI: 10.1111/pbi.12200.

Zhang, J., Khan, S.A., Hasse, C., Ruf, S., Heckel, D.G., and Bock, R. (2015). Full crop protection from an insect pest by expression of long double-stranded RNAs in plastids. *Science* 347**,** 991. DOI: 10.1126/science.1261680.

Zhang, J.L., Simmons, C., Yalpani, N., Crane, V., Wilkinson, H., and Kolomiets, M. (2005). Genomic analysis of the *12-OXO-PHYTODIENOIC ACID REDUCTASE* gene family of *Zea mays*. *Plant Molecular Biology* 59**,** 323-343. DOI: 10.1007/s11103-005-8883-z.

Zhang, N., Roberts, H.M., Van Eck, J., and Martin, G.B. (2020). Generation and molecular characterization of CRISPR/Cas9-induced mutations in 63 immunity-associated genes in tomato reveals specificity and a range of gene modifications. *Frontiers in Plant Science* 11**,** 13. DOI: 10.3389/fpls.2020.00010.

Zhang, Y., Bai, Y., Wu, G., Zou, S., Chen, Y., Gao, C., and Tang, D. (2017). Simultaneous modification of three homoeologs of *TaEDR1* by genome editing enhances powdery mildew resistance in wheat. *Plant J* 91**,** 714-724. DOI: 10.1111/tpj.13599.

Zhang, Y., Zhang, F., Li, X.H., Baller, J.A., Qi, Y.P., Starker, C.G., Bogdanove, A.J., and Voytas, D.F. (2013). Transcription activator-like effector nucleases enable efficient plant genome engineering. *Plant Physiology* 161**,** 20-27. DOI: 10.1104/pp.112.205179.

Zhou, H.B., Liu, B., Weeks, D.P., Spalding, M.H., and Yang, B. (2014). Large chromosomal deletions and heritable small genetic changes induced by CRISPR/Cas9 in rice. *Nucleic Acids Research* 42**,** 10903-10914. DOI: 10.1093/nar/gku806.

Zhou, Y., Xu, J., Zhu, Y., Duan, Y., and Zhou, M. (2016). Mechanism of action of the benzimidazole fungicide on *Fusarium graminearum*: interfering with polymerization of monomeric tubulin but not polymerized microtubule. *Phytopathology* 106**,** 807-813. DOI: 10.1094/phyto-08-15-0186-r.

Zhu, J.J., Song, N., Sun, S.L., Yang, W.L., Zhao, H.M., Song, W.B., and Lai, J.S. (2016). Efficiency and inheritance of targeted mutagenesis in maize using CRISPR-Cas9. *Journal of Genetics and Genomics* 43**,** 25-36. DOI: 10.1016/j.jgg.2015.10.006.

Zhu, L., Zhu, J., Liu, Z.X., Wang, Z.Y., Zhou, C., and Wang, H. (2017a). Host-induced gene silencing of rice blast fungus *Magnaporthe oryzae* pathogenicity genes mediated by the Brome mosaic virus. *Genes* 8**,** 14. DOI: 10.3390/genes8100241.

Zhu, X.G., Qi, T., Yang, Q., He, F.X., Tan, C.L., Ma, W., Voegele, R.T., Kang, Z.S., and Guo, J. (2017b). Host-induced gene silencing of the *MAPKK* gene *PsFUZ7* confers stable resistance to wheat stripe rust. *Plant Physiology* 175**,** 1853-1863. DOI: 10.1104/pp.17.01223.

Zipfel, C. (2008). Pattern-recognition receptors in plant innate immunity. *Curr Opin Immunol* 20**,** 10-16. DOI: 10.1016/j.coi.2007.11.003.

Zong, Y., Song, Q., Li, C., Jin, S., Zhang, D., Wang, Y., Qiu, J.L., and Gao, C. (2018). Efficient C-to-T base editing in plants using a fusion of nCas9 and human APOBEC3A. *Nat Biotechnol*. DOI: 10.1038/nbt.4261.

Zong, Y., Wang, Y., Li, C., Zhang, R., Chen, K., Ran, Y., Qiu, J.L., Wang, D., and Gao, C. (2017). Precise base editing in rice, wheat and maize with a Cas9-cytidine deaminase fusion. *Nat Biotechnol* 35**,** 438-440. DOI: 10.1038/nbt.3811.

Zou, G., Ying, S.H., Shen, Z.C., and Feng, M.G. (2006). Multi-sited mutations of β-Tubulin are involved in benzimidazole resistance and thermotolerance of fungal biocontrol agent *Beauveria bassiana*. *Environmental Microbiology* 8**,** 2096-2105. DOI: 10.1111/j.1462-2920.2006.01086.x.

Zuker, M. (2003). Mfold web server for nucleic acid folding and hybridization prediction. *Nucleic Acids Research* 31**,** 3406-3415. DOI: 10.1093/nar/gkg595.

Zuker, M., and Jacobson, A.B. (1998). Using reliability information to annotate RNA secondary structures. *RNA* 4**,** 669-679. DOI: 10.1017/s1355838298980116.

Zuo, T., Zhang, J., Lithio, A., Dash, S., Weber, D.F., Wise, R., Nettleton, D., and Peterson, T. (2016). Genes and small RNA transcripts exhibit dosage-dependent expression pattern in maize copy-number alterations. *Genetics* 203**,** 1133-1147. DOI: 10.1534/genetics.116.188235.

7. Supplementary data

Supplemental Table 1: Antibiotics used in this study

Antibiotic	Stock concentration	Final concentration
Ampicillin	100 mg/mL	100 µg/mL
Spectinomycin	100 mg/mL	100 µg/mL
Rifampicin*	10 mg/mL	50 µg/mL
Kanamycin	10 mg/mL	50 µg/mL
Hygromycin**	50 mg/mL	30 mg/mL
Bialaphos	10 mg/mL	5 mg/mL
Ticarcillin	250 mg/mL	400 mg/mL
* dissolved in DMSO, without filter sterilization		
**purchased as ready-to-use stock solution from Roche (Mannheim, Germany)		

Supplemental Table 2: Oligonucleotides used in this study

Sequences of oligonucleotides used for *C. graminicola* quantification		
Target gene	**Primer name**	**Sequence 5'-3'**
C. graminicola ITS (Internal Transcribed Spacer)	Cg-ITS2-qPCR-Fw	CGTCGTAGGCCCTTAAAGGTAG
	Cg-ITS2-qPCR-Rv	TTACGGCAAGAGTCCCTC
pUC18	M13-qPCR-Fw	GTAAAACGACGGCCAGTGC
	M13-qPCR-Rv	CACAGGAAACAGCTATGACC

Sequences of oligonucleotides used for *U. maydis* quantification		
Target gene	**Primer name**	**Sequence 5'-3'**
U. maydis Ppi (Peptidyl-prolyl isomerase)	UmPpi (BMQ)-F	ACATCGTCAAGGCTATCG
	UmPpi(BMQ)-R	AAAGAACACCGGACTTGG
Maize GAPDH (Glyceraldehyde 3-phosphate dehydrogenase)	ZmGAPDH (BMQ)-F	CTTCGGCATTGTTGAGGGTTTG
	ZmGAPDH (BMQ)-R	TCCTTGGCTGAGGGTCCGTC

Sequences of oligonucleotides used for the detection of T-DNA by PCR		
Target gene	**Primer name**	**Sequence 5'-3'**
cas9	Bie475	TTTAGCCCTGCCTTCATACG
	Zm cas9 R4	AGCGGAGCCTTCGTAATC
gRNA	NBPSH114R1 (forward)	CCAAGCTCAAGCTAAGCTC
	Zmlox3-G1R	AAACTCGATGATCCCGCTCAGCAT
	Zmlox3-G2R	AAACCCGTCAGCCCGTCGATGATC
	Zmlox3-G3R	AAACCCTTGCCGAGGAACTCGCT
	Zmlox3-G4R	AAACCCGTGCCCTTGAGCCGCGC
	Zmlox3-G5R	AAACCCGTCGTTGACAGCATCAGC
hpt	NB2X35SPF	AGAGGACACGCTGAAATC
	GH HYG R5	GATTCCTTGCGGTCCGAATG
β-Tubulin2 (β-Tub2)	βTUB2F1	GAGATTGTTCACCTCCAGAC
	βTUB2R1	TTAAACCTCCTCCTCCAG
Sdh1	SDH1F1	ATGGCCTCATCAATGGCG
	SDH1R1	CACACGCTTGAAAGGAGG
Sdh2	SDH2F1	TCTTCCTCCCGAGTCTTG
	SDH2R1	GCCATCTGCTTCTTGATCTC
Sdh3	SDH3F1	ATGATTGCGCAGCGGGTG
	SDH3R1	CTACCACGCAAAGGCCAG
Sdh4	SDH4F1	ATGGCTTCGATTGTGCGACC
	SDH4R1	TTACGCCCTCCAGAGAC
pNB96/97 sense	Bie372	AAACAAATGCAGTATGAAGATACAC
	NB2X35SPF	AGAGGACACGCTGAAATC
pNB96/97 anti-sense	Bie371	GAAGGGATAGCCCTCATAGATAG
	35S term catin	CATGAGCGAAACCCTATAAGAACCC
pNB98/99 Sense	Bie475	TTTAGCCCTGCCTTCATACG
	Bie372	AAACAAATGCAGTATGAAGATACAC
pNB98/99 anti-sense	Bie371	GAAGGGATAGCCCTCATAGATAG
	35S term catin	CATGAGCGAAACCCTATAAGAACCC

Sequences of oligonucleotides used for reverse transcriptase quantitative PCR			
Target gene	**Primer name**	**Sequence 5'-3'**	**Literature source for primer**
ZmLOX1	zmLOX1qRTF	TCTGTCTGAGCTGAGGACGTA	Christensenet al., 2015
	zmLOX1qRTR	CACAAAGTAACTTCATTATTGAGGA	
ZmLOX2	zmLOX2qRTF	TTCCATCTGATTCGATCGAG	
	zmLOX2qRTR	CACATTATTATTGGGAAACCAAC	
ZmLOX4	zmLOX4qRTF	TGAGCGGATGGTTTGTAGAT	
	zmLOX4qRTR	ATTATCCAGACGTGGCTCCT	
ZmLOX5	zmLOX5qRTF	GGGCAGATTGTGTCTCGTAGTA	
	zmLOX5qRTR	ATATTCAAGCGTGGACTCCTCT	
ZmLOX6	zmLOX6qRTF	ACAGCCCTGACTGGTGCTC	
	zmLOX6qRTR	TTCACGTTTATGTGGTGGAGA	
ZmLOX8	zmLOX8qRTF	CAGTACCGACAGACAGCCAT	
	zmLOX8qRTR	GTTTCGGACCACCAAATCAA	
ZmLOX9	zmLOX9qRTF	TGAGTGCATCGTTCGTTGT	
	zmLOX9qRTR	TCAATCCTCATTCTTGGCAG	
ZmLOX10	zmLOX10qRTF	ATCCTCAGCATGCATTAGTCC	
	zmLOX10qRTR	AGTCTCAAACGTGCCTCTTGT	
ZmLOX11	zmLOX11qRTF	GTCCGTCCTCTCCATCCAA	
	zmLOX11qRTR	GGATCTGCTAGTAATGTCATCC	
ZmLOX12	zmLOX12qRTF	AATTGACAAGCTCGCTCCTT	
	zmLOX12qRTR	TCCAAACCAATCATCGCAA	
ZmGST2	zmGST2qRTF	TGTGCTTGATTAGTTAATTGG	
	zmGST2qRTR	CGTGGAGAAAGCAGCAAAAT	
ZmHYD	zmHYDqRTF	TGTGCCAGGTGCTTGCGTT	
	zmHYDqRTR	TGAAAGCAGGATAAACACCAA	
ZmOPR2	zmOPR2qRTF	GACCGACCGAGAGCAAATAG	
	zmOPR2qRTR	ATCTTGTAAGGCGTCAGCAG	
P450	zmP450qRTF	CTGACCGCATATGTAGAAA	
	zmP450qRTR	TCGCAATGCATACAAGGGA	
ZmPR1	zmPR1qRTF2	GCGAGAGCTCCTACTAGACTGT	Nasinet al., 2013
	zmPR1qRTR2	CGCCTGCATGGTTTTATTGACT	
ZmPAL1	zmPAL1qRTF	TCAAGTAAAAGAACGCCAAGGA	
	zmPAL1qRTR	GAAGAAAGAGCAACGCCACA	
Corn cystatin	zmCC9qRTF2	TAGCAGACCTGCAGATGGCTA	Doehlemannet al., 2008
	zmCC9qRTR2	GAAGAGCAAGCATCCGTGG	
ZmPR3	zmPR3qRTF	GAACAACTACAGCAGCCAGGTG	
	zmPR3qRTR	GAGACAATAGCTGACATGCGTC	
ZmPR4	zmPR4qRTF1	GCGTTCAAGCCCATCGACA	
	zmPR4qRTR1	CGTGTGGGATCACATCCATATAAC	
ZmPR5	zmPR5qRTF2	TATCGGCCGGAATAGGCTCTG	Doehlmann et al., 2012
	zmPR5qRTR2	CGCGTACATACAAATGCGTGC	
ZmUbiquitin*	zmUBIqRTF1	TGATAATGTGAAGGCCAAGATCCAG	Shivajiet al., 2010
	zmUBIqRTR1	GGTCTGGGGGAATCCCCTCCTTGTC	
ZmOPR6	zmOPR6qRTF	AGCAGGCTTTGATGGAGTGGA	
	zmOPR6qRTR	TTGGCAAAACGCATCGGAAGG	
ZmOPR7	zmOPR7qRTF	CGGCTGTTCATCGCTAATCCCGA	
	zmOPR7qRTR	CAATCGCGGCATTACCCAGATGT	
Maize protease inhibitor (MPI)	zmMPIqRTF	ATGAGCTCCACGGAGTGC	
	zmMPIqRTR	TCAGCCGATGTGGGGCGTC	
PRm3 (chitinase)	zmPRM3qRTF	CGCCGCAGTGCCCCTACCC	
	zmPRM3qRTR	TCTCCCGATGATCCGCTCTTATATTA	
ZmLOX3	zmLOX-3qRTF1	TCACGAGCCAGATCCAGACCA	
	zmLOX-3qRTR1	ATTCGATTCACCAGCCCACACG	
Allene oxide synthase (AOS)	zmAOSqRTF1	CCAGGTGAGGAAGGGCGAGATGCT	
	zmAOSqRTR1	GTGAAGGTGGGGCCGAGGGTGAGA	
ZmACX	zmACXqRTF	GTCCTCGTCTTCCACGTTGT	Maschiettoa et al., 2015
	zmACXqRTR	CGAGGTCAAGACCAAAGCTC	
ZmOPR8	zmOPR8qRTF1	TACTGATGCCCGATGGATCC	
	zmOPR8qRTR1	AACCTGCTTTGATGGCGTTT	
Zm18S*	zm18SqRTF	CCATCCCTCCGTAGTTAGCTTCT	Manoli et al., 2011
	zm18SqRTR	CCTGTCGGCCAAGGCTATATAC	
ZmOPR5	zmOPR5qRTF	CTCGGAGGTTTGAAGTAGACGC	Yanet al., 2012
	zmOPR5qRTR	CAACTTGACAACTGACTGATCTT	
* used as reference gene for normalization			

**Supplemental Table 3:** Software's used in this study

List of softwares used in this study			
Name of the Software	**Company /source**	**Company Headquarters**	**Web Page**
Clone Manager 9 Professional Edition	Scientific & Educational Software	Morrisville. NC. USA	https://www.scied.com/pr_cmbas.htm
Endnote® X5	Thomson Reuters	Philadelphia. PA. USA	https://endnote.com
Microsoft Office Excel 2010	Microsoft Corporation	Redmond. WA. USA	https://www.microsoft.com
GIMP (GNU Image Manipulation)	Free and open-source	Charlotte. North Carolina	https://www.gimp.org
ApE (A plasmid Editor)	Software is Freeware	M. Wayne Davis (developer)	https://jorgensen.biology.utah.edu/wayned/ape
ImageJ (image processing)	LOCI. University of Wisconsin	University of Wisconsin	https://imagej.nih.gov/ij/index.html
Sigma stat	Jandel Scientific Software	San Jose, California	http://www.systat.de

Supplemental Table 4: Sequences of gRNA oligonucleotides used for cas9/gRNA vector

Sequences of oligonucleotides used for the cloning of RNA-guided cas9 vectors		
Target motif	**Primer name**	**Sequence 5'-3'**
Zmlox3-G1	Zmlox3-G1F	TGGCATGCTGAGCGGGATCATCGA
	Zmlox3-G1R	AAACTCGATGATCCCGCTCAGCAT
Zmlox3-G2	Zmlox3-G2F	TGGCGATCATCGACGGGCTGACGG
	Zmlox3-G2R	AAACCCGTCAGCCCGTCGATGATC
Zmlox3-G3	Zmlox3-G3F	TGGCAGCGAGTTCCTCGGCAAGG
	Zmlox3-G3R	AAACCCTTGCCGAGGAACTCGCT
Zmlox3-G4	Zmlox3-G4F	TGGCGCGCGGCTCAAGGGCACGG
	Zmlox3-G4R	AAACCCGTGCCCTTGAGCCGCGC
Zmlox3-G5	Zmlox3-G5F	TGGCGCTGATGCTGTCAACGACGG
	Zmlox3-G5R	AAACCCGTCGTTGACAGCATCAGC

Supplemental Table 5: Solutions used in protoplast experiment

| Solutions used for protoplast experiments	
cell wall digestion enzymes	**PEG solution**
1.5% cellulase	40% (W/V) PEG4000
0.4% macerozyme R10	100 mmol/L CaCl2
0.4 mol/L mannitol	0.2 mol/L mannitol
20 mmol/L KCl	**MMG solution**
20 mmol/L MES pH 5.7	4 mmol/L MES pH 5.7
10 mmol/L CaCl2	0.4 mol/L mannitol
0.1% BSA	15 mmol/L MgCl2
5 mmol/L b-mercaptoethanol	**WI solution**
W5 solution	4 mmol/L MES pH 5.7
154 mmol/L NaCl	0.5 mol/L mannitol
5 mmol/L KCl	15 mmol/L KCl
125 mmol/L CaCl2	
2 mmol/L MES pH 5.7	
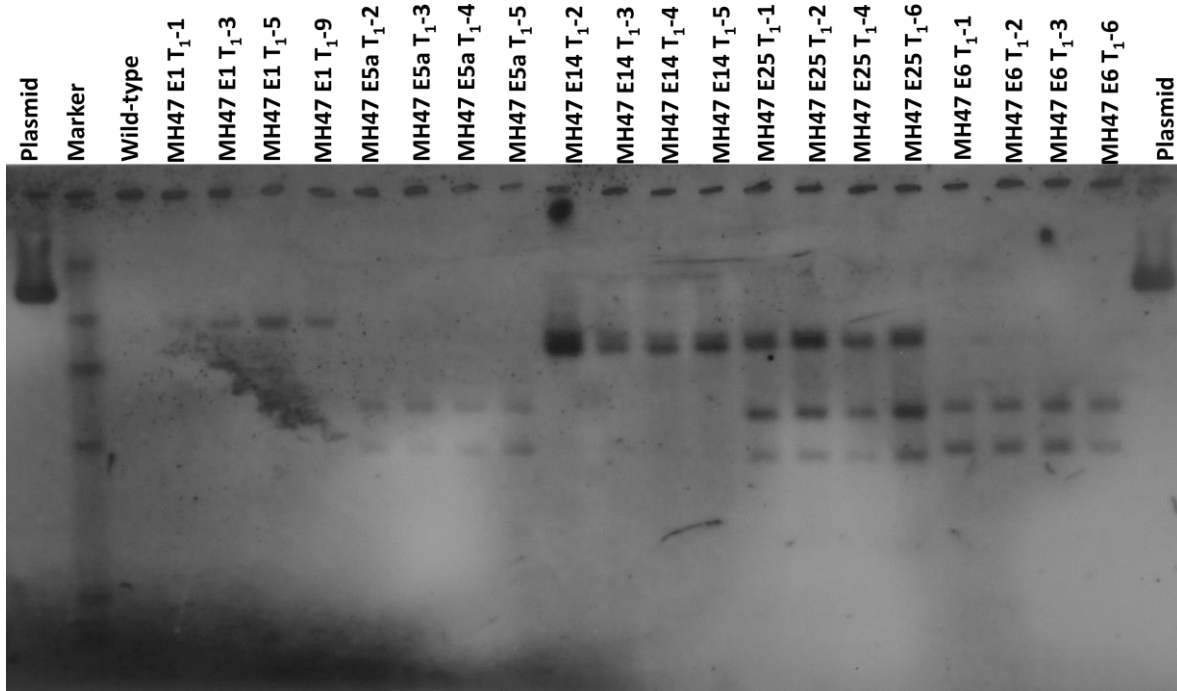
Supplemental Figure 1: DNA gel blot analysis of transgenic segregants of T_1 (from self-pollinated T_0) transgenic plants from the transformation experiment with pNB97 carrying an RNAi unit addressing the *C. graminicola Sdh1*. 20 μg genomic DNA each were digested with *HinDIII* and the fragments were separated into 0.8% (w/v) agarose gel. Hybridization of the specific DNA sequences was performed with a *hygromycin hosphotransferase* (*hpt*) specific probe. The names of the individual plants belonging to three T_1 families are given above the picture. Wild-type used as a negative control, plasmid as a positive control. Alphabets a, b indicates transgenic siblings.
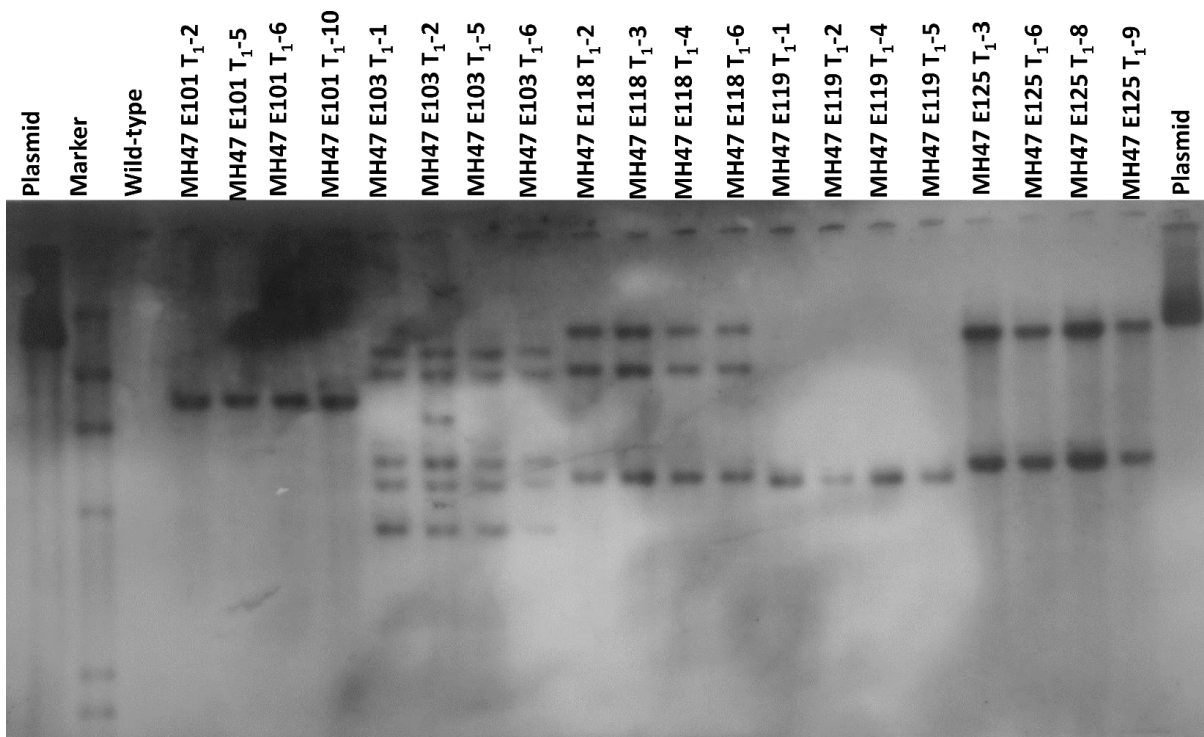
Supplemental Figure 2: DNA gel blot analysis of transgenic segregants of T_1 (from self-pollinated T_0) transgenic plants from the transformation experiment with pNB98 carrying an RNAi unit addressing the *C. graminicola β-Tub2*. 20 µg genomic DNA each were digested with *HinDIII* and the fragments were separated into 0.8% (w/v) agarose gel. Hybridization of the specific DNA sequences was performed with a *hygromycin hosphotransferase* (*hpt*) specific probe. The names of the individual plants belonging to three T_1 families are given above the picture. Wild-type used as a negative control, plasmid as a positive control. Alphabets a, b indicates transgenic siblings.
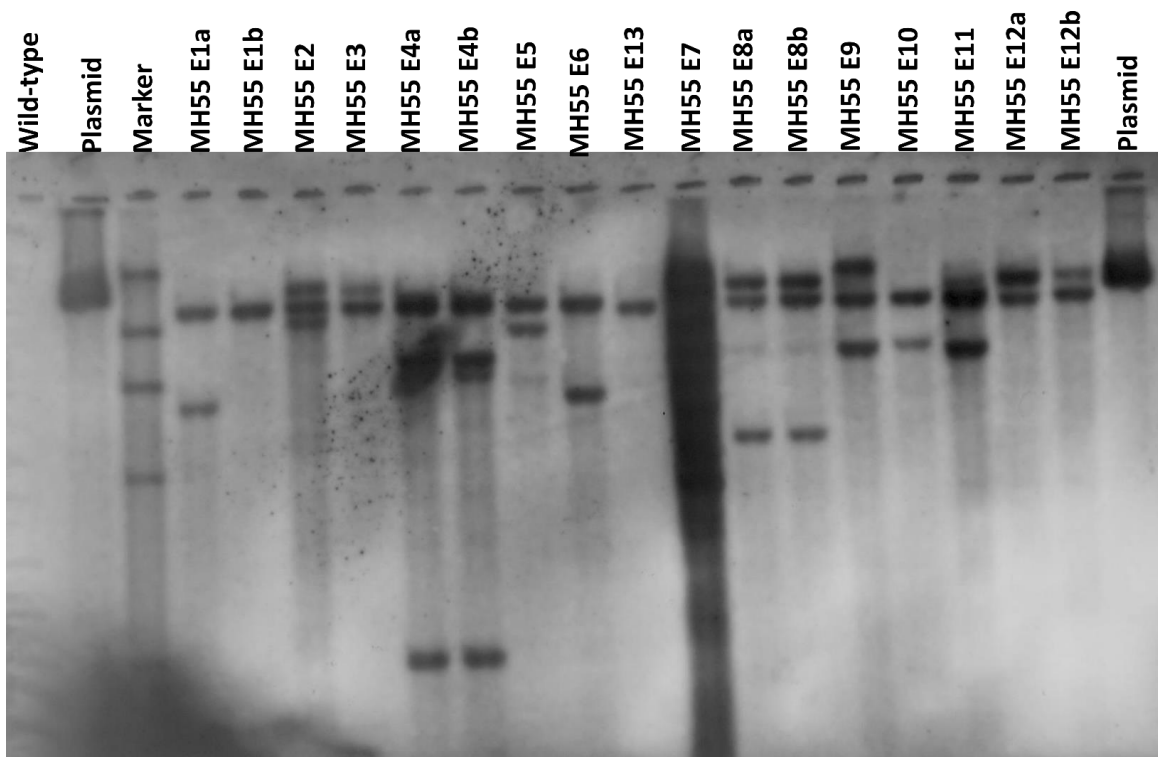
Supplemental Figure 3: DNA gel blot analysis of primary transgenic T_0 plants from the transformation experiment with pNB99 carrying an RNAi unit addressing the *C. graminicola Sdh1*. 20 µg genomic DNA each were digested with *HinDIII* and the fragments were separated into 0.8% (w/v) agarose gel. Hybridization of the specific DNA sequences was performed with a *hygromycin hosphotransferase* (*hpt*) specific probe. The names of the individual plants are given above the picture. Wild-type used as a negative control, plasmid as a positive control. Alphabets a, b indicates transgenic siblings.
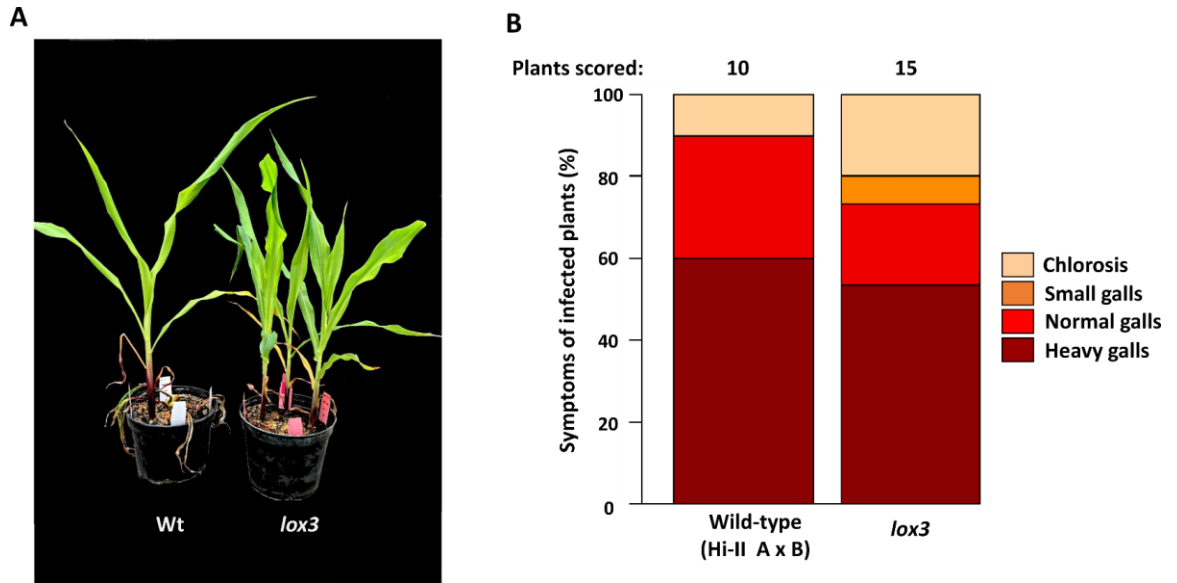
Supplemental Figure 4: Comparison of wild-type and *lox3* mutant lines for susceptibility towards *U. maydis*. (A) Typical symptom development 8 dpi. (B) Quantification of infection symptoms on maize seedlings at 8 dpi.

8. Acknowledgements

9. Curriculum vitae

Personal Information

Name	Krishna Mohan Pathi
Address	Hans-Stubbe-Str.20
	06466 Gatersleben
	Germany
Date/place of birth	06.07.1986/Alamur
Nationality	Indian

Work Experience

01/2017-Present	PhD Student
	Leibniz Institute of Plant Genetics and Crop Plant Research (IPK)
	Plant Reproductive Biology Group, Gatersleben, Germany
01/2014-12/2016	Research Fellow
	Leibniz Institute of Plant Genetics and Crop Plant Research (IPK)
	Plant Reproductive Biology Group, Gatersleben, Germany
06/2011-12/2014	Research Fellow
	International Centre for Genetic Engineering and Biotechnology (ICGEB)
	Plant Molecular Biology Research Group, New Delhi, INDIA
09/2008-05/2011	Research Officer
	BIOSEED RESEARCH INDIA Pvt. Ltd
	Genetic Transformation Lab. (R & D unit), Agri Science Park
	International Crop Research Institute for Semi-Arid Tropics (ICRISAT),
	Patancheru (Hyderabad), India

Education

07/2006-07/2008	Master of Biotechnology
	Periyar University, India (secured 65%)
Master Thesis	**Title**: **Antimicrobial activity of *Catharanthus roseus***
07/2003-07/2006	Bachelor of Science (Botany, Zoology, Chemistry)
	Sri Krishna Devaraya University, India (secured 65%)
2001-2003	Intermediate education (secured 70%)
	Board of Intermediate Education, India

Academic Awards

- Achieved **Elevator Pitch award** in the **PLANT 2030 Status Seminar 2019** for excellent presentation
- Honored with **The Best Discussion Award** in **PSSC-2017** for an outstanding discussion during the conference
- Awarded **DBT-JRF** (Department of Bio-Technology - Junior Research Fellowship) Ministry of Science & Technology, Govt of India (06-2011 till 12-2014)

Publications

- **Pathi KM**, Rink P, Budhagatapalli N, Betz R, Saado I, Hiekel S, Becker M, Djamei A, J Kumlehn J (**2020**). Engineering smut resistance in maize by site-directed knockout of *LIPOXYGENASE 3*. **Frontiers in Plant Science.** 2020.543895
- Beier S, Ulpinnis C, Schwalbe M, Münch T, Hoffie R, Koeppel I, Hertig C,

Budhagatapalli N, Hiekel S, **Pathi KM**, Hensel G, Grosse M, Chamas S, Gerasimova S, Kumlehn J, Scholz U, Schmutzer T **(2019)**. Kmasker plants - a tool for assessing complex sequence space in plant species. *The plant journal*. 102 (3), 631-642.

- **Pathi KM**, Tula S, Huda KMK, Kumar V S, Tuteja N (**2013**) Regeneration of elite Indian maize (*Zea mays L*.) inbreds from mature zygotic embryo through callus initiation. *Plant Signalling and Behaviour.* 8: (10)

- KMdK Huda, SA Banu, **Pathi KM**,Tuteja N **(2013)** Functional analysis of rice plasma membrane Ca2+ATPase promoter in response to environmental stimuli in transgenic tobacco plants. *PLOS ONE*. (8):3

- **Pathi KM**, Tula S, Tuteja N (**2013**) High Frequency regeneration via direct somatic embryogenesis and efficient *Agrobacterium* mediated transformation of *Nicotiana. Plant Signalling and Behaviour*. (8):6

- **Pathi KM**, Tuteja N (**2012**) High-frequency regeneration via multiple shoot induction of elite recalcitrant cotton (*Gossypium hirsutum* L. cv. Narashima*. Plant Signalling and Behaviour*. (8):1

Conference Talks	- **Krishna Mohan Pathi**, Nagaveni Budhagatapalli, Götz Hensel, Heike Büchner, Maximilian Groß, Holger Deising, Jochen Kumlehn.(2019). Establishment of maize resistance to fungal diseases by host-induced gene silencing and site-directed mutagenesis. **German Society of Plant Biotechnology**. Geisenheim

- **Krishna Mohan Pathi**, Nagaveni Budhagatapalli, Götz Hensel, Heike Büchner, Maximilian Groß, Holger Deising, Jochen Kumlehn.(2019). Establishment of anthracnose disease resistance of maize by Cas endonuclease-mediated mutagenesis and host-induced gene silencing. **PSSC** Halle

- **Krishna Mohan Pathi**, Nagaveni Budhagatapalli, Maximilian Groß, Holger Deising, Jochen Kumlehn. (2018). Establishment of anthracnose disease resistance of maize by RNA interference and site-directed mutagenesis. **German Society of Plant Biotechnology.** Neustadt a.d. Weinstraße

- **Krishna Mohan Pathi**, Nagaveni Budhagatapalli, Maximilian Groß, Holger Deising, Jochen Kumlehn. (2017). Pathogen resistance achieved by plant-induced silencing of fungicide target genes. **PSSC**. IPB Halle

- **Krishna Mohan Pathi**, Ingrid Otto, Friederike Göhring, Heike Büchner, Andrea Müller and Jochen Kumlehn. (2016). Induction of adventitious roots from *Nicotiana attenuata* shoots generated in vitro. **PSSC** IPK Gatersleben

- **Krishna Mohan Pathi**, Heike Büchner and Jochen Kumlehn. (2014). Embryogenic callus and multiple shoot formation from coleoptilar node explants of maize**. PSSC.** IPK Gatersleben

Posters	- **Krishna Mohan Pathi**, Nagaveni Budhagatapalli, Götz Hensel, Heike Büchner, Diaa Eldin S. Daghma,Maximilian Groß, Holger Deising, Jochen Kumlehn.(2019). Establishment of anthracnose disease resistance of maize by Cas endonuclease-mediated mutagenesis and host-induced gene silencing. **IS-MPMI**. Glasgow Scotland.

- **Krishna Mohan Pathi**, Nagaveni Budhagatapalli, Götz Hensel, Heike Büchner, Diaa Eldin S. Daghma,Maximilian Groß, Holger Deising, Jochen Kumlehn.(2019). Establishment of anthracnose disease resistance of maize by Cas endonuclease-mediated mutagenesis and host-induced gene silencing. **PLANT 2030 Status Seminar 2019**. Potsdam.
- **Krishna Mohan Pathi**, Nagaveni Budhagatapalli, Götz Hensel, Heike Büchner, Maximilian Groß, Holger Deising, Jochen Kumlehn.(2017). Pathogen resistance achieved by plant-induced silencing of fungicide target genes. **Workshop on Molecular Plant Breeding**. JKI Braunschweig
- **Krishna Mohan Pathi**, Heike Büchner, Cornelia Marthe and Jochen Kumlehn. (2015). Generation of instantly homozygous transgenic tobacco plants by gene transfer to haploid cells. **PSSC.** IPB Halle
- **Krishna Mohan Pathi**, Heike Büchner, Cornelia Marthe and Jochen Kumlehn. (2015). Generation of instantly homozygous transgenic tobacco plants by gene transfer to haploid cells. **German Society of Plant Biotechnology**. Einbeck, Germany

Language Skills	

- English-Fluent
- German-B1 level
- Hindi-Good
- Telugu-Mother tongue